Toni Jernfors

Metabolic and Genomic Characteristics of Bank Voles Exposed to Radionuclides

UNIVERSITY OF JYVÄSKYLÄ

FACULTY OF MATHEMATICS
AND SCIENCE

Toni Jernfors

Metabolic and genomic characteristics of bank voles exposed to radionuclides

Esitetään Jyväskylän yliopiston matemaattis-luonnontieteellisen tiedekunnan suostumuksella
julkisesti tarkastettavaksi yliopiston vanhassa juhlasalissa S212
huhtikuun 29. päivänä 2022 kello 12.

Academic dissertation to be publicly discussed, by permission of
the Faculty of Mathematics and Science of the University of Jyväskylä,
in building Seminarium, Old Festival Hall S212 on April 29, 2022 at 12 o'clock noon..

JYVÄSKYLÄN YLIOPISTO
UNIVERSITY OF JYVÄSKYLÄ

JYVÄSKYLÄ 2022

Editors
Jari Haimi
Department of Department of Biological and Environmental Science, University of Jyväskylä
Timo Hautala
Open Science Centre, University of Jyväskylä

ABSTRACT

Organisms defend against external disturbances using various metabolic and genomic methods. Organisms experience stress when the disturbances grow severe enough to debilitate survival or reproduction. Low dose ionising radiation of environmental radionuclides is a form of contamination whose long-term metabolic and genomic effects on wild populations on the molecular level are not well understood. In this thesis I assess the metabolic and genomic consequences of inhabiting an environment polluted by radionuclides derived from the 1984 nuclear accident of Chernobyl, Ukraine, in the bank vole (*Myodes glareolus*) using techniques such as quantitative PCR, RNA-sequencing, 16S amplicon sequencing of gut microbiota, high precision liquid chromatography and gut tissue histology. I show that environmental radionuclides elicit expression changes in DNA repair mechanisms, fatty acid energy metabolism and mitochondrial function, which may facilitate oxidative balance. I also show that direct impact of radiation on the host rather than indirect effects through changes in gut microbiota composition better explain the observed metabolic changes. Moreover, bank voles exposed to radiation show immunosuppression and reduced mucus production in the colon, which may increase risk of infection. Furthermore, I show that voles exposed to radionuclides exhibit higher ribosomal DNA copy number, possibly improving genomic stability. Overall, inhabiting an environment contaminated by radionuclides possibly impacts metabolic and other regulatory mechanisms, causing diverse symptoms. Study of wildlife's responses and its capabilities to survive anthropogenic disturbances continues to increase in importance along with increase in human population and land use.

Keywords: Chernobyl; environmental stress; low dose ionising radiation; metabolism; ribosomal DNA; RNA-sequencing; short chain fatty acids.

Toni Jernfors, University of Jyväskylä, Department of Biological and Environmental Science, P.O. Box 35, FI-40014 University of Jyväskylä, Finland

TIIVISTELMÄ

Jernfors, Toni
Radionuklideille altistuneiden metsämyyrien metaboliset ja genomiset ominaisuudet
Jyväskylä: Jyväskylän yliopisto, 2021, 55 p.
(JYU Dissertations
ISSN 2489-9003; 507)
ISBN 978-951-39-9108-1
Diss.

Eliöt puolustautuvat ulkoisia häiriötekijöitä vastaan erilaisin metabolisin ja genomisin keinoin. Stressiksi kutsutaan tilannetta, jossa häiriöiden suuruus tai kesto alkaa vaikuttaa haitallisesti eläimen selviytymiseen tai lisääntymiseen. Ympäristön radionuklideista johtuva jatkuva matala-annoksinen säteily on saastumisen muoto, jonka pitkän aikavälin vaikutuksia eliöihin on vain vähän tutkittu molekyylitasolla. Väitöskirjassani tutkin, millaisia metabolisia ja genomisia seurauksia radionuklidien saastuttamalla Tshernobylin (Ukraina) ydinonnettomuusalueella eläminen aiheuttaa villeillä metsämyyräpopulaatioilla (*Myodes glareolus*) käyttäen useita menetelmiä kuten kvantitatiivista PCR:ää, RNA-sekvensointia, suolistomikrobiomin 16S-amplikonisekvensointia, korkean erotuskyvyn nestekromatografiaa ja paksusuolen kudosvärjäyksiä. Osoitan, että ympäristön radionuklidit aiheuttavat muutoksia DNA:n korjaukseen, rasvahappojen energia-aineenvaihduntaan ja mitokondrioiden toimintaan liittyvien geenien ilmenemiseen, mikä mahdollisesti parantaa oksidatiivista tasapainoa. Osoitan myös, että säteilyn suorat vaikutukset todennäköisemmin selittävät aineenvaihdunnallisia muutoksia myyrissä kuin epäsuorat vaikutukset suoliston mikrobiston kautta. Lisäksi säteilylle altistuneilla metsämyyrillä havaittiin immuunijärjestelmän tukahduttamista ja madaltunutta paksusuolen limakalvon eritystä, mikä voi lisätä infektion riskiä. Lopuksi osoitan, että säteilylle altistuneilla myyrillä havaittiin korkeampaa ribosomaalisen DNA:n kopiolukumäärää, mikä saattaa lisätä genomin tasapainoa. Tulokset osoittavat yleistetysti, että pitkäaikainen ympäristön stressi todennäköisesti vaikuttaa aineenvaihdunnallisiin ja muihin sääntelevim mekanismeihin aiheuttaen monipuolista oireilua. Luonnonvaraisen eliöstön kykyyn vastata ihmisperäisiin häiriöihin liittyvän tutkimuksen tärkeys lisääntyy sitä mukaa, kun väestön määrä ja maankäyttö lisääntyvät.

Avainsanat: Aineenvaihdunta; lyhytketjuiset rasvahapot; ionisoiva säteily; ribosomaalinen DNA; RNA-sekvensointi; Tšernobyl; ympäristöstressi.

Toni Jernfors, Jyväskylän yliopisto, Bio- ja ympäristötieteiden laitos PL 35, 40014 Jyväskylän yliopisto

Author's address   Toni Jernfors
Department of Biological and Environmental Science
P.O. Box 35
FI-40014 University of Jyväskylä
Finland
toni.m.jernfors@jyu.fi

Supervisors   Professor Phillip C Watts
Department of Biological and Environmental Science
P.O. Box 35
FI-40014 University of Jyväskylä
Finland

Dr. Jenni Kesäniemi
Department of Biological and Environmental Science
P.O. Box 35
FI-40014 University of Jyväskylä
Finland

Reviewers   Docent Miia Rainio
Department of Biology
FI-20014 University of Turku
Finland

Professor Andrea Bonisoli-Alquati
Department of Biological Sciences
California State Polytechnic University, Pomona
CA, USA

Opponent   Professor Heidi Hauffe
Department of Biodiversity and Molecular Ecology
Research and Innovation Centre
Fondazione Edmund Mach
38098 San Michele all'Adige
TN, Italy

LIST OF ORIGINAL PUBLICATIONS

The thesis is based on the following original papers, which will be referred to in the text by their Roman numerals I–IV.

I   Jernfors T, Kesäniemi J, Lavrinienko A, Mappes T, Milinevsky G, Møller AP, Mousseau TA, Tukalenko E & Watts PC. 2018. Transcriptional Upregulation of DNA Damage Response Genes in Bank Voles (Myodes glareolus) Inhabiting the Chernobyl Exclusion Zone. *Frontiers in Environmental Science* 5: 95. https://doi.org/10.3389/fenvs.2017.00095

II Kesäniemi J, Jernfors T, Lavrinienko A, Kivisaari K, Kiljunen M, Mappes T & Watts PC. 2019. Exposure to environmental radionuclides is associated with altered metabolic and immunity pathways in a wild rodent. *Molecular Ecology* 28: 4620–4635. https://doi.org/10.1111/mec.15241

III Jernfors T. Lavrinienko A, Vareniuk I, Landberg R, Fristed R, Tkachenko O, Taskinen S, Tukalenko E, Kesäniemi J, Mappes T, Watts PC. 2022. Association between gut health and gut microbiota in a polluted environment. *Manuscript*.

IV Jernfors T, Danforth J, Kesäniemi J, Lavrinienko A, Tukalenko E, Fajkus J, Dvořáčková M, Mappes T & Watts PC. 2021. Expansion of rDNA and pericentromere satellite repeats in the genomes of bank voles Myodes glareolus exposed to environmental radionuclides. *Ecology and Evolution* 00: 1–14. https://doi.org/10.1002/ece3.7684

The following table shows authors' contributions to the original papers.

	I	II	III	IV
Study design	TJ, PCW, TM	TJ, PCW, JK	TJ, AL, PCW	TJ, JD, PCW
Data collection	AL, TM, GM, APM, TAM, ET	JK, AL, TM	TJ, AL, ET, TM, JK	AL, ET, TM
Laboratory work	TJ, JK	TJ, JK, KK, MK	TJ, AL, IV, RL, RF, OT	TJ, JD, JK, ET, JF, MD
Data analysis	TJ	TJ, JK	TJ, AL, ST	TJ, JD
Manuscript writing	TJ, PCW	TJ, JK, PCW	TJ, PCW	TJ, PCW

Toni Jernfors (TJ), Phillip C. Watts (PCW), Anton Lavrinienko (AL), Jenni Kesäniemi (JK), Tapio Mappes (TM), Gennadi Milinevsky (GM), Anders P. Møller (APM), Timothy A. Mousseau (TAM), Eugene Tukalenko (ET), Kati Kivisaari (KK), Mikko Kiljunen (MK), Igor Vareniuk (IV), Rikard Landberg (RL), Rikard Fristed (FR), Olena Tkachenko (OT), Sara Taskinen (ST), John Danforth, (JD), Jiří Fajkus (JF), Martina Dvořáčková (MD)

ABBREVIATIONS

CEZ	Chernobyl exclusion zone
CNV	copy number variation
FAO	fatty acid oxidation
GO	gene ontology
IR	ionizing radiation
rDNA	ribosomal DNA
SCFA	short chain fatty acid
qPCR	quantitative PCR

CONTENTS

ORIGINAL PUBLICATIONS

1 INTRODUCTION

1.1 Environmental change and stress in the anthropocene

Anthropogenic effects such as land use, pollution, climate change, habitat loss and propagation of invasive species have made humanity a major selective force in the ecosphere (Palumbi 2001, Acevedo-Whitehouse and Duffus 2009). Anthropogenic factors impose "stress" on wildlife, and the human ecological footprint has led to accelerated rates of local extinctions and species loss (Barnosky *et al.* 2011), suggesting that processes of genetic adaptation are insufficient to promote survival in changing environments as they can take tens of generations to take effect (Urban *et al.* 2014). Organisms can cope with homeostatic disturbances in the short term by metabolic adjustments or in the long term by inducing acclimatized phenotypes during development. However, when stress occurs chronically or at high intensity, overproduction of stress response mediators can begin to cause pathological damage or otherwise fail to control homeostasis, thus harming health (Del Giudice *et al.* 2018). Indeed, anthropogenic effects have accelerated phenotypic change in wildlife (Hendry *et al.* 2008, Merilä and Hendry 2014, Urban *et al.* 2014, Lourenço *et al.* 2016, Alberti *et al.* 2017). As biodiversity is closely linked to human health, wellbeing and societal needs (Romanelli *et al.* 2015), study of wildlife's responses and its capabilities to survive anthropogenic disturbances continues to increase in importance as the human population and land use are likely to rise in the future.

1.2 Homeostatic control mechanisms

1.2.1 Homeostatic control and stress

Although the concept of stress is impossibly broad, in biological systems it can generally be understood that stress occurs when a **biological control system fails to control** a fitness-maintaining variable that can be either internal or ex-

ternal to the organism. On systemic level, organisms respond to homeostatic disturbances by mounting a wide variety of responses such as maintenance and control of physiological variables (e.g., blood pressure, blood electrolytes, body temperature), mode of primary metabolism (emphasis of glycolysis or fatty acid oxidation), and cellular homeostasis (oxidative balance, DNA repair) (Del Giudice *et al.* 2018) (Fig. 1). Control of homeostatic variables is broadly categorized under two strategies, the feedback and feedforward mechanisms. Briefly, in feedback control, a variable e.g. blood pressure is monitored and, in instance of deviation from a reference level, a response occurs. Feedforward controllers in turn can incorporate information from past and present stressors, predicting future disturbances and allowing rapid response. "Stress" occurs when a disturbance cannot be controlled for due to its amplitude of frequency, impacting survival or reproductive success (Koolhaas *et al.* 2011).

Chronic, health-impairing stress is exemplified by the immunosuppressive effects of stress hormones such as glucocorticoids. The immune system is expensive in resources and energy, thus in the short-term immunosuppression helps reroute energy to more immediate responses such as wound healing or detoxification. However, prolonged stress can have debilitating effects on an organism's immunocompetence. Indeed, increased parasite load and risk of disease in wildlife is a common consequence of environmental pollution (Acevedo-Whitehouse and Duffus 2009).

The capability to mount suitable stress responses is an integral component of plasticity and thus survival in environments that are being changed by human action. Recently, there has been growing evidence on diverse mechanisms that may provide additional flexibility for coping with stress in the long-term due to their (1) effects on the organism's phenotype, (2) inducibility by the environment and (3) partial heritability, potentially promoting survival in changing environments on a population level (Alberdi *et al.* 2016, Danchin *et al.* 2019). In the next section I present two such elements of interest: the gut microbiota and ribosomal DNA copy number variation (Fig. 1).
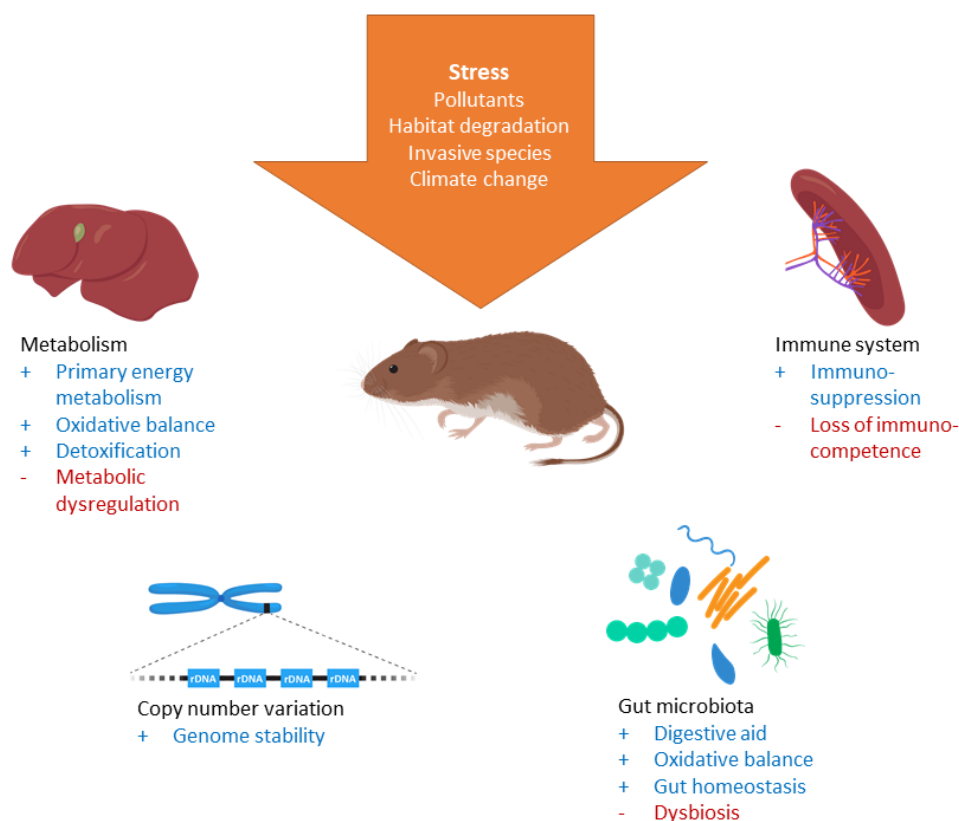
FIGURE 1   Stress-responsive physiological and genomic characteristics studied in this thesis. Organisms mount various systemic responses when subjected to environmental stress that can fail when the duration or intensity of stress factors exceed the scope of responses.

1.2.2 Gut microbiota

The gut microbiota is a community of predominantly bacteria, microfungi and protists that reside in the animal gastrointestinal tract in a symbiotic relationship with the host (Shreiner *et al.* 2015). Gut microbiota provides various services to the host, such as aid in digestion of foodstuffs (Gentile and Weir 2018), regulation of gut development and physiology (Birchenough *et al.* 2015, Schroeder 2019), regulation of host metabolism (den Besten *et al.* 2013, Canfora *et al.* 2015), facilitation of host immune system (Hooper *et al.* 2012) and preventing colonization by pathogenic microbes in the gut (Pickard *et al.* 2017). The gut microbiota affect host feeding behavior and neuronal development (Sampson and Mazmanian 2015), exemplifying the close symbiotic relationship with the host.

The composition of gut microbiota is affected by various factors, most notably by diet (David *et al.* 2014), and by other environmental factors such as season (Maurice *et al.* 2015, Sommer *et al.* 2016), parasites (Cortés *et al.* 2020), habitat degradation (Amato *et al.* 2013) and social interactions (Dill-McFarland *et al.* 2019). While environmental factors can change gut microbiota composition rap-

idly, a portion of the microbiota is also determined by host genetics (Goodrich *et al.* 2014) and maternal inheritance (Ferretti *et al.* 2018).

The gut microbiota produce short chain fatty acids (SCFA) as fermentation side products, most abundantly acetate, propionate and butyrate (den Besten *et al.* 2013). These metabolites mediate most of the host–microbiota interactions and affect the host in diverse ways, e.g. by providing host colon cells with additional energy, acting as signaling molecules to influence metabolism and promoting health through their antioxidative capabilities (Huang *et al.* 2017). Disruption to the relationship between host and gut microbiota, dysbiosis, is implicated in various diseases and conditions such as inflammatory bowel disease, diabetes (both type I and II), cancer, depression and autism spectrum disorders (DeGruttola *et al.* 2016). In humans, many of these health issues can be traced to a gut microbiota composition resulting from diet, lifestyle and environment typical to industrialized societies (Sonnenburg and Sonnenburg 2019).

The gut metagenome accounts for a significant portion of host organism's potential for phenotypic variation, for instance, a winter-type metagenome promotes energy storage in the brown bear preparing it for overwintering (Sommer *et al.* 2016), and transplantation of a cold-adapted gut microbiota into germ-free mice improves their cold tolerance through modulating energy homeostasis in the host (Chevalier *et al.* 2015). Reciprocally, environmental conditions such as diet, stress and infections drive evolution within the gut microbiota. Exemplifying this circular interaction, desert woodrat (*Neotoma lepida*) populations in contact with toxic plants have developed a gut microbiota with enhanced detoxification capabilities (Kohl *et al.* 2014). Considering the deep host-microbiota interactions and partial heritability of the microbiota, it has been proposed that the combined genomes of the host and microbiota form a single unit, the hologenome, that undergoes selection (Zilber-Rosenberg and Rosenberg 2008).

1.2.3 Genomic tandem repeat loci as environmental sensors

Interest in structural genomic variants and their effect as drivers of ecological and evolutionary processes is increasing (Mérot *et al.* 2020). Ribosomal DNA (rDNA) copy number variation (CNV) is a form of structural variation that garners special attention due to characteristics such as rapid copy number mutability and possibility to act as an environmental sensor (Bughio and Maggert 2019). rDNA is the originating genomic region of ribosomal RNAs that, together with riboproteins, form the protein translating organelles, ribosomes (Gibbons *et al.* 2015). rDNA loci are among the most ancient and most studied loci of the genome, and research on rDNA has advanced understanding of cytogenetics, cancer and ageing (Kobayashi 2014, Schöfer and Weipoltshammer 2018, Symonová 2019). In eukaryotes, rDNA is arranged as tandemly repeating units of large (>10 kb) 45S sequences that can exist in multiple chromosomes (e.g., in chromosomes 13, 14, 15, 21 and 22 in humans) and the separately occurring 5S locus. The 45S units are transcribed and then processed into 18S, 5.8S and 28S rRNAs, which form the small and large ribosomal subunits (Fig. 2).
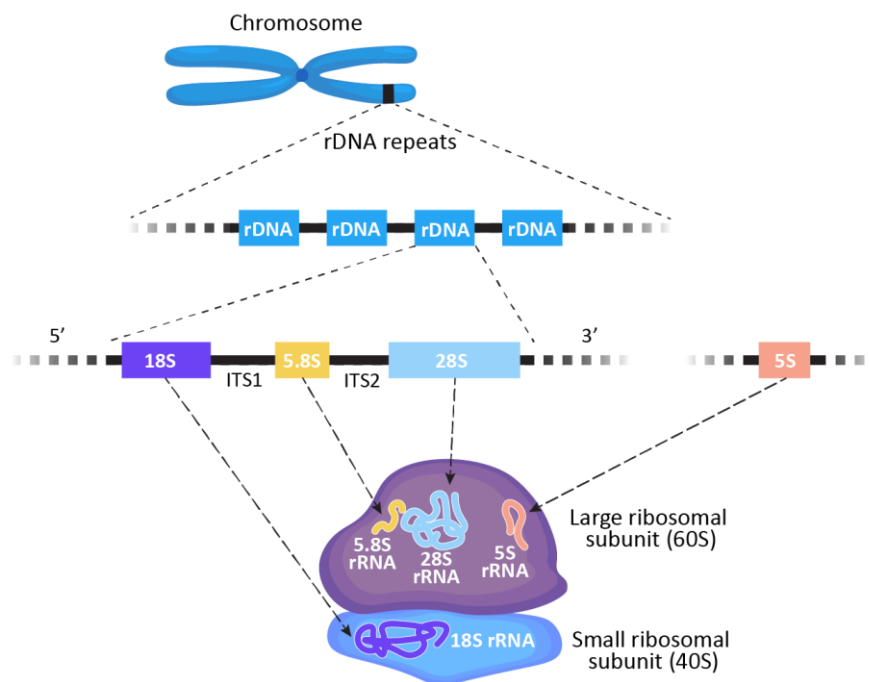
FIGURE 2   General structure of ribosomal DNA in animals.

Characteristic to rDNA is its very high CNV, which can vary between tens to thousands depending on species (Prokopowich *et al.* 2003, Symonová 2019, Lavrinienko *et al.* 2021b) and showing upwards tenfold variation in rDNA copy number even within species (e.g. 40 – 400 copies in humans) (Parks *et al.* 2018, Symonová 2019, Lavrinienko *et al.* 2021b). rDNA copy number shows geographic variation in diverse taxa, such as humans (Parks *et al.* 2018), conifers (Strauss and Tsai 1988) and *Daphnia* (Harvey *et al.* 2020).

rDNA CNV can be induced by environmental factors such as diet and genotoxic stress (Kobayashi 2011, Aldrich and Maggert 2015, Jack *et al.* 2015, Salim *et al.* 2017), with observable changes arising as soon as one generation (van Cann 2019). While details on the mechanics of rDNA CNV are still not fully known, one factor is rDNA's instability. As a repetitive genomic region, rDNA is prone to copy number changes resulting from unequal sister chromatid exchange during meiosis or homologous recombination DNA repair (Bughio and Maggert 2019). Moreover, there appear to be species-specific mechanisms that facilitate copy number expansion, for instance, the interaction of replication fork barrier protein Fob1 and barrier sequences in *Saccharomyces cerevisiae* (Kobayashi *et al.* 1998) and meiotic magnification in *Drosophila* (Bianciardi *et al.* 2012).

rDNA CNV is known to affect cell processes, and loss in rDNA copy number is often associated with genomic instability (Kobayashi 2011), cellular senescence (Saka *et al.* 2013, Kobayashi 2014) and cancer (Xu *et al.* 2017). Con-

versely, high rDNA copy number is associated with genomic stability, for instance, *S. cerevisiae* strains with high rDNA copy number are more resistant to mutagens (Ide *et al.* 2010). Indeed, rDNA CNV is correlated with mitochondrial abundance and regulation of gene expression for a range of genes involved in chromatin maintenance and the nucleolus (Paredes *et al.* 2011, Gibbons *et al.* 2014, Kobayashi and Sasaki 2017, Salim and Gerton 2019), although it is not known whether this is a feature of rDNA *per se* or of genomic heterochromatin content, of which rDNA is a major constituent of.

Another major constituent of heterochromatin are the satellite repeats of the centromeric and pericentromeric regions that have been found to affect gene expression possibly by containing originating sequences for noncoding RNAs (Ideue and Tani 2020), although evidence on CNV of centromeric satellites in response to environmental factors is scarce. However, repetitive constituents of heterochromatin such as rDNA, telomeres (Goytisolo *et al.* 2000, Zhang *et al.* 2016) or heterochromatic content in general (Yan *et al.* 2011, Larson *et al.* 2012) commonly show correlation between repeat copy number and genomic stability (i.e. radioresistance or lower frequency of DNA damage) and ageing (Qiu 2015). According to genomic safeguard hypothesis, heterochromatin content may confer protective effects for more vulnerable, active genomic regions by forming a barrier and localizing DNA damage to peripheral genomic regions (Qiu 2015).

1.3 The Chernobyl nuclear power plant accident and the wildlife of the exclusion zone as a model system

1.3.1 The accident and establishment of the exclusion zone

The nuclear accident of the former Chernobyl nuclear power plant (CNPP) is one of the most severe environmental disasters. On April 26th, 1986, CNPP reactor 4 exploded due to an erroneous safety experiment, exposing the reactor core (International Atomic Energy Agency 2006). The reactor continued to burn for ten days, releasing more than 9 million terabecquerels of radioactive material into the atmosphere. The nuclear fallout affected large areas of Europe, with much of the radionuclides being deposited in Ukraine, Belarus, and Eastern Russia. The accident caused a substantial socioeconomic cost due to large-scale evacuations, with a total of over 350,000 people affected in Ukraine, Belarus, and Russia. To limit human access to the contaminated area, The Chernobyl Nuclear Power Plant Zone of Alienation, or Chernobyl Exclusion Zone (CEZ) was established around ca. 30 km radius of the CNPP.

Radionuclide contamination in the CEZ today mostly consists of particles with long half-lives, most notably strontium-90 (^{90}Sr), cesium-137 (^{137}Cs) and plutonium-239 (^{239}Pu), with highly volatile fuel particles such as ^{131}I and ^{134}Cs having since been mostly decayed after over thirty years (Chesser *et al.* 2000, Beresford *et al.* 2016). Ambient radiation levels in the CEZ are still considered too high for permanent human habitation. Lack of human activity and land use

the CEZ has effectively transformed into a wildlife sanctuary through inadvertent rewilding (International Atomic Energy Agency 2006, Perino *et al.* 2019), and in 2016, roughly two thirds of the CEZ was organized as a wildlife reserve, the Chernobyl Radiation and Ecological Biosphere Reserve. The absence of human action, free movement of wildlife and heterogeneous patterns of radionuclide contamination on the local scale facilitating effective control area setups has made the CEZ a remarkable natural laboratory to study effects of radionuclide contamination on wildlife in their natural environment.

1.3.2 Ionizing radiation and its effects on tissues

Ionizing radiation (IR) consists of charged particles (alpha and beta particles) and photons containing sufficient energy (gamma and X-rays) to excite and detach electrons from atoms and molecules, ionizing impacted matter (International Atomic Energy Agency 2010). All organisms are exposed to very low doses of IR from natural sources such as cosmic background radiation and radioactive materials in Earth's crust such as radon gas. Impacts of IR on biological matter are divided in two categories of direct and indirect action (Ward 1988, Desouky *et al.* 2015). In direct action, radiation impacts biomolecules, causing structural damage. This is particularly damaging towards DNA, as disruption of DNA's double-helical structure leaves the DNA sequence vulnerable to mutations. Indirect action mainly consists of reactive oxygen species (ROS) such as hydroxyl and peroxide radicals that are released when radiation breaks down water and other molecules in cells, increasing the level of oxidative stress within the biological system (Desouky *et al.* 2015, Einor *et al.* 2016). An organism's total absorbed radiation dose consists of external dose from ambient radiation as well as internal dose received from internalized radionuclides, mostly from ^{137}Cs due to its water-soluble salts and ^{90}Sr for its tendency to deposit in bones as a calcium analogue (Chesser *et al.* 2000, Beresford *et al.* 2020a).

The detrimental effects of IR on tissues are well known in context of medical use and accidents with large, rapidly delivered doses, and recommendations for radioprotection are based on exposure models from controlled laboratory studies (International Atomic Energy Agency 2010, Rühm *et al.* 2018). United Nations Scientific Committee on the Effects of Atomic Radiation (UNSCEAR) and other international radioprotection organizations consider absorbed doses and dose rates below 100 mGy and 0.1 mGy/min as low dose, where effect sizes of most responses to IR become negligible. Ambient radiation dose rates encountered in contaminated areas of the CEZ today are in the low-dose range (4–40 µGy/h), which is an equivalent of several (2-5) chest X-ray scans (0.1 mSv) per day.

1.3.3 Effects of radionuclides on wildlife in the Chernobyl Exclusion Zone

Even at dose rates perceived as low dose, harmful effects have been observed in wildlife inhabiting contaminated areas such as Chernobyl and Fukushima, as well as uranium mines and nuclear test sites (reviewed by Mousseau *et al.* 2014,

Lourenço *et al.* 2016). Various effects of low dose IR have been recorded across several taxa, suggesting that organisms exhibit differing radiosensitivities. Wildlife inhabiting contaminated areas may be more radiosensitive in general, potentially due to interacting effects from multiple stressors (Garnier-Laplace *et al.* 2013, Real and Garnier-Laplace 2020) thus highlighting the need to further study populations exposed to chronic low-dose IR in natural settings.

At the population level, exposure to radionuclides associates with decrease of abundance in various taxa, such as birds (Garnier-Laplace *et al.* 2015), soil invertebrates (Møller and Mousseau 2018) and mammals (Mappes *et al.* 2019, Beaugelin-Seiller *et al.* 2020), although other studies have found conflicting results for instance with abundances of large mammals (Deryabina *et al.* 2015). The apparent flourishing of wildlife in the CEZ has made it an effective wildlife sanctuary, although this is more likely representative of the absence of detrimental human presence than insignificance of radiation effects. At the individual level exposure to environmental radionuclides has been associated for instance with size reduction in brain (Møller *et al.* 2011) and other organs, reduced sperm quality (Møller *et al.* 2014), tumors and albinism (Møller *et al.* 2013), increased parasite load (Morley 2012) and change in gut microbiota composition (Lavrinienko *et al.* 2018). On the molecular level, elevated DNA damage and chromosomal aberrations are a common consequence of IR in both humans and wildlife (Dzyubenko and Gudkov 2009, Bonisoli-Alquati *et al.* 2010, Salnikova *et al.* 2012), with similar effects observed due to accident of Fukushima NPP as well (Hiyama *et al.* 2012, Chen *et al.* 2014). Further effects observed in wildlife in the CEZ include increased oxidative stress (Einor *et al.* 2016), telomere shortening (Kesäniemi *et al.* 2019b) and mitochondrial DNA damage (Kesäniemi *et al.* 2020).

Despite the numerous effects of IR observed in wildlife inhabiting the CEZ, it is surprising that by the start of this thesis project few studies examined molecular effects other than standard DNA damage markers and mutation rates or nucleotide diversity (Lourenço *et al.* 2016). As such, little is known about the effects of radionuclide contamination on metabolism or the genome in a natural setting, and what kind of systemic stress responses organisms subjected to chronic low dose IR utilize in the wild. Radiosensitivity differences between species may be explained by differences in diet, metabolism, or lifestyle. For instance, species utilizing carotenoid- and pheomelanin-based pigments in plumage experience stronger negative effects of IR, as synthesis of these pigments are costly in antioxidants that are also needed to maintain oxidative balance (Einor *et al.* 2016). Alternately, antioxidative potential may be allocated to mitigate impact of IR at the cost of fur coloration (Boratyński *et al.* 2015), which in turn can have ecological costs. Interaction of direct and indirect effects of IR can be exemplified in the bank vole, where abundance loss that correlates IR can be mitigated with food supplementation to a degree (Mappes *et al.* 2019). The bank vole (*Myodes glareolus*) provides an especially intriguing model species to study impacts of environmental radionuclides on a wild population as they carry some of the highest radionuclide loads among wildlife in the CEZ.

1.4   Aims of the study

My aims in this thesis are to characterize genomic and metabolic effects of inhabiting an environment contaminated by radionuclides. I will use a multidisciplinary approach (Table 1) using the bank vole population inhabiting the CEZ as a model to gather data on various biological systems across four studies.

Objective 1: Surveying markers of DNA repair (Study I)

As bank voles inhabiting the CEZ show little to no genetic damage i.e. micronuclei (Rodgers and Baker 2000, Rodgers *et al.* 2001) despite evidence of increased oxidative stress in the form of cataracts (Lehmann *et al.* 2016), I expected upregulation in DNA repair pathways in response to radionuclides. In Study I, I thus quantified impact of chronic environmental IR on gene expression using qPCR in a pilot experiment in five candidate DNA repair–related genes *Atm, Mre11, Brca1, p53* and *p21* in bank vole liver tissue.

Objective 2: Transcriptomics of low dose IR exposure (Study II)

What physiological systems and pathways are affected in response to chronic low-dose IR in a natural environment? While evidence on increased mutation rates in the bank vole is disputable (Baker *et al.* 2017), fibroblasts isolated from bank voles inhabiting the CEZ display increased tolerance to oxidative and genotoxic stresses (Mustonen *et al.* 2018). I hypothesised that bank voles in the CEZ have identified efficient mechanisms to maintain genome integrity in response to chronic stress from radionuclides. Here I mainly used RNA sequencing techniques to examine broad metabolic effects in liver tissue and the immune system in spleen tissue.

Objective 3: Metabolism-microbiota interactions (Study III)

Animals exposed to persistent environmental contamination are commonly characterized by compromised immune system (Acevedo-Whitehouse and Duffus 2009). Also, exposure to radionuclides is known to affect gut microbiota composition in bank voles (Lavrinienko *et al.* 2018) which may affect the amounts of short chain fatty acids (SCFA) produced by the gut microbiota. As SCFA affect gut health and host metabolism (Canfora *et al.* 2015), I investigated whether changes in host metabolism observed in objective 2 are driven by changes in gut health and gut microbiota. I measured several features of rodent health: morphology and gene expression of colon tissue, SCFAs in blood plasma, gut microbiota composition using 16S amplicon sequencing and microbiota-derived metabolites in faecal samples using liquid and gas chromatography.

Objective 4: Genomic tandem repeat copy number variation (Study IV)

Here, I hypothesized that change in rDNA and pericentromere content will be a feature of the genomes of organisms exposed to radionuclides. rDNA has been identified as an environmental sensor with impact on gene expression reminiscent of epigenetic markers e.g. methylation (Bughio and Maggert 2019), but studies placing rDNA copy number variation in ecological context are lacking. Non-coding heterochromatin content has also been suggested to have protective functions against IR (Qiu 2015). I used qPCR to quantify the relative amounts of (1) 18S rDNA and (2) Msat-160 (a pericentromeric satellite sequence) as proxies for heterochromatin content in genomes of bank voles exposed to radionuclides.

2 METHODS

2.1 The bank vole as a model organism

The bank vole (*Myodes glareolus*) (Fig. 3) is a small, burrowing woodland rodent ubiquituous to deciduous and coniferous forests in Europe and northern Asia (Macdonald 2006). The bank vole has an opportunistic diet that mainly consists of forest floor items such as forbs, grasses, invertebrates, berries, lichen and fungi (Calandra *et al.* 2015). The species has a litter size of 2-10 pups and a short period until sexual maturity (ca. 20 days), allowing it to have up to four reproduction cycles per breeding season typically from May to September, depending on latitude (Koivula *et al.* 2003, Mappes and Koskela 2004). Breeding females are highly territorial and have home ranges of ca. 1 km, with males being slightly more mobile (Kozakiewicz *et al.* 2007). Overall, the species has a range expansion rate of 1–5 km per breeding season (White *et al.* 2012). The bank vole's lifespan in the wild is up to 1.5 years, which includes one breeding and one overwintering season (Innes and Millar 1994).

FIGURE 3   The bank vole (*Myodes glareolus*). Photo: Pinja Rautio

The bank vole is one of the first mammals to recolonize the Chernobyl exclusion zone following the 1986 CNPP disaster (Chesser *et al.* 2000) and has since become a central model organism in studying the effects of chronic low-dose IR on a wild animal population. It is commonly occurring in the CEZ and trappable even in highly contaminated areas such as the Red Forest. Its burrowing lifestyle and diet brings it to constant contact to external and ingested radionuclides (Chesser *et al.* 2000), and its territoriality makes it highly likely that individuals are exposed to radionuclides throughout their whole lives in the CEZ, where radiation levels substantially vary along geographical patterns. An estimated 50 generations of bank voles have inhabited the CEZ since the accident (Baker *et al.* 2017).

2.2   Field expeditions and sampling in the Chernobyl exclusion zone

The datasets used in this thesis consist of various bank vole tissues and fecal samples, collected during field seasons in 2015–2017 in the Chernobyl exclusion zone (CEZ) and other locations in Ukraine (Fig. 4). Please see Table 1 for an overview of datasets and methods across the four studies in this project.
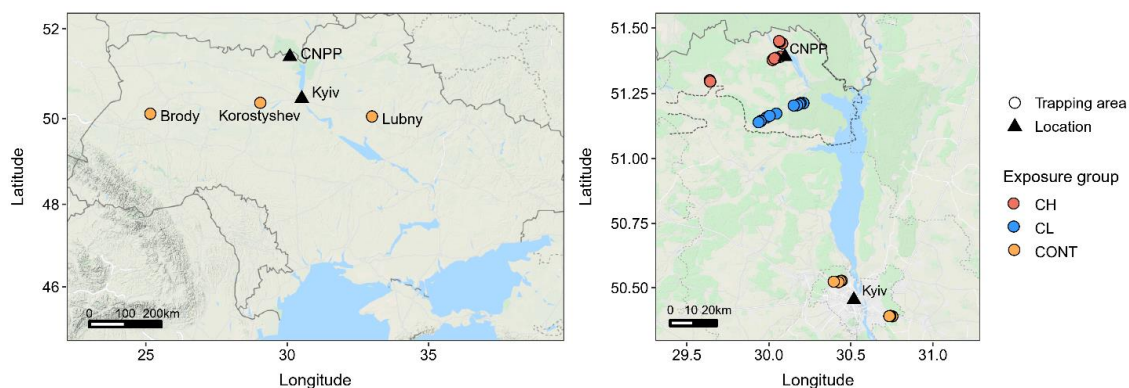
FIGURE 4   Sampling locations in Ukraine and the CEZ (dashed border). CNPP = Chernobyl Nuclear Power Plant. Map data © 2021 Google.

TABLE 1   Sample size, source tissues and main methods used in each subproject.

Study	Sample size	Sources	Methods
I	71	Liver	qPCR (candidate DNA damage response genes)
II	40	Liver, spleen	RNA-seq, stable isotope analysis
III	45	Colon, blood, feces	RNA-seq, tissue histology, liquid & gas chromatography (SCFA quantification), 16S amplicon sequencing (gut microbiota composition)
IV	202	Skin (ear)	qPCR (ribosomal DNA + pericentromeric satellite Msat-160 copy number)

As I targeted wild bank vole populations exposed to radionuclides in this project, I attempted to control for confounding factors by using a study area strategy that includes geographically close areas within the CEZ with differing levels of ambient radiation as well as radionuclide-free control areas outside the CEZ with similar mixed forest habitats, made possible by the heterogenous patterns of radiation levels in the CEZ. Please refer to the individual chapters for details on number and distribution of trapping locations. Ambient radiation was measured at each location by averaging repeated measurements at a height of one cm from the ground, using a handheld Geiger counter (Gamma- Scout GmbH & Co. KG, Germany). Generally, for the purposes of analyses, bank voles were assigned in three exposure groups based on ambient radiation dose rates: CEZ-High (CH, ~4–40 µGy/h, ref), CEZ-Low (CL, near background level dose rate), and control areas outside the CEZ (CONT). This scheme was applied in studies I and IV but limited in studies II and III due to high cost of analyses involved, where only CH and CONT groups were used.

Bank voles were trapped using Ugglan Special2 live traps with potato and sunflower seed bait at several trapping locations that were separated by at least 500 m. Generally, at each trapping location, traps were placed in 3x3 or 4x4 grids with 15-20 m intertrap distance. Traps were set late afternoon and

checked in the next morning over three consecutive trapping nights. In the CEZ, captured bank voles were transferred to a laboratory in the town of Chernobyl for processing and tissue collection within the same day. Bank voles were sexed and measured for length, weight and head width and internal absorbed dose and sacrificed by cervical dislocation. Collected samples included blood, skin, liver, spleen and colon tissues as well as fecal samples (Table 1). In addition, the bank voles' habitats were sampled for putative food items such as fungi, nuts, invertebrates and herbaceous plants to survey for a potential bank vole diet (Study II). Details on procedures and tissues collected are presented in the individual studies.

While ambient radiation in the CEZ can vary at very small scales (down to ~200 m distances, Beresford *et al.* 2020b), external radiation at trapping location has been found to correlate well with external absorbed dose rates in the bank vole (Lavrinienko *et al.* 2020). However, external measurements fail to account for internal absorbed dose, which can comprise a considerable portion of an organism's total absorbed dose rate, depending on diet and overall lifestyle of a species (Beresford *et al.* 2020a, Lavrinienko *et al.* 2021a). In studies II–IV, captured bank voles were measured for internal absorbed dose rate from ^{137}Cs using whole-body gamma spectrometry using a SAM 940 radionuclide identifier system (Berkeley Nucleonics Corporation, San Rafael, CA, USA). Internal dose rates in the bank vole have been found to be consistent over repeated measurements, giving an accurate estimate of total lifetime absorbed doses combined with external dose rates (Lavrinienko *et al.* 2020). For technical details of internal absorbed dose measurements, please refer to supplementary information of studies II and IV.

2.3   Quantification of gene expression

2.3.1 Quantitative PCR

In Study I, I quantified gene expression of five DNA repair genes, *Atm, Mre11, Brca1, p53* and *p21*, in bank voles inhabiting the CEZ. The target genes' mRNA homologs in the prairie vole *Microtus ochrogaster* were aligned to a draft bank vole genome (Genbank accession no. GCA_001305785) using web BLAST (Altschul *et al.* 1990). Primer3 web (Untergasser *et al.* 2012) was then used to design primers on resulting alignments. Total RNA was extracted from liver tissue of bank voles exposed to radionuclides using RNeasy Mini Kit (Qiagen) according to manufacturer's protocol, followed by reverse transcription into cDNA using iScript cDNA Synthesis Kit (Bio-Rad). Quantitative PCRs were conducted on the LightCycler 480 platform (Roche) using SYBR Green I Master chemistry (Roche).

2.3.2 RNA sequencing

In studies II and III, I used high-throughput RNA sequencing (Wang *et al.* 2009, Stark *et al.* 2019) that provides a comprehensive approach to gene expression. Total RNA was isolated from liver and spleen tissues of 40 female bank voles (Study II) and distal colonic tissue of 44 female bank voles (Study III) exposed to radionuclides using RNeasy Mini Kit (Qiagen) according to manufacturer's protocol. RNA samples were sent to Beijing Genomics Institute (BGI) Hong Kong (www.bgi.com/global/) for library preparation and sequencing. mRNA-focused sequencing libraries were prepared with TruSeq RNA Library Prep Kit (Illumina) and sequenced for 100bp paired-end (PE) reads on Illumina HiSeq4000 platform (BGI Hong Kong) resulting in sequencing depth of ~16 million PE reads per sample library.

2.4   Stable isotope analysis

In Study II, I used stable isotope analysis (SIA) to analyze variation in bank vole diet. Foods differ in their isotopic composition, and thus analysis of isotope profiles of nitrogen and carbon in animal tissue can provide information on routine diet when compared to a background of isotope profiles of putative food items from the animal's habitat (Baltensperger *et al.* 2015). Due to isotope fractionation and metabolic differences in macronutrient routing, ^{15}N tends to become enriched in animals consuming a protein-rich diet, thus ratio of ^{15}N/^{14}N (δ^{15}N) informs of an animal's trophic level. Ratio of ^{13}C/^{12}C (δ^{13}C) informs mainly of plant diversity in diet, although factors of ^{13}C enrichment are diverse and not entirely known. Isotope turnover rate differs according to tissue. For instance, fur retains signal from diet in rodents for several months (Kurle *et al.* 2014). Here, δ^{15}N and δ^{13}C isotope profiles were analyzed from fur samples of 40 bank voles used in Study II. Briefly, dried fur samples were analysed for stable isotopes of carbon and nitrogen using a Thermo Finnigan DELTAplus Advantage CF-IRMS connected to a Carlo Erba Flash EA1112 elemental analyser. Dried pike (*Esox lucius* L.) white muscle was used as an internal working standard for the fur samples. For details on methods, please refer to appendix S1 of Study II.

2.5   Colon tissue histology

In Study III, I performed histological analyses to investigate health and condition of colon epithelium in bank voles exposed to radionuclides. Colon tissue samples were fixed in 10% formalin solution and in metha-Carnoy solution (60% methanol, 30% chloroform, 10% glacial acetic acid). After fixation, the samples were dehydrated, embedded in paraffin with a vertical orientation and cut into 5 μm thick sections. Tissue sections fixed in 10% formalin solution were

stained with hematoxylin and eosin (H&E), a gold standard method for inspection of general tissue condition, and tissue sections fixed in metha-Carnoy solution were stained with alcian blue with carmine as counterstain for visualization of mucus-secreting goblet cells in the colon epithelium (Suvarna *et al.* 2013). For details on staining protocol please see Study III. For the morphometrical analysis, the digital microphotographs of stained colon sections were taken at a magnification of ×100 or ×400 using a computer-assisted image analyzing system consisting of Olympus BX41 microscope and Olympus C-5050 Zoom digital camera. Crypt depth (µm), colonocyte height (µm), colonocyte nucleus cross-sectional area (µm2) and goblet cell cross-sectional area (µm2) were measured using Image J v1.42q software. Samples were assigned a colonic goblet cell state classification (normal, hypo- or hypertrophic) based on goblet cell size and amount of mucus-containing vesicles.

2.6   Quantification of short chain fatty acids

To determine the gut microbiota's effect on host metabolism (Study III), concentrations of short-chain fatty acids (SCFAs) were quantified in both fecal matter and blood in bank voles exposed to radionuclides. Fecal and blood samples were sent to Division of Food and Nutrition Science in Chalmers University of Technology, Sweden, for SCFA quantification. In feces, concentrations of seven SCFAs, acetic, propionic, isobutyric, butyric, isovaleric, valeric and caproic acids were analyzed using a GCMS-TQ8030 gas chromatography–mass spectrometry system (Shimadzu) according to (Cheng *et al.* 2020). In blood, concentrations of nine SCFAs, formic, acetic, propionic, isobutyric, butyric, succinic, isovaleric, valeric and caproic acids were analyzed by Triple Quad 6500+ LC-MS/MS System (SCIEX) according to (Han *et al.* 2015). Detailed descriptions of methods can be found in Study III.

2.7   Gut microbiome sequencing

Composition of the gut microbiota in bank voles inhabiting the CEZ and near Kyiv (Study III) was determined using thigh-throughput amplicon sequencing of the V4 region of the 16S ribosomal RNA (rRNA) locus. Briefly, DNA was isolated from fecal samples using PowerFecal DNA Isolation kit (Qiagen) according to manufacturer's protocol. DNA was sent to BGI Hong Kong for library preparation following the Earth Microbiome Project protocol (www.earthmicrobiome.org/protocols-and-standards/) and sequencing on an Illumina HiSeq 2500 platform to provide 250 bp paired end reads.

2.8 Quantification of ribosomal DNA and pericentromeric satellite copy number

In Study IV, I measured relative copy number of two tandemly repeated loci, ribosomal 18S DNA and a pericentromeric satellite Msat-160 in bank voles exposed to radionuclides using qPCR. DNA was extracted from ear tissue samples using DNeasy Blood Tissue Kit (Qiagen), following manufacturer's protocol. rDNA and Msat-160 sequences were identified in bank vole draft genome (Genbank GCA_001305785) by BLAST alignments 18S rDNA (GenBank NR_003278.3) and Msat-160 (GenBank FN859393) homologues in mouse (*Mus musculus*) and Eurasian water vole (*Arvicola amphibius*), respectively. Aligned sequences were used to design primers in Primer3 web. Quantitative PCRs were conducted on the LightCycler 480 platform (Roche) using SYBR Green I Master chemistry (Roche), using gene *36b4* as single-copy control (Cawthon 2002). Raw quantification cycle (Cq) data were corrected for PCR efficiency (E) and transformed into relative values using the Pfaffl method (Pfaffl 2001). See Study IV for details.

2.9 Bioinformatics

2.9.1 Transcriptomics

Two transcriptome assemblies, a combined liver and spleen assembly (Study II) and a colon tissue assembly (Study III) were assembled from read data generated by RNA sequencing (section 2.3.1) using *de novo* transcriptome assembler Trinity (Grabherr *et al.* 2011). The assemblies were annotated using Trinotate annotation pipeline (Bryant *et al.* 2017). Subsequent mapping, transcript count estimation, quality checking and statistical analysis steps were performed according to the extended Trinity transcriptomics pipeline (github.com/trinityrnaseq/trinityrnaseq/wiki) (Haas *et al.* 2013) using default settings unless stated otherwise. Transcriptome completeness was estimated using BUSCO (Simão *et al.* 2015), which scans the assembly for the presence of near-universal single-copy orthologs (BUSCOs) and relating the number of identified BUSCOs to a database of related species, in this case, the mammalian BUSCO database. Transcriptomes were annotated using Trinotate automated annotation pipeline (Bryant *et al.* 2017). Reads from all individual samples were mapped to the transcriptomes using Bowtie (Langmead *et al.* 2009), and read counts were estimated on both transcript and gene level using RSEM (Li and Dewey 2011), producing expression tables to be used in statistical testing. Please refer to Studies II and III for further details on analysis pipeline and software.

2.9.2 Gut microbiomics

Read data were de-multiplexed, and adapters and primers were removed by BGI. The paired end sequences were processed using qiime2 (Bolyen *et al.* 2019) analysis platform. Briefly, reads were truncated at the 3′ end to remove low-quality bases, after which data were denoised using default parameters in dada2 (Callahan *et al.* 2016) to produce the amplicon sequence variant (ASV) table. Taxonomies were assigned using a naïve Bayes classifier, pretrained on the Greengenes version 13_8 16S rRNA gene sequences (Bokulich *et al.* 2018). Please refer to Study III for details.

2.10 Statistical analyses

The studies in this project utilize generalized linear and mixed models as well as nonparametric tests in R (The R Core Team 2018) to examine differences in various variables such as organ sizes, body condition index (= standardized residuals from linear model of weight and head width, Labocha *et al.* 2014) and genes of interest either among exposure groups or using total absorbed dose rate as a continuous variable. Detailed information about methods as well as relevant R packages can be found in the individual thesis chapters.

This project utilizes large datasets produced by high-throughput sequencing methods i.e., RNA sequencing data of bank vole tissues (Studies II and III) and 16S rRNA amplicon sequencing data of bank vole gut microbiome (Study III). Due to the large amount of data generated, these datasets were analyzed in an exploratory manner using best practice guidelines (Conesa *et al.* 2016, Bryant *et al.* 2017, Knight *et al.* 2018). Briefly, transcript count data was first examined using principal component analysis (PCA) to explore and visualize sample clustering patterns based on similarities in gene expression. The sample scores on principal components representing treatment-related clustering were further used in hypothesis-based tests, for example to examine the effect of IR and other factors such as colon goblet cell state (Study III) on gene expression. Specific differentially expressed genes between exposure groups CH and CONT were identified using 'DESeq2' (Love *et al.* 2014) in R. Finally, to examine functional differences in gene expression between exposure groups, gene ontology (GO) term enrichment analysis using R package 'GOSeq' (Young *et al.* 2016) was used. GO terms are hierarchical identifiers assigned to genes that describe gene functions and related metabolic pathways. GO term enrichment analysis identifies commonly occurring (significantly enriched) GO terms among differentially expressed genes, providing an overview of biological pathways affected by treatment.

Analyses of microbial communities (microbiota) were performed using tools in the Qiime2 platform (Bolyen *et al.* 2019) in three categories: 1) within-sample diversity, or *alpha diversity*, measured in species richness (number of ASVs) and evenness (Shannon index), 2) population-wide structure in abun-

dance and composition of taxa, *beta diversity*, measured in metrics of dissimilarity (Bray-Curtis) and phylogenetic distances (UniFrac, Lozupone *et al.* 2007), and 3) differential abundance of ASVs or agglomerated taxonomical groups between samples. Beta diversity matrices were further reduced using principal coordinates analysis (PCoA) to visualize sample clustering patterns. Permutational analysis of variance (PERMANOVA) in R package 'vegan' (Oksanen *et al.* 2018) was used to examine amount of variance in beta diversity explained by exposure group, total received dose rate and goblet cell state.

3   MAIN RESULTS AND DISCUSSION

3.1   Overview of the results

In this thesis, I examine the metabolic and genomic effects of chronic exposure to radionuclide contamination in a bank vole population inhabiting the Chernobyl Exclusion Zone, producing four manuscripts. An overview of the main results and conclusions in each study is presented in Table 2. In this section I summarize and discuss the main results discovered in this project.

TABLE 2   Main results and conclusions from each subproject.

Study	Main results	Conclusions
I	Bank voles inhabiting the CEZ exhibit upregulation of *Atm, Mre11*	Bank voles inhabiting the CEZ experience oxidative stress.
II	Upregulation of hepatic FAO, immuno-suppression with evidence of inflammation, increase in dietary ^{15}N	Metabolic shift towards FAO may act as a systemic response towards chronic low dose IR. Evidence of chronic stress reducing immunocompetence.
III	Weakened colonic mucus layer, radiation-associated reduction in circulating propionate, butyrate and formate	Stress-related poor health of bank vole gut. Radiation likely impacts host metabolism directly instead of gut microbiota-related changes.
IV	Increase in copy number of rDNA and pericentromeric satellite Msat-160	Highly localized patterns of CN variation on studied loci. Evidence supports heterochromatin safeguard hypothesis.

3.2 Bank voles inhabiting the CEZ are characterized by a metabolic shift towards fatty acid oxidation

3.2.1 Gene expression profile implies persistent oxidative stress and metabolic shift in primary metabolism (Studies I and II)

In Study I, I found significant upregulation in two genes, *Atm* and *Mre11* among bank voles inhabiting the CEZ (Study I: Fig. 2). *Atm* is an upstream signaling protein that is activated by DNA double-strand breaks and increased cellular oxidative stress, and regulates multiple pathways related to genomic stability, including initiation of DNA repair functions and regulation of oxidative balance (Guo *et al.* 2010, Cosentino *et al.* 2011). *Mre11* is a constituent protein of the MRN complex, which has multiple functions in DNA damage sensing, repair, genome maintenance and telomere homeostasis (Lee and Paull 2007, Lamarche *et al.* 2010, Deng *et al.* 2011). With no observed change in *Brca1*, *p53* and *p21* expression, and the measured radiation levels being generally insufficient to induce DNA double-strand breaks, it suggested that upregulation of *Atm* and *Mre11* in bank voles in the CEZ was mainly indicative of oxidative stress response without gross genomic damage. These findings were concomitant with results on increased cellular resistance to oxidative stress (Mustonen *et al.* 2018) and altered telomere homeostasis (Kesäniemi *et al.* 2019b) from concurrent studies.

Contrary to expectations from Study I, in Study II, I did not observe upregulation in enzymatic pathways regulating oxidative balance such as oxidoreductases that are typically used as markers of oxidative stress. Instead, the stress response appears to be focused on the endoplasmic reticulum and mitochondria via upregulation of *Atf5*, *Slc25a27* and *Pycr1* (Study II: Table 2). Also, I found upregulation in synthesis and metabolism of scavenger molecules such as haptoglobin and vitamins B5, A and C. As a novel observation, bank voles inhabiting the CEZ appear to have emphasized fatty acid oxidation (FAO) as evidenced by enrichment of GO terms such as fatty acid beta-oxidation and lipid catabolic process (Fig. 5), upregulation of key FAO-promoting genes such as *Cpt1a* and *Fgf21* as well as glycolysis-inhibiting gene *Pdk4* (Fig. 6). These results indicate a shift in primary metabolism, which may act as a system-wide coping mechanism against persistent oxidative stress (Martínez *et al.* 2013).

Normally, FAO is associated with fasting, starvation or a high-fat diet in human and rodent models (Kersten 2014), which is striking as the studied voles did not display reduced body condition. However, the FAO-emphasizing phenotype is also associated with a 'preserving' mode of metabolism with links to improved oxidative balance and genomic stability, possibly by association with NAD+ and sirtuins (Poljsak and Milisav 2016, Mei *et al.* 2016) as opposed to cellular growth–emphasizing energy pathways (Yuan *et al.* 2013). That FAO is associated with stability and maintenance is exhibited by increased lifespan in rodents under caloric restriction (Heydari *et al.* 2007). To determine whether bank

vole diet factored in the observed metabolic changes, I conducted stable isotope analysis (SIA). I observed a higher $\delta 15N$ value in bank voles inhabiting the CEZ compared to control, suggesting that the voles inhabiting the CEZ are placed on a higher trophic level (Study II: Fig. 4). Combined with shift in gut microbiota composition (Lavrinienko *et al.* 2018) this suggested a possible diet-based origin with increased animal protein sources for the apparent shift in metabolism, although previous studies have shown decrease in invertebrate abundance in the CEZ (Møller and Mousseau 2018). Alternatively, shift in trophic level can also be caused by self-digestion from starvation (Petzke *et al.* 2010), although the bank voles inhabiting the CEZ did not exhibit reduced body condition index. Regardless, these findings on metabolic shift were particularly interesting, as prior to this experiment change in lipid metabolism in response to IR had been described only in Atlantic salmon and at much high dose rates than encountered in the CEZ (Song *et al.* 2016). A FAO-emphasizing metabolic phenotype may offer advantages in an environment characterized by chronic low dose IR due to its association with genomic stability.

3.2.2 Possible role of mitochondria in response to chronic low dose ionizing radiation (Studies II and III)

Several findings from this project (Studies II and III) as well as further evidence from a later study examining protein-level signals of metabolic shift (Kesäniemi et al. in preparation) point toward mitochondrial function being affected by radionuclide contamination, either directly causing or otherwise reflecting the signals of metabolic rewiring.

Mitochondrial myopathies are neuromuscular diseases caused by damaged mitochondria, and are known to induce a FAO-emphasizing phenotype that is mediated by AKT signaling and secretion of FGF21 in skeletal muscle (Tyynismaa *et al.* 2010, Forsström *et al.* 2019). Bank voles inhabiting the CEZ show some signals of this, i.e. upregulation in transcription of *Fgf21* and stress response factor *Atf5* in the liver (Study II), increased damage in mitochondrial DNA (mtDNA) (Kesäniemi *et al.* 2020), and increased protein-level expression of FGF21 in skeletal muscle (Kesäniemi et al. in preparation), implying that mitochondria of bank voles exposed to radionuclides experience oxidative stress. Furthermore, bank voles inhabiting the CEZ exhibit increased formate concentration in blood plasma (Study III). Formate acts as a pool of methyl groups in one carbon metabolism, which is largely controlled by mitochondrial function (Pietzke *et al.* 2019). Indeed, the liver gene expression profile shows enrichment of GO terms for one carbon metabolism (Fig. 5). Also, Kesäniemi et al. (in preparation) found consistent dephosphorylation of AKT in several tissues in bank voles inhabiting the CEZ. Dephosphorylation of AKT promotes the metabolic mode of catabolism and cell survival as opposed to anabolic pathways and cell growth and division (Manning and Toker 2017), which together with FAO-promoting gene expression profile in the liver and expression of systemic FGF21 provides a strong case for metabolic rewiring in bank voles exposed to radionuclides.

Ultimately, these results are correlative across several studies utilizing captured wild animals, and thus some inconsistencies cannot be explained. For instance, mitochondrial dysfunction should not result in increased formate production. Interestingly, change in mitochondrial function and fatty acid metabolism are implicated in response to effects of spaceflight (da Silveira *et al.* 2020). This suggests a crucial role for mitochondrial homeostasis in relation to radiation exposure and thus offering intriguing new areas for future research.

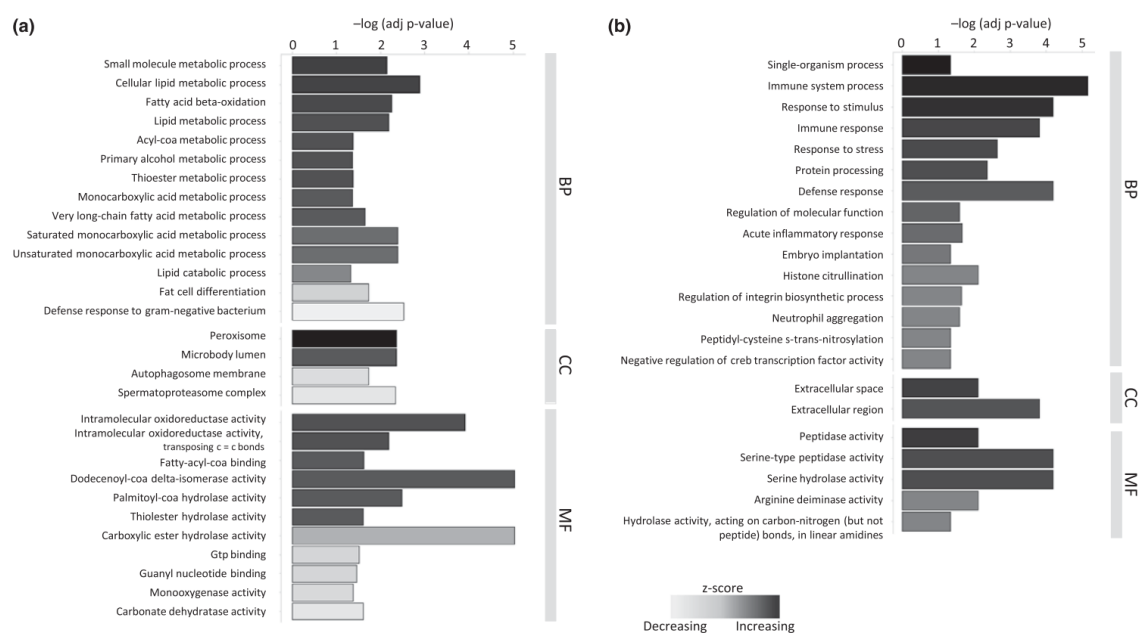FIGURE 5   Summarized list of significantly enriched GO terms (FDR < 0.05) among DEGs between uncontaminated Kyiv control and CEZ populations for (a) liver and (b) spleen. GO terms are ordered by category. BP: biological pathway, CC: cell compartment, MF: molecular function and by Z-score, which indicates the general direction of expression difference of a group of genes containing a given GO term (Study II).
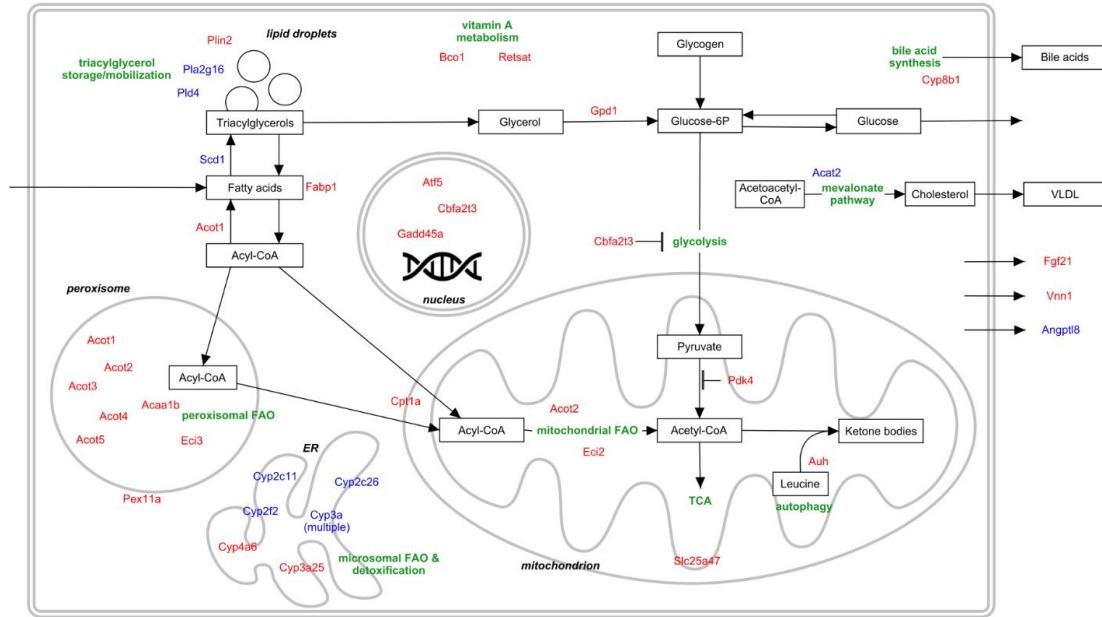
FIGURE 6   Overview of affected liver metabolic pathways between uncontaminated control and CEZ populations of bank voles based on gene expression data from Study II. Gene names in red colour indicate upregulation and blue colour downregulation in bank voles of the CEZ compared to control voles. ER: endoplasmic reticulum, FAO: fatty acid oxidation, VLDL: very-low-density lipoprotein (Study II).

3.3 Gene expression and gut tissue histology implies immunosuppression (Studies II and III)

RNA sequencing and differential expression analysis conducted in Study II revealed enriched GO terms relating to immune system function in bank voles inhabiting the CEZ (Fig. 5), with specific DEGs indicating immunosuppression in the liver (e.g. downregulation of immunoproteasome subunits and parts of the JAK-STAT signaling pathway, Study II: Table 2) as well as activation of innate immunity via granulocytes in the spleen (e.g. upregulation of proinflammatory mediators such as *Cma1* and *Lox5*, Study II: Table 2). Moreover, in Study III, upregulated transcripts in colon tissue of bank vole exposed to radionuclides contained several enriched GO terms relating to immune system signaling (Study III: Table S8), although noise in the data prevented meaningful examination of details.

Relation between the immune system and IR is complex (Di Maggio *et al.* 2015, Frey *et al.* 2015), however, the observed immunosuppressive effects parallel known impacts of chronic stress on immune system. As part of stress response, glucocorticoids (stress hormones) typically suppress the immune system for a short-term boost in performance to deal with an immediate stressor. A prolonged stress reaction however can be detrimental to long-term immunocompetence and increase vulnerability to pathogen infection (Acevedo-

Whitehouse and Duffus 2009), signs of which are exhibited by bank voles inhabiting the CEZ with upregulation of genes related to granulocyte function. Indeed, small mammals in the CEZ, including bank voles, show higher loads of protozoan parasites (Morley 2012) and helminth infections (Sazykina and Kryshev 2006), although viral load in bank voles does not show relationship with environmental radiation (Kesäniemi *et al.* 2019c). These changes in immune system along with upregulation in certain stress response and cell cycle inhibiting genes *Atf5* and *Gadd45a* provide additional evidence of an ongoing stress response to low dose IR even after 50 generations of inhabitation of an environment contaminated by radionuclides. This observation is notable due to both the control populations' proximity to a metropolis and lack of human presence in the CEZ, as human presence in general forms a major stress factor to wildlife (Acevedo-Whitehouse and Duffus 2009).

In Study III, I did not observe visual cues of pathological damage or inflammation such as edema or structural disturbance of the epithelium by visual examination of colon tissue cuts, which was surprising considering the upregulation of proinflammatory factors in spleen. Instead, bank voles from the CEZ exhibited hypotrophic goblet cells with a smaller area and reduced amount of mucus bodies at a risk ratio of 5.8 (95% confidence interval of 1.34-25.17) compared to control (Fig. 7). Also, the hypotrophic cell condition was correlated with downregulation of *Clca1* and *Agr2* (Study III: Fig. 6), genes that are involved in secretion and formation of the outer mucus layer (Park *et al.* 2009, Nyström *et al.* 2018). Goblet cells of the colonic epithelium produce and secrete the mucus layer which functions as an important barrier against pathogens (Birchenough *et al.* 2015). The observed reduction in mucus production may present an increased risk of infection, signs of which were observed in gene expression data from liver and spleen tissue in Study II as activation of granulocytes in the spleen. While the reason for goblet cell hypotrophy remains unknown, bank voles inhabiting the CEZ were also associated with increased abundance of Bacteroidetes family *Muribaculaceae*, with concomitant decrease in Firmicute families *Ruminococcaceae* and *Lachnospiraceae* (Study III: Fig. 10B). These three families have been found to be sensitive to radiation in other studies as well (Lavrinienko *et al.* 2020, 2021a, Antwis *et al.* 2021), possibly in a way that interacts with season. While *Ruminococcaceae* and *Lachnospiraceae* are known to contain several mucus layer inhabiting members, further research is needed to identify exact radiosensitive species and their interactions with the mucus layer.
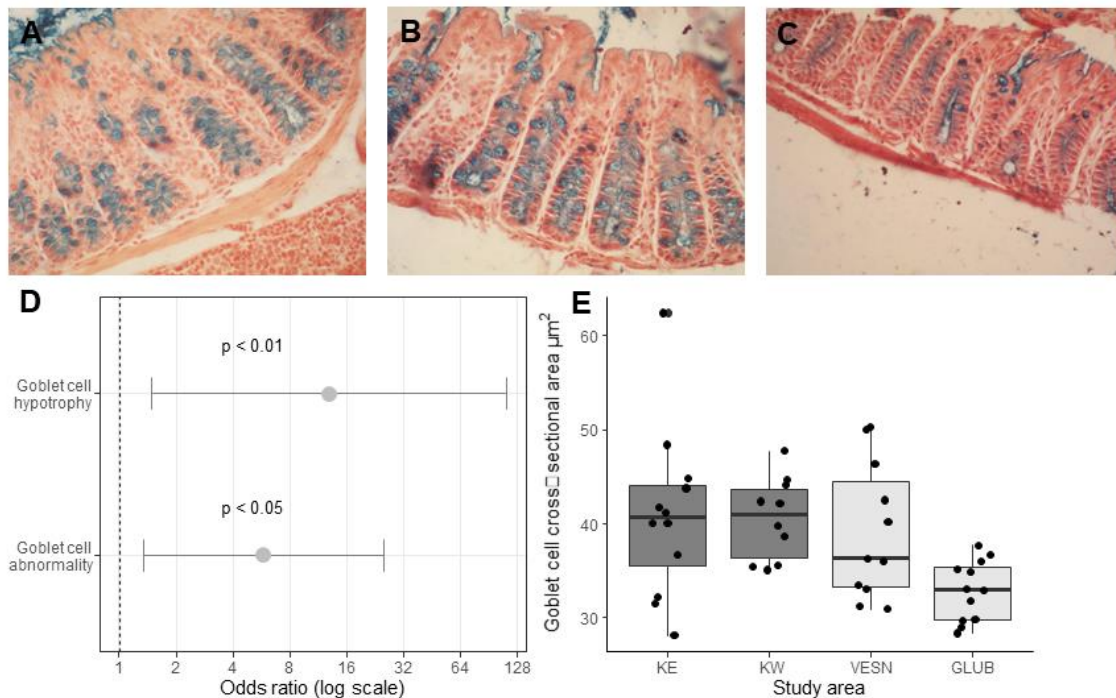
FIGURE 7   A) normal, B) hyper- and C) hypotrophic colonic mucous goblet cells (alcian blue with carmine supplementation, × 400). Mucin bodies (in blue) appear smaller and fewer in number in hypotrophic goblet cells than normal. D) Odds ratio of bank voles exposed to radionuclides exhibiting goblet cell hypotrophy and abnormality (hyper+hypotrophic cells). E) Goblet cell cross-sectional area across study areas (Study III).

3.4 Radiation impacts host metabolism directly rather than through microbiota-mediated changes (Study III)

While I observed radiation-associated reduction in concentrations of circulating propionate and butyrate, fecal concentrations of the three major fecal SCFAs (acetate, propionate and butyrate) were more representative of individual study areas rather than radiation (Study III: Fig. 7). A portion of SCFAs is absorbed from the gut into the portal vein, through which they are transported to the liver and then to peripheral circulation. Circulating SCFAs better represent host metabolism than fecal SCFAs, as the colonic concentration of SCFAs is subject to many factors such as time of day, host absorption rate and microbiota composition (Boets *et al.* 2017, Müller *et al.* 2019). Here, radiation appears to directly impact uptake, regulation by the liver or usage by peripheral tissues of propionate and butyrate. SCFAs affect gene expression in liver and peripheral tissues mainly by acting as signaling molecules for G protein coupled receptors and by histone acetylase inhibition, typically increasing fatty acid oxidation and reducing inflammation (Liu *et al.* 2018, Müller *et al.* 2019). While reduction in circulating SCFAs appears to conflict with observed upregulation of FAO (Study II), butyrate has previously shown paradoxical effects on metabolism depending

on tissue condition (Liu *et al.* 2018, van der Hee and Wells 2021), highlighting the need for further research on metabolic effects of SCFAs.

3.5 Genomic architecture as a responsive element to environmental contamination (Study IV)

Here, I observed increase in mean copy number of both rDNA and Msat-160 repeats among bank voles inhabiting contaminated areas of the CEZ (Fig. 8). Copy number increase in contaminated areas was significantly higher than in noncontaminated areas within the CEZ, revealing capability for copy number variation (CNV) in heterochromatic repeats over a fine geographic scale. Both rDNA and Msat-160 may contribute to genomic stability as part of heterochromatin by physically surrounding and protecting the more vulnerable, actively transcribed genomic regions in the nucleolar center (Geyer *et al.* 2011, Qiu 2015). In addition, rDNA CNV is known to have multiple associations with genomic stability (Ide *et al.* 2010, Paredes *et al.* 2011, Kobayashi 2011, 2014, Saka *et al.* 2013, Gibbons *et al.* 2014, Xu *et al.* 2017, Kobayashi and Sasaki 2017). As such, increased copy number in rDNA and Msat-160 may provide a fitness advantage against IR in the CEZ, either through selection from standing CNV in the population or by inducing copy number maintaining mechanisms during developmental phase.

Another important finding of this study was a positive correlation between rDNA and Msat-160 CN among bank voles in noncontaminated areas both within and outside the CEZ, which however was not observed among bank voles exposed to radionuclides (Study IV: Table 3). It is notable that loss of correlation between various processes is a common observation among bank voles inhabiting the CEZ, as with the weakening of gene co-expression networks (Study II), lack of relationship between mtDNA CN and expression of mitochondrial synthesis–modulating gene PCG1α (Kesäniemi *et al.* 2020) and lack of correlation in telomere content between tissues (Kesäniemi *et al.* 2019b), suggesting that chronic radiation stress disrupts a putative mechanism that normally maintains typical genome architecture.
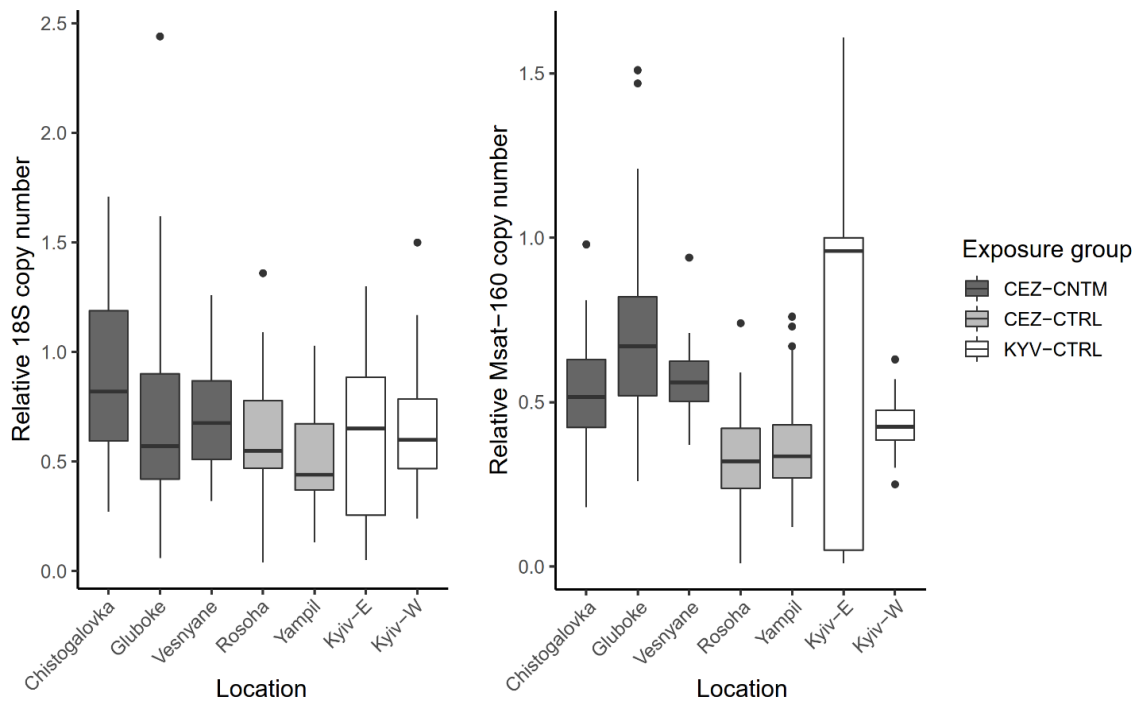
FIGURE 8   Relative rDNA and Msat-160 copy numbers (Study IV).

4 CONCLUSIONS AND FUTURE DIRECTIONS

These results provide a wealth of new information on how inhabitation of environments contaminated by radionuclides and the resultant chronic exposure to low dose IR both internally and externally affect wildlife on a molecular level. The apparent immunosuppression and upregulation of stress response genes such as *Atf5* inform of an ongoing stress response. One of the definitions of stress is the failure to control a fitness-critical variable (Del Giudice *et al.* 2018). Indeed, breeding success is reduced in bank voles in the CEZ along a radiation gradient (Mappes *et al.* 2019).

Stress responses are regulated by complex, interconnected signaling networks, and thus a repeated failure to control homeostasis caused by chronic stress can result in various harmful effects that at first glance do not appear to be connected (Del Giudice *et al.* 2018), as exemplified by the extremely complex pathophysiology of metabolic syndrome in humans (Rochlani *et al.* 2017). Here, observations that may reflect a loss of regulative function caused by lifelong (including development) habitation of LDIR environment include the weakening of gene co-expression networks (Study II), high interindividual variation in various host parameters and gut microbiota among CEZ samples compared to control (Study III), the lack of relationship between mtDNA CN and expression of mitochondrial synthesis–modulating gene PCG1α (Kesäniemi *et al.* 2020), and lack of correlation in telomerase expression and telomere content between tissues (Kesäniemi *et al.* 2019b). In community microbiology, the instabilization of gut community composition due to failure to control homeostasis has been dubbed Anna Karenina principle, following the quote by Leo Tolstoy: "All happy families are alike, each unhappy family is unhappy in its own way" (Zaneveld *et al.* 2017). Here, the stress-related "failure to control" may be central in understanding several observations in this thesis as well as other studies investigating bank voles of the CEZ.

The expression of the FAO-emphasizing phenotype in bank voles exposed to radionuclides is a novel observation, which had previously been observed only in a controlled experiment with the Atlantic salmon (*Salmo salar*) (Song *et al.* 2016), and later, as an effect of spaceflight in humans and mice (da Silveira *et al.* 2020). One of the most important questions raised by these results is whether

the observed metabolic shift is adaptive given its potentially beneficial health effects, or a sign of a low-dose IR related radiation syndrome given the similarity to symptoms of mitochondrial myopathy (Forsström *et al.* 2019). Accordingly, protein level expression of FGF21 should be examined as a potential new marker for low dose IR stress. Future research on effects of radiation on circulating SCFAs should also incorporate temporal sampling as well as sampling from the portal vein for a more accurate representation of SCFA influx from the gut. Research focusing on fatty acid metabolism and mitochondrial function as a response to low-dose IR should be of great interest in the future, given that radiation dose rates in space are similar to the CEZ (Blue *et al.* 2019), and that interest in space development and exploration is increasing in the private sector (Weinzierl 2018).

With the recent construction of enclosures in the CEZ in collaboration with Taras Shevchenko National University of Kyiv, reciprocal transplant experiments can be conducted to unravel the genetic basis of phenotypes from developmental plastic effects. While there is some evidence of adaptation as shown by fibroblasts extracted from bank voles exposed to radionuclides being more viable under stress *in vitro* (Mustonen *et al.* 2018), experiments investigating local adaptation in the CEZ are still scarce. Recently, reciprocal transplant experiments have been used to great effect in conjunction with modern genomic methods such as SNP calling and RNA sequencing (Leinonen *et al.* 2013, Lovell *et al.* 2016, Gould *et al.* 2018). Here, for instance, gene expression data can be examined for number and habitat specificity of differentially expressed genes or transcripts, as divergence in regulatory elements typically manifests as a specific response to "home conditions" in locally adapted populations. If evidence of local adaptation is found, further information on *cis-* and *trans*-acting regulatory variation can be obtained from allele specific expression analysis (ASE), which incorporates parental genotypes with gene expression data (Lovell *et al.* 2016). Challenges include intensive labor of handling mammals and cost of sequencing to secure the depth necessary for investigation of isoform-specific expression.

Study IV of this thesis provides much needed new data on local rDNA CN variation in animals and encourages further research on rDNA dynamics in evolution, for instance by using selection line experiments. Study of rDNA in mammals as opposed to e.g., yeast or *Drosophila* however presents major challenges: 1) large inherent variation in rDNA CN requires large sample numbers to resolve, a problem which is 2) exacerbated by generation time and workload required to rear rodents. Moreover, 3) the molecular characteristics of the rDNA locus (e.g., nonviability of rDNA knockouts and large proportion of transcriptionally silent copies) makes rDNA difficult to manipulate and to make direct correlations between copy number and phenotypic characteristics. Fortunately, as rDNA CN is a feature of genomic DNA it can be easily quantified using qPCR or ddPCR at low cost and interested investigators may already have samples of various taxa available from past sampling expeditions and selection line projects as frozen tissue or isolated DNA.

Acknowledgements

So many different people have contributed to this work that at times it became incredibly difficult to use the first-person pronoun while writing this thesis. In fact, my editor told me to go back and fix the language by removing the "we"-words I somehow unconsciously ended up using. I am enormously thankful for all my co-workers and friends for their support over the years.

First, I am grateful to Prof. Heidi Hauffe for agreeing to be my honourable opponent, Prof. Andrea Bonisoli-Alquati and Miia Rainio for review of my thesis, and Jari Haimi for your help in editing and finalizing.

I would like to thank the Finnish Cultural Foundation, University of Oulu, University of Jyväskylä and the Finnish Centre for Scientific Computing (CSC) for providing the funding and resources to make this research possible. Thank you Soile Alatalo, Sari Viinikainen and Elina Virtanen for the best technical support in the laboratory and keeping my wetwork (and me) in one piece! Thank you to international collaborators and fixers for making work in the Zone possible. Special thanks go to Maksym Ivanenko, Igor Chizhevsky, Gennadi Milinevsky, Timothy A. Mousseau and Anders P. Møller.

I would like to thank my supervisor Phillip Watts for introducing me to this hugely interesting topic and supporting me from all the way from the time I caught you during a post-seminar coffee break to this moment. You have been there for every step of the way and your dedication to your students, including me has been inspiring. A big thank you to my second supervisor Jenni Kesäniemi as well. While Phill's torrents of new ideas during group meetings felt overwhelming at times, your stoic mindset and dark coffee break humour has been helpful with keeping things focused.

The vole lab group has provided an incredible work environment both for interesting discussions and for fun bar nights and outings! Thanks Anton, I have found a colleague and a friend in you that I hope lasts for a long time to come. Thank you Ilze for bringing much needed party mentality to the group! It was just in time – by the time you joined Anton was becoming too affected by Jenni's and my Finnish gloom. Thank you Anni, Eugene, Tiffany, Yinying, Lucy, Nosheen, Tapio, Esa, Kikka and all the rest!

Thanks to the university and PhD student communities, both in Oulu and Jyväskylä, for all the peer support over the years. Special thanks to the Sauna and Support Group for bringing in much needed motivation during the worst stretch of Covid-19, and to Emily Knott for all the help with surviving University bureaucracy!

Special thanks to my high school biology teacher Esa Härmä, for making biology cool! I might have become a chemist otherwise.

Most of my family in the generation above me are teachers of various sorts, no doubt due to influence of a very special woman. I am enormously thankful to my late grandmother for cultivating my curiosity over how earthly things work, together with my father and aunt Ira. I was still finishing my masters when we had our last meeting, where you said you were so proud of me

for choosing this path. Well, the one who set me on this path was you, and I am now proud to say I that made it, as promised.

REFERENCES

Acevedo-Whitehouse K. & Duffus A.L.J. 2009. Effects of environmental change on wildlife health. *Philos. Trans. R. Soc. B Biol. Sci.* 364: 3429–3438.

Alberdi A., Aizpurua O., Bohmann K., Zepeda-Mendoza M.L. & Gilbert M.T.P. 2016. Do Vertebrate Gut Metagenomes Confer Rapid Ecological Adaptation? *Trends Ecol. Evol.* 31: 689–699.

Alberti M., Correa C., Marzluff J.M., Hendry A.P., Palkovacs E.P., Gotanda K.M., Hunt V.M., Apgar T.M. & Zhou Y. 2017. Global urban signatures of phenotypic change in animal and plant populations. *Proc. Natl. Acad. Sci. U. S. A.* 114: 8951–8956.

Aldrich J.C. & Maggert K.A. 2015. Transgenerational Inheritance of Diet-Induced Genome Rearrangements in Drosophila. *PLoS Genet.* 11: 1–21.

Altschul S.F., Gish W., Miller W., Myers E.W. & Lipman D.J. 1990. Basic local alignment search tool. *J. Mol. Biol.* 215: 403–410.

Amato K.R., Yeoman C.J., Kent A., Righini N., Carbonero F., Estrada A., Rex Gaskins H., Stumpf R.M., Yildirim S., Torralba M., Gillis M., Wilson B.A., Nelson K.E., White B.A. & Leigh S.R. 2013. Habitat degradation impacts black howler monkey (Alouatta pigra) gastrointestinal microbiomes. *ISME J.*

Antwis R.E., Beresford N.A., Jackson J.A., Fawkes R., Barnett C.L., Potter E., Walker L., Gaschak S. & Wood M.D. 2021. Impacts of radiation exposure on the bacterial and fungal microbiome of small mammals in the Chernobyl Exclusion Zone. *J. Anim. Ecol.*: 1365-2656.13507.

Baker R.J., Dickins B., Wickliffe J.K., Khan F.A.A.A., Gaschak S., Makova K.D. & Phillips C.D. 2017. Elevated mitochondrial genome variation after 50 generations of radiation exposure in a wild rodent. *Evol. Appl.* 10: 784–791.

Baltensperger A.P., Huettmann F., Hagelin J.C. & Welker J.M. 2015. Quantifying trophic niche spaces of small mammals using stable isotopes (δ 15 N and δ 13 C) at two scales across Alaska. *Can. J. Zool.* 93: 579–588.

Barnosky A.D., Matzke N., Tomiya S., Wogan G.O.U., Swartz B., Quental T.B., Marshall C., McGuire J.L., Lindsey E.L., Maguire K.C., Mersey B. & Ferrer E.A. 2011. Has the Earth's sixth mass extinction already arrived? *Nature* 471: 51–57.

Beaugelin-Seiller K., Garnier-Laplace J., Della-Vedova C., Métivier J.M., Lepage H., Mousseau T.A. & Møller A.P. 2020. Dose reconstruction supports the interpretation of decreased abundance of mammals in the Chernobyl Exclusion Zone. *Sci. Rep.* 10: 14083.

Beresford N.A., Barnett C.L., Gashchak S., Maksimenko A., Guliaichenko E., Wood M.D. & Izquierdo M. 2020a. Radionuclide transfer to wildlife at a 'Reference site' in the Chernobyl Exclusion Zone and resultant radiation exposures. *J. Environ. Radioact.* 211: 105661.

Beresford N.A., Fesenko S., Konoplev A., Skuterud L., Smith J.T. & Voigt G. 2016. Thirty years after the Chernobyl accident: What lessons have we learnt? *J. Environ. Radioact.* 157: 77–89.

Beresford N.A., Scott E.M. & Copplestone D. 2020b. Field effects studies in the Chernobyl Exclusion Zone: Lessons to be learnt. *J. Environ. Radioact.* 211: 105893.

Besten G. den, Eunen K. van, Groen A.K., Venema K., Reijngoud D.-J. & Bakker B.M. 2013. The role of short-chain fatty acids in the interplay between diet, gut microbiota, and host energy metabolism. *J. Lipid Res.* 54: 2325–2340.

Bianciardi A., Boschi M., Swanson E.E., Belloni M. & Robbins L.G. 2012. Ribosomal DNA organization before and after magnification in Drosophila melanogaster. *Genetics* 191: 703–723.

Birchenough G.M.H., Johansson M.E.V., Gustafsson J.K., Bergström J.H. & Hansson G.C. 2015. New developments in goblet cell mucus secretion and function. *Mucosal Immunol.* 8: 712–719.

Blue R.S., Chancellor J.C., Suresh R., Carnell L.S., Reyes D.P., Nowadly C.D. & Antonsen E.L. 2019. Challenges in Clinical Management of Radiation-Induced Illnesses During Exploration Spaceflight. *Aerosp. Med. Hum. Perform.* 90: 966–977.

Boets E., Gomand S. V., Deroover L., Preston T., Vermeulen K., Preter V. De, Hamer H.M., Mooter G. Van den, Vuyst L. De, Courtin C.M., Annaert P., Delcour J.A. & Verbeke K.A. 2017. Systemic availability and metabolism of colonic-derived short-chain fatty acids in healthy subjects: a stable isotope study. *J. Physiol.* 595: 541–555.

Bokulich N.A., Kaehler B.D., Rideout J.R., Dillon M., Bolyen E., Knight R., Huttley G.A. & Gregory Caporaso J. 2018. Optimizing taxonomic classification of marker-gene amplicon sequences with QIIME 2's q2-feature-classifier plugin. *Microbiome* 6: 90.

Bolyen E., Rideout J.R., Dillon M.R., Bokulich N.A., Abnet C.C., Al-Ghalith G.A., Alexander H., Alm E.J., Arumugam M., Asnicar F., Bai Y., Bisanz J.E., Bittinger K., Brejnrod A., Brislawn C.J., Brown C.T., Callahan B.J., Caraballo-Rodríguez A.M., Chase J., Cope E.K., Silva R. Da, Diener C., Dorrestein P.C., Douglas G.M., Durall D.M., Duvallet C., Edwardson C.F., Ernst M., Estaki M., Fouquier J., Gauglitz J.M., Gibbons S.M., Gibson D.L., Gonzalez A., Gorlick K., Guo J., Hillmann B., Holmes S., Holste H., Huttenhower C., Huttley G.A., Janssen S., Jarmusch A.K., Jiang L., Kaehler B.D., Kang K. Bin, Keefe C.R., Keim P., Kelley S.T., Knights D., Koester I., Kosciolek T., Kreps J., Langille M.G.I., Lee J., Ley R., Liu Y.-X., Loftfield E., Lozupone C., Maher M., Marotz C., Martin B.D., McDonald D., McIver L.J., Melnik A. V., Metcalf J.L., Morgan S.C., Morton J.T., Naimey A.T., Navas-Molina J.A., Nothias L.F., Orchanian S.B., Pearson T., Peoples S.L., Petras D., Preuss M.L., Pruesse E., Rasmussen L.B., Rivers A., Robeson M.S., Rosenthal P., Segata N., Shaffer M., Shiffer A., Sinha R., Song S.J., Spear J.R., Swafford A.D., Thompson L.R., Torres P.J., Trinh P., Tripathi A., Turnbaugh P.J., Ul-Hasan S., Hooft J.J.J. van der, Vargas F., Vázquez-Baeza Y., Vogtmann E., Hippel M. von, Walters W., Wan Y., Wang M., Warren J., Weber K.C., Williamson C.H.D., Willis A.D., Xu Z.Z., Zaneveld J.R., Zhang Y., Zhu Q., Knight R. & Caporaso J.G. 2019. Reproducible, interactive, scalable and extensible microbiome data science using QIIME 2. *Nat.*

Biotechnol. 37: 852–857.

Bonisoli-Alquati A., Voris A., Mousseau T.A., Møller A.P., Saino N. & Wyatt M.D. 2010. DNA damage in barn swallows (Hirundo rustica) from the Chernobyl region detected by use of the comet assay. *Comp. Biochem. Physiol. Part C Toxicol. Pharmacol.* 151: 271–277.

Boratyński Z., Lehmann P., Mappes T., Mousseau T.A. & Møller A.P. 2015. Increased radiation from Chernobyl decreases the expression of red colouration in natural populations of bank voles (Myodes glareolus). *Sci. Rep.* 4: 7141.

Bryant D.M., Johnson K., DiTommaso T., Tickle T., Couger M.B., Payzin-Dogru D., Lee T.J., Leigh N.D., Kuo T.H., Davis F.G., Bateman J., Bryant S., Guzikowski A.R., Tsai S.L., Coyne S., Ye W.W., Freeman R.M., Peshkin L., Tabin C.J., Regev A., Haas B.J. & Whited J.L. 2017. A Tissue-Mapped Axolotl De Novo Transcriptome Enables Identification of Limb Regeneration Factors. *Cell Rep.* 18: 762–776.

Bughio F. & Maggert K.A. 2019. The peculiar genetics of the ribosomal DNA blurs the boundaries of transgenerational epigenetic inheritance. *Chromosom. Res.* 27: 19–30.

Calandra I., Labonne G., Mathieu O., Henttonen H., Lévêque J., Milloux M.-J., Renvoisé É., Montuire S. & Navarro N. 2015. Isotopic partitioning by small mammals in the subnivium. *Ecol. Evol.* 5: 4132–4140.

Callahan B.J., McMurdie P.J., Rosen M.J., Han A.W., Johnson A.J.A. & Holmes S.P. 2016. DADA2: High-resolution sample inference from Illumina amplicon data. *Nat. Methods* 13: 581–583.

Canfora E.E., Jocken J.W. & Blaak E.E. 2015. Short-chain fatty acids in control of body weight and insulin sensitivity. *Nat Rev Endocrinol* 11: 577–591.

Cann J. van. 2019. Intergenerational responses to a changing environment: maternal and paternal early life shape fitness components in the bank vole.

Chen Y., Zhou P.-K., Zhang X.-Q., Wang Z.-D., Wang Y. & Darroudi F. 2014. Cytogenetic studies for a group of people living in Japan 1 year after the Fukushima nuclear accident. *Radiat. Prot. Dosimetry* 159: 20–25.

Cheng K., Brunius C., Fristedt R. & Landberg R. 2020. An LC-QToF MS based method for untargeted metabolomics of human fecal samples. *Metabolomics* 16: 46.

Chesser R.K., Sugg D.W., Lomakin M.D., Bussche R.A. van den, DeWoody J.A., Jagoe C.H., Dallas C.E., Whicker F.W., Smith M.H., Gaschak S.P., Chizhevsky I. V, Lyabik V. V, Buntova E.G., Holloman K. & Baker R.J. 2000. Concentrations and dose rate estimates of 134137 cesium and 90 strontium in small mammals at chornobyl, Ukraine. *Environ. Toxicol. Chem.* 19: 305–312.

Chevalier C., Stojanović O., Colin D.J., Suarez-Zamorano N., Tarallo V., Veyrat-Durebex C., Rigo D., Fabbiano S., Stevanović A., Hagemann S., Montet X., Seimbille Y., Zamboni N., Hapfelmeier S. & Trajkovski M. 2015. Gut Microbiota Orchestrates Energy Homeostasis during Cold. *Cell* 163: 1360–1374.

Conesa A., Madrigal P., Tarazona S., Gomez-Cabrero D., Cervera A.,

McPherson A., Szcześniak M.W., Gaffney D.J., Elo L.L., Zhang X. & Mortazavi A. 2016. A survey of best practices for RNA-seq data analysis. *Genome Biol.* 17: 13.

Cortés A., Clare S., Costain A., Almeida A., McCarthy C., Harcourt K., Brandt C., Tolley C., Rooney J., Berriman M., Lawley T., MacDonald A.S., Rinaldi G. & Cantacessi C. 2020. Baseline Gut Microbiota Composition Is Associated With Schistosoma mansoni Infection Burden in Rodent Models. *Front. Immunol.* 11: 1.

Cosentino C., Grieco D. & Costanzo V. 2011. ATM activates the pentose phosphate pathway promoting anti-oxidant defence and DNA repair. *EMBO J.* 30: 546–555.

Danchin E., Pocheville A., Rey O., Pujol B. & Blanchet S. 2019. Epigenetically facilitated mutational assimilation: epigenetics as a hub within the inclusive evolutionary synthesis. *Biol. Rev.* 94: 259–282.

David L.A., Maurice C.F., Carmody R.N., Gootenberg D.B., Button J.E., Wolfe B.E., Ling A. V., Devlin A.S., Varma Y., Fischbach M.A., Biddinger S.B., Dutton R.J. & Turnbaugh P.J. 2014. Diet rapidly and reproducibly alters the human gut microbiome. *Nature* 505: 559–563.

DeGruttola A.K., Low D., Mizoguchi A. & Mizoguchi E. 2016. Current Understanding of Dysbiosis in Disease in Human and Animal Models. *Inflamm. Bowel Dis.* 22: 1137–1150.

Deng R., Tang J., Ma J.-G., Chen S.-P., Xia L.-P., Zhou W.-J., Li D.-D., Feng G.-K., Zeng Y.-X. & Zhu X.-F. 2011. PKB/Akt promotes DSB repair in cancer cells through upregulating Mre11 expression following ionizing radiation. *Oncogene* 30: 944–955.

Deryabina T.G., Kuchmel S.V., Nagorskaya L.L., Hinton T.G., Beasley J.C., Lerebours A. & Smith J.T. 2015. Long-term census data reveal abundant wildlife populations at Chernobyl. *Curr. Biol.* 25: R824–R826.

Desouky O., Ding N. & Zhou G. 2015. Targeted and non-targeted effects of ionizing radiation. *J. Radiat. Res. Appl. Sci.* 8: 247–254.

Dill-McFarland K.A., Tang Z.Z., Kemis J.H., Kerby R.L., Chen G., Palloni A., Sorenson T., Rey F.E. & Herd P. 2019. Close social relationships correlate with human gut microbiota composition. *Sci. Rep.* 9: 1–10.

Dzyubenko E. V & Gudkov D.I. 2009. Cytogenetical and haematological effects of long-term irradiation on freshwater gastropod snails in the Chernobyl accident Exclusion Zone. *Radioprotection* 44: 933–936.

Einor D., Bonisoli-Alquati A., Costantini D., Mousseau T.A.A. & Møller A.P.P. 2016. Ionizing radiation, antioxidant response and oxidative damage: A meta-analysis. *Sci. Total Environ.* 548–549: 463–471.

Ferretti P., Pasolli E., Tett A., Asnicar F., Gorfer V., Fedi S., Armanini F., Truong D.T., Manara S., Zolfo M., Beghini F., Bertorelli R., Sanctis V. De, Bariletti I., Canto R., Clementi R., Cologna M., Crifò T., Cusumano G., Gottardi S., Innamorati C., Masè C., Postai D., Savoi D., Duranti S., Lugli G.A., Mancabelli L., Turroni F., Ferrario C., Milani C., Mangifesta M., Anzalone R., Viappiani A., Yassour M., Vlamakis H., Xavier R., Collado C.M., Koren O., Tateo S., Soffiati M., Pedrotti A., Ventura M., Huttenhower C., Bork P.

& Segata N. 2018. Mother-to-Infant Microbial Transmission from Different Body Sites Shapes the Developing Infant Gut Microbiome. *Cell Host Microbe* 24: 133-145.e5.

Forsström S., Jackson C.B., Carroll C.J., Kuronen M., Pirinen E., Pradhan S., Marmyleva A., Auranen M., Kleine I.M., Khan N.A., Roivainen A., Marjamäki P., Liljenbäck H., Wang L., Battersby B.J., Richter U., Velagapudi V., Nikkanen J., Euro L. & Suomalainen A. 2019. Fibroblast Growth Factor 21 Drives Dynamics of Local and Systemic Stress Responses in Mitochondrial Myopathy with mtDNA Deletions. *Cell Metab.* 30: 1040-1054.e7.

Frey B., Hehlgans S., Rödel F. & Gaipl U.S. 2015. Modulation of inflammation by low and high doses of ionizing radiation: Implications for benign and malign diseases. *Cancer Lett.* 368: 230–237.

Garnier-Laplace J., Beaugelin-Seiller K., Della-Vedova C., Métivier J.M., Ritz C., Mousseau T.A. & Pape Møller A. 2015. Radiological dose reconstruction for birds reconciles outcomes of Fukushima with knowledge of dose-effect relationships. *Sci. Rep.* 5: 1–13.

Garnier-Laplace J., Geras'kin S., Della-Vedova C., Beaugelin-Seiller K., Hinton T.G., Real A. & Oudalova A. 2013. Are radiosensitivity data derived from natural field conditions consistent with data from controlled exposures? A case study of Chernobyl wildlife chronically exposed to low dose rates. *J. Environ. Radioact.* 121: 12–21.

Gentile C.L. & Weir T.L. 2018. The gut microbiota at the intersection of diet and human health. *Science.* 362: 776–780.

Geyer P.K., Vitalini M.W. & Wallrath L.L. 2011. Nuclear organization: Taking a position on gene expression. *Curr. Opin. Cell Biol.* 23: 354–359.

Gibbons J.G., Branco A.T., Godinho S.A., Yu S. & Lemos B. 2015. Concerted copy number variation balances ribosomal DNA dosage in human and mouse genomes. *Proc. Natl. Acad. Sci. U. S. A.* 112: 2485–2490.

Gibbons J.G., Branco A.T., Yu S. & Lemos B. 2014. Ribosomal DNA copy number is coupled with gene expression variation and mitochondrial abundance in humans. *Nat Commun* 5: 4850.

Giudice M. Del, Buck C.L., Chaby L.E., Gormally B.M., Taff C.C., Thawley C.J., Vitousek M.N. & Wada H. 2018. What Is Stress? A Systems Perspective. *Integr. Comp. Biol.* 58: 1019–1032.

Goodrich J.K., Waters J.L., Poole A.C., Sutter J.L., Koren O., Blekhman R., Beaumont M., Treuren W. Van, Knight R., Bell J.T., Spector T.D., Clark A.G. & Ley R.E. 2014. Human Genetics Shape the Gut Microbiome. *Cell* 159: 789–799.

Gould B.A., Chen Y. & Lowry D.B. 2018. Gene regulatory divergence between locally adapted ecotypes in their native habitats. *Mol. Ecol.* 27: 4174–4188.

Goytisolo F.A., Samper E., Martín-Caballero J., Finnon P., Herrera E., Flores J.M., Bouffler S.D. & Blasco M.A. 2000. Short Telomeres Result in Organismal Hypersensitivity to Ionizing Radiation in Mammals. *J. Exp. Med.* 192: 1625–1636.

Grabherr M.G., Haas B.J., Yassour M., Levin J.Z., Thompson D.A., Amit I.,

48

Adiconis X., Fan L., Raychowdhury R., Zeng Q., Chen Z., Mauceli E., Hacohen N., Gnirke A., Rhind N., Palma F. di, Birren B.W., Nusbaum C., Lindblad-Toh K., Friedman N. & Regev A. 2011. Full-length transcriptome assembly from RNA-Seq data without a reference genome. *Nat. Biotechnol.* 29: 644–652.

Guo Z., Kozlov S., Lavin M.F., Person M.D. & Paull T.T. 2010. ATM Activation by Oxidative Stress. *Science.* 330: 517–521.

Haas B.J., Papanicolaou A., Yassour M., Grabherr M., Blood P.D., Bowden J., Couger M.B., Eccles D., Li B., Lieber M., MacManes M.D., Ott M., Orvis J., Pochet N., Strozzi F., Weeks N., Westerman R., William T., Dewey C.N., Henschel R., LeDuc R.D., Friedman N. & Regev A. 2013. De novo transcript sequence reconstruction from RNA-seq using the Trinity platform for reference generation and analysis. *Nat. Protoc.* 8: 1494–1512.

Han J., Lin K., Sequeira C. & Borchers C.H. 2015. An isotope-labeled chemical derivatization method for the quantitation of short-chain fatty acids in human feces by liquid chromatography–tandem mass spectrometry. *Anal. Chim. Acta* 854: 86–94.

Harvey E.F., Cristescu M.E., Dale J., Hunter H., Randall C. & Crease T.J. 2020. Metal exposure causes rDNA copy number to fluctuate in mutation accumulation lines of Daphnia pulex. *Aquat. Toxicol.* 226: 105556.

Hee B. van der & Wells J.M. 2021. Microbial Regulation of Host Physiology by Short-chain Fatty Acids. *Trends Microbiol.* 29: 700–712.

Hendry A.P., Farrugia T.J. & Kinnison M.T. 2008. Human influences on rates of phenotypic change in wild animal populations. *Mol. Ecol.* 17: 20–29.

Heydari A.R., Unnikrishnan A., Lucente L.V. & Richardson A. 2007. Caloric restriction and genomic stability. *Nucleic Acids Res.* 35: 7485–7496.

Hiyama A., Nohara C., Kinjo S., Taira W., Gima S., Tanahara A. & Otaki J.M. 2012. The biological impacts of the Fukushima nuclear accident on the pale grass blue butterfly. *Sci. Rep.* 2: 570.

Hooper L. V., Littman D.R. & Macpherson A.J. 2012. Interactions between the microbiota and the immune system. *Science.*

Huang W., Guo H.-L., Deng X., Zhu T.-T., Xiong J.-F., Xu Y.-H. & Xu Y. 2017. Short-Chain Fatty Acids Inhibit Oxidative Stress and Inflammation in Mesangial Cells Induced by High Glucose and Lipopolysaccharide. *Exp. Clin. Endocrinol. Diabetes* 125: 98–105.

Ide S., Miyazaki T., Maki H. & Kobayashi T. 2010. Abundance of Ribosomal RNA Gene Copies Maintains Genome Integrity. *Science.* 327: 693–696.

Ideue T. & Tani T. 2020. Centromeric Non-Coding RNAs: Conservation and Diversity in Function. *Non-Coding RNA* 6: 4.

Innes D.G.L. & Millar J.S. 1994. Life histories of Clethrionomys and Microtus (Microtinae). *Mamm. Rev.* 24: 179–207.

International Atomic Energy Agency. 2006. *Environmental consequences of the chernobyl accident and their remediation: twenty years of experience. Report of the chernobyl forum expert group 'environment'*. IAEA, Vienna, Austria.

International Atomic Energy Agency. 2010. *Radiation Biology: A handbook for teachers and students*. IAEA, Vienna, Austria.

Jack C. V., Cruz C., Hull R.M., Keller M.A., Ralser M. & Houseley J. 2015. Regulation of ribosomal DNA amplification by the TOR pathway. *Proc. Natl. Acad. Sci.* 112: 9674–9679.

Jernfors T., Danforth J., Kesäniemi J., Lavrinienko A., Tukalenko E., Fajkus J., Dvořáčková M., Mappes T. & Watts P.C. 2021. Expansion of rDNA and pericentromere satellite repeats in the genomes of bank voles Myodes glareolus exposed to environmental radionuclides. *Ecol. Evol.*: ece3.7684.

Jernfors T., Kesäniemi J., Lavrinienko A., Mappes T., Milinevsky G., Møller A.P., Mousseau T.A., Tukalenko E. & Watts P.C. 2018. Transcriptional Upregulation of DNA Damage Response Genes in Bank Voles (Myodes glareolus) Inhabiting the Chernobyl Exclusion Zone. *Front. Environ. Sci.* 5: 95.

Kersten S. 2014. Integrated physiology and systems biology of PPARα. *Mol. Metab.* 3: 354–371.

Kesäniemi J., Jernfors T., Lavrinienko A., Kivisaari K., Kiljunen M., Mappes T. & Watts P.C. 2019a. Exposure to environmental radionuclides is associated with altered metabolic and immunity pathways in a wild rodent. *Mol. Ecol.*: mec.15241.

Kesäniemi J., Lavrinienko A., Tukalenko E., Boratyński Z., Kivisaari K., Mappes T., Milinevsky G., Møller A.P., Mousseau T.A. & Watts P.C. 2019b. Exposure to environmental radionuclides associates with tissue-specific impacts on telomerase expression and telomere length. *Sci. Rep.* 9: 850.

Kesäniemi J., Lavrinienko A., Tukalenko E., Mappes T., Watts P.C. & Jurvansuu J. 2019c. Infection Load and Prevalence of Novel Viruses Identified from the Bank Vole Do Not Associate with Exposure to Environmental Radioactivity. *Viruses* 12: 44.

Kesäniemi J., Lavrinienko A., Tukalenko E., Moutinho A.F., Mappes T., Møller A.P., Mousseau T.A. & Watts P.C. 2020. Exposure to environmental radionuclides alters mitochondrial DNA maintenance in a wild rodent. *Evol. Ecol.* 34: 163–174.

Knight R., Vrbanac A., Taylor B.C., Aksenov A., Callewaert C., Debelius J., Gonzalez A., Kosciolek T., McCall L.I., McDonald D., Melnik A. V., Morton J.T., Navas J., Quinn R.A., Sanders J.G., Swafford A.D., Thompson L.R., Tripathi A., Xu Z.Z., Zaneveld J.R., Zhu Q., Caporaso J.G. & Dorrestein P.C. 2018. Best practices for analysing microbiomes. *Nat. Rev. Microbiol.* 16: 410–422.

Kobayashi T. 2011. Regulation of ribosomal RNA gene copy number and its role in modulating genome integrity and evolutionary adaptability in yeast. *Cell. Mol. Life Sci.* 68: 1395–1403.

Kobayashi T. 2014. Ribosomal RNA gene repeats, their stability and cellular senescence. *Proc. Japan Acad. Ser. B* 90: 119–129.

Kobayashi T. & Sasaki M. 2017. Ribosomal DNA stability is supported by many 'buffer genes'—introduction to the Yeast rDNA Stability Database. *FEMS Yeast Res.* 17: 1–8.

Kobayashi T., Heck D.J., Nomura M. & Horiuchi T. 1998. Expansion and contraction of ribosomal DNA repeats in Saccharomyces cerevisiae:

Requirement of replication fork blocking (Fob1) protein and the role of RNA polymerase I. *Genes Dev.* 12: 3821–3830.

Kohl K.D., Weiss R.B., Cox J., Dale C. & Denise Dearing M. 2014. Gut microbes of mammalian herbivores facilitate intake of plant toxins Dam N. van (ed.). *Ecol. Lett.* 17: 1238–1246.

Koivula M., Koskela E., Mappes T. & Oksanen T.A. 2003. Cost of reproduction in the wild: manipulation of reproductive effort in the bank vole. *Ecology* 84: 398–405.

Koolhaas J.M., Bartolomucci A., Buwalda B., Boer S.F. de, Flügge G., Korte S.M., Meerlo P., Murison R., Olivier B., Palanza P., Richter-Levin G., Sgoifo A., Steimer T., Stiedl O., Dijk G. van, Wöhr M. & Fuchs E. 2011. Stress revisited: A critical evaluation of the stress concept. *Neurosci. Biobehav. Rev.* 35: 1291–1301.

Kozakiewicz M., Chołuj A. & Kozakiewicz A. 2007. Long-distance movements of individuals in a free-living bank vole population: an important element of male breeding strategy. *Acta Theriol. (Warsz).* 52: 339–348.

Kurle C.M., Koch P.L., Tershy B.R. & Croll D.A. 2014. The effects of sex, tissue type, and dietary components on stable isotope discrimination factors (Δ 13 C and Δ 15 N) in mammalian omnivores. *Isotopes Environ. Health Stud.* 50: 307–321.

Labocha M.K., Schutz H. & Hayes J.P. 2014. Which body condition index is best? *Oikos* 123: 111–119.

Lamarche B.J., Orazio N.I. & Weitzman M.D. 2010. The MRN complex in double-strand break repair and telomere maintenance. *FEBS Lett.* 584: 3682–3695.

Langmead B., Trapnell C., Pop M. & Salzberg S.L. 2009. Ultrafast and memory-efficient alignment of short DNA sequences to the human genome. *Genome Biol.* 10: R25.

Larson K., Yan S.-J., Tsurumi A., Liu J., Zhou J., Gaur K., Guo D., Eickbush T.H. & Li W.X. 2012. Heterochromatin Formation Promotes Longevity and Represses Ribosomal RNA Synthesis Kim S.K. (ed.). *PLoS Genet.* 8: e1002473.

Lavrinienko A., Hämäläinen A., Hindström R., Tukalenko E., Boratyński Z., Kivisaari K., Mousseau T.A., Watts P.C. & Mappes T. 2021a. Comparable response of wild rodent gut microbiome to anthropogenic habitat contamination. *Mol. Ecol.*: mec.15945.

Lavrinienko A., Jernfors T., Koskimäki J.J., Pirttilä A.M. & Watts P.C. 2021b. Does Intraspecific Variation in rDNA Copy Number Affect Analysis of Microbial Communities? *Trends Microbiol.* 29: 19–27.

Lavrinienko A., Mappes T., Tukalenko E., Mousseau T.A., Møller A.P., Knight R., Morton J.T., Thompson L.R. & Watts P.C. 2018. Environmental radiation alters the gut microbiome of the bank vole Myodes glareolus. *ISME J.* 12: 2801–2806.

Lavrinienko A., Tukalenko E., Kesäniemi J., Kivisaari K., Masiuk S., Boratyński Z., Mousseau T.A., Milinevsky G., Mappes T. & Watts P.C. 2020. Applying the Anna Karenina principle for wild animal gut microbiota: Temporal

stability of the bank vole gut microbiota in a disturbed environment. *J. Anim. Ecol.*: 1365-2656.13342.

Lee J.-H. & Paull T. 2007. Activation and regulation of ATM kinase activity in response to DNA double-strand breaks. *Oncogene* 26: 7741–7748.

Lehmann P., Boratyński Z., Mappes T., Mousseau T.A. & Møller A.P. 2016. Fitness costs of increased cataract frequency and cumulative radiation dose in natural mammalian populations from Chernobyl. *Sci. Rep.* 6: 19974.

Leinonen P.H., Remington D.L., Leppälä J. & Savolainen O. 2013. Genetic basis of local adaptation and flowering time variation in Arabidopsis lyrata. *Mol. Ecol.* 22: 709–723.

Li B. & Dewey C.N. 2011. RSEM: accurate transcript quantification from RNA-Seq data with or without a reference genome. *BMC Bioinformatics* 12: 323.

Liu H., Wang J., He T., Becker S., Zhang G., Li D. & Ma X. 2018. Butyrate: A Double-Edged Sword for Health? *Adv. Nutr.* 9: 21–29.

Lourenço J., Mendo S. & Pereira R. 2016. Radioactively contaminated areas: Bioindicator species and biomarkers of effect in an early warning scheme for a preliminary risk assessment. *J. Hazard. Mater.* 317: 503–542.

Love M.I., Huber W. & Anders S. 2014. Moderated estimation of fold change and dispersion for RNA-seq data with DESeq2. *Genome Biol.* 15: 550.

Lovell J.T., Schwartz S., Lowry D.B., Shakirov E. V., Bonnette J.E., Weng X., Wang M., Johnson J., Sreedasyam A., Plott C., Jenkins J., Schmutz J. & Juenger T.E. 2016. Drought responsive gene expression regulatory divergence between upland and lowland ecotypes of a perennial C 4 grass. *Genome Res.* 26: 510–518.

Lozupone C.A., Hamady M., Kelley S.T. & Knight R. 2007. Quantitative and Qualitative β Diversity Measures Lead to Different Insights into Factors That Structure Microbial Communities. *Appl. Environ. Microbiol.* 73: 1576–1585.

Macdonald D.W. 2006. *The Encyclopedia of Mammals*. Oxford University Press.

Maggio F. Di, Minafra L., Forte G., Cammarata F., Lio D., Messa C., Gilardi M. & Bravatà V. 2015. Portrait of inflammatory response to ionizing radiation treatment. *J. Inflamm.* 12: 14.

Manning B.D. & Toker A. 2017. AKT/PKB Signaling: Navigating the Network. *Cell* 169: 381–405.

Mappes T. & Koskela E. 2004. Genetic basis of the trade-off between offspring number and quality in the bank vole. *Evolution (N. Y).* 58: 645–650.

Mappes T., Boratyński Z., Kivisaari K., Lavrinienko A., Milinevsky G., Mousseau T.A., Møller A.P., Tukalenko E. & Watts P.C. 2019. Ecological mechanisms can modify radiation effects in a key forest mammal of Chernobyl. *Ecosphere* 10: e02667.

Martínez P., Gómez-López G., García F., Mercken E., Mitchell S., Flores J.M., deCabo R. & Blasco M.A. 2013. RAP1 Protects from Obesity through Its Extratelomeric Role Regulating Gene Expression. *Cell Rep.* 3: 2059–2074.

Maurice C.F., CL Knowles S., Ladau J., Pollard K.S., Fenton A., Pedersen A.B. & Turnbaugh P.J. 2015. Marked seasonal variation in the wild mouse gut microbiota. *ISME J.* 9: 2423–2434.

Mei Z., Zhang X., Yi J., Huang J., He J. & Tao Y. 2016. Sirtuins in metabolism, DNA repair and cancer. *J. Exp. Clin. Cancer Res.* 35: 182.

Merilä J. & Hendry A.P. 2014. Climate change, adaptation, and phenotypic plasticity: The problem and the evidence. *Evol. Appl.* 7: 1–14.

Mérot C., Oomen R.A., Tigano A. & Wellenreuther M. 2020. A Roadmap for Understanding the Evolutionary Significance of Structural Genomic Variation. *Trends Ecol. Evol.* 35: 561–572.

Møller A.P. & Mousseau T.A. 2018. Reduced colonization by soil invertebrates to irradiated decomposing wood in Chernobyl. *Sci. Total Environ.* 645: 773–779.

Møller A.P., Bonisoli-Alquati A. & Mousseau T.A. 2013. High frequency of albinism and tumours in free-living birds around Chernobyl. *Mutat. Res. Toxicol. Environ. Mutagen.* 757: 52–59.

Møller A.P., Bonisoli-Alquati A., Mousseau T.A. & Rudolfsen G. 2014. Aspermy, Sperm Quality and Radiation in Chernobyl Birds Singh S.R. (ed.). *PLoS One* 9: e100296.

Møller A.P., Bonisoli-Alquati A., Rudolfsen G. & Mousseau T.A. 2011. Chernobyl Birds Have Smaller Brains Brembs B. (ed.). *PLoS One* 6: e16862.

Morley N.J. 2012. The effects of radioactive pollution on the dynamics of infectious diseases in wildlife. *J. Environ. Radioact.* 106: 81–97.

Mousseau T.A., Moller A.P., Møller A.P., Moller A.P., Møller A.P. & Moller A.P. 2014. Genetic and ecological studies of animals in Chernobyl and Fukushima. *J. Hered.* 105: 704–709.

Müller M., Hernández M.A.G., Goossens G.H., Reijnders D., Holst J.J., Jocken J.W.E., Eijk H. van, Canfora E.E. & Blaak E.E. 2019. Circulating but not faecal short-chain fatty acids are related to insulin sensitivity, lipolysis and GLP-1 concentrations in humans. *Sci. Reports 2019 91* 9: 1–9.

Mustonen V., Kesäniemi J., Lavrinienko A., Tukalenko E., Mappes T., Watts P.C. & Jurvansuu J. 2018. Fibroblasts from bank voles inhabiting Chernobyl have increased resistance against oxidative and DNA stresses. *BMC Cell Biol.* 19: 17.

Nyström E.E.L., Birchenough G.M.H., Post S. van der, Arike L., Gruber A.D., Hansson G.C. & Johansson M.E.V. 2018. Calcium-activated Chloride Channel Regulator 1 (CLCA1) Controls Mucus Expansion in Colon by Proteolytic Activity. *EBioMedicine* 33: 134–143.

Oksanen J., Blanchet F.G., Kindt R., Legen- P., Minchin P.R., Hara R.B.O., Simpson G.L., Soly- P., Stevens M.H.H. & Wagner H. 2018. Package ' vegan ' version 2.5-2. *Community Ecol. Packag.*

Palumbi S.R. 2001. Humans as the World's Greatest Evolutionary Force. *Science.* 293: 1786–1790.

Paredes S., Branco A.T., Hartl D.L., Maggert K.A. & Lemos B. 2011. Ribosomal dna deletions modulate genome-wide gene expression: 'rDNA-sensitive' genes and natural variation. *PLoS Genet.* 7: 1–10.

Park S.W., Zhen G., Verhaeghe C., Nakagami Y., Nguyenvu L.T., Barczak A.J., Killeen N. & Erle D.J. 2009. The protein disulfide isomerase AGR2 is essential for production of intestinal mucus. *Proc. Natl. Acad. Sci. U. S. A.*

106: 6950–6955.

Parks M.M., Kurylo C.M., Dass R.A., Bojmar L., Lyden D., Vincent C.T. & Blanchard S.C. 2018. Variant ribosomal RNA alleles are conserved and exhibit tissue-specific expression. *Sci. Adv.* 4: eaao0665.

Perino A., Pereira H.M., Navarro L.M., Fernández N., Bullock J.M., Ceauşu S., Cortés-Avizanda A., Klink R. Van, Kuemmerle T., Lomba A., Pe'er G., Plieninger T., Benayas J.M.R., Sandom C.J., Svenning J.C. & Wheeler H.C. 2019. Rewilding complex ecosystems. *Science.* 364.

Petzke K.J., Fuller B.T. & Metges C.C. 2010. Advances in natural stable isotope ratio analysis of human hair to determine nutritional and metabolic status. *Curr. Opin. Clin. Nutr. Metab. Care* 13: 532–540.

Pfaffl M.W. 2001. A new mathematical model for relative quantification in real-time RT-PCR. *Nucleic Acids Res.* 29: 45e – 45.

Pickard J.M., Zeng M.Y., Caruso R. & Núñez G. 2017. Gut microbiota: Role in pathogen colonization, immune responses, and inflammatory disease. *Immunol. Rev.*

Pietzke M., Meiser J. & Vazquez A. 2019. Formate metabolism in health and disease. *Mol. Metab.*: 1–15.

Poljsak B. & Milisav I. 2016. NAD+ as the Link Between Oxidative Stress, Inflammation, Caloric Restriction, Exercise, DNA Repair, Longevity, and Health Span. *Rejuvenation Res.* 19: 406–413.

Prokopowich C.D., Gregory T.R. & Crease T.J. 2003. The correlation between rDNA copy number and genome size in eukaryotes. *Genome* 46: 48–50.

Qiu G.H. 2015. Protection of the genome and central protein-coding sequences by non-coding DNA against DNA damage from radiation. *Mutat. Res. - Rev. Mutat. Res.* 764: 108–117.

Real A. & Garnier-Laplace J. 2020. The importance of deriving adequate wildlife benchmark values to optimize radiological protection in various environmental exposure situations. *J. Environ. Radioact.* 211: 105902.

Rochlani Y., Pothineni N.V., Kovelamudi S. & Mehta J.L. 2017. Metabolic syndrome: pathophysiology, management, and modulation by natural compounds. *Ther. Adv. Cardiovasc. Dis.* 11: 215–225.

Rodgers B.E. & Baker R.J. 2000. Frequencies of micronuclei in bank voles from zones of high radiation at Chornobyl, Ukraine. *Environ. Toxicol. Chem.* 19: 1644–1648.

Rodgers B.E., Wickliffe J.K., Phillips C.J., Chesser R.K. & Baker R.J. 2001. Experimental exposure of naive bank voles (Clethrionomys glareolus) to the Chornobyl, Ukraine, environment: A test of radioresistance. *Environ. Toxicol. Chem.* 20: 1936–1941.

Romanelli C., Cooper D., Campbell-Lendrum D., Maiero M., Karesh W., Hunter D. & Golden C. 2015. *Connecting global priorities: biodiversity and human health: a state of knowledge review.* WHO/CBD.

Rühm W., Azizova T., Bouffler S., Cullings H.M., Grosche B., Little M.P., Shore R.S., Walsh L. & Woloschak G.E. 2018. Typical doses and dose rates in studies pertinent to radiation risk inference at low doses and low dose rates. *J. Radiat. Res.* 59: ii1–ii10.

54

Saka K., Ide S., Ganley A.R.D. & Kobayashi T. 2013. Cellular senescence in yeast is regulated by rDNA noncoding transcription. *Curr. Biol.* 23: 1794–1798.

Salim D. & Gerton J.L. 2019. Ribosomal DNA instability and genome adaptability. *Chromosom. Res.* 27: 73–87.

Salim D., Bradford W.D., Freeland A., Cady G., Wang J., Pruitt S.C. & Gerton J.L. 2017. DNA replication stress restricts ribosomal DNA copy number. *PLoS Genet.* 13: 1–20.

Salnikova L., Chumachenko A., Belopolskaya O. & Rubanovich A. 2012. Correlations between DNA polymorphism and frequencies of gamma-radiation tnduced and spontaneous cytogenetic damage. *Health Phys.* 103: 37–41.

Sampson T.R. & Mazmanian S.K. 2015. Control of Brain Development, Function, and Behavior by the Microbiome. *Cell Host Microbe* 17: 565–576.

Sazykina T. & Kryshev I.I. 2006. Radiation effects in wild terrestrial vertebrates – the EPIC collection. *J. Environ. Radioact.* 88: 11–48.

Schöfer C. & Weipoltshammer K. 2018. Nucleolus and chromatin. *Histochem. Cell Biol.* 150: 209–225.

Schroeder B.O. 2019. Fight them or feed them: how the intestinal mucus layer manages the gut microbiota. *Gastroenterol. Rep.* 7: 3–12.

Shreiner A.B., Kao J.Y. & Young V.B. 2015. The gut microbiome in health and in disease. *Curr. Opin. Gastroenterol.* 31: 69–75.

Silveira W.A. da, Fazelinia H., Rosenthal S.B., Laiakis E.C., Kim M.S., Meydan C., Kidane Y., Rathi K.S., Smith S.M., Stear B., Ying Y., Zhang Y., Foox J., Zanello S., Crucian B., Wang D., Nugent A., Costa H.A., Zwart S.R., Schrepfer S., Elworth R.A.L., Sapoval N., Treangen T., MacKay M., Gokhale N.S., Horner S.M., Singh L.N., Wallace D.C., Willey J.S., Schisler J.C., Meller R., McDonald J.T., Fisch K.M., Hardiman G., Taylor D., Mason C.E., Costes S. V. & Beheshti A. 2020. Comprehensive Multi-omics Analysis Reveals Mitochondrial Stress as a Central Biological Hub for Spaceflight Impact. *Cell* 183: 1185-1201.e20.

Simão F.A., Waterhouse R.M., Ioannidis P., Kriventseva E. V. & Zdobnov E.M. 2015. BUSCO: assessing genome assembly and annotation completeness with single-copy orthologs. *Bioinformatics* 31: 3210–3212.

Sommer F., Ståhlman M., Ilkayeva O., Arnemo J.M., Kindberg J., Josefsson J., Newgard C.B., Fröbert O. & Bäckhed F. 2016. The Gut Microbiota Modulates Energy Metabolism in the Hibernating Brown Bear Ursus arctos. *Cell Rep.* 14: 1655–1661.

Song Y., Salbu B., Teien H.-C., Evensen Ø., Lind O.C., Rosseland B.O. & Tollefsen K.E. 2016. Hepatic transcriptional responses in Atlantic salmon (Salmo salar) exposed to gamma radiation and depleted uranium singly and in combination. *Sci. Total Environ.* 562: 270–279.

Sonnenburg E.D. & Sonnenburg J.L. 2019. The ancestral and industrialized gut microbiota and implications for human health. *Nat. Rev. Microbiol.* 17: 383–390.

Stark R., Grzelak M. & Hadfield J. 2019. RNA sequencing: the teenage years. *Nat. Rev. Genet.* 20: 631–656.

Strauss S.H. & Tsai C.-H. 1988. Ribosomal Gene Number Variability in Douglas-Fir. *J. Hered.* 79: 453–458.

Suvarna K.S., Layton C. & Bancroft J.D. 2013. *Bancroft's Theory and Practise of Histological Techniques (7th edition)*. Churchill Livingstone, London, UK.

Symonová. 2019. Integrative rDNAomics—Importance of the Oldest Repetitive Fraction of the Eukaryote Genome. *Genes (Basel).* 10: 345.

The R Core Team. 2018. *R: A language and environment for statistical computing.*

Tyynismaa H., Carroll C.J., Raimundo N., Ahola-erkkilä S., Wenz T., Ruhanen H., Guse K., Hemminki A., Peltola-Mjøsund K.E., Tulkki V., Orešič M., Moraes C.T., Pietiläinen K., Hovatta I. & Suomalainen A. 2010. Mitochondrial myopathy induces a starvation-like response. *Hum. Mol. Genet.* 19: 3948–3958.

Untergasser A., Cutcutache I., Koressaar T., Ye J., Faircloth B.C., Remm M. & Rozen S.G. 2012. Primer3--new capabilities and interfaces. *Nucleic Acids Res.* 40: e115.

Urban M.C., Richardson J.L. & Freidenfelds N.A. 2014. Plasticity and genetic adaptation mediate amphibian and reptile responses to climate change. *Evol. Appl.* 7: 88–103.

Wang Z., Gerstein M. & Snyder M. 2009. RNA-Seq: a revolutionary tool for transcriptomics.

Ward J.F. 1988. DNA Damage Produced by Ionizing Radiation in Mammalian Cells: Identities, Mechanisms of Formation, and Reparability. In: pp. 95–125.

Weinzierl M. 2018. Space, the Final Economic Frontier. *J. Econ. Perspect.* 32: 173–192.

White T.A., Lundy M.G., Montgomery W.I., Montgomery S., Perkins S.E., Lawton C., Meehan J.M., Hayden T.J., Heckel G., Reid N. & Searle J.B. 2012. Range expansion in an invasive small mammal: Influence of life-history and habitat quality. *Biol. Invasions* 14: 2203–2215.

Xu B., Li H., Perry J.M., Singh V.P., Unruh J., Yu Z., Zakari M., McDowell W., Li L. & Gerton J.L. 2017. Ribosomal DNA copy number loss and sequence variation in cancer. *PLoS Genet.* 13: 1–25.

Yan S.-J., Lim S.J., Shi S., Dutta P. & Li W.X. 2011. Unphosphorylated STAT and heterochromatin protect genome stability. *FASEB J.* 25: 232–241.

Young M.D., Wakefield M.J. & Smyth G.K. 2016. goseq : Gene Ontology testing for RNA-seq datasets Reading data. : 1–25.

Yuan H.-X.X., Xiong Y. & Guan K.-L.L. 2013. Nutrient Sensing, Metabolism, and Cell Growth Control. *Mol. Cell* 49: 379–387.

Zaneveld J.R., McMinds R. & Thurber R.V. 2017. Stress and stability: Applying the Anna Karenina principle to animal microbiomes. *Nat. Microbiol.* 2.

Zhang X., Ye C., Sun F., Wei W., Hu B. & Wang J. 2016. Both Complexity and Location of DNA Damage Contribute to Cellular Senescence Induced by Ionizing Radiation Li J.J. (ed.). *PLoS One* 11: e0155725.

Zilber-Rosenberg I. & Rosenberg E. 2008. Role of microorganisms in the evolution of animals and plants: the hologenome theory of evolution. *FEMS Microbiol. Rev.* 32: 723–735.

ORIGINAL P**UBLICATIONS**

I

TRANSCRIPTIONAL UPREGULATION OF DNA DAMAGE
RESPONSE GENES IN BANK VOLES (MYODES GLAREOLUS)
INHABITING THE CHERNOBYL EXCLUSION ZONE

by

Jernfors T, Kesäniemi J, Lavrinienko A, Mappes T, Milinevsky G, Møller AP,

Mousseau TA, Tukalenko E & Watts PC. 2018

Transcriptional Upregulation of DNA Damage Response Genes in Bank Voles (*Myodes glareolus*) Inhabiting the Chernobyl Exclusion Zone

Toni Jernfors[1]*, Jenni Kesäniemi[1], Anton Lavrinienko[1], Tapio Mappes[2], Gennadi Milinevsky[3], Anders P. Møller[4], Timothy A. Mousseau[5], Eugene Tukalenko[3] and Phillip C. Watts[1]

[1] Ecology and Genetics, University of Oulu, Oulu, Finland, [2] Department of Biological and Environmental Science, University of Jyväskylä, Jyvaskyla, Finland, [3] Taras Shevchenko National University of Kyiv, Kyiv, Ukraine, [4] Ecologie Systématique Evolution, Université Paris-Sud, CNRS, AgroParisTech, Université Paris-Saclay, Orsay, France, [5] Department of Biological Sciences, University of South Carolina, Columbia, SC, United States

Exposure to ionizing radiation (IR) from radionuclides released into the environment can damage DNA. An expected response to exposure to environmental radionuclides, therefore, is initiation of DNA damage response (DDR) pathways. Increased DNA damage is a characteristic of many organisms exposed to radionuclides but expression of DDR genes of wildlife inhabiting an area contaminated by radionuclides is poorly understood. We quantified expression of five central DDR genes *Atm, Mre11, p53, Brca1,* and *p21* in the livers of the bank vole *Myodes glareolus* that inhabited areas within the Chernobyl Exclusion Zone (CEZ) that differed in levels of ambient radioactivity, and also from control areas outside the CEZ (i.e., sites with no detectable environmental radionuclides) in Ukraine. Expression of these DDR genes did not significantly differ between male and female bank voles, nor among sites within the CEZ. We found a near two-fold upregulation in the DDR initiators *Mre11* and *Atm* in animals collected from the CEZ compared with samples from control sites. As *Atm* is an important regulator of oxidative stress, our data suggest that antioxidant activity may be a key component of the defense against exposure to environmental radioactivity.

Keywords: chernobyl, ionizing radiation, DNA damage, DNA repair, oxidative stress, *Atm*, *Mre11*

INTRODUCTION

Accidental release of radionuclides into the environment presents a potential health risk to humans and wildlife (Møller and Mousseau, 2006; Lourenço et al., 2016). On 26 April 1986, reactor 4 of the Chernobyl Nuclear Power Plant (NPP) exploded, releasing an estimated 9×10^3 to 1×10^4 petabecquerels (Pbq) of radionuclides over much of Eastern Europe, Russia, and Fennoscandia (Dreicer et al., 1996). This accident, together with the accident at the Fukushima Daiichi NPP in 2011, stimulated public and scientific interest in the impacts of environmental radionuclides on natural ecosystems (Wheatley et al., 2016). To limit human exposure to radionuclides, the Chernobyl Exclusion Zone (CEZ) was established at ∼30 km radius around the accident site. The CEZ still contains elevated levels of isotopes with long half-lives, notably strontium-90,

caesium-137, and plutonium-239 (about 29, 30, and 24,100 years, respectively). The wildlife inhabiting the CEZ provide the best-studied model of the biological impact of exposure to radionuclides (Møller and Mousseau, 2006).

One harmful effect of exposure to ionizing radiation (IR) from radionuclides is elevated DNA damage, either directly or by generating reactive oxygen species (ROS) through radiolysis of intracellular water (Ward, 1988; Einor et al., 2016). Elevated DNA damage, for example as chromosomal aberrations (Dzyubenko and Gudkov, 2009) or DNA breaks (Bonisoli-Alquati et al., 2010; Fujita et al., 2014), has been observed in wildlife and humans inhabiting areas affected by the accidents at Chernobyl and Fukushima (reviewed by Lourenço et al., 2016). That not all studies find elevated DNA damage in areas with increased radioactivity (e.g., Bonisoli-Alquati et al., 2015) points to interspecific differences in response to environmental radionuclides (Møller and Mousseau, 2015). Somewhat surprisingly, despite the many (>200) studies of DNA damage, few studies have quantified activity of DNA repair pathway genes on organisms exposed to environmental radionuclides (Lourenço et al., 2016).

In eukaryotes, DNA repair is activated and regulated by the DNA damage response (DDR) pathway, which is a multi-branched signaling cascade initiated by the serine/threonine kinases ATR and ATM upon detection of single-strand DNA breaks (SSBs) and double-strand DNA breaks (DSBs), respectively (Giglia-Mari et al., 2011). DSBs typically result from exposure to highly genotoxic agents and IR (Ward, 1990) and pose a serious problem for genomic integrity as they cannot always be repaired without incorporating mutations, thus increasing the risk of cancer (Cannan and Pederson, 2016). DSBs are detected by the MRE11-RAD50-NBS1 complex, which activates ATM. Pathways activated by ATM include p53-mediated cell cycle checkpoint and apoptosis, increased antioxidant production, and DNA repair, where the choice between non-homologous end joining (NHEJ) and homologous recombination (HR) repair is regulated by BRCA1 (Daley and Sung, 2014).

Just three studies, all on plants, have quantified DNA repair activity in wildlife affected by the Chernobyl and Fukushima accidents. After exposure to high doses (750 Gy) of IR, DNA repair activity in pollen and seed from two species of plant depended upon the composition of radionuclides in the soil in which the parental plants had grown (Boubriak et al., 2008). Progeny of *Arabidopsis* inhabiting areas around Chernobyl exhibited low recombination rates, despite X-ray induced upregulation of homologous recombination repair-related *Rad54-like* in samples from a contaminated area (Kovalchuk et al., 2014). Unfortunately these studies within the CEZ did not use replicate samples from contaminated and uncontaminated sites, making it challenging to determine whether radiation or a third variable accounts for these effects. In rice (*Oryza sativa*) seedlings, exposure to low-dose IR affected expression of stress response and DNA repair associated genes (Hayashi et al., 2014), with some single-strand break repair genes initially upregulated but suppressed after 24 h of IR exposure. Ultimately, plants have been found to be sensitive to
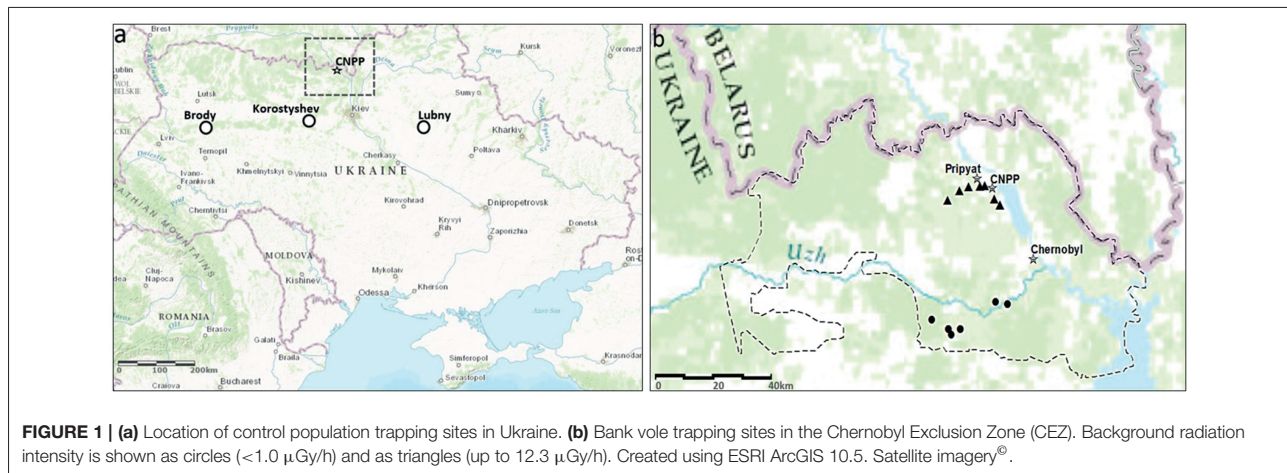
environmental radiation, and it has been suggested that they could serve as bioindicator species for assessing radiation risk (Nikitaki et al., 2017). The DDR of wild vertebrates exposed to environmental radionuclides has rarely been studied, although, for example, upregulation in the *p53* gene has been observed in wood mice (*Apodemus sylvaticus*) inhabiting a former uranium mine area (Lourenço et al., 2013).

The subject of the physiological and ecological effects of low-dose IR is highly controversial, as evidenced by several conflicting studies concerning species diversity and abundance in the CEZ. Populations of large mammals, such as the wild boar (*Sus scrofa*), appear especially abundant (Deryabina et al., 2015), but it is difficult to quantify the effect of human absence on these populations. Here, we quantify mRNA transcription in five DDR and repair genes in livers of the bank vole *Myodes glareolus,* a small rodent that inhabits areas within and outside the CEZ. Multiple populations from both experimental and control regions were studied to ensure spatial replication of study sites that differ in contamination levels. The bank vole is abundant (typically 10–80 animals per hectare) in forest habitats in much of Europe and Asia (Hutterer et al., 2016) and was one of the first mammals to re-colonize the CEZ after the nuclear accident (Baker et al., 1996). Bank voles inhabiting the CEZ show an increased frequency of chromosomal aberrations (Goncharova and Ryabokon, 1995) and increased oxidative stress in the form of cataracts (Lehmann et al., 2016), although estimates of DNA damage have returned conflicting results (Cristaldi et al., 1991; Rodgers and Baker, 2000). We hypothesize that exposure to low-dose IR stimulates the expression of key genes in the DDR pathway.

MATERIALS AND METHODS

Sample Collection

Animals were caught using Ugglan Special live traps (Grahnab, Sweden), with sunflower seeds and potato as bait, during 6th−11th May 2015, at 14 locations within the CEZ that differed in levels of soil radionuclides (**Figure 1**). Bank voles were also caught during 16th−27th August 2015 at three separate regions outside the CEZ, where elevated levels of soil radionuclides have not been detected: Brody (50°0594 N, 25°10752 E), Lubny (50°05564 N, 32°98566 E), and Korostyshev (50°34422 N, 29°23673 E) in order to control for habitat effects. At each trapping location, 20 traps were placed in a line, with each trap separated by about 10 m and with trapping locations separated by at least 500 m. Procedures were performed in accordance with relevant guidelines and regulations, approved by the Finnish Animal Experiment Board and the Finnish Ministry of the Environment (under the authorization ESAVI/3834/04.10.03/2011 and ESAVI/7256/04.10.07/2014). Ambient radiation levels at the trapping locations were measured at 1 cm above the ground with a hand-held GM dosimeter (Inspector, International Medcom INC, Sebastopol, CA, USA) calibrated to measure Sieverts (Sv); such measurements of radiation are repeatable among days and even years (Møller and Mousseau, 2013). Mean ambient radiation levels varied among trapping locations from 0.1 to 12.3 μSv/h within

FIGURE 1 | (a) Location of control population trapping sites in Ukraine. **(b)** Bank vole trapping sites in the Chernobyl Exclusion Zone (CEZ). Background radiation intensity is shown as circles (<1.0 μGy/h) and as triangles (up to 12.3 μGy/h). Created using ESRI ArcGIS 10.5. Satellite imagery[©].

the CEZ (**Figure 1**) and was 0.135 μSv/h at the three areas outside the CEZ. To estimate lifetime external doses, animals were allocated to two age groups based on head width, which is often used as a proxy of age in small mammals (Kallio et al., 2014): juveniles (<12.0 mm) and adults (≥12.1 mm). Accumulated external doses were calculated for 1 month (juveniles, ranging from 0.07 to 9.01 mGy) and for the range of 2–5 months (adults, ranging from 0.20 to 28.64 mGy; **Datasheet 1**).

After measuring head width (to 0.1 mm) and body mass (to 0.1 g), animals were euthanized by cervical dislocation and liver tissue samples transferred to Allprotect Tissue Reagent (Qiagen). We selected bank voles with 10–14 mm head width to reduce variation associated with maturation. Samples were stored at −80°C until processing.

Quantitative PCR (qPCR)

Intron-exon boundaries in five DSB damage response genes *Atm, Mre11, Brca1, p53,* and *p21* were identified using sequences from a draft bank vole genome (Genbank accession no. GCA_001305785). Bank vole gene sequences were aligned using online BLAST (Altschul et al., 1990) with default parameters against their putative mRNA homologs in the prairie vole (*Microtus ochrogaster*) available in Genbank: *p53* (XM_005349777), *Brca1* (XM_013354463), *Atm* (XM_013346263), *Mre11a* (XM_013355380), and *p21* (XM_005360336). For normalization of gene expression, we amplified two reference genes: beta-actin (*Actb*) and retention in endoplasmic reticulum sorting receptor 1 (*Rer1*). Beta-actin primers are based on a sequence from mouse (*Mus musculus*) and primers for *Rer1* were based on the putative gene sequence derived from bank vole genome. Primers were designed using Primer3 (Rozen and Skaletsky, 2000; **Table 1**). The mouse nucleotide database in Genbank was used to identify common transcripts and avoid potentially rare splice variants.

Up to 30 mg liver tissue per sample was homogenized using TissueLyser II (Qiagen) bead mill (2 × 2 min at 25 Hz),

TABLE 1 | qPCR primer information.

Gene	Primer sequence (5' –> 3')	Size (bp)	E
p53	CCA ACA CAA GCT CCT CTC CC ATT CGC GTC CTG AGC ATC C	145	1.900
Brca1	AGT TCC AGC CAC AAC CTT CAG CCT CTT GAG ATG GGC AGT TCC	156	1.900
Atm	GGA TGG CAT TGT GGT GAA GC AGG ACC TAT TTC TCC CAA ACA CC	121	1.944
Mre11a	GGC ACA ACA TCT AGC AAA CGG TGG CTG CTC ATG AAA GGG TC	101	2.038
Actb	TGC GTG ACA TCA AAG AGA AG GAT GCC ACA GGA TTC CAT A	197	1.906
Rer1	GGC CGA TCC TGG TGA TGT AC CCA CGT CCT CCT TCC CTT TG	132	1.986

and total RNA was extracted with RNeasy Mini Kit (Qiagen) that incorporated a DNase digestion step according to the manufacturer's protocol. Four hundred nanograms of total RNA per sample was used for reverse transcription in 20 μl reaction volumes using iScript cDNA synthesis kit (Bio-Rad) according to the manufacturer's protocol.

Quantitative PCRs were completed for each individual sample in 16 μl final reaction volumes that contained 4 ng cDNA template, 400 nM both forward and reverse primers and 8 μl LightCycler 480 SYBR Green I Master (Roche). Thermal cycling profiles were: 95°C for 5 min followed by, 95°C for 10 s, 60°C for 15 s (for all primers), and 72°C for 10 s (with recording), using a LightCycler 480 Real-Time PCR System (Roche). Primer specificity was determined by melt curve analysis and PCR efficiencies were calculated from standard curves using five-fold serial dilutions of mixed-sample liver cDNA (**Table 1**). All qPCRs were run as three technical replicates and a sample was re-analyzed if the standard deviation among replicates was >0.4. *Actb* showed slightly greater variation in expression ($SD = 0.97$ cycles, $n = 25$) than *Rer1* ($SD = 0.65$ cycles, $n = 25$) across samples.

Data Analysis

Raw data were imported into GenEx v.6.1 to allow PCR efficiency correction ($Cq = CqE\frac{\log 1+E}{\log 2}$, where CqE is the uncorrected C_q value and E is the PCR efficiency). Each sample was normalized against the geometric mean expression of two internal reference genes *Actb* and *Rer1* ($Cq_{norm} = CqGOI - \frac{1}{n}\sum_{i=1}^{n}CqRGi$) to control for outlying values (Vandesompele et al., 2002). C_q values were converted to relative linear scale with average expression of the control groups set as the reference level, after which all data were converted to $\log_2$ scale (**Datasheet 2**). Subsequent statistical analyses were performed in SPSS v.24.0 (IBM Corp. 2016).

First, we examined differences in gene expression between three groups of samples: (1) animals within the CEZ caught from areas with elevated ambient radiation dose rates ($>1.0 \mu$Gy/h, mean 4.8 μGy/h, conferring a yearly external radiation dose of between ~10 and 110 mGy at the most irradiated location), (2) animals from within the CEZ where ambient radiation was not dramatically elevated ($<1.0 \mu$Gy/h, mean 0.20 μGy/h) and (3) animals from outside the CEZ (mean 0.13 μGy/h). While the levels of soil radiation do not differ significantly between the latter two groups, bank voles inhabiting the CEZ may have moved among areas prior to capture. Variation in gene expression among the three groups and possible sex interaction was analyzed using two-way analysis of variance (ANOVA), followed by a Tukey's *post-hoc* test. Second, as no significant differences in gene expression could be attributed to an animal's sex or among samples within the CEZ (see *Results*), we made a comparison in gene expression between animals collected (1) from within the CEZ and (2) the three control areas, using a Student's *t*-test.

RESULTS

We quantified gene expression in five DDR genes *Atm, Mre11, p53, Brca1,* and *p21* in bank voles populating the CEZ. We chose these genes for their positions and signaling roles at the top of the DDR cascade to investigate possible activation of DDR response in a natural low-dose radiation environment. Our analyses were based on data from 57 animals: 30 (14 males, 16 females) from the CEZ, and 27 (14 m, 13 f) from Brody, Lubny, and, Korostyshev. Samples from the CEZ were further divided into two groups of "elevated" (7 m, 5 f) and "near-background" (7 m, 11 f) levels of environmental radioactivity as described above. Lifetime external doses within the "elevated" group were estimated to range between 1.14 and 9.01 mGy for juveniles and 2.82 to 28.64 mGy for adults, while in "near-background group" ranges were 0.07–0.34 mGy for juveniles and 0.13–1.68 mGy for adults. Gene expression levels were found to be similar between the three external control locations (**Datasheet 2**), and thus were considered as a single control group. Liver was selected as the tissue of interest as it is radiosensitive in a clinical context (Christiansen et al., 2007; Stryker, 2007); moreover, liver tissue appears sensitive to DNA damage, with liver tissue from bank voles exposed to environmental radionuclides having shorter telomeres compared with samples from control areas (Kesäniemi et al. unpublished).
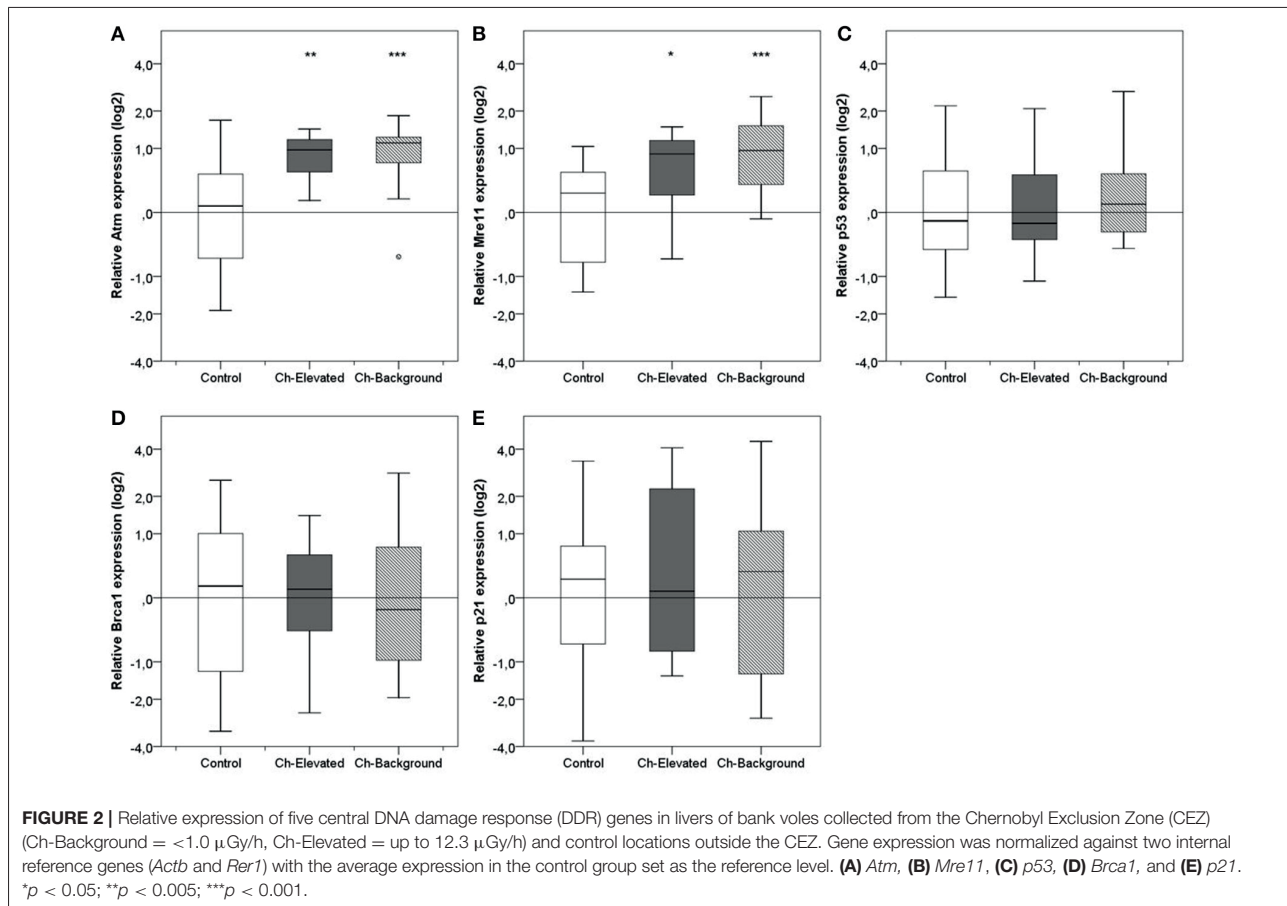
We found significant differential expression in *Mre11* and *Atm*, which could be explained by radioactivity [2-way ANOVA, Atm $F_{(2, 51)} = 9.52$, $P < 0.001$; Mre11 $F_{(2, 51)} = 10,18$, $P < 0.001$; p53 $F_{(2, 51)} = 0.34$, $P > 0.05$; Brca1 $F_{(2, 51)} = 0.04$, $P > 0.05$; p21 $F_{(2, 51)} = 0.62$, $P > 0.05$]. No significant differences in the expression of any of the five genes could be explained by sex [*Atm* $F_{(2, 51)} = 0.19$, $P > 0.05$; *Mre11* $F_{(2, 51)} = 0.60$, $P > 0.05$; *p53* $F_{(2, 51)} = 0.07$, $P > 0.05$; *Brca1* $F_{(2, 51)} = 1.82$, $P > 0.05$; *p21* $F_{(2, 51)} = 0.03$, $P > 0.05$]. Significant upregulation (compared with samples from control areas) of *Atm* and *Mre11* was observed in both "elevated" ($P_{Atm} < 0.01$, $P_{Mre11} < 0.05$) and "near-background" ($P_{Atm} < 0.001$, $P_{Mre11} < 0.001$) groups of samples from the CEZ, despite the significantly lower amount of environmental radiation in the latter group of samples (**Figure 2**); upregulation of *Mre11* was in fact slightly stronger (but non-significantly so) in the "near-background" treatment.

Hence, relative quantification of five DDR genes among samples (males and females) from (1) the CEZ and (2) the control areas outside the CEZ revealed significant upregulation in *Atm* and *Mre11* in bank voles inhabiting the CEZ compared with bank voles taken from control areas: transcription of mRNA increased almost two-fold in *Atm* (1.93-fold increase, $t_{(55)} = 4.51$, $P < 0.001$) and *Mre11* (1.87-fold increase, $t_{(55)} = 4.56$, $P < 0.001$), whereas no significant differences in mRNA levels of *p53, Brca1,* or *p21* were detected (**Figure 2**).

DISCUSSION

Exposure to IR causes DNA damage, and elevated DNA damage is characteristic of wildlife inhabiting areas affected by nuclear accident sites. An appropriate response from DNA repair pathways is an expected response to exposure to environmental radioactivity. We identified a significant, almost two-fold, upregulation in expression of *Atm* and *Mre11* in the livers of bank voles living within the CEZ, which is the first evidence that expression of DNA repair-related genes is stimulated in vertebrates exposed to low-dose environmental radioactivity.

A notable feature of these data is the similar gene expression in animals caught from within the CEZ, irrespective of the level of soil radionuclides at the trapping location. The CEZ comprises a mosaic of radionuclide contamination (Chesser et al., 2004) where the variation in radionuclide levels in soil and vegetation introduce small scale (few hundred meters) heterogeneity in the overall received doses for bank voles (Chesser et al., 2000). One explanation for the common upregulation effect is that bank voles can readily disperse over 1 km during the breeding season (Kozakiewicz et al., 2007) and thus individuals trapped from the areas with little or no soil radionuclides within the CEZ could have been exposed to substantial levels of radionuclides prior to capture. Bank voles inhabit burrows and have an opportunistic diet (Butet and Delettre, 2011), and are thus exposed to a wide variety of ingested radionuclides including the common fission product caesium-137. Caesium-137 is particularly problematic for ecosystems due to its capacity to form various water-soluble salts. Bank voles can carry potentially high amounts of

FIGURE 2 | Relative expression of five central DNA damage response (DDR) genes in livers of bank voles collected from the Chernobyl Exclusion Zone (CEZ) (Ch-Background = <1.0 μGy/h, Ch-Elevated = up to 12.3 μGy/h) and control locations outside the CEZ. Gene expression was normalized against two internal reference genes (*Actb* and *Rer1*) with the average expression in the control group set as the reference level. **(A)** *Atm*, **(B)** *Mre11*, **(C)** *p53*, **(D)** *Brca1*, and **(E)** *p21*. *$p < 0.05$; **$p < 0.005$; ***$p < 0.001$.

internal radiation sources (Baker et al., 2017). In this scenario, the common upregulation effect between contaminated and non-contaminated areas represents an average expression for inhabiting the CEZ especially if there are carry forward effects from exposure to very high amounts of radionuclides in prior generations. Such effects of past exposures have been reported with respect to mitochondrial mutation rates in these same voles (Baker et al., 2017) and would have the effect of averaging effects over broader geographic scales. Another possibility is that observed patterns reflect local adaptations that have spread from populations at contaminated regions to adjacent areas via gene flow (Møller et al., 2006; Fedorka et al., 2012) which could also account for a "higher than expected" level of expression in less contaminated areas within the CEZ.

Upregulation of DDR pathways of animals residing within the CEZ may seem intuitive, but these pathways have not been studied in wildlife inhabiting areas contaminated by radioactivity. That *Atm* is upregulated is relevant as this gene is positioned at the top of the DBS repair pathway. ATM is primarily regulated at the protein level when subjected to IR (Bakkenist and Kastan, 2003), but *Atm* promoter activity, and protein abundance, is stimulated by exposure to IR in mice tissues, including liver (Gueven et al., 2006); moreover, silencing

of ATM decreases radioresistance of glioma *in vitro* and *in vivo* (Li et al., 2016). Perhaps crucially, ATM is an important regulator of cellular oxidative stress (Barzilai et al., 2002), promoting the production of NADPH (Cosentino et al., 2011). Moreover, ATM can be activated by oxidative stress independently from DBS-related activation by the MRN complex (Guo et al., 2010). Antioxidant production likely constitutes a major part of the adaptive response against environmental radioactivity in birds within and around the CEZ (Galván et al., 2014) and in cell lines of fibroblasts from bank voles (Mustonen et al., submitted). Moreover, a change in fur color of bank voles within the CEZ was attributed to downregulation of pheomelanin to reallocate antioxidants to ROS defense (Boratynski et al., 2014). Indeed, upregulation of oxidative stress response genes *Cat* and *Fsd3* in *Arabidopsis* (Kovalchuk et al., 2014) indicate that increased ROS defense could be a key coping strategy against exposure to environmental radionuclides.

MRE11 is a constituent protein of the MRE11-RAD50-NBS1 complex, a multi-purpose maintainer of genomic stability whose tasks include DSB detection and subsequent activation of ATM protein (Lee and Paull, 2005) as well as DNA repair functions and telomeric maintenance (Lamarche et al., 2010). Reduced expression of the *Mre11* gene often leads to genomic instability,

and increased protein levels of ATM and MRE11 in some tumors are associated with resistance against radiotherapy (Tribius et al., 2001; Deng et al., 2011). An apparently low frequency of micronuclei in bank voles from the CEZ might indicate that this species has some degree of radioresistance (Rodgers and Baker, 2000). Given our results, *Atm* and *Mre11* represent important candidate genes that regulate genomic stability in bank voles exposed to environmental radionuclides.

Our observation of no significant variation in expression of *p53* may be explained by this gene being primarily regulated through post-translational modification of cellular protein (Kruse and Gu, 2009), although transcriptional upregulation has previously been detected in the livers of European wood mice inhabiting an abandoned uranium mine area (Lourenço et al., 2013). Significant enrichment of heavy metals (uranium and cadmium) were also detected in these mice, contributing to toxicity alongside radiation. Thus, radionuclide levels comparable to studied areas in the CEZ are not severe enough to induce transcription in *p53*. *P21* is under transcriptional regulation by p53 and is required for DNA damage related cell cycle inhibition (Bunz, 1998). That *p21* expression is not altered in animals inhabiting the CEZ implies cell cycle control pathways are not activated in response to increased *Atm* expression. *Brca1* is upregulated in response to genotoxic stress (De Siervi et al., 2010). A lack of change in expression of *Brca1* in bank voles from the CEZ indicates that the homologous recombination repair pathway is not a key component of the response to environmental radionuclides, consistent with a recent study of expression of DBS repair pathways during exposure to IR (Liu et al., 2016). *Arabidopsis* from the CEZ show reduced recombination, which might prevent gross chromosomal rearrangements (Kovalchuk et al., 2014).

As the expression of *p21* and *Brca1* is not stimulated it is plausible that the low-dose IR environment of Chernobyl does not cause sufficient DNA damage to warrant cell cycle arrest and activation of DSB repair. Nonetheless, some genomic impact is

derived from exposure to radionuclides as bank voles from the CEZ have shorter telomeres than bank voles from control areas (Kesäniemi et al., unpublished), likely reflecting an increase in oxidative stress that is widely associated with telomere shortening (von Zglinicki, 2002). Hence is it interesting that ATM can be activated by oxidation independently from MRN interaction. Altered telomere homeostasis may affect the expression of *Mre11* as a telomere maintainer and the role of this gene warrants further investigation.

AUTHOR CONTRIBUTIONS

TJ and PW: designed the outline of the study; AL, ET, AM, TM, TAM, and GM: were involved in setup of infrastructure in the field and animal sample collection, and TJ and JK: conducted molecular analyses and performed calculations; TJ: wrote the manuscript with input from all other authors.

ACKNOWLEDGMENTS

SUPPLEMENTARY MATERIAL

The Supplementary Material for this article can be found online at: https://www.frontiersin.org/articles/10.3389/fenvs.2017.00095/full#supplementary-material

Datasheet 1 | Accumulated external dose estimations by age groups.

Datasheet 2 | qPCR raw and normalized quantification cycle data.

REFERENCES

Altschul, S. F., Gish, W., Miller, W., Myers, E. W., and Lipman, D. J. (1990). Basic local alignment search tool. *J. Mol. Biol.* 215, 403–410. doi: 10.1016/S0022-2836(05)80360-2

Baker, R. J., Dickins, B., Wickliffe, J. K., Khan, F. A., Gaschak, S., Makova, K., et al. (2017). Elevated mitochondrial genome variation after 50 generations of radiation exposure in a wild rodent. *Evol. Appl.* 10, 784–791. doi: 10.1111/eva.12475

Baker, R. J., Hamilton, M. J., Van Den Bussche, R. A., Wiggins, L. E., Sugg, D. W., Smith, M. H., et al. (1996). Small mammals from the most radioactive sites near the chornobyl nuclear power plant. *J. Mammal.* 77, 155–170. doi: 10.2307/1382717

Bakkenist, C. J., and Kastan, M. B. (2003). DNA damage activates ATM through intermolecular autophosphorylation and dimer dissociation. *Nature* 421, 499–506. doi: 10.1038/nature01368

Barzilai, A., Rotman, G., and Shiloh, Y. (2002). ATM deficiency and oxidative stress: a new dimension of defective response to DNA damage. *DNA Repair* 1, 3–25. doi: 10.1016/S1568-7864(01)00007-6

Bonisoli-Alquati, A., Voris, A., Mousseau, T. A., Møller, A. P., Saino, N., and Wyatt, M. D. (2010). DNA damage in barn swallows (*Hirundo rustica*) from the Chernobyl region detected by use of the comet assay. *Comp. Biochem. Physiol. C Toxicol. Pharmacol.* 151, 271–277. doi: 10.1016/j.cbpc.2009.11.006

Bonisoli-Alquati, A., Koyama, K., Tedeschi, D. J., Kitamura, W., Sukuzi, H., Ostermiller, S., et al. (2015). Abundance and genetic damage of barn swallows from Fukushima. *Sci. Rep.* 5:9432. doi: 10.1038/srep09432

Boratynski, Z., Lehmann, P., Mappes, T., Mousseau, T. A., and Møller, A. P. (2014). Increased radiation from Chernobyl decreases the expression of red colouration in natural populations of bank voles (*Myodes glareolus*). *Sci. Rep.* 4:7141. doi: 10.1038/srep07141

Boubriak, I. I., Grodzinsky, D. M., Polischuk, V. P., Naumenko, V. D., Gushcha, N. P., Micheev, A. N., et al. (2008). Adaptation and impairment of DNA repair function in pollen of *Betula verrucosa* and seeds of *Oenothera biennis* from differently radionuclide- contaminated sites of Chernobyl. *Ann. Bot.* 101, 267–276. doi: 10.1093/aob/mcm276

Bunz, F. (1998). Requirement for p53 and p21 to sustain G2 arrest after DNA damage. *Science* 282, 1497–1501. doi: 10.1126/science.282.5393.1497

Butet, A., and Delettre, Y. R. (2011). Diet differentiation between European *Arvicoline* and *Murine* rodents. *Acta Theriol.* 56, 297–304. doi: 10.1007/s13364-011-0049-6

Cannan, W. J., and Pederson, D. S. (2016). Mechanisms and consequences of double-strand break formation in chromatin. *J. Cell. Physiol.* 231, 3–14. doi: 10.1002/jcp.25048

Chesser, R. K., Bondarkov, M., Baker, R. J., Wickliffe, J. K., and Rodgers, B. E. (2004). Reconstruction of radioactive plume characteristics

along Chernobyl's Western Trace. *J. Environ. Radioact.* 71, 147–157. doi: 10.1016/S0265-931X(03)00165-6

Chesser, R. K., Sugg, D. W., Lomakin, M. D., van den Bussche, R. A., DeWoody, J. A., Jagoe, C. H., et al. (2000). Concentrations and dose rate estimates of ^{134137}cesium and ^{90}strontium in small mammals at chornobyl, Ukraine. *Environ. Toxicol. Chem.* 19, 305–312. doi: 10.1002/etc.5620190209

Christiansen, H., Sheikh, N., Saile, B., Reuter, F., Rave-Fränk, M., Hermann, R. M., et al. (2007). x-Irradiation in rat liver: consequent upregulation of hepcidin and downregulation of hemojuvelin and ferroportin-1 gene expression. *Radiology* 242, 189–197. doi: 10.1148/radiol.2421060083

Cosentino, C., Grieco, D., and Costanzo, V. (2011). ATM activates the pentose phosphate pathway promoting anti-oxidant defence and DNA repair. *EMBO J.* 30, 546–555. doi: 10.1038/emboj.2010.330

Cristaldi, M., Ieradi, L. A., Mascanzoni, D., and Mattei, T. (1991). Environmental impact of the Chernobyl accident: mutagenesis in bank voles from Sweden. *Int. J. Radiat. Biol.* 59, 31-40. doi: 10.1080/09553009114550031

Daley, J. M., and Sung, P. (2014). 53BP1, BRCA1, and the choice between recombination and end joining at DNA double-strand breaks. *Mol. Cell. Biol.* 34, 1380–1388. doi: 10.1128/MCB.01639-13

Deng, R., Tang, J., Ma, J.-G., Chen, S.-P., Xia, L.-P., Zhou, W.-J., et al. (2011). PKB/Akt promotes DSB repair in cancer cells through upregulating Mre11 expression following ionizing radiation. *Oncogene* 30, 944–955. doi: 10.1038/onc.2010.467

Deryabina, T. G., Kuchmel, S. V., Nagorskaya, L. L., Hinton, T. G., Beasley, J. C., Lerebours, A., et al. (2015). Long-term census data reveal abundant wildlife populations at Chernobyl. *Curr. Biol.* 25, R824–R826. doi: 10.1016/j.cub.2015.08.017

De Siervi, A., De Luca, P., Byun, J. S., Di, L. J., Fufa, T., Haggerty, C. M., et al. (2010). Transcriptional autoregulation by BRCA1. *Cancer Res.* 70:532. doi: 10.1158/0008-5472.CAN-09-1477

Dreicer, M., Aarkrog, A., Alexakhin, R., Anspaugh, L., Arkhipov, N. P., and Johansson, K.-J. (1996). "Consequences of the Chernobyl accident for the natural and human environments," in *International Conference on "One Decade after Chernobyl: Summing up the Consequences of the Accident"* (Vienna) (IAEA), 319–361.

Dzyubenko, E. V., and Gudkov, D. I. (2009). Cytogenetical and haematological effects of long-term irradiation on freshwater gastropod snails in the Chernobyl accident exclusion zone. *Radioprotection* 44, 933–936. doi: 10.1051/radiopro/20095166

Einor, D., Bonisoli-Alquati, A., Costantini, D., Mousseau, T. A., and Møller, A. P. (2016). Ionizing radiation, antioxidant response and oxidative damage: a meta-analysis. *Sci. Total Environ.* 548–549, 463–471. doi: 10.1016/j.scitotenv,.2016.01.027

Fedorka, K. M., Winterhalter, W. E., Shaw, K. L., Brogan, W. R., and Mousseau, T. A. (2012). The role of gene flow asymmetry along an environmental gradient in constraining local adaptation and range expansion. *J. Evol. Biol.* 25, 1676–1685. doi: 10.1111/j.1420-9101.2012.02552.x

Fujita, Y., Yoshihara, Y., Sato, I., and Sato, S. (2014). Environmental radioactivity damages the DNA of earthworms of Fukushima Prefecture, Japan. *Eur. J. Wildl. Res.* 60, 145–148. doi: 10.1007/s10344-013-0767-y

Galván, I., Bonisoli-Alquati, A., Jenkinson, S., Ghanem, G., Wakamatsu, K., Mousseau, T. A., et al. (2014). Chronic exposure to low-dose radiation at Chernobyl favours adaptation to oxidative stress in birds. *Funct. Ecol.* 28, 1387–1403. doi: 10.1111/1365-2435.12283

Giglia-Mari, G., Zotter, A., and Vermeulen, W. (2011). DNA damage response. *Cold Spring Harb. Perspect. Biol.* 3, 1–19. doi: 10.1101/cshperspect.a000745

Goncharova, R. I., and Ryabokon, N. I. (1995). Dynamics of cytogenetic injuries in natural populations of bank vole in the Republic of Belarus. *Radiat. Prot. Dosimetry* 62, 37–40. doi: 10.1093/oxfordjournals.rpd.a082816

Gueven, N., Fukao, T., Luff, J., Paterson, C., Kay, G., Kondo, N., et al. (2006). Regulation of the Atm promoter *in vivo*. *Genes Chromosomes Cancer* 45, 61–71. doi: 10.1002/gcc.20267

Guo, Z., Kozlov, S., Lavin, M. F., Person, M. D., and Paull, T. T. (2010). ATM activation by oxidative stress. *Science* 330, 517–521. doi: 10.1126/science.1192912

Hayashi, G., Shibato, J., Imanaka, T., Cho, K., Kubo, A., Kikuchi, S., et al. (2014). Unraveling low-level gamma radiation-responsive changes in expression of

early and late genes in leaves of rice seedlings at litate Village, Fukushima. *J. Hered.* 105, 723–738. doi: 10.1093/jhered/esu025

Hutterer, R., Kryštufek, B., Yigit, N., Mitsain, G., Palomo, L. J., Henttonen, H., et al. (2016). *Myodes glareolus*. *IUCN Red List Threat. Species* 2016.

Kallio, E. R., Begon, M., Birtles, R. J., Bown, K. J., Koskela, E., Mappes, T., et al. (2014). First report of *Anaplasma phagocytophilum* and *Babesia microti* in rodents in Finland. *Vector Borne Zoonotic Dis.* 14, 389–393. doi: 10.1089/vbz.2013.1383

Kovalchuk, I., Abramov, V., Pogribny, I., Kovalchuk, O., Physiology, S. P., and May, N. (2014). Molecular aspects of plant adaptation to life in the chernobyl zone. *Plant Physiol.* 135, 357–363. doi: 10.1104/pp.104.040477

Kozakiewicz, M., Chołuj, A., and Kozakiewicz, A. (2007). Long-distance movements of individuals in a free-living bank vole population: an important element of male breeding strategy. *Acta Theriol.* 52, 339–348. doi: 10.1007/BF03194231

Kruse, J.-P., and Gu, W. (2009). Modes of p53 regulation. *Cell* 137, 609–622. doi: 10.1016/j.cell.2009.04.050

Lamarche, B. J., Orazio, N. I., and Weitzman, M. D. (2010). The MRN complex in double-strand break repair and telomere maintenance. *FEBS Lett.* 584, 3682–3695. doi: 10.1016/j.febslet.2010.07.029

Lee, J.-H., and Paull, T. T. (2005). ATM activation by DNA double-strand breaks through the Mre11-Rad50-Nbs1 complex. *Science* 308, 551–554. doi: 10.1126/science.1108297

Lehmann, P., Boratynski, Z., Mappes, T., Mousseau, T. A., and Møller, A. P. (2016). Fitness costs of increased cataract frequency and cumulative radiation dose in natural mammalian populations from Chernobyl. *Sci. Rep.* 6:19974. doi: 10.1038/srep19974

Li, Y., Li, L., Li, B., Wu, Z., Wu, Y., Wang, Y., et al. (2016). Silencing of ataxia-telangiectasia mutated by siRNA enhances the *in vitro* and *in vivo* radiosensitivity of glioma. *Oncol. Rep.* 35, 3303-3312. doi: 10.3892/or.2016.4754

Liu, M., Wang, H., Lee, S., Liu, B., Dong, L., and Wang, Y. (2016). DNA repair pathway choice at various conditions immediately post irradiation. *Int. J. Radiat. Biol.* 92, 819–822. doi: 10.1080/09553002.2016.1230243

Lourenço, J., Mendo, S., and Pereira, R. (2016). Radioactively contaminated areas: bioindicator species and biomarkers of effect in an early warning scheme for a preliminary risk assessment. *J. Hazard. Mater.* 317, 503–542. doi: 10.1016/j.jhazmat.2016.06.020

Lourenço, J., Pereira, R., Gonçalves, F., and Mendo, S. (2013). Metal bioaccumulation, genotoxicity and gene expression in the European wood mouse (*Apodemus sylvaticus*) inhabiting an abandoned uranium mining area. *Sci. Total Environ.* 443, 673–680. doi: 10.1016/j.scitotenv.2012.10.105

Møller, A. P., Hobson, K. A., Mousseau, T. A., and Peklo, A. M. (2006). Chernobyl as a population sink for barn swallows: tracking dispersal using stable-isotope profiles. *Ecol. Appl.* 16, 1696–1705. doi: 10.1890/1051-0761(2006)016[1696:CAAPSF]2.0.CO;2

Møller, A. P., and Mousseau, T. A. (2013). Assessing effects of radiation on abundance of mammals and predator-prey interactions in Chernobyl using tracks in the snow. *Ecol. Indic.* 26, 112–116. doi: 10.1016/j.ecolind.2012.10.025

Møller, A. P., and Mousseau, T. A. (2015). Strong effects of ionizing radiation from Chernobyl on mutation rates. *Sci. Rep.* 5:8363. doi: 10.1038/srep08363

Møller, A. P., and Mousseau, T. A. (2006). Biological consequences of Chernobyl: 20 years on. *Trends Ecol. Evol.* 21, 200–207. doi: 10.1016/j.tree.2006.01.008

Nikitaki, Z., Pavlopoulou, A., Holá, M., Donà, M., Michalopoulos, I., Balestrazzi, A., et al. (2017). Bridging plant and human radiation response and DNA repair through an *in silico* approach. *Cancers* 9:E65. doi: 10.3390/cancers9060065

Rodgers, B. E., and Baker, R. J. (2000). Frequencies of micronuclei in bank voles from zones of high radiation at chornobyl, Ukraine. *Environ. Toxicol. Chem.* 19, 1644–1648. doi: 10.1002/etc.5620190623

Rozen, S., and Skaletsky, H. (2000). Primer3 on the WWW for general users and for biologist programmers. *Methods Mol. Biol.* 132, 365–386. doi: 10.1385/1-59259-192-2:365

Stryker, J. A. (2007). Science to practice: why is the liver a radiosensitive organ? *Radiology* 242, 1–2. doi: 10.1148/radiol.2421061103

Tribius, S., Pidel, A., and Casper, D. (2001). ATM protein expression correlates with radioresistance in primary glioblastoma cells in culture. *Int. J. Radiat. Oncol. Biol. Phys.* 50, 511–523. doi: 10.1016/S0360-3016(01)01489-4

Vandesompele, J., De Preter, K., Pattyn, F., Poppe, B., Van Roy, N., De Paepe, A., et al. (2002). Accurate normalization of real-time quantitative RT-PCR

data by geometric averaging of multiple internal control genes. *Genome Biol.* 3:RESEARCH0034. doi: 10.1186/gb-2002-3-7-research0034

von Zglinicki, T. (2002). Oxidative stress shortens telomeres. *Trends Biochem. Sci.* 27, 339–344. doi: 10.1016/S0968-0004(02)02110-2

Ward, J. F. (1988). DNA damage produced by ionizing radiation in mammalian cells: identities, mechanisms of formation, and reparability, *Prog. Nucleic Acid Res. Mol. Biol.* 35, 95–125.

Ward, J. F. (1990). The yield of DNA double-strand breaks produced intracellularly by ionizing radiation: a review. *Int. J. Radiat. Biol.* 57, 1141–1150. doi: 10.1080/09553009014551251

Wheatley, S., Sovacool, B. K., and Sornette, D. (2016). Reassessing the safety of nuclear power. *Energy Res. Soc. Sci.* 15, 96–100. doi: 10.1016/j.erss.2015.12.026

Supplementary material for this article: https://doi.org/10.17011/jyx/dataset/80621

II

EXPOSURE TO ENVIRONMENTAL RADIONUCLIDES
IS ASSOCIATED WITH ALTERED METABOLIC AND
IMMUNITY PATHWAYS IN A WILD RODENT

by

Kesäniemi J, Jernfors T, Lavrinienko A, Kivisaari K, Kiljunen M,
Mappes T & Watts PC. 2019

ORIGINAL ARTICLE

MOLECULAR ECOLOGY WILEY

Exposure to environmental radionuclides is associated with altered metabolic and immunity pathways in a wild rodent

Jenni Kesäniemi[1] [iD] | Toni Jernfors[1] [iD] | Anton Lavrinienko[1] [iD] | Kati Kivisaari[2] [iD] |
Mikko Kiljunen[2] [iD] | Tapio Mappes[2] [iD] | Phillip C. Watts[1,2] [iD]

[1]Ecology and Genetics Research Unit, University of Oulu, Oulu, Finland

[2]Department of Biological and Environmental Science, University of Jyväskylä, Jyväskylä, Finland

Correspondence
Jenni Kesäniemi, Ecology and Genetics Research Unit, University of Oulu, Oulu, Finland.
Email: jenni.e.kesaniemi@jyu.fi

Funding information
Academy of Finland, Grant/Award Number: 287153 and 268670

Abstract

Wildlife inhabiting environments contaminated by radionuclides face putative detrimental effects of exposure to ionizing radiation, with biomarkers such as an increase in DNA damage and/or oxidative stress commonly associated with radiation exposure. To examine the effects of exposure to radiation on gene expression in wildlife, we conducted a de novo RNA sequencing study of liver and spleen tissues from a rodent, the bank vole *Myodes glareolus*. Bank voles were collected from the Chernobyl Exclusion Zone (CEZ), where animals were exposed to elevated levels of radionuclides, and from uncontaminated areas near Kyiv, Ukraine. Counter to expectations, we did not observe a strong DNA damage response in animals exposed to radionuclides, although some signs of oxidative stress were identified. Rather, exposure to environmental radionuclides was associated with upregulation of genes involved in lipid metabolism and fatty acid oxidation in the livers – an apparent shift in energy metabolism. Moreover, using stable isotope analysis, we identified that fur from bank voles inhabiting the CEZ had enriched isotope values of nitrogen: such an increase is consistent with increased fatty acid metabolism, but also could arise from a difference in diet or habitat between the CEZ and elsewhere. In livers and spleens, voles inhabiting the CEZ were characterized by immunosuppression, such as impaired antigen processing, and activation of leucocytes involved in inflammatory responses. In conclusion, exposure to low dose environmental radiation impacts pathways associated with immunity and lipid metabolism, potentially as a stress-induced coping mechanism.

KEYWORDS
DNA repair, *Myodes glareolus*, pollution, radionuclides, RNAseq, stable isotope

1 | INTRODUCTION

Human actions pose numerous stressors such as warming, extreme weather and pollutants, to wildlife at both global and local scales, with loss and deterioration of habitat presenting major impacts to many species (Acevedo-Whitehouse & Duffus, 2009). Organisms that persist in the face of a changing environment need to mount an appropriate genomic response, often achieved using altered transcriptional activity. Analyses of these transcriptional changes provide key insights into the biological pathways that underline

---

any physiological response (Evans, Pespeni, Hofmann, Palumbi, & Sanford, 2017; Pujolar et al., 2012).

Exposure to radionuclides is a source of genotoxicity to wildlife, with numerous human activities, for example processes involved in uranium mining, nuclear energy production and its waste treatment, or nuclear tests, having left many contaminated areas worldwide (reviewed by Lourenço, Mendo, & Pereira, 2016). Perhaps the most notable areas of radionuclide contamination in the natural environment are derived from the accidents at the Nuclear Power Plants (NPPs) at Chernobyl (Ukraine, 1986) and at Fukushima (Japan, 2011). Wildlife inhabiting the area surrounding the former NPP at Chernobyl provide the best-studied models of the biological impacts of exposure to environmental radionuclides. The accident at the Chernobyl NPP Reactor 4 released more than 9 million terabecquerels (TBq) of radionuclides over a wide area (>200,000 km^2) of Europe and eastern Russia. Subsequently, the Chernobyl Exclusion Zone (CEZ) was established at an approximately 30 km radius (~4,300 km^2 area) around the accident site to limit human exposure to the radioactive fallout. However, the wildlife inhabiting the CEZ are exposed to elevated levels of persistent radioisotopes, notably strontium-90 (^{90}Sr), cesium-137 (^{137}Cs), and plutonium-239 (^{239}Pu) (Møller & Mousseau, 2006).

Detrimental effects of chronic exposure to radiation in wildlife have been reported at multiple biological scales (reviewed by Lourenço et al., 2016). For example, the community diversity of soil bacteria (Romanovskaya, Sokolov, Rokitko, & Chernaya, 1998), abundance of soil invertebrates (Møller & Mousseau, 2018) and the density of mammals (Møller & Mousseau, 2013) negatively correlate with levels of radiation within and around the CEZ. At the organismal level, wildlife affected by Chernobyl fallout exhibit a suite of phenotypic effects such as aspermy and reduced sperm motility (Møller, Bonisoli-Alquati, Mousseau, & Rudolfsen, 2014) and smaller brains (Møller, Bonisoli-Alquati, Rudolfsen, & Mousseau, 2011): comparable impacts have been reported in studies of organisms affected by the Fukushima nuclear accident (Lourenço et al., 2016). Conversely, many studies fail to find notable biological impacts of exposure to environmental radionuclides, for example on the community diversity of macro-organisms (Murphy, Nagorskaya, & Smith, 2011), or in the abundance or density of wildlife (Deryabina et al., 2015). At a molecular level, an apparent increase of DNA damage, chromosomal aberrations (Lourenço et al., 2016), oxidative stress (Einor, Bonisoli-Alquati, Costantini, Mousseau, & Møller, 2016) and/or mutation rate (Møller & Mousseau, 2015) have been associated with exposure to environmental radionuclides (but cf. [Kesäniemi et al., 2018] who found no evidence that mutation rate was elevated in bank voles inhabiting the CEZ). Despite the numerous and often contradictory studies on the diverse impacts of exposure to environmental radionuclides, changes in genome-wide gene expression associated with exposure to low dose environmental radionuclides are poorly understood.

While exposure to environmental radionuclides impacts gene expression, it is hard to identify a general response of organisms because studies typically quantify expression of candidate genes from

DNA repair and oxidative stress pathways. For example, the level of soil radionuclides within and around the CEZ is associated with the activity of some candidate radical scavenging and DNA damage response genes in plants (Kovalchuk, 2004) and in a rodent, the bank vole *Myodes glareolus* (Jernfors et al., 2018). Away from Chernobyl, increased DNA damage and elevated expression of selected DNA damage and repair candidate genes were observed in European wood mice (*Apodemus sylvaticus*) exposed to uranium mining waste (Lourenço, Pereira, Gonçalves, & Mendo, 2013) and marine mussels (*Mytilus* sp.) from sediments with low (0.61 μGy/hr) levels of radionuclides (Alamri, Cundy, Di, Jha, & Rotchell, 2012). A clear limitation of the candidate gene approach is that it overlooks the potential action of many other cellular and molecular processes. For example, biomedical studies have shown that in addition to inducing DNA repair pathways, exposure to acute, high dose (>1 Gy) radiation can repress the adaptive immune system while stimulating a proinflammatory response (Di Maggio et al., 2015; Hekim, Cetin, Nikitaki, Cort, & Saygili, 2015). The effects of chronic exposure to relatively low environmental radiation in wildlife immunity is not well known. However, a microarray study has shown that exposure to environmental radionuclides correlates with upregulation of the inflammatory cytokine IFNγ in the intestines of pigs affected by radionuclide fallout from Fukushima (Morimoto et al., 2017). Here, we used RNAseq to analyze the transcriptional response by wildlife (the bank vole) exposed to environmental radionuclides.

The bank vole *Myodes glareolus* is a small rodent that inhabits deciduous or coniferous forests throughout much of northern Europe and Asia (Macdonald, 2007). This species is an ideal model to quantify the genomic effects of exposure to environmental radiation as it was one of the first mammals to recolonize areas contaminated by radionuclides following the Chernobyl accident (Chesser et al., 2000). As bank voles burrow in soil and have a varied diet (including fungi, invertebrates and plants; Butet & Delettre, 2011), animals living within the CEZ can experience considerable absorbed doses of radiation (either from the soil or by consuming contaminated food); for example, bank voles from the Red Forest had average absorbed doses of radiocesium of 6.7 mGy/day (Baker et al., 2017; Chesser et al., 2000).

To examine the effects of environmental radionuclide exposure on gene expression in wild bank voles, RNAseq data were obtained for the liver and spleen tissues, as they have contrasting biological functions and different radiosensitivities. The liver is an organism's metabolic centre where it regulates energy metabolism, detoxification processes and produces diverse metabolites. The spleen has a central role in maintaining immune system function, for example via its association with storage and activation of immune cells, antibody release, and production of inflammatory mediators. The spleen, like other lymphoid organs, has a high radiosensitivity, in contrast to the liver that apparently has a fairly low radiosensitivity (Rubin & Casarett, 1968). We predicted that exposure to radionuclides will (a) elicit changes in transcriptional activity of DNA repair and oxidative stress response pathway genes, given the prevalence of studies reporting the impact of exposure to radionuclides on these molecular

functions (reviewed by Einor et al., 2016; Lourenço et al., 2016). Also, we expected to find (b) changes in gene expression affecting the immune and inflammatory pathways given the prominence of these pathways in biomedical literature examining molecular impacts of exposure to radiation (Hekim et al., 2015; Kam & Banati, 2013). Finally, we predicted (c) more pronounced transcriptional differences in immune responses in the spleen than in the liver, due to its role in immune functions and its apparently high radiosensitivity.

2 | MATERIALS AND METHODS

2.1 | Sample collection

Bank voles were collected from four sampling areas (*n* = 40, 10 voles from each area) in Ukraine (18th-25th of July, 2016): two locations (Vesnyane and Gluboke, 33 km apart) within the Chernobyl Exclusion Zone (CEZ) that were contaminated by radionuclides, and two uncontaminated locations near Kyiv (Kyiv west and east, 26 km apart; see map in Figure S1). We sampled voles from both sides of the Dnieper and Pripyat rivers, which represent a population genetic barrier. As bank voles from locations to the east of these rivers are genetically more similar than bank voles from locations on the west of these rivers (Kesäniemi, J., Lavrinienko, A., Tukalenko, E., Boratyński, Z., Kivisaari, K., Mappes, T., Milinevsky, G., Møller, A.P., Mousseau, T.A. & Watts, P.C., unpublished data), our sampling design incorporates two genetically different samples within each treatment, while maintaining genetically similar samples among treatments (e.g., the locations Vesnyane, CEZ and Kyiv west were similar). Animals were sampled from similar mixed forest habitats.

Bank voles were trapped using the Ugglan Special2 live traps (Grahnab, Sweden), with sunflower seeds and potato as bait. Environmental radiation was measured at ground level at each trapping site using a hand-held GM dosimeter (Inspector, International Medcom INC, Sebastopol, CA, USA). The mean level of ambient radiation dose rate (measured in μGy/hr) within the CEZ locations was significantly higher than at the locations outside the CEZ (μGy/hr, mean ± *SD*: Vesnyane = 18.03 ± 0.9, Gluboke = 14.74 ± 5.3, Kyiv west = 0.15 ± 0.0, Kyiv east = 0.30 ± 0.0; Kruskal–Wallis test, χ^2 = 34.871, *df* = 3, *p* < .001).

We estimated ^{137}Cs activity (whole-body burden) for each vole using a SAM 940 radionuclide identifier system (Berkeley Nucleonics Corporation, San Rafael, CA, USA) equipped with a 3″ × 3″ NaI detector. The detector was shielded by 10 cm of lead to reduce noise from the background radioactivity. With corrections for laboratory background, the activity of ^{137}Cs was evaluated from the obtained spectra in energies window 619–707 keV with cesium photopeak at 662 keV. Reliable measurements of cesium activity could not be made for 14 voles from Kyiv, because the ^{137}Cs activity in these animals was below the detectability level, i.e. the decision threshold (the level of 95% probability that the signal from detector is caused by background fluctuation). Cesium activity (radiocesium Becquerels per kg, Bq/kg) was thus estimated for six bank voles from the Kyiv locations (Bq/kg, median [lower quartile;upper quartile]: Kyiv = 542

[506; 594]) and all CEZ voles (Bq/kg, median [lower quartile; upper quartile]: Vesnyane = 4,117 [2,620; 22,215], Gluboke = 12,319 [2,797; 27,044]). Cesium activity was significantly higher in voles from the CEZ than from Kyiv locations (Mann-Whitney *U* test, *U* = 120.00, *p* < .001, *n* = 26).

Animals were euthanized by cervical dislocation and the livers and spleens immediately stored in AllProtect Tissue Reagent (Qiagen). Body size (weight, head width) was recorded for all individuals. As a general estimation of physiological condition of the voles, a body condition index was calculated for each individual as the standardized residual value from a linear regression of weight (dependent variable) against head width: a positive body condition index value reflects a better condition, i.e., heavier animals with greater energy reserves (Schulte-Hostedde, Millar, & Hickling, 2001).

2.2 | RNA extraction, library preparation and sequencing

Total RNA was extracted using RNeasy Mini Kit (Qiagen) according to the manufacturer's protocol. Samples from both tissues and all sampling locations were processed (RNA extractions and sequencing) at random order (see Appendix S1). Libraries were prepared using an Illumina TruSeq RNA Sample Prep Kit version 2 for 100 bp paired-end (PE) sequencing. Individually barcoded samples were sequenced on an Illumina HiSeq4000 (Beijing Institute of Genomics, Hong Kong).

2.3 | De novo transcriptome assembly, annotation and data analysis

Liver and spleen reads from four voles (one from each location) were combined (a total of 156,478,452 PE reads) for de novo transcriptome assembly. The transcriptome was assembled using Trinity version 2.4.0 (Grabherr et al., 2011) with default parameters. Most downstream analyses followed Trinity best-practice guidelines (Haas et al., 2013; see Appendix S1). The transcriptome was annotated using Trinotate version 3.0.1 (https://trinotate.github.io/). Reads from liver (*n* = 39, as sequencing of one liver RNA sample from Kyiv east failed, see Table S1) and spleen (*n* = 40) samples were mapped to the transcriptome using Bowtie version 1.1.1 (Langmead, Trapnell, Pop, & Salzberg, 2009), with number of aligned reads quantified using RSEM version 1.3.0 (Li & Dewey, 2011). Transcript abundance was examined by principal component analysis, which revealed one individual (from Vesnyane, CEZ; Figure S2) to be clearly positioned outside the cluster of all other samples (in both tissues). This outlier individual was removed from all subsequent analyses (leaving final sample sizes of *n* = 38 for liver and *n* = 39 for spleen, Figure S2). Analysis of differential expression comparing CEZ sites and uncontaminated Kyiv sites for the two tissues separately were performed at the gene level using DESEQ2 version 1.10.1 (Love, Huber, & Anders, 2014), with a two-fold minimum change and a maximum false discovery rate (FDR) threshold of 0.001. Biological functions and pathways affected by environmental radiation were identified using gene ontology (GO) enrichment analysis implemented

TABLE 1 Transcriptome assembly statistics

Number of transcripts	445,192
Number of genes	273,880
GC%	48.10
Median contig length	453
Average contig length	1,050.39
N50	2,258
Number of transcripts in E90 set	51,173
E90N50	2,874

by GOseq Bioconductor version 1.26.0 (Young, Wakefield, Smyth, & Oshlack, 2010) on the DE genes (DEGs) within each tissue and the assembled and annotated transcriptome as a background set.

2.4 | Gene coexpression networks

To investigate whether inhabiting the CEZ impacted gene expression interactions, weighted topological overlap gene coexpression networks were constructed using wTO (Gysi, Voigt, Fragoso, Almaas, & Nowick, 2018) in R 3.5.0 (R Core Team, 2018). For both tissues separately, pairwise correlation networks with positive and negative interactions between genes were built for each of the four sites (using wTO. Complete mode with Pearson correlations and 1,000 bootstraps), using 3,000 of the most highly expressed genes in both tissues (TPM count data). Consensus networks were then built for the CEZ and Kyiv sites. To identify similarities and differences between the consensus networks, the networks were compared using CoDiNA (Gysi, de Miranda Fragoso, Buskamp, Almaas, & Nowick, 2018) in R, where only the significant correlations were retained (links with not significant wTO values [$p > .001$] were set to zero). CoDiNA assigns each link into one of three categories; α links are present in both consensus networks with the same sign (negative or positive correlation between genes), β links are present in both networks but with a different sign of the link's weight (different interaction between the genes), and γ links are specific to one of the networks (see Appendix S1).

2.5 | Stable isotope analysis

As voles from the CEZ showed differences in metabolic pathways compared to the voles from uncontaminated areas, bank vole dietary preferences were examined using stable isotope analysis (SIA). SIA from consumers' tissues reflects the isotopic composition of the diet, since food sources, such as plant types, seeds or invertebrates, differ in their isotopic compositions (Baltensperger, Huettmann, Hagelin, & Welker, 2015; Calandra et al., 2015). Animal fur has a slow isotopic turnover rate and reflects the isotopic signal of consumed food from the past several months in rodents (Kurle, Koch, Tershy, & Croll, 2014). Abundance of ^{15}N increase with transfer between trophic levels relative to ^{14}N, and the ratio of these stable isotopes ($\delta^{15}N$) can be used to define an organism's trophic position. Due to the difference in assimilation of stable isotopes of carbon by primary producers in ecosystems, ratio of carbon isotopes ($\delta^{13}C$) can be used as an indicator of the food source (Ben-David & Flaherty, 2012). Samples of bank vole fur and putative food items (collected from the vole sample locations) were analyzed for $\delta^{15}N$ and $\delta^{13}C$ (Appendix S1 and Table S2). Fur $\delta^{15}N$ values were correlated with gene expression changes (TMM-normalized count values of all annotated DEGs in both tissues) using Pearson correlations in R 3.5.0 (function 'rcorr'; R Core Team, 2018), with p-values corrected by Benjamini-Hochberg method and considered significant at FDR < 0.05.

3 | RESULTS

3.1 | Bank vole body condition

All individuals were adult females with no significant difference in either weight (g, mean ± SD: Vesnyane = 22.4 ± 4.8, Gluboke = 21.8 ± 3.0, Kyiv west = 21.0 ± 2.6, Kyiv east = 22.2 ± 3.3; ANOVA, $F = 0.319$, $df = 3$, $p = .812$) or head width, a proxy for age (Kallio et al., 2014) (mm, mean ± SD: Vesnyane = 13.0 ± 0.4, Gluboke = 12.8 ± 0.5, Kyiv west = 13.1 ± 0.3, Kyiv east = 12.8 ± 0.2; ANOVA $F = 1.109$, $df = 3$, $p = .356$) among the four sampling locations. Animals from the CEZ and Kyiv area did not differ significantly in body condition index (BCI, mean ± SD: Vesnyane = 0.09 ± 1.3, Gluboke = 0.16 ± 0.9, Kyiv west = −0.56 ± 0.5, Kyiv east = 0.31 ± 0.9; ANOVA $F = 1.565$, $df = 3$, $p = .215$).

3.2 | De novo transcriptome assembly and annotation

De novo assembly resulted in 445,192 transcripts (contigs) that clustered in 273,880 'genes' (clusters of contigs traced from the same De Bruijn graph during Trinity assembly), with a transcript N50 = 2,258 bp and E90N50 = 2,874 bp (Table 1). Mapping read data against this transcriptome yielded an overall alignment rate of 93%, with 85% of reads aligning as proper pairs. BUSCO analysis of the combined liver-spleen transcriptome identified a comprehensive transcriptome, with 80% complete mammalian BUSCOs. Furthermore, 11% of BUSCOs were fragmented, while only 9% were missing. BLASTX search against SwissProt found 10,376 uniproteins that are represented by near full-length transcripts (>80% alignment coverage) in the transcriptome (Figure S3). A total of 128,907 transcripts (31,517 'genes') were annotated with at least one GO term leveraged from the top BLASTX hit(s) (Dryad Data file 1, file 2, file 3).

3.3 | Variation in liver and spleen gene expression associated with inhabiting the CEZ

A total of 444 differentially expressed genes (DEGs; fold change ≥2, FDR <0.001) were identified in the livers of bank voles, with 292 genes being upregulated in the CEZ voles and 152 downregulated (Table S3, Dryad Data file 4a). Of these, 188 genes were successfully
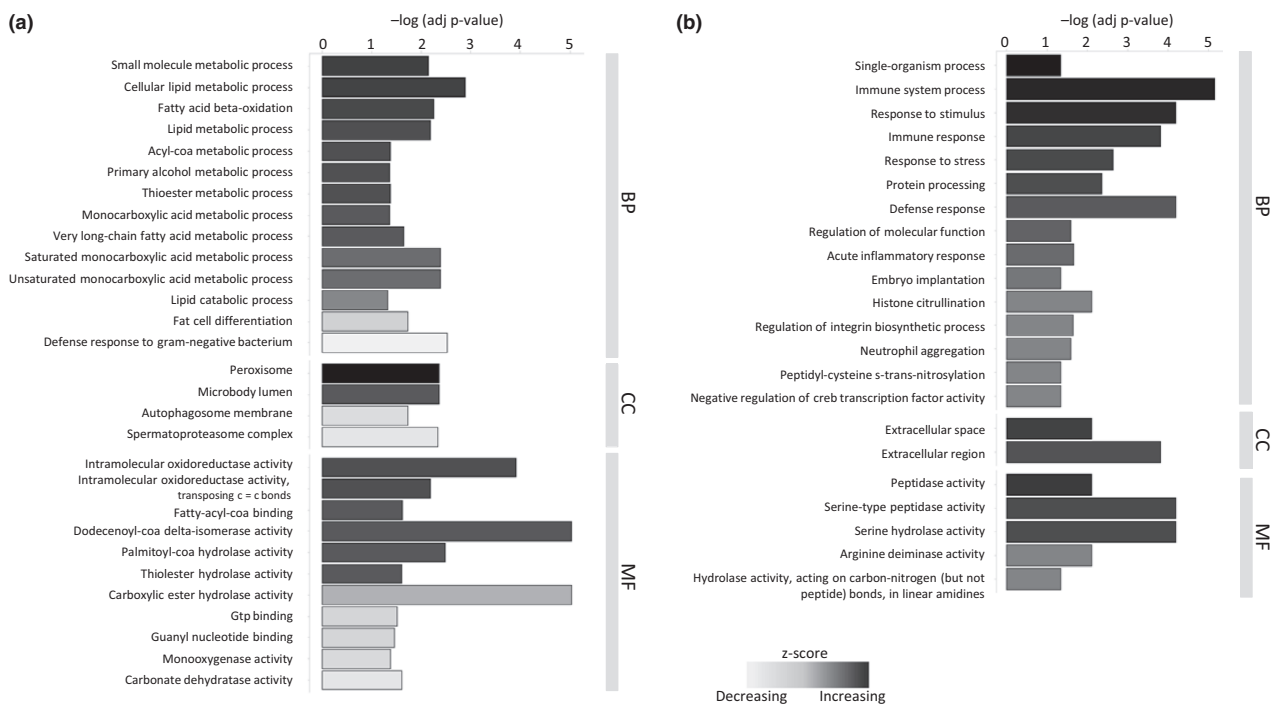
FIGURE 1 Summarized list of significantly enriched GO terms (FDR < 0.05) among DEGs between uncontaminated Kyiv control and CEZ populations for (a) liver and (b) spleen. GOseq results have been further reduced in REVIGO to remove overlap. GO terms are ordered by category. BP, biological pathway; CC, cell compartment; MF, molecular function and by Z-score, which indicates the general direction of expression difference of a group of genes containing a given GO term

annotated (i.e., receiving at least one GO term annotation) to a best matching protein with a known function (Swiss-Prot 2017_04). In spleens, 97 genes were identified as DE, of which were 61 upregulated and 36 downregulated in the voles from the CEZ (Table S3, Dryad Data file 4b), and with 62 genes obtaining at least one GO term. The gene expression profiles cluster by treatment i.e. the contaminated and control areas; hence, variation in transcriptional activity is associated with variation in the radiation levels (Figure S4). Within the CEZ, liver tissue profiles show higher individual variation (Vesnyane and Gluboke comparison with 40 up- and 176 downregulated DE genes, Dryad Data file 5) compared to spleen tissue (two nonannotated DE genes).

From the differentially expressed genes, the most significantly enriched GO terms in the biological pathway category in the liver tissue of animals from CEZ were related to lipid metabolic processes, more specifically catabolic processes such as fatty acid beta-oxidation, metabolic processing of fatty acids and retinols, as well as the acyl-CoA metabolic processing. Repressed pathways (downregulated DEGs) in the liver include fat cell differentiation and defence responses against bacteria and protozoa. Additionally, immune processes such as cytokine signalling related pathways, antigen processing and virus defence pathways were repressed (Figure 1a, Table S4a,b, Figure S5a,b). The enriched pathways in spleens of animals from CEZ were associated with immune system processes, defence and stress responses and acute inflammatory responses, as well as processing of proteins, e.g., citrullination (Figure 1b, Table S4c). GO term analysis between the two

Chernobyl sites showed additional enrichment of peroxisomal activation processes in the genes upregulated in Gluboke liver tissue (See Dryad Data file 5 for GO analysis results).

3.4 | Metabolic pathways

Primary energy metabolism pathways were affected in the livers of voles from the CEZ (Table 2). In particular, genes typically associated with mitochondrial fatty acid oxidation (FAO) and accelerated peroxisomal activity were induced (Figure 2), indicating a shift to the use of fatty acids (FA) as a primary energy source. Notable genes that were upregulated include *Cpt1a* (mitochondrial importer of FA; Kersten, 2014), *Pdk4* (a regulator of metabolic flexibility; Zhang, Hulver, McMillan, Cline, & Gilbert, 2014), *Gpd1* (enables gluconeogenesis from glycerol), and *Fgf21* (coordinator of FA utilization, secreted as a hormone by the liver; Fisher & Maratos-Flier, 2016), which together can promote FAO and gluconeogenesis, while inhibiting oxidation of glucose derived pyruvates in the liver (Fisher & Maratos-Flier, 2016; Kersten, 2014). Additionally, mitochondrial *Auh*, a central gene of the leucine degradation pathway, where the ketogenic amino acid is converted to ketones, was upregulated. A common theme among these upregulated key metabolic genes is transcriptional control by peroxisomal proliferator activated receptor alpha (PPARα), the master regulator of FAO (Kersten, 2014). While the catabolic processes of FAO were induced in the liver tissue of CEZ voles, a key gene in the FA biosynthetic pathways, *Scd1*, was downregulated.

TABLE 2 Differentially expressed genes in the liver and spleen. Positive fold change values indicate upregulation in bank voles inhabiting the CEZ. PPARa in parenthesis indicate known target of peroxisomal proliferator activated receptor alpha

Gene	Function/description	Fold change (log2)
Liver		
Metabolism and stress		
Acot1-5	Acyl-CoA thioesterases, peroxisomal FAO, regulation of FA/CoA levels (PPARa)	~1.30
Fgf21	Fibroblast growth factor 21, fasting hormone (PPARa)	2.40
Eci3	Enoyl-CoA delta isomerase 3, peroxisomal FAO, very long chain fatty acids	2.24
Cbfa2t3	Inhibition of glycolysis. TF	2.05
Rgn	Regucalcin, vitamin C synthesis, Ca2+ homeostasis	1.82
Plin2	Perilipin-2, intracellular lipid accumulation marker (PPARa)	1.77
Eci2	Enoyl-CoA delta isomerase 2, mitochondrial FAO (PPARa)	1.67
Nedd4	E3 ubiquitin-protein ligase	1.59
Cyp4a6	Cytochrome P450, lipid metabolism	1.58
G0s2	G0/G1 switch protein 2, apoptosis, adipogenesis (PPARa)	1.51
Cyp3a25	Cytochrome P450, drug & lipid metabolism	1.45
Gpd1	Glycerol-3-phosphate dehydrogenase, enables gluconeogenesis from glycerol	1.45
Cyp8b1	Cytochrome P450, bile acid synthesis (PPARa)	1.43
Pdk4	Pyruvate dehydrogenase kinase, regulation of FAO, glycolysis and gluconeogenesis by inhibition of PDC (PPARa)	1.41
Retsat	Retinoid (vitamin A derivate) metabolism (PPARa)	1.34
Cdk3	Cyclin-dependent kinase 3, cell cycle regulation	1.31
Vnn1	Pantetheinase, vitamin B5 metabolism, AO activity (PPARa)	1.27
Pex11a	Peroxisomal membrane protein, peroxisome proliferation	1.23
Atf5	Hepatic stress response TF	1.20
Acaa1b	Peroxisomal FAO (PPARa)	1.18
Gadd45a	Growth arrest and DNA damage-inducible protein, DNA repair, response to DNA damage	1.16
Cpt1a	Carnitine O-palmitoyltransferase, mitochondrial FAO, rate-limiting (PPARa)	1.14
Bco1	Retinoid (vitamin A derivate) metabolism	1.14
Pycr1	Proline synthesis, mitochondrial, OS response	1.14
Fabp1	Fatty acid binding protein, binding and transport of intracellular FA, AO activity (PPARa)	1.13
Slc25a47	Respiratory uncoupling, mitochondrial	1.10
Auh	Methylglutaconyl-CoA hydratase, mitochondrial, AA degradation (ketogenic)	1.07
Pla2g16	Regulation of adipocyte lipolysis (phospholipids), lipid metabolism	−1.00
Acat2	Acetyl-CoA acetyltransferase, mevalonate pathway (cholesterol biosynthesis)	−1.10
Cyp2c11	Cytochrome P450	−1.14
Angptl8	Angiopoietin-like protein 8, regulation of serum TAG levels	−1.16
Pld4	Phospholipase, phospholipid synthesis	−1.17
Cyp2c26	Cytochrome P450	−1.22
Lpl	Lipoprotein lipase, cholesterol homeostasis	−1.25
Cyp2f2	Cytochrome P450, drug metabolism	−1.27
Cyp3a family	Cytochrome P450, various members, drug & lipid metabolism	~ −1.40
Scd1	Stearoyl-CoA desaturase 1, MUFA synthesis, rate-limiting (PPARa)	−1.85
Immune response		
Irgm1	Immunity-related GTPase, IFNg induced, innate immunity	−1.02
Tap1	Antigen peptide transporter 1, antigen processing (MHC-I), adaptive immunity	−1.07
Iigp1	Interferon-inducible GTPase, resistance to intracellular pathogens, innate immunity	−1.07

(Continues)

TABLE 2 (Continued)

Gene	Function/description	Fold change (log2)
Gstm4	Glutathione S-transferase	−1.14
Psmb8	Proteasome subunit, antigen processing (MHC-I), immunity	−1.23
Batf2	TF, immune responses	−1.25
Stat1	JAK-STAT cascade, response to IFNs, antiviral	−1.27
Rnf213	E3 ubiquitin-protein ligase	−1.28
Nlrc5	Innate immunity, antiviral	−1.32
Psmb9	Proteasome subunit, antigen processing (MHC-I), immunity	−1.40
Tgtp2	Innate immunity, resistance to intracellular pathogens, T-cell-specific	−1.42
Ccl19	Cytokine, chemokine receptor binding, inflammatory response	−1.43
Socs1	JAK-STAT cascade, IFNg signaling	−1.44
H2 MHC-I	Histocompatibility antigens, antigen presenting	−1.46
Cfhr1	Regulation of complement cascade, immunity	−1.81
Spleen		
Immune response		
Mrgprb2	Mas-related G-protein coupled receptor	1.64
Mcpt8	Mast cell protease 8	1.48
Ms4a2	High affinity immunoglobulin epsilon receptor subunit beta, mast cell activation, IgE binding	1.36
Cpa3	Mast cell carboxypeptidase A, angiotensin metabolism	1.35
Padi4	Transcription regulation, innate immune responses	1.30
Cma1	Mast cell chymase, protease	1.28
Kng1	Kininogen, inflammatory response (vasodilation)	1.25
Prg2	Proteoglycan, cytotoxin, helminthotoxin, antiparasitic, immunity	1.23
Mmp9	Matrix metalloproteinase-9, inflammatory response, tissue remodeling	1.21
Spdya	Speedy protein A, cell cycle regulation, response to DNA damage	1.14
Hp	Haptoglobin, antimicrobial, AO, immunity	1.11
S100A9	Innate immunity, inflammatory response, antimicrobial, AO, apoptosis	1.11
Lcn2	Neutrophil gelatinase-associated lipocalin, antimicrobial, AO, innate immunity	1.11
Mcemp1	Mast cell-expressed membrane protein 1	1.10
Alox5	Arachidonate 5-lipoxygenase, leukotriene metabolism, inflammatory response	1.08
Pglyrp1	Peptidoglycan recognition protein 1, antimicrobial, innate immune response	1.07
Cebpb	TF in immune and inflammatory responses	−1.01
Ube2q2	Ubiquitin-conjugating enzyme E2 Q2, protein ubiquitination	−1.01
Zxdb	Transcription regulation (MHC class I and MHC class II genes)	−1.03
Zfp91	E3 ubiquitin-protein ligase	−1.69
Znrf2	E3 ubiquitin-protein ligase, antigen processing	−2.04
Metabolism		
Pdk4	Regulation of FAO, glycolysis and gluconeogenesis	1.57
Fabp4	Fatty acid binding protein 4	1.47
Plin5	Lipid droplet protein perilipin	1.27
Angl4	Angiopoietin-related protein 4	1.22

Abbreviations: AA, amino acid; AO, antioxidant; FA, fatty acid; FAO, fatty acid oxidation; MUFA, monounsaturated fatty acid; OS, oxidative stress; PDC, pyruvate dehydrogenase complex; TAG, triacylglycerol; TF, transcription factor.

This pattern supports the observed change in fatty acid metabolism, since *Scd1* repression is linked to increased FAO (Paton & Ntambi, 2009). The pattern of elevated FAO was observed in both CEZ sites, with Gluboke voles showing additional upregulation of peroxisomal activity (associated with processing of very long chain fatty acids, see Dryad Data file 5). In the spleen, some genes induced by the PPARγ (peroxisome proliferator-activated receptors) signalling pathway involved in fatty acid and glucose metabolisms were upregulated in
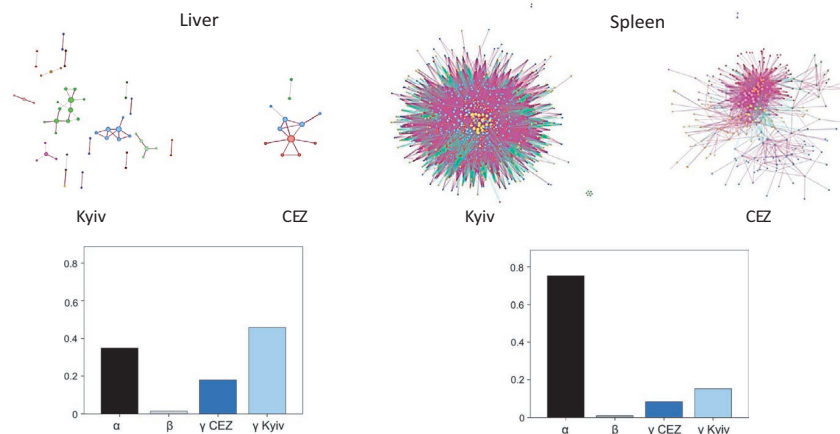
FIGURE 2 Overview of affected liver metabolic pathways between uncontaminated control and CEZ populations of bank voles. Gene names in red colour indicate upregulation and blue colour downregulation in bank voles of the CEZ compared to control voles. ER, endoplasmic reticulum; FAO, fatty acid oxidation; VLDL, very-low-density lipoprotein

bank voles from Chernobyl (Table 2), but their specific functions in the spleen are unknown.

3.5 | Response of the innate and active immune system

Genes involved with the innate immune response via granulocytes such as mast cells, neutrophils, eosinophils and basophils, were upregulated in the spleen tissue of voles from the CEZ (Table 2). Genes associated with the release of proinflammatory mediators were upregulated (e.g., *Cma1* chymase, Table 2). For example, upregulation of the lipoxygenase *Lox5* implies increased production of proinflammatory lipid leukotrienes (Caughey, 2007; Metz et al., 2007). Inflammatory reaction was also supported by the upregulation of *Mmp9*, which is involved with mast cell degranulation and inflammation-associated tissue remodelling processes (Caughey, 2007; Heissig et al., 2005). Activation of innate immune responses was further supported by upregulation of genes involved in pathogen defence responses, such as antimicrobial peptides (*Lcn2*, *S100A9*) (Levy, 2004), and *Padi4*, which is associated with defence against helminths and other extracellular pathogens (Li et al., 2010). Additionally, genes related to protein ubiquitination, a process involved in regulation of immune responses and degradation of damaged proteins were downregulated in the spleen tissue of voles from the CEZ. For example, the two E3 ubiquitin protein ligases (*Znrf2* and *Zfp91*) are also involved in regulation of adaptive immune responses, such

as MHC-I antigen presenting (Gao & Karin, 2005). Regulation of adaptive immunity responses might be compromised in the spleen tissue by lowered antibody-producing activity of B-cells, since expression of some immunoglobulin heavy and light chains was repressed (Table S3).

In contrast to upregulation of some innate immune response pathways in the spleen, key components of the adaptive immune pathway regulating the activity of MHC-I and antigen processing were downregulated in the livers of bank voles from the CEZ. For example, there was downregulation of immune proteasome genes (*Psmb9* and *Psmb8*), class I histocompatibility antigens and *Tap1*, a transporter protein involved the antigen processing (Kincaid et al., 2012). Additionally, parts of the Janus kinase/signal transducers and activators of transcription, JAK-STAT signalling pathway (*Stat1* and *Socs1*) (Gao, Wang, Lafdil, & Feng, 2012), were also downregulated in livers of animals from the CEZ.

3.6 | Cellular response to stress

Bank voles inhabiting the CEZ upregulated transcription of some genes induced by oxidative stress in the liver. For example, mitochondrial oxidative stress response genes were upregulated (e.g., *Atf5*, mitochondrial *Slc25a47*, *Pycr1* [Fiorese et al., 2016; Kuo et al., 2016; Tan, Ooi, Aw, & Hui, 2004]) and there was an increased activation of genes involved in metabolism of extracellular antioxidants (vitamins B5, A and C) in voles from the CEZ. In the spleen, *Hp* for haptoglobin, an antioxidant that enhances cells' tolerance to

FIGURE 3 Gene coexpression networks for liver and spleen. The consensus network data is filtered with *p*-value (.001) and contains only links with high correlation (wTO values for liver: 0.44 for CEZ and 0.47 for Kyiv; wTO for spleen: 0.70 for CEZ and 0.72 for Kyiv). Networks were clustered with the Louvain algorithm, and the clusters are colour-coded. The colour of the links represents the sign of the interaction, with purple links being positive and green links being negative interactions. The barplots show the proportion of categories of links[†] when networks from Kyiv and the CEZ were compared. CoDiNA identified 179,133 links and 2,863 nodes in the liver network, whereas 1,841,074 links and 2,960 nodes were detected in the spleen network

†α links, in both networks with the same sign (negative or positive correlation), β links, in both networks but with a different sign; γ links, specific to one network

oxidative stress (Gutteridge, 1995), was upregulated. In addition, upregulation of two genes generally induced by genotoxic stress or DNA damage was observed (*Gadd45a* in the liver and *Spdya* in the spleen (Liebermann & Hoffman, 2008; McAndrew, Gastwirt, & Donoghue, 2009)), although there were no signs of increased DNA repair efforts, such as increased expression of genes involved in repair of DNA damage, in either tissue. Transcriptional repression of cytochrome P450 genes, such as few members of Cyp2 and several Cyp3a isoforms (families involved in detoxification reactions) was seen in the livers of voles inhabiting Chernobyl.

3.7 | Gene coexpression networks

Inhabiting the CEZ affected the interactions among genes in both tissues, with a general pattern of lower amount of coexpressed gene connections in the networks of the CEZ animals. In the spleen, five densely connected clusters of coexpressed genes with high significant correlation (*p* < .001, and see wTO correlation values in Figure 3) were identified in the networks from the samples from uncontaminated areas (Kyiv), whereas fewer genes and links (connections between two genes) were identified in the networks from CEZ. In the liver, gene networks in animals from Kyiv contained more links and clustered gene groups than the networks from the CEZ samples (17 and 5 clusters, respectively; Figure 3). When the coexpression networks from CEZ and Kyiv liver tissues were compared, more than half of the connections among the genes were assigned to either Kyiv or CEZ network (γ links), not shared by both (α links), and high frequency of gene correlation patterns specific especially to Kyiv control voles were observed (Figure 3). Genes with strong correlation patterns in the Kyiv network were associated with pathways of energy metabolism, response to stress, antibiotic metabolism, mitochondrion organization, ROS metabolism and

antigen presenting (including DEGs: innate immune response genes *Irgm1*, *Iigp1* & *Tgtp2*, and MHC-I genes such as *Stat1* and the proteasome genes), whereas the CEZ animals' networks included genes related to energy metabolism processes (including DEGs: vitamin metabolism genes *Rgn*, *Vnn1*, *Restat* and FAO genes *Cpt1a* and *Gpd1* [Figure S6a,b]). Comparatively, in the spleen, most gene coexpression patterns were shared between the treatments (α links) (Figure 3). Highly connected genes in both treatments were involved in RNA and cellular metabolism processes, with some additional immune response genes specific to Kyiv network (DEGs such as the antimicrobial *s100a9* and *Prg2*) (Figure S7a,b). The differentially expressed genes were not strongly represented in the networks of either tissue. However, a pattern of lower amount of coexpression patterns among genes (links) in the CEZ voles compared to Kyiv networks was visible in both tissues (Figure 3, Figure S8).

3.8 | Stable isotopes

Carbon stable isotope values (δ^{13}C) had wide interindividual variation at all locations except at Gluboke from CEZ, where marked interindividual homogeneity was observed (Figure 4); hence, there was significant difference in the variance of δ^{13}C among groups (Levene's *F*-statistics, *F* = 4.92, *df* = 3,36, *p* = .006). There was no significant difference in variance in values of δ^{15}N among sampling sites (Levene's *F*-statistics, *F* = 2.76, *df* = 3,36, *p* = .056), albeit with high variation present among individuals from Vesnyane (Figure 4, Table S5). Mean δ^{15}N values were significantly higher in the animals from CEZ compared with animals from the uncontaminated sites (Kruskal–Wallis test, χ^2 = 27.70, *df* = 3, *p* < .001; Table S6 for pairwise tests), with the mean δ^{15}N being on average 3.22‰ greater in the samples of fur from animals inhabiting the CEZ. There was no significant difference

FIGURE 4 Carbon (δ^{13}C) vs. nitrogen (δ^{15}N) isotopic values for the fur samples of *Myodes glareolus* inhabiting the CEZ and uncontaminated locations near Kyiv (with mean values of each group in the centre), and their potential dietary sources. Fur isotopic values were corrected downwards (by factors of 2.2‰ for δ^{13}C and 2.8‰ for δ^{15}N, see Kurle et al., 2014) to account for differences between isotopic values of animal tissue and food sources. Dietary sources[‡] are presented with means and *SD*
‡FN, fungi; HP, herbaceous plants; IN, insects; LI, lichens; MO, mosses; WP, woody plants
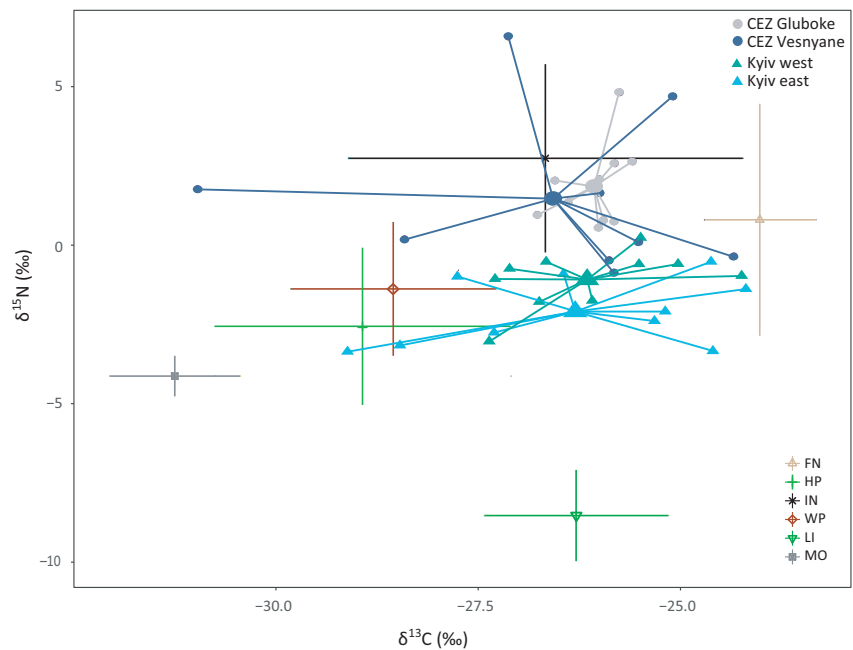
in the mean δ^{13}C values among sampling sites (Kruskal–Wallis test, $\chi^2 = 0.035$, $df = 3$, $p = 1.000$). In general, bank vole diets from Kyiv animals place in between fungi and woody & herbaceous plants in the dual isotope space, whereas voles from the CEZ were placed closer to insects (Figure 4). In the liver tissue, the expression levels of nearly half of the DEGs (107 out of 188 annotated DEGs) correlate with δ^{15}N. The positive correlation with many of metabolically relevant genes related to induction of fatty acid oxidation, such as *Cpt1a*, *Pdk4* and *Fabp1* (Table S7), suggest that the affected metabolic pathways are largely associated with an apparent increase in fur nitrogen isotope levels in the CEZ animals.

4 | DISCUSSION

Detrimental effects of exposure to radionuclides have been reported at multiple biological scales in wildlife, with elevated levels of DNA damage and oxidative stress as the common characteristic associated biomarkers. Counter to our predictions, the major gene pathways associated with exposure to radionuclides in bank voles inhabiting the CEZ were related to fatty acid metabolism, consistent with an increase in stable isotope values of nitrogen in samples of bank vole fur. We also note that bank voles inhabiting the CEZ show changes in immune response and inflammatory pathways.

4.1 | Low dose IR is associated with altered metabolic pathways in the liver

Gene expression profiles of bank voles inhabiting the CEZ associate with maintenance of a metabolic state with induced fatty acid oxidation (FAO; Table 2), with the impacted pathways controlled largely by PPARα. PPARα is typically activated by a prolonged negative

energy balance (for example starvation or fasting) or ketogenic (low carbohydrate, high fat) diet (Kersten, 2014). Energy stress exhausts liver glycogen, after which fatty acids and glycerol are expected to be mobilized from body fats (triacylglycerols) for energy use. Subsequently, most tissues can switch to FAO as a main energy source via *Cpt1a* upregulation to increase mitochondrial import of Acyl-CoA (Figure 2), as is observed in the livers of voles inhabiting the CEZ (Table 2).

However, alterations of lipid metabolism can have wider impacts on organismal bioenergetics. When FAO is promoted, the liver typically initiates gluconeogenesis and the production of ketone bodies. However, support for these processes in our data was ambiguous: upregulation of *Gpd1* and *Pdk4* can promote both gluconeogenesis and FAO, and increased leucine degradation can contribute to increased ketone levels (IJlst et al., 2002), though no further support for ketogenesis was seen (Table 2, Figure 2). One consequence of failure to induce ketogenesis or gluconeogenesis in response to an increase in FAO is insufficient resources for the brain, as the brain disfavours long chain fatty acids (Schönfeld & Reiser, 2013) and requires glucose or ketones as a source of energy. With this in mind, there is a negative correlation between brain size and radionuclide levels in birds nesting within the CEZ (Møller et al., 2011). Direct measurements of whether brain size or developmental processes are impacted by metabolic alterations or direct exposure effects in bank voles and other species from the contaminated areas within the CEZ are needed.

An important but unresolved issue is whether the increased FAO in the CEZ bank voles is a direct consequence of exposure to radiation (and possibly adaptive in animals exposed to radionuclides) or represents a more passive indirect response to differences in habitat within and outside the CEZ. In addition, the enrichment (>3‰) of fur nitrogen isotope values (δ^{15}N) associated with inhabiting the CEZ

is fairly high, i.e., comparable to a shift in trophic level (e.g., Ben-David & Flaherty, 2012). Elevated radionuclide levels are associated with altered community structure and a reduction in biodiversity (Geras'kin, Fesenko, & Alexakhin, 2008), raising the possibility that altered metabolism reflects some change in habitat or diet associated with bank voles inhabiting the CEZ. Some support for an altered diet might be derived from the different gastrointestinal microbiota communities in bank voles from areas contaminated by radionuclides compared with animals from uncontaminated areas (Lavrinienko et al., 2018). Bank voles have a diverse diet (Butet & Delettre, 2011), and the elevated nitrogen isotope levels in the CEZ animals could arise from an increase in consumption of food with higher $\delta^{15}N$, such as invertebrates, fungi or seeds (Calandra et al., 2015). However, a reduction in the abundance of invertebrates in areas with high levels of environmental radioactivity within the CEZ (Møller & Mousseau, 2018) argues against a more invertebrate-rich diet in animals from the CEZ. In general, the large variation in dietary carbon indicates that bank voles exploit a diversity of plant resources (Calandra et al., 2015), with no apparent dietary difference among our sample areas.

Besides diet, another explanation for the nitrogen enrichment in bank voles inhabiting the CEZ is induction of metabolic pathways associated with catabolic processes, and this is consistent with the transcriptional signature of increased FAO. Generally, nutritional stress (such as starvation or fasting) increases $\delta^{15}N$ in tissues and fur due to catabolism (Hobson, Alisauskas, & Clark, 1993; Petzke, Fuller, & Metges, 2010). Despite the metabolic signals associated with nutritional stress, neither weight loss nor poor body condition characterize the voles from the CEZ, suggesting that the bank voles inhabiting the CEZ are not starving or deprived of food. Hence, maintaining a metabolic state with increased FAO without obvious loss of body weight can be a part of a strategy to cope with a stressful environment. An increase of FAO as a response to environmental pollution is not commonly reported, although some evidence of altered lipid metabolism can be found in the Atlantic cod (*Gadus morhua*) exposed to methylmercury (Yadetie et al., 2013). Also, exposure to depleted Uranium and gamma rays caused activation of PPARα in the Atlantic salmon (*Salmo salar*) (Song et al., 2016). Altered expression of PPARα-associated genes is also linked with metabolic diseases (Seo et al., 2008). Nevertheless, a metabolic switch from glycolysis towards FAO might also be beneficial as an antitumoural strategy within an oxidative environment as tumours commonly depend on glycolysis-related anabolic pathways to support their growth (Vander Heiden, Cantley, & Thompson, 2009).

4.2 | DNA repair and oxidative stress response

Given that increased DNA damage such as strand breaks is associated with exposure to radionuclides (reviewed by Lourenço et al., 2016), it is interesting that bank voles inhabiting the CEZ exhibited few signs of increased DNA repair activity (see Table 2). However, the altered metabolic pathways may have wider influence here, as both energetic and cellular stress may boost DNA repair pathways, decrease age-related oxidative stress (Heydari, Unnikrishnan,

Lucente, & Richardson, 2007), promote catabolic pathways (such as FAO) and repress growth signalling pathways while promoting cell survival (Yuan, Xiong, & Guan, 2013) and genomic stability. Elevated expression of cell cycle regulators can also increase resistance to oxidative and genotoxic stress as well as to starvation in *Drosophila* (Moskalev et al., 2012). Indeed, fibroblast cells isolated from bank voles from the CEZ show increased resistance to cell death against DNA damaging agents, and can more efficiently recover after irradiation (acute high dose of 10 Gy) (Mustonen et al., 2018), contrary to a pattern of premature senescence and loss of proliferation ability commonly seen in cells sensitive to radiation (Loseva et al., 2014). Within the approximately 50 generations of inhabiting the CEZ (Baker et al., 2017), bank voles may have evolved some resistance to radiation induced DNA damage and oxidative stress (see also Galvan et al., 2014), or are not receiving a sufficiently high dose of radiation to inflict a DNA repair response. Although altered telomere homeostasis is a sign of cellular stress in bank voles inhabiting the CEZ (Kesäniemi, Lavrinienko, et al., 2019), no increases in DNA damage (measured as chromosomal aberrations [Rodgers & Baker, 2000]) or mutation rate, i.e., heteroplasmy (Kesäniemi et al., 2018) in bank voles from contaminated CEZ areas have been reported.

Species affected by the Chernobyl nuclear accident show divergent levels of oxidative damage and antioxidant defences (Einor et al., 2016), such as increased glutathione levels in birds inhabiting the CEZ (reviewed by Lourenço et al., 2016). Counter to our expectations of elevated oxidative stress response, glutathione peroxidase or other antioxidant metabolism genes, such as superoxide dismutases (SOD) and catalase (Kam & Banati, 2013; Limón-Pacheco & Gonsebatt, 2009) were not differentially expressed in bank vole livers or spleens. However, inhabiting the CEZ may enhance the levels of extracellular antioxidants derived from the diet. Genes involved in vitamin metabolism pathways were induced in bank vole livers (Table 2), such as *Vnn1*, which can enhance production of the radioprotective agent cysteamine (Ferreira, Naquet, & Manautou, 2015), and retinoid metabolism related genes, which also act as antioxidants (Shiota, Tsuchiya, & Hoshikawa, 2006). However, interpreting activity of these vitamin metabolism genes in terms of oxidative stress is difficult as they can have pleiotropic effects on key pathways such as fatty acid metabolism and inflammation (Naquet, Giessner, & Galland, 2016; Shiota et al., 2006). Elevated levels of oxidative stress can damage mitochondria, leading to further increased ROS (reactive oxygen species) production and severe cellular oxidative stress (Kam & Banati, 2013). Therefore, responding to oxidative stress threats and maintaining functional mitochondria is particularly relevant to wildlife within the CEZ.

4.3 | Tissues differ in their stress response

Based on clinical radiotherapy studies in humans, spleen tissue is considered as more radiosensitive than liver (Rubin & Casarett, 1968). In bank voles, the data suggests that on a transcriptional level, chronic low dose radiation exposure leads to more pronounced stress

response in the liver tissue compared to spleen, supported by the higher number of DE genes. Additionally, several processes related to immune responses and lipid metabolism were either repressed or enhanced in the liver. In the spleen, repression of biological processes was limited in voles from the CEZ, and for example, minimal signs of oxidative stress was seen (Table 2). In rodents, radiation exposure induces tissue specific changes also in epigenetic markers (Pogribny, Raiche, Slovack, & Kovalchuk, 2004). Additionally, inhabiting the CEZ changes or disrupts interactions among genes or their regulatory pathways, with treatment specific (CEZ/Kyiv) changes on coregulation more obvious in liver tissue of bank voles, despite its lower suggested radiosensitivity. Previous studies have also shown that coexpressed gene networks are shaped by environmental factors or stressors (Des Marais, Guerrero, Lasky, & Scarpino, 2017; Rose, Seneca, & Palumbi, 2016). As liver and spleen differ in their biological function, differences in their stress responses on a gene expression level is not unexpected. However, immune responses were sensitive to environmental radiation contamination in bank vole liver and spleen tissues, as immune system GO terms were identified in DE genes from both tissues, and the coexpression patterns of genes involved in immune system processes responded to radionuclide contamination. Similarly, pollution induced oxidative stress impacts expression profiles and coregulation of immune response genes in human endothelial cells (Gong et al., 2007).

4.4 | Immunosuppression in the liver tissue

Exposure to radioactivity affects inflammatory and immune systems in clinical settings (Di Maggio et al., 2015; Frey, Hehlgans, Rödel, & Gaipl, 2015), and our data show comparable processes in wildlife exposed to radionuclides. Immune cells, especially T-lymphocytes, are sensitive to radiation (Soule et al., 2007) and thus vertebrates exposed to radionuclides typically show immunosuppression and reduced white blood cell (lymphocyte) numbers or a change in the proportion of leucocyte types (Lourenço et al., 2016; Mikryakov, Gudkov, Mikryakov, Pomortseva, & Balabanova, 2013). Immunosuppression (e.g. downregulation of antigen processing pathways) in the livers of bank voles inhabiting the CEZ (Table 2) could imply lowered cellular immunity against intracellular pathogens, such as viruses. For example, MHC-I and immune proteasomes are vital for lymphocyte mediated antigen presenting and processing (Ferrington & Gregerson, 2012); also, our data are consistent with proteasome function being sensitive to a wide dose range (0.17–20 Gy) of ionizing radiation in mouse and human cell lines (Pajonk & McBride, 2001). The inflammatory response of the liver tissue from bank voles from the CEZ is not consistent with the high dose radiotherapy (single dose of >1 Gy) induced activation of cytokine induced proinflammatory pathways. Bank voles exposed to chronic low dose radiation rather show signs of repression of interferon induced (especially IFNγ) pathways, such as JAK-STAT signalling, which can lead to lowered antiviral defences (Gao et al., 2012; Rauch, Müller, & Decker, 2013).

4.5 | Inhabiting the CEZ is associated with activation of granulocytes in spleen tissue

Activation of granulocytes is a common, inflammatory response to radiation in clinical studies (Soule et al., 2007). Accordingly, evidence of inflammation in bank voles inhabiting the CEZ include increased expression of genes involved in activation of mast cells and other granulocytes (Table 2), via the release and synthesis of proinflammatory signalling molecules (such as proteases and leukotrienes, Table 2) (Caughey, 2007; Metz et al., 2007). Mast cells can also release cytokines and be activated by them; however in our data, there was no evidence of differential expression of cytokine genes (Table 2).

Despite the predominantly proinflammatory role of mast cells, favorable anti-inflammatory functions have also been reported, for example in response to UV-B irradiation in mouse skin cells (Hart et al., 1998; Metz et al., 2007). Altered expression of mast cells may have fitness consequences as these cells defend against diverse pathogens and parasites (Caughey, 2007) and appear to be more resistant than other immune cells to radiation induced cytotoxicity (Soule et al., 2007). Mast cell activation may be important for wildlife immunity and host-parasite dynamics. For example, an acute exposure to high radiation (2–5 Gy or above) increases susceptibility to infectious pathogens in birds and mammals (reviewed by Morley, 2012). An increased susceptibility to infection is associated with radiation exposure in humans and fish exposed to radionuclides also in the CEZ (Lourenço et al., 2016; Morley, 2012). Small mammals inhabiting areas of elevated radionuclides had higher ectoparasite burdens and increased prevalence of protozoan parasites (Morley, 2012), and bank voles from contaminated areas within the CEZ had an increased prevalence of helminth infections (Sazykina & Kryshev, 2006). The association of radionuclide exposure and parasites is not well studied, therefore measurements of parasite burdens and blood cell counts are needed to better understand how the suite of impacts associated with suppression and activation of active immunity and mast cells respectively.

To conclude, inhabiting an area with elevated radionuclide contamination affects multiple biological pathways in wild bank voles, highlighting processes associated with lipid metabolism and immune responses in a tissue specific manner. As human actions continue pose new environmental challenges to wildlife, it becomes increasingly important to examine how species react to chronic environmental stressors, such as exposure to radiation or other pollutants.

AUTHOR CONTRIBUTIONS

J.K., and P.W. designed the experiment, J.K., T.J., A.L., K.K., M.K., T.M., and P.W. performed the research, J.K. and T.J. analyzed the results. J.K., and T.J. wrote the manuscript in collaboration with all authors.

DATA AVAILABILITY STATEMENT

Additional details on the transcriptome assembly & annotation (files 1–3) and additional results from DESeq and GOseq analyses (files 4–5) are accessible from Dryad Digital Repository (https://doi.org/10.5061/dryad.j3c6r69; Kesäniemi, Jernfors, et al., 2019). Raw transcriptome reads are accessible from Genbank (NCBI SRA SRP15797).

ORCID

Jenni Kesäniemi https://orcid.org/0000-0001-8328-558X

Toni Jernfors https://orcid.org/0000-0002-8657-574X

Anton Lavrinienko https://orcid.org/0000-0002-9524-8054

Kati Kivisaari https://orcid.org/0000-0001-8892-2947

Mikko Kiljunen https://orcid.org/0000-0002-7411-1331

Tapio Mappes https://orcid.org/0000-0002-5936-7355

Phillip C. Watts https://orcid.org/0000-0001-7755-187X

REFERENCES

Acevedo-Whitehouse, K., & Duffus, A. L. J. (2009). Effects of environmental change on wildlife health. *Philosophical Transactions of the Royal Society of London. Series B, Biological Sciences*, *364*(1534), 3429–3438. https://doi.org/10.1098/rstb.2009.0128

Alamri, O. D., Cundy, A. B., Di, Y., Jha, A. N., & Rotchell, J. M. (2012). Ionizing radiation-induced DNA damage response identified in marine mussels, *Mytilus* sp. *Environmental Pollution*, *168*, 107–112. https://doi.org/10.1016/j.envpol.2012.04.015

Baker, R. J., Dickins, B., Wickliffe, J. K., Khan, F. A. A., Gaschak, S., Makova, K. D., & Phillips, C. D. (2017). Elevated mitochondrial genome variation after 50 generations of radiation exposure in a wild rodent. *Evolutionary Applications*, *10*(8), 784–791. https://doi.org/10.1111/eva.12475

Baltensperger, A. P., Huettmann, F., Hagelin, J. C., & Welker, J. M. (2015). Quantifying trophic niche spaces of small mammals using stable isotopes (δ^{15}N and δ^{13}C) at two scales across

Alaska. *Canadian Journal of Zoology*, *93*(7), 579–588. https://doi.org/10.1139/cjz-2015-0025

Ben-David, M., & Flaherty, E. A. (2012). Stable isotopes in mammalian research: A beginner's guide. *Journal of Mammalogy*, *93*(2), 312–328. https://doi.org/10.1644/11-MAMM-S-166.1

Butet, A., & Delettre, Y. R. (2011). Diet differentiation between European arvicoline and murine rodents. *Acta Theriologica*, *56*(4), 297. https://doi.org/10.1007/s13364-011-0049-6

Calandra, I., Labonne, G., Mathieu, O., Henttonen, H., Lévêque, J., Milloux, M.-J., … Navarro, N. (2015). Isotopic partitioning by small mammals in the subnivium. *Ecology and Evolution*, *5*(18), 4132–4140. https://doi.org/10.1002/ece3.1653

Caughey, G. H. (2007). Mast cell tryptases and chymases in inflammation and host defense. *Immunological Reviews*, *217*, 141–154. https://doi.org/10.1111/j.1600-065X.2007.00509.x

Chesser, R. K., Sugg, D. W., Lomakin, M. D., Van den Bussche, R. A., DeWoody, J. A., Jagoe, C. H., … Baker, R. J. (2000). Concentrations and dose rate estimates of (134,137)cesium and (90)strontium in small mammals at Chornobyl, Ukraine. *Environmental Toxicology and Chemistry*, *19*(2), 305–312. https://doi.org/10.1002/etc.5620190209

Deryabina, T. G., Kuchmel, S. V., Nagorskaya, L. L., Hinton, T. G., Beasley, J. C., Lerebours, A., & Smith, J. T. (2015). Long-term census data reveal abundant wildlife populations at Chernobyl. *Current Biology*, *25*(19), R824–R826. https://doi.org/10.1016/j.cub.2015.08.017

Des Marais, D. L., Guerrero, R. F., Lasky, J. R., & Scarpino, S. V. (2017). Topological features of a gene co-expression network predict patterns of natural diversity in environmental response. *Proceedings of the Royal Society B: Biological Sciences*, *284*(1856), 20170914. https://doi.org/10.1098/rspb.2017.0914

Di Maggio, F., Minafra, L., Forte, G., Cammarata, F., Lio, D., Messa, C., … Bravatà, V. (2015). Portrait of inflammatory response to ionizing radiation treatment. *Journal of Inflammation*, *12*, 14. https://doi.org/10.1186/s12950-015-0058-3

Einor, D., Bonisoli-Alquati, A., Costantini, D., Mousseau, T. A., & Møller, A. P. (2016). Ionizing radiation, antioxidant response and oxidative damage: A meta-analysis. *Science of the Total Environment*, *548–549*, 463–471. https://doi.org/10.1016/j.scitotenv.2016.01.027

Evans, T. G., Pespeni, M. H., Hofmann, G. E., Palumbi, S. R., & Sanford, E. (2017). Transcriptomic responses to seawater acidification among sea urchin populations inhabiting a natural pH mosaic. *Molecular Ecology*, *26*(8), 2257–2275. https://doi.org/10.1111/mec.14038

Ferreira, D. W., Naquet, P., & Manautou, J. E. (2015). Influence of vanin-1 and catalytic products in liver during normal and oxidative stress conditions. *Current Medicinal Chemistry*, *22*(20), 2407–2416.

Ferrington, D. A., & Gregerson, D. S. (2012). Immunoproteasomes: Structure, function, and antigen presentation. *Progress in Molecular Biology and Translational Science*, *109*, 75–112. https://doi.org/10.1016/B978-0-12-397863-9.00003-1

Fiorese, C. J., Schulz, A. M., Lin, Y. F., Rosin, N., Pellegrino, M. W., & Haynes, C. M. (2016). The transcription factor ATF5 mediates a mammalian mitochondrial UPR. *Current Biology*, *26*(15), 2037–2043. https://doi.org/10.1016/j.cub.2016.06.002

Fisher, F. M., & Maratos-Flier, E. (2016). Understanding the physiology of FGF21. *Annual Review of Physiology*, *78*(1), 223–241. https://doi.org/10.1146/annurev-physiol-021115-105339

Frey, B., Hehlgans, S., Rödel, F., & Gaipl, U. S. (2015). Modulation of inflammation by low and high doses of ionizing radiation: Implications for benign and malign diseases. *Cancer Letters*, *368*, 230–237. https://doi.org/10.1016/j.canlet.2015.04.010

Galván, I., Bonisoli-Alquati, A., Jenkinson, S., Ghanem, G., Wakamatsu, K., Mousseau, T. A., & Møller, A. P. (2014). Chronic exposure to low-dose radiation at Chernobyl favours adaptation to oxidative

stress in birds. *Functional Ecology*, *28*(6), 1387–1403. https://doi.org/10.1111/1365-2435.12283

Gao, B., Wang, H., Lafdil, F., & Feng, D. (2012). STAT proteins – Key regulators of anti-viral responses, inflammation, and tumorigenesis in the liver. *Journal of Hepatology*, *57*, 430–441. https://doi.org/10.1016/j.jhep.2012.01.029

Gao, M., & Karin, M. (2005). Regulating the regulators: Control of protein ubiquitination and ubiquitin-like modifications by extracellular stimuli. *Molecular Cell*, *19*, 581–593. https://doi.org/10.1016/j.molcel.2005.08.017

Geras'kin, S. A., Fesenko, S. V., & Alexakhin, R. M. (2008). Effects of non-human species irradiation after the Chernobyl NPP accident. *Environment International*, *34*(6), 880–897. https://doi.org/10.1016/j.envint.2007.12.012

Gong, K. E., Zhao, W., Li, N., Barajas, B., Kleinman, M., Sioutas, C., … Araujo, J. A. (2007). Air-pollutant chemicals and oxidized lipids exhibit genome-wide synergistic effects on endothelial cells. *Genome Biology*, *8*(7), R149. https://doi.org/10.1186/gb-2007-8-7-r149

Grabherr, M. G., Haas, B. J., Yassour, M., Levin, J. Z., Thompson, D. A., Amit, I., … Regev, A. (2011). Full-length transcriptome assembly from RNA-Seq data without a reference genome. *Nature Biotechnology*, *29*(7), 644–652. https://doi.org/10.1038/nbt.1883

Gutteridge, J. M. C. (1995). Lipid peroxidation and antioxidants as biomarkers of tissue damage. *Clinical Chemistry*, *41*, 1819–1828.

Gysi, D. M., de Miranda Fragoso, T., Buskamp, V., Almaas, E., & Nowick, K. (2018). Comparing multiple networks using the Co-expression Differential Network Analysis (CoDiNA). *arXiv*, Preprint arXiv, 1802.00828.

Gysi, D. M., Voigt, A., Fragoso, T. D. M., Almaas, E., & Nowick, K. (2018). WTO: An R package for computing weighted topological overlap and a consensus network with integrated visualization tool. *BMC Bioinformatics*, *19*(1), 392. https://doi.org/10.1186/s12859-018-2351-7

Haas, B. J., Papanicolaou, A., Yassour, M., Grabherr, M., Blood, P. D., Bowden, J., … Regev, A. (2013). De novo transcript sequence reconstruction from RNA-seq using the Trinity platform for reference generation and analysis. *Nature Protocols*, *8*(8), 1494–1512. https://doi.org/10.1038/nprot.2013.084

Hart, P. H., Grimbaldeston, M. A., Swift, G. J., Jaksic, A., Noonan, F. P., & Finlay-Jones, J. J. (1998). Dermal mast cells determine susceptibility to ultraviolet B-induced systemic suppression of contact hypersensitivity responses in mice. *The Journal of Experimental Medicine*, *187*(12), 2045–2053. https://doi.org/10.1084/jem.187.12.2045

Heissig, B., Rafii, S., Akiyama, H., Ohki, Y., Sato, Y., Rafael, T., … Hattori, K. (2005). Low-dose irradiation promotes tissue revascularization through VEGF release from mast cells and MMP-9-mediated progenitor cell mobilization. *The Journal of Experimental Medicine*, *202*(6), 739–750. https://doi.org/10.1084/jem.20050959

Hekim, N., Cetin, Z., Nikitaki, Z., Cort, A., & Saygili, E. I. (2015). Radiation triggering immune response and inflammation. *Cancer Letters*, *368*, 156–163. https://doi.org/10.1016/j.canlet.2015.04.016

Heydari, A. R., Unnikrishnan, A., Lucente, L. V., & Richardson, A. (2007). Caloric restriction and genomic stability. *Nucleic Acids Research*, *35*(22), 7485–7496. https://doi.org/10.1093/nar/gkm860

Hobson, K. A., Alisauskas, R. T., & Clark, R. G. (1993). Stable-nitrogen isotope enrichment in avian tissues due to fasting and nutritional stress: Implications for isotopic analyses of diet. *The Condor*, *95*(2), 388. https://doi.org/10.2307/1369361

IJlst, L., Loupatty, F. J., Ruiter, J. P. N., Duran, M., Lehnert, W., & Wanders, R. J. A. (2002). 3-Methylglutaconic aciduria type I is caused by mutations in AUH. *American Journal of Human Genetics*, *71*(6), 1463–1466. https://doi.org/10.1086/344712

Jernfors, T., Kesäniemi, J., Lavrinienko, A., Mappes, T., Milinevsky, G., Møller, A. P., … Watts, P. C. (2018). Transcriptional upregulation of DNA damage response genes in bank voles (*Myodes glareolus*) inhabiting the Chernobyl Exclusion Zone. *Frontiers in Environmental Science*, *5*, https://doi.org/10.3389/fenvs.2017.00095

Kallio, E. R., Begon, M., Birtles, R. J., Bown, K. J., Koskela, E., Mappes, T., & Watts, P. C. (2014). First report of *Anaplasma phagocytophilum* and *Babesia microti* in rodents in Finland. *Vector-Borne and Zoonotic Diseases*, *14*(6), 389–393. https://doi.org/10.1089/vbz.2013.1383

Kam, W.-W.-Y., & Banati, R. B. (2013). Effects of ionizing radiation on mitochondria. *Free Radical Biology and Medicine*, *65*, 607–619. https://doi.org/10.1016/j.freeradbiomed.2013.07.024

Kersten, S. (2014). Integrated physiology and systems biology of PPARα. *Molecular Metabolism*, *3*, 354–371. https://doi.org/10.1016/j.molmet.2014.02.002

Kesäniemi, J., Boratyński, Z., Danforth, J., Itam, P., Jernfors, T., Lavrinienko, A., & Watts, P. C. (2018). Analysis of heteroplasmy in bank voles inhabiting the Chernobyl exclusion zone: A commentary on Baker et al. (2017) "Elevated mitochondrial genome variation after 50 generations of radiation exposure in a wild rodent". *Evolutionary Applications*, *11*(5), 820–826. https://doi.org/10.1111/eva.12578

Kesäniemi, J., Jernfors, T., Lavrinienko, A., Kivisaari, K., Kiljunen, M., Mappes, T., & Watts, P. C. (2019). Data from: Exposure to environmental radionuclides is associated with altered metabolic and immunity pathways in a wild rodent. Dryad Digital Repository. https://doi.org/10.5061/dryad.j3c6r69

Kesäniemi, J., Lavrinienko, A., Tukalenko, E., Boratyński, Z., Kivisaari, K., Mappes, T., … Watts, P. C. (2019). Exposure to environmental radionuclides associates with tissue-specific impacts on telomerase expression and telomere length. *Scientific Reports*, *9*, 850. https://doi.org/10.1038/s41598-018-37164-8

Kincaid, E. Z., Che, J. W., York, I., Escobar, H., Reyes-Vargas, E., Delgado, J. C., … Rock, K. L. (2012). Mice completely lacking immunoproteasomes show major changes in antigen presentation. *Nature Immunology*, *13*(2), 129–135. https://doi.org/10.1038/ni.2203

Kovalchuk, I., Abramov, V., Pogribny, I., & Kovalchuk, O. (2004). Molecular aspects of plant adaptation to life in the Chernobyl zone. *Plant Physiology*, *135*, 357–363. https://doi.org/10.1104/pp.104.040477

Kuo, M.-L., Lee, M.-E., Tang, M., den Besten, W., Hu, S., Sweredoski, M. J., … Yen, Y. (2016). PYCR1 and PYCR2 interact and collaborate with RRM2B to protect cells from overt oxidative stress. *Scientific Reports*, *6*, 18846. https://doi.org/10.1038/srep18846

Kurle, C. M., Koch, P. L., Tershy, B. R., & Croll, D. A. (2014). The effects of sex, tissue type, and dietary components on stable isotope discrimination factors (Δ^{13}C and Δ^{15}N) in mammalian omnivores. *Isotopes in Environmental and Health Studies*, *50*(3), 307–321. https://doi.org/10.1080/10256016.2014.908872

Langmead, B., Trapnell, C., Pop, M., & Salzberg, S. L. (2009). Ultrafast and memory-efficient alignment of short DNA sequences to the human genome. *Genome Biology*, *10*(3), R25. https://doi.org/10.1186/gb-2009-10-3-r25

Lavrinienko, A., Mappes, T., Tukalenko, E., Mousseau, T. A., Møller, A. P., Knight, R., … Watts, P. C. (2018). Environmental radiation alters the gut microbiome of the bank vole Myodes glareolus. *ISME Journal*, *12*, 2801. https://doi.org/10.1038/s41396-018-0214-x

Levy, O. (2004). Antimicrobial proteins and peptides: Anti-infective molecules of mammalian leukocytes. *Journal of Leukocyte Biology*, *76*(5), 909–925. https://doi.org/10.1189/jlb.0604320

Li, B., & Dewey, C. N. (2011). RSEM: Accurate transcript quantification from RNA-Seq data with or without a reference genome. *BMC Bioinformatics*, *12*(1), 323. https://doi.org/10.1186/1471-2105-12-323

Li, P., Li, M., Lindberg, M. R., Kennett, M. J., Xiong, N., & Wang, Y. (2010). PAD4 is essential for antibacterial innate immunity mediated by neutrophil extracellular traps. *The Journal of Experimental Medicine*, *207*(9), 1853–1862. https://doi.org/10.1084/jem.20100239

Liebermann, D. A., & Hoffman, B. (2008). Gadd45 in stress signaling. *Journal of Molecular Signaling*, *3*, 15. https://doi.org/10.1186/1750-2187-3-15

Limón-Pacheco, J., & Gonsebatt, M. E. (2009). The role of antioxidants and antioxidant-related enzymes in protective responses to environmentally induced oxidative stress. *Mutation Research - Genetic Toxicology and Environmental Mutagenesis.*, *674*, 137–147. https://doi.org/10.1016/j.mrgentox.2008.09.015

Loseva, O., Shubbar, E., Haghdoost, S., Evers, B., Helleday, T., & Harms-Ringdahl, M. (2014). Chronic low dose rate ionizing radiation exposure induces premature senescence in human fibroblasts that correlates with up regulation of proteins involved in protection against oxidative stress. *Proteomes*, *2*(3), 341–362. https://doi.org/10.3390/proteomes2030341

Lourenço, J., Mendo, S., & Pereira, R. (2016). Radioactively contaminated areas: Bioindicator species and biomarkers of effect in an early warning scheme for a preliminary risk assessment. *Journal of Hazardous Materials*, *317*, 503–542. https://doi.org/10.1016/j.jhazmat.2016.06.020

Lourenço, J., Pereira, R., Gonçalves, F., & Mendo, S. (2013). Metal bioaccumulation, genotoxicity and gene expression in the European wood mouse (*Apodemus sylvaticus*) inhabiting an abandoned uranium mining area. *Science of the Total Environment*, *443*, 673–680. https://doi.org/10.1016/j.scitotenv.2012.10.105

Love, M. I., Huber, W., & Anders, S. (2014). Moderated estimation of fold change and dispersion for RNA-seq data with DESEQ2. *Genome Biology*, *15*, 550. https://doi.org/10.1186/s13059-014-0550-8

Macdonald, D. W. (2007). *The encyclopedia of mammals* (3rd. ed.). Oxford, UK: Oxford University Press.

McAndrew, C. W., Gastwirt, R. F., & Donoghue, D. J. (2009). The atypical CDK activator Spy1 regulates the intrinsic DNA damage response and is dependent upon p53 to inhibit apoptosis. *Cell Cycle*, *8*(1), 66–75. https://doi.org/10.4161/cc.8.1.7451

Metz, M., Grimbaldeston, M. A., Nakae, S., Piliponsky, A. M., Tsai, M., & Galli, S. J. (2007). Mast cells in the promotion and limitation of chronic inflammation. *Immunological Reviews*, *217*, 304–328. https://doi.org/10.1111/j.1600-065X.2007.00520.x

Mikryakov, V. R., Gudkov, D. I., Mikryakov, D. V., Pomortseva, N. L., & Balabanova, L. V. (2013). Comparative characteristics of leucocytes compositions in the crucian carp *Carassius carassius* (Cyprinidae) from the waterbodies of the Chernobyl exclusion zone and from the Rybinsk reservoir. *Journal of Ichthyology*, *53*(9), 753–757. https://doi.org/10.1134/S0032945213060076

Møller, A. P., Bonisoli-Alquati, A., Mousseau, T. A., & Rudolfsen, G. (2014). Aspermy, sperm quality and radiation in chernobyl birds. *PLoS ONE*, *9*(6), https://doi.org/10.1371/journal.pone.0100296

Møller, A. P., Bonisoli-Alquati, A., Rudolfsen, G., & Mousseau, T. A. (2011). Chernobyl birds have smaller brains. *PLoS ONE*, *6*(2), e16862. https://doi.org/10.1371/journal.pone.0016862

Møller, A. P., & Mousseau, T. A. (2006). Biological consequences of Chernobyl: 20 years on. *Trends in Ecology and Evolution.*, *21*(4), 200–207. https://doi.org/10.1016/j.tree.2006.01.008

Møller, A. P., & Mousseau, T. A. (2013). Assessing effects of radiation on abundance of mammals and predator-prey interactions in Chernobyl using tracks in the snow. *Ecological Indicators*, *26*, 112–116. https://doi.org/10.1016/j.ecolind.2012.10.025

Møller, A. P., & Mousseau, T. A. (2015). Strong effects of ionizing radiation from Chernobyl on mutation rates. *Scientific Reports*, *5*, 8363. https://doi.org/10.1038/srep08363

Møller, A. P., & Mousseau, T. A. (2018). Reduced colonization by soil invertebrates to irradiated decomposing wood in Chernobyl. *Science of the Total Environment*, *645*, 773–779. https://doi.org/10.1016/j.scitotenv.2018.07.195

Morimoto, M., Kato, A., Kobayashi, J., Okuda, K., Kuwahara, Y., Kino, Y., ... Fukumoto, M. (2017). Gene expression analyses of the small intestine of pigs in the ex-evacuation zone of the Fukushima Daiichi Nuclear Power Plant. *BMC Veterinary Research*, *13*(1), https://doi.org/10.1186/s12917-017-1263-5

Morley, N. J. (2012). The effects of radioactive pollution on the dynamics of infectious diseases in wildlife. *Journal of Environmental Radioactivity*, *106*, 81–97. https://doi.org/10.1016/j.jenvrad.2011.12.019

Moskalev, A., Plyusnina, E., Shaposhnikov, M., Shilova, L., Kazachenok, A., & Zhavoronkov, A. (2012). The role of D-GADD45 in oxidative, thermal and genotoxic stress resistance. *Cell Cycle*, *11*(22), 4222–4241. https://doi.org/10.4161/cc.22545

Murphy, J. F., Nagorskaya, L. L., & Smith, J. T. (2011). Abundance and diversity of aquatic macroinvertebrate communities in lakes exposed to Chernobyl-derived ionising radiation. *Journal of Environmental Radioactivity*, *102*(7), 688–694. https://doi.org/10.1016/j.jenvrad.2011.04.007

Mustonen, V., Kesäniemi, J., Lavrinienko, A., Tukalenko, E., Mappes, T., Watts, P. C., & Jurvansuu, J. (2018). Fibroblasts from bank voles inhabiting Chernobyl have increased resistance against oxidative and DNA stresses. *BMC Cell Biology*, *19*(1), 17. https://doi.org/10.1186/s12860-018-0169-9

Naquet, P., Giessner, C., & Galland, F. (2016). Metabolic adaptation of tissues to stress releases metabolites influencing innate immunity. *Current Opinion in Immunology*, *38*, 30–38. https://doi.org/10.1016/j.coi.2015.10.005

Pajonk, F., & McBride, W. H. (2001). Ionizing radiation affects 26s proteasome function and associated molecular responses, even at low doses. *Radiotherapy and Oncology*, *59*, 203–212. https://doi.org/10.1016/S0167-8140(01)00311-5

Paton, C. M., & Ntambi, J. M. (2009). Biochemical and physiological function of stearoyl-CoA desaturase. *American Journal of Physiology-Endocrinology Metabolism*, *297*(1), 28–37. https://doi.org/10.1152/ajpendo.90897.2008

Petzke, K. J., Fuller, B. T., & Metges, C. C. (2010). Advances in natural stable isotope ratio analysis of human hair to determine nutritional and metabolic status. *Current Opinion in Clinical Nutrition and Metabolic Care*, *13*(5), 532–540. https://doi.org/10.1097/MCO.0b013e32833c3c84

Pogribny, I., Raiche, J., Slovack, M., & Kovalchuk, O. (2004). Dose-dependence, sex- and tissue-specificity, and persistence of radiation-induced genomic DNA methylation changes. *Biochemical and Biophysical Research Communications*, *320*(4), 1253–1261. https://doi.org/10.1016/j.bbrc.2004.06.081

Pujolar, J., Marino, I. A. M., Milan, M., Coppe, A., Maes, G. E., Capoccioni, F., ... Zane, L. (2012). Surviving in a toxic world: Transcriptomics and gene expression profiling in response to environmental pollution in the critically endangered European eel. *BMC Genomics*, *13*(1), 507. https://doi.org/10.1186/1471-2164-13-507

R Core Team (2018). *R: A language and environment for statistical computing*. Vienna, Austria: R Foundation for Statistical Computing. Retrieved from http://www.R-project.org/

Rauch, I., Müller, M., & Decker, T. (2013). The regulation of inflammation by interferons and their STATs. *JAK-STAT*, *2*(1), e23820. https://doi.org/10.4161/jkst.23820

Rodgers, B. E., & Baker, R. J. (2000). Frequencies of micronuclei from bank voles from zones of high radiation at Chornobyl, Ukraine. *Environmental Toxicology and Chemistry*, *19*(6), 1644–1648.

Romanovskaya, V. A., Sokolov, I. G., Rokitko, P. V., & Chernaya, N. A. (1998). Effect of radioactive contamination on soil bacteria in the 10-km zone around the Chernobyl Nuclear Power Plant. *Microbiology*, *67*(2), 226–231.

Rose, N. H., Seneca, F. O., & Palumbi, S. R. (2016). Gene networks in the wild: Identifying transcriptional modules that mediate coral resistance to experimental heat stress. *Genome Biology and Evolution*, *8*(1), 243–252. https://doi.org/10.1093/gbe/evv258

Rubin, P., & Casarett, G. W. (1968). Clinical radiation pathology as applied to curative radiotherapy. *Cancer*, *22*(4), 767–778. https://doi.org/10.1002/1097-0142(196810)22:4<767:AID-CNCR2820220412>3.0.CO;2-7

Sazykina, T., & Kryshev, I. I. (2006). Radiation effects in wild terrestrial vertebrates – The EPIC collection. *Journal of Environmental Radioactivity*, *88*, 11–48. https://doi.org/10.1016/j.jenvrad.2005.12.009

Schönfeld, P., & Reiser, G. (2013). Why does brain metabolism not favor burning of fatty acids to provide energy? – Reflections on disadvantages of the use of free fatty acids as fuel for brain. *Journal of Cerebral Blood Flow & Metabolism*, *33*(10), 1493–1499. https://doi.org/10.1038/jcbfm.2013.128

Schulte-Hostedde, A. I., Millar, J. S., & Hickling, G. J. (2001). Evaluating body condition in small mammals. *Canadian Journal of Zoology*, *79*(6), 1021–1029. https://doi.org/10.1139/cjz-79-6-1021

Seo, Y. S., Kim, J. H., Jo, N. Y., Choi, K. M., Baik, S. H., Park, J. J., ... Kim, A. (2008). PPAR agonists treatment is effective in a nonalcoholic fatty liver disease animal model by modulating fatty-acid metabolic enzymes. *Journal of Gastroenterology and Hepatology*, *23*(1), 102–109.

Shiota, G., Tsuchiya, H., & Hoshikawa, Y. (2006). The liver as a target organ of retinoids. *Hepatology Research*, *36*(4), 248–254. https://doi.org/10.1016/j.hepres.2006.08.010

Song, Y., Salbu, B., Teien, H. C., Evensen, Ø., Lind, O. C., Rosseland, B. O., & Tollefsen, K. E. (2016). Hepatic transcriptional responses in Atlantic salmon (*Salmo salar*) exposed to gamma radiation and depleted uranium singly and in combination. *Science of the Total Environment*, *562*, 270–279. https://doi.org/10.1016/j.scitotenv.2016.03.222

Soule, B. P., Brown, J. M., Kushnir-Sukhov, N. M., Simone, N. L., Mitchell, J. B., & Metcalfe, D. D. (2007). Effects of gamma radiation on FcεRI and TLR-mediated mast cell activation. *Journal of Immunology*, *179*(5). https://doi.org/10.4049/jimmunol.179.5.3276

Tan, M. G. K., Ooi, L. L. P. J., Aw, S. E., & Hui, K. M. (2004). Cloning and identification of hepatocellular carcinoma down-regulated mitochondrial carrier protein, a novel liver-specific uncoupling protein. *Journal of Biological Chemistry*, *279*(43), 45235–45244. https://doi.org/10.1074/jbc.M403683200

Vander Heiden, M. G., Cantley, L. C., & Thompson, C. B. (2009). Understanding the warburg effect: The metabolic requirements of cell proliferation. *Science*, *324*, 1029–1033. https://doi.org/10.1126/science.1160809

Yadetie, F., Andre, O., Lanzén, A., Berg, K., Olsvik, P., Hogstrand, C., & Goksøyr, A. (2013). Global transcriptome analysis of Atlantic cod (*Gadus morhua*) liver after in vivo methylmercury exposure suggests effects on energy metabolism pathways. *Aquatic Toxicology*, *126*, 314–325. https://doi.org/10.1016/j.aquatox.2012.09.013

Young, M. D., Wakefield, M. J., Smyth, G. K., & Oshlack, A. (2010). Gene ontology analysis for RNA-seq: Accounting for selection bias. *Genome Biology*, *11*(2), R14. https://doi.org/10.1186/gb-2010-11-2-r14

Yuan, H. X., Xiong, Y., & Guan, K. L. (2013). Nutrient sensing, metabolism, and cell growth control. *Molecular Cell*, *49*(3), 379–387. https://doi.org/10.1016/j.molcel.2013.01.019

Zhang, S., Hulver, M. W., McMillan, R. P., Cline, M. A., & Gilbert, E. R. (2014). The pivotal role of pyruvate dehydrogenase kinases in metabolic flexibility. *Nutrition & Metabolism*, *11*(1), 10. https://doi.org/10.1186/1743-7075-11-10

SUPPORTING INFORMATION

Additional supporting information may be found online in the Supporting Information section at the end of the article.

Supplementary material for this article: https://doi.org/10.17011/jyx/dataset/80622

III

ASSOCIATION BETWEEN GUT HEALTH AND GUT
MICROBIOTA IN A POLLUTED ENVIRONMENT

by

Jernfors T. Lavrinienko A, Vareniuk I, Landberg R, Fristed R, Tkachenko O,
Taskinen S, Tukalenko E, Kesäniemi J, Mappes T, &Watts PC. 2022

Manuscript

Association between gut health and gut microbiota in a polluted environment.

Toni Jernfors[1], Anton Lavrinienko[1], Igor Vareniuk[2], Rikard Landberg[3], Rikard Fristed[3], Olena Tkachenko[2], Sara Taskinen[4], Eugene Tukalenko[1,5], Jenni Kesäniemi[1], Tapio Mappes[1], Phillip C. Watts[1]

[1]Department of Biological and Environmental Science, University of Jyväskylä, FI-40014, Finland
[2]Department of Cytology, Histology and Reproductive Medicine, National Taras Shevchenko University of Kyiv, 01033, Ukraine
[3]Division of Food and Nutrition Science, Chalmers University of Technology, SE-412 96 Gothenburg, Sweden
[4]Department of Mathematics and Statistics, University of Jyväskylä, FI-40014, Finland
[5]Laboratory for Radiological Protection, National Research Center for Radiation Medicine, National Academy of Medical Sciences of Ukraine, 04050, Ukraine

Corresponding author: Toni Jernfors, toni.m.jernfors@jyu.fi

Abstract

Animals host complex bacterial communities in their gastrointestinal tracts, with which they share a mutualistic interaction. The numerous effects these interactions grant to the host include regulation of the immune system, defense against pathogen invasion, aid in digestion of otherwise indigestible foodstuffs and even changing host behaviour. Stress, such as environmental pollution, parasites, predators and intraspecies competition, can alter the composition of the gut microbiome, which in turn can change host-microbiome interactions in ways that are detrimental to the host such as causing metabolic dysfunction and inflammation. While host-microbiome interactions have been extensively studied in humans and captive animals, studies into wild animal microbiomes have been scarce. We assessed effects of disturbed environment on gut health of bank voles exposed to radionuclides in natural habitat using a combined approach of transcriptomics, microbial community analysis by 16S amplicon sequencing, histological staining analyses of colon tissue and quantification of gut microbiota -produced short-chain fatty acids in faecal matter and blood that act as mediators of host-microbiome interactions. We found signs of weakened mucus layer and related changes in *Clca1* and *Agr2* gene expression and microbiome composition in animals exposed to radionuclides. These results imply that disturbed environment can have widely reaching effects through gut health.

Introduction

Gut microbiota, the community of microbes that reside within animals' gastrointestinal tracts, make important contributions to the health of their hosts. Gut microbiota can comprise species of bacteria, archaea, microfungi, protists and viruses, but are typically thought to be dominated by bacteria (Shreiner *et al.* 2015). Some of the useful services provided by the gut microbiota to their hosts include digestion of complex and otherwise indigestible foodstuffs to produce key metabolites (Gentile and Weir 2018), defending against colonisation by pathogens (Pickard *et al.* 2017, Iacob *et al.* 2019), and/or training and regulation of the host's immune system (Hooper *et al.* 2012). It is therefore important to understand the processes that affect the composition of the gut microbiota.

Gut microbiota composition is largely determined by the host's experience of the environment, and thus may is impacted by diet (Zmora *et al.* 2019), season (Maurice *et al.* 2015), social interactions (Dill-McFarland *et al.* 2019), parasite burden (Cortés *et al.* 2020) and habitat quality (Amato *et al.* 2013) or pollution (Lavrinienko *et al.* 2018a, Brila *et al.* 2021). As such the gut microbiota composition can be dynamic, potentially reflecting the host's state of health and/or influencing the host's capacity to mount an appropriate response to its environment (Alberdi *et al.* 2016). Understanding the interplay between the host, its gut microbiota and the environment is important, given the current diversity and extent of anthropogenic impacts on natural environments that impact wildlife health (Acevedo-Whitehouse and Duffus 2009). But while many studies on wild animals have identified associations between some feature of the host or its environment and gut microbiota composition, few studies have examined whether changes in the gut microbiota associate with key aspects of host health.

Given the multifunctional role of the gut microbiota, there are inherent difficulties in identifying the most relevant services that would be impacted by a change in gut microbiota. Nonetheless, one of the primary services provided by the gut microbiota is the supply of metabolites to the host (Morrison and Preston 2016). Key metabolites derived from fermentation by gut bacteria are the short-chain fatty acids (SCFAs), most prominently acetic, propionic and butyric acids (den Besten *et al.* 2013, van der Hee and Wells 2021). Production of SCFAs provides a link between the gut microbiota and host physiology, for example by acting as signaling molecules (Kim 2021), having antioxidative properties (Huang *et al.* 2017) and by representing a key source of energy to the host (Lopetuso *et al.* 2013). For example, colonocytes of ruminants may obtain up to 70% of their energy by metabolising SCFAs, especially butyrate. Butyrate can also affect gene expression in the host by acting as histone deacetylase inhibitors, promoting fatty acid oxidation and having anti-inflammatory effects (Chang *et al.* 2014, van der Hee and Wells 2021). A disruption to the gut microbiota is thus likely to impact provision of such services, shaping host metabolism and health.

A healthy gut helps limit exposure of the host tissues to gut microbiota, antigens and other harmful substances. One of the primary actors of this barrier

function is the mucus barrier, which is a mesh of glycoproteins (mucins) and antibacterial proteins covering the surface of gut epithelium (Paone and Cani 2020). The rigid inner mucus layer consists of transmembrane mucins expressed by epithelial enterocytes, and a healthy inner mucus layer is impenetrable to microbes. The outer mucus layer is produced by specialized epithelial cells, goblet cells, that express and secrete the outer mucus layer's main mucin component MUC2 along with other components such as chloride channel accessory 1 (CLCA1), Fc fragment of IgG-binding protein (FCGBP), zymogen granule protein 16 (ZG16) and anterior gradient homolog (AGR2) into the gut lumen by exocytosis. In the gut lumen, several factors such as change in pH and Ca^{+2} concentration and interaction with the accompanying secreted components cause the formation and 100-1000 fold expansion of the MUC2 mesh structure (Park *et al.* 2009, Birchenough *et al.* 2015, Nyström *et al.* 2018). Many gut microbes inhabit the porous outer mucus layer, where they derive nutrients and can interface with the host's immune system (Schroeder 2019). Not only do properties of the gut mucus layer affect the gut microbiota composition, but the gut microbiota can affect the development and composition of the mucus layer (Hooper *et al.* 1999, Birchenough *et al.* 2015, Schroeder 2019). Indeed, gut mucus layer defects are often observed in diseases such as metabolic syndrome–related dysglycemia (Chassaing *et al.* 2017) and colitis (Johansson *et al.* 2014). It is not known how environmental impacts that are manifest as an altered gut microbiota affect features of the host's gut health or the services provided by the gut microbiota in wildlife.

An example of anthropogenic impacts on the composition of wildlife gut microbiota are rodents exposed to environmental radionuclides (Lavrinienko *et al.* 2018a, b, 2020, 2021, Antwis *et al.* 2021). On April 26 1986, an accident at reactor 4 of the former nuclear power plant at Chernobyl, Ukraine, resulted in the release of about 9 million terabecquerels of radionuclides into the atmosphere, with nuclear fallout largely affecting Eastern Europe, Western Russia and Fenno-Scandinavia (Møller and Mousseau 2006, Beresford *et al.* 2016). Because exposure to elevated levels of ionising radiation can cause cellular damage, either by direct damage to DNA or by elevating oxidative stress through the radiolysis of intracellular water (Ward 1988, Desouky *et al.* 2015, Einor *et al.* 2016), the Chernobyl Exclusion Zone (CEZ) was established at an approximately 30 km radius around the accident site to limit human exposure to persistent environmental radionuclides, notably strontium-90, cesium-137 and plutonium-239 (Beresford *et al.* 2016). Wildlife inhabiting the CEZ provide the best-studied models of the biological impacts of exposure to environmental radionuclides (Beresford *et al.* 2016, Bréchignac *et al.* 2016, Lourenço *et al.* 2016). The specific impacts of exposure to radionuclide contamination depend on, for example, the received dose and characteristics of the species examined (Beresford *et al.* 2020a), but a number of studies have found that animal wildlife exposed to elevated levels of ionizing radiation (IR) within the CEZ experience signs of poor condition, such as cataracts, increased oxidative stress and delayed maturation (Geras'kin *et al.* 2008, Einor *et al.* 2016, Lourenço *et al.* 2016, Cannon and Kiang 2020).

The bank vole *Myodes glareolus* is a small rodent that inhabits mixed woodlands of much of northern Europe and Asia (Macdonald 2006). This species was among the first mammals to recolonize the highly contaminated areas within the CEZ following the nuclear accident (Baker *et al.* 1996). While there is no clear evidence of DNA damage and/or elevated mutation rates associated with exposure to radionuclides (Rodgers *et al.* 2001, Kesäniemi *et al.* 2018), bank voles inhabiting contaminated areas within the CEZ are likely in worse health than those in uncontaminated areas. For example, bank vole populations in contaminated areas exhibit an increase in frequency of cataracts (Lehmann *et al.* 2016) and a reduction in population densities and litter sizes (Mappes *et al.* 2019), moreover, bank voles exposed to radionuclides show signs of metabolic remodeling (Kesäniemi *et al.* 2019a), telomere and mitochondrial damage (Kesäniemi *et al.* 2019b, 2020), and changes in genome architecture (Jernfors *et al.* 2021). An association between the condition of the environment and gut health is plausible because the gut microbiota of bank voles inhabiting areas contaminated by radionuclides differs to the gut microbiota of animals that are not exposed to radionuclides (Lavrinienko *et al.* 2018a, 2020, Antwis *et al.* 2021). A comparable association between mammal gut microbiota and exposure to radionuclides occurs in other species of rodent within the CEZ and also at the Fukushima nuclear accident site in Japan (Lavrinienko *et al.* 2021). However, it is not known whether the changes in gut microbiota associated with radionuclide exposure affect key services provided by the gut microbiota (such as SCFA supply) and/or impacts on the host's gut health (*e.g.* immune function, cell morphology).

Here, we quantify whether the change in gut microbiota elicited by exposure to environmental radionuclides associated with tangible impacts on gut health in the bank vole *Myodes glareolus*. To achieve this aim, we measured key features of animal health (*e.g.* gene expression and cell morphology of colon tissue, SCFAs in plasma) and quantified the gut microbiota (using 16S amplicon sequencing) and faecal SCFAs. Changes in host physiology and gut microbiota are associated with radionuclide contamination but there are few impacts on faecal SCFAs, implying that the possible impacts of radiation exposure on the host are not derived from a major change in services provided by the gut microbiota.

Materials & methods

Sample collection

Forty-five female bank voles were live-captured (using Ugglan Special2 live traps) from mixed forest habitats in October 2017 from four general study areas in Ukraine: the (1) east and (2) west side of Dnieper river near Kyiv, and from (3) Gluboke lake and (4) Vesnyane within the CEZ (Fig. 1), henceforth referred as uncontaminated (areas 1 and 2) and contaminated (areas 3 and 4) groups. At each location 9 or 16 traps were placed in a grid with an inter-trap distance of 15-20 m over one trapping night per trapping site, except at Gluboke lake where

two trapping nights were required to obtain sufficient samples. Traps were checked in the following morning and caught animals were transferred to the laboratory for internal absorbed dose rate estimation, body size measurement (body weight and head width), and tissue and feces sampling.

Fecal samples for microbiota analysis were collected from live animals immediately after capture as in Lavrinienko *et al.* 2018a. After fecal sample collection, sample of whole blood was taken from orbital sinus in heparinized capillary tubes. Animals were euthanized by cervical dislocation and dissected to collect additional fecal samples from the colon for SCFA quantification, and tissue samples from mid- and distal colon for histological analyses and RNA sequencing. All fecal samples were immediately stored in dry ice until archived in -80°C freezer. Colon tissue samples were stored in Allprotect Tissue Reagent (Qiagen) for RNA extraction and in two different fixatives, 10% formalin solution or metha-Carnoy solution (60% methanol, 30% chloroform, 10% glacial acetic acid) for histological analyses.

Dosimetry

Ambient radiation levels at each trapping location were measured by averaging at least 9 measurements with a hand-held Geiger counter (Gamma-Scout, GmbH & Co., Germany), placed one cm above the ground. Ambient dose rate measurements give a reasonable approximation of external absorbed dose rate for bank voles (Chesser *et al.* 2000, Beresford *et al.* 2008, Lavrinienko *et al.* 2020). The average external absorbed dose rates were 0.3±0 µGy/h (mean±*SD*) at east Kyiv, 0.15±0 µGy/h at west Kyiv, 24.12±19.18 µGy/h at Gluboke lake, and 16.23±1.29 µGy/h at Vesnyane.

Internal absorbed dose rates of bank voles were estimated by measuring ^{137}Cs activity with SAM 940 radionuclide identifier system (Berkeley Nucleonics Corporation, San Rafael, CA, USA) equipped with a 3"x3" NaI detector (Supplementary Methods 1). A sum of internal and external absorbed dose rates was considered as a total absorbed dose rate per animal (mGy/d) (Table S1), providing means (±*SD*) of 0.007±0.002 mGy/d and 0.735±0.504 mGy/d for uncontaminated and contaminated groups, respectively. Internal and external absorbed dose rates had a correlation coefficient R = 0.91.

Histological analysis of colon tissue

Fixed samples were dehydrated, embedded in paraffin with a vertical orientation, and cut into 5 µm sections. Tissue sections, fixed in 10% formalin, were stained with hematoxylin and eosin (H&E) for general inspection of tissue condition according to standard protocol (Suvarna *et al.* 2013). Tissue sections fixed in metha-Carnoy solution were stained with alcian blue (Suvarna *et al.* 2013), but counterstained with carmine for visualization of goblet cells. To remove potential bias, histological examination of the colon tissue was performed without knowledge of the treatment groups (e.g. in "blind"). Digital microphotographs of stained colon sections were taken at ×100 or ×400 magnification using a com-

puter-assisted image analyzing system consisting of Olympus BX41 microscope and Olympus C-5050 Zoom digital camera. Depth of crypts (µm), height of colonocytes (µm), area of colonocytes' nucleus (µm²) from H&E images, and the cellular area of goblet cells (µm²) from alcian blue–carmine images were measured using Image J v.1.42q (Schneider *et al.* 2012). Goblet cells were defined as normal, hypertrophic or hypotrophic states based on cell size and prevalence of mucus-containing vesicles.

SCFA quantification in blood plasma and fecal samples

SCFAs (formic, acetic, propionic, isobutyric, butyric, succinic, isovaleric, valeric and caproic acids) in plasma were analyzed by liquid chromatography–mass spectrometry (LC–MS) according to method described by (Han *et al.* 2015) (see Supplementary Methods 2 for details and modifications). Samples were analyzed using a 6500+ QTRAP triple-quadrupole mass spectrometer (AB Sciex, 11432 Stockholm, Sweden), which was equipped with an APCI source and operated in the negative-ion mode. Chromatographic separations were performed on a Phenomenex Kinetix Core-Shell C18 (2.1, 100 mm, 1.7 um 100Å) UPLC column with SecurityGuard ULTRA Cartridges (C18 2.1mm ID). SCFAs (acetic, propionic, isobutyric, butyric, isovaleric, valeric and caproic acids) in fecal samples were analyzed by gas chromatography–mass spectrometry (GC–MS) using a Shimadzu GC–MS-TQ8030 (Tokyo, Japan), fast scanning triple quadrupole gas chromatography system with a PAL autosampler, see (Cheng *et al.* 2020), with details and modifications to the protocol described in Supplementary Methods 2.

RNA sequencing of colon tissue and de novo assembly

Total RNA was extracted from colonic tissue samples using an RNeasy Mini Kit (Qiagen) according to manufacturer's protocol. Samples were sent to the Beijing Institute of Genomics (BGI), Hong Kong (https://www.bgi.com/global/) for library preparation and sequencing. RNA libraries were prepared using TruSeq Stranded mRNA Library Prep Kit (Illumina) and sequenced for 100 bp paired end (PE) reads on two lanes on Illumina HiSeq4000 resulting in depth of ~16 million PE reads per sample (Table S5). Adapters and low quality reads were removed using SOAPnuke (<20 Q).

Reads from eight samples (two samples from each study area, providing a total of 143,691,087 PE reads) were pooled for *de novo* transcriptome assembly using Trinity v.2.5.1 (parameters: default) (Grabherr *et al.* 2011), followed by transcript clustering using cd-hit-est v.4.6.8 (parameters: -c 0.98 -p 1 -d 0 -b 3) (Fu *et al.* 2012). Transcriptome completeness was estimated by the presence of assembled single copy orthologs using BUSCO v.2.0 with mammalian lineage dataset odb9 as a reference (Simão *et al.* 2015). Transcriptome was annotated using Trinotate v.3.0.1 pipeline (Bryant *et al.* 2017), leveraging UniProt (SwissProt) 2018_2 for transcript identification. Downstream analyses followed Trinity best-practice guidelines (Haas *et al.* 2013) using default parameters, with Bowtie

v.1.2.2 (Langmead *et al.* 2009) used to align reads against the transcriptome and RSEM v.1.3.1 (Li and Dewey 2011) used for alignment counting (transcripts and genes).

Gut microbiome amplicon sequencing and bioinformatics analyses

Total DNA was extracted from faecal samples (*n*=45) using a PowerFecal DNA Isolation Kit (Qiagen) following the manufacturer's instructions. All library preparation and sequencing work was performed at the BGI. Briefly, samples were processed using the Earth Microbiome Project protocol to amplify the V4 region of the 16S ribosomal RNA (rRNA) gene using the original 515F/806R primers (Caporaso *et al.* 2011). Libraries were sequenced on an Illumina HiSeq 2500 platform at BGI to provide 250 bp paired-end (PE) reads.

Read data were de-multiplexed, and adapters and primers were removed by BGI. The PE sequences (total =9,790,549, mean =217,567, range 129,304–268,333) were processed using qiime2 version 2018.8 (Bolyen *et al.* 2019). Briefly, reads were truncated at the 3′ end to remove low-quality bases (reverse reads at 186 bp), after which data were denoised using default parameters in dada2 (Callahan *et al.* 2016). The resulting feature-table contained 5,208,639 sequences, with 3,453 amplicon sequence variants (ASVs). Low-abundance (frequency < 10 across all samples) ASVs were removed. This step left 5,207,788 sequences (mean =115,728, range 74,172–137,640 sequences per sample) and 3,310 ASVs. We assigned taxonomy using a naïve Bayes classifier that has been pretrained on the Greengenes version 13_8 16S rRNA gene sequences (reads trimmed to the V4 region amplified by 515F/806R primers, and clustered at 99% identity) (Bokulich *et al.* 2018)). The final feature-table was rarefied to 74,172 sequences per sample to avoid biases caused by variation in sequencing depth among samples (Weiss *et al.* 2017).

Statistical analyses

Statistical testing was conducted using R v.4.0.2 (The R Core Team 2018), using Wilcoxon rank sum tests or Kruskal-Wallis tests when comparing medians of various parameters among contaminated and uncontaminated groups or among all four study areas, respectively. Various statistical methods were used to examine potential differences *(a)* in bank vole health and physiology, *(b)* RNAseq and *(c)* gut microbiota data among treatment groups.

(a) Bank vole health and physiology. Body condition index (BCI) reflecting general physiological condition of the voles was calculated as standardized residuals from linear regression of weight and head width (Labocha *et al.* 2014). Also, normalized liver and spleen weights were calculated as standardized residuals from a linear regression of organ weight and head width. An odds ratio for risk of incidence of abnormality classification in colonic goblet cells was calculated using package 'fmsb' v.0.7.1 (Nakazawa 2019). Exploratory data analysis of host variables (logarithm of total absorbed dose rate, morphometric and histological measurements of the colon and SCFA concentration in blood and

fecal samples) was conducted using pairwise Pearson correlations with 'corrplot' v.0.84 (Wei and Simko 2017) and by principal component analysis (PCA) using the package 'FactoMineR' v.1.34 (Lê *et al.* 2008).

(b) Gene expression. A principal component analysis of transcript counts was performed within the Trinity pipeline to summarise the main differences in transcript (gene) expression among samples. Differential expression (DE) analysis between uncontaminated and contaminated groups and between categories of goblet cell (normal, hypotrophic, and hypertrophic) was conducted using DESeq2 in Bioconductor v.3.7 (Love *et al.* 2014) with DE threshold fold change >2 and a false discovery rate (Benjamini–Hochberg's *FDR*) <0.05. Gene ontology (GO) (Ashburner *et al.* 2000) term enrichment analysis among differentially expressed transcripts and genes was performed using GOseq in Bioconductor v.3.7 (Young *et al.* 2010) to identify significantly enriched GO terms at *FDR*<0.05. We also specifically tested difference in expression of five mucosal secreted genes, *Muc2, Clca1, Fcgbp, Agr2* and *Zg16* (Birchenough *et al.* 2015, Paone and Cani 2020) between the three goblet cell classification types using Kruskal-Wallis test.

(c) Gut microbiota composition. Alpha diversity in samples was estimated using a number of observed ASVs. Linear discriminant analysis Effect Size (LEfSe) (Segata *et al.* 2011) was calculated using Galaxy web interface (https://galaxyproject.org/learn/visualization/custom/lefse/) to determine the microbial families that explain compositional differences between contaminated and uncontaminated groups, using LDA score thresholds of >2 and <-2, *p*<0.05. Package ALDEx2 v.1.11.0 (Fernandes *et al.* 2014) was used to identify differentially abundant ASVs between contaminated and uncontaminated groups, as well as between animals exhibiting hypotrophic goblet cells and other goblet cell conditions at *FDR*<0.05.

PERMANOVA with Bray-Curtis and UniFrac distances that represent compositional differences between samples (β-diversity) was used to simultaneously test the response of the gut microbiota to three environmental factors (total dose, radiation group, study area) and four general measures of phenotype (body condition index, colon goblet cell state and principal component scores on components 1 and 2 of transcript count PCA data (Anderson 2001). PERMANOVA was carried out using the adonis function (999 permutations) in vegan v.2.5-6 (Oksanen *et al.* 2018).

Results

Effects of radionuclide contamination on bank vole phenotype

Animals inhabiting areas contaminated by radionuclides did not show evidence of a major change in body condition or gut health, however exposure to radionuclides was associated with changes in the concentration of some plasma SCFAs and had an impact on transcription in the colon and goblet cell morphology.

Bank vole BCI and organ size

Bank vole BCI or organ weight did not significantly differ among the four study areas or between contaminated and uncontaminated areas. Also, total received dose rate did not correlate significantly with bank vole BCI or organ size (Fig. 2).

Plasma short chain fatty acid (SCFA) concentrations

Notably, concentrations of plasma formate in bank voles were high, averaging 346.3 μM (sd ±84.9 μM) across all samples (Table S4). Median plasma SCFA concentrations exhibited significant study area-specific differences in four of the SCFAs: propionate (Kruskal-Wallis H=10.92, p<0.05), formate (H=20.42, p<0.001), valerate (H=12.07, p<0.01) and caproate (H=15.19, p<0.01) (Table S2, Fig. S3). Plasma concentrations of propionate (R=-0.53, p<0.001) and butyrate (R=-0.34, p<0.05) had significant negative correlations with the logarithm of total dose rate, while the concentration of plasma formate exhibited a positive correlation with total dose rate (R=0.48, p<0.001) (Fig. 2). Plasma and fecal SCFA concentrations did not correlate with each other aside from isovalerate (R=0.32, p<0.05).

Colon cell morphology

We observed no obvious signs of gross pathological change (such as edema, leukocyte infiltration, disturbance in crypt structure or superficial epithelium) in the colon tissue of bank voles inhabiting contaminated areas. Colon epithelial cell nuclei in ten animals appeared hyperchromatic, which potentially indicate a decrease in transcriptional activity due to the denser staining of transcriptionally silent heterochromatin, although animals with hyperchromatic nuclei were present in all study areas.

There were no significant differences in colon cell morphometry (cell height, nuclear cross-sectional area, and crypt depth) between samples from contaminated and uncontaminated areas (Table S3). About a third of the animals from contaminated areas (8 out of 23, with three from Vesnyane and five from Gluboke) exhibited abnormally hypotrophic goblet cells, characterized by a reduction in the amount of stained mucin bodies and a low cross-sectional cell area (Fig. 4C), which indicates an impaired mucus-producing capability by these cells. Hypotrophic goblet cells were not observed in the animals inhabiting uncontaminated areas. Six animals (three from uncontaminated areas and three from Vesnyane) had hypertrophic goblet cells, indicative of increased mucus production (Fig. 4B). The odds of animals inhabiting contaminated areas exhibiting an abnormality (hypertrophy or hypotrophy) in colonic goblet cells was 5.8 times higher than uncontaminated animals (95% confidence interval=1.34-25.17) (Fig. 4D). The median goblet cell cross-sectional area was significantly lower in samples from Gluboke (Kruskal-Wallis H=11.463, df=3, p<0.01) compared with samples from the uncontaminated areas East Kyiv (post-hoc Wilcoxon test p<0.05) and West Kyiv (p<0.01). Median goblet cell area in sam-

ples from Vesnyane did not significantly differ from either uncontaminated areas or Gluboke due to high variance from presence of both hypertrophic and hypotrophic goblet cells (Fig. 4E).

Transcriptional changes in the colon

The colon transcriptome assembly (after clustering with cd-hit-est) consisted of 356050 transcripts (237,648 genes) that had a contig N50=2109 and an E90N50=3145 (Table S6). The assembly contained 86% complete mammalian BUSCOs, and 105799 transcripts received at least one GO-term annotation.

Samples from contaminated and uncontaminated areas were separated on the first two principal components, and predominantly on the second principal component (PC2) (Fig. 5), with sample scores along PC2 having a significant correlation with total dose rate (R=-0.431, $p<0.01$), indicating that general transcriptional activity differed between contaminated and uncontaminated groups. We identified 98 transcripts (66 genes) that were significantly differentially expressed (DE) (fold change >2, FDR<0.05) between samples from contaminated and uncontaminated areas. Of these DE transcripts (and genes), 68 (and 43) were up-regulated in samples from areas contaminated with radionuclides (Table S7) that represented significantly enriched gene ontology (GO) terms associated with innate immunity, including GO:0002429 'immune response-activating cell surface receptor signaling pathway', GO:0038096 'Fc-gamma receptor signaling pathway involved in phagocytosis', GO:0030449 'regulation of complement activation' and GO:0002673 'regulation of acute inflammatory response' (Table S8). There appeared to be too few significantly downregulated transcripts to identify the associated significantly enriched GO terms.

We found significant difference in expression of two genes associated with mucosal secretion, *Clca1* (Kruskal-Wallis *H*=11.02, *df*=2, $p<0.01$) and *Agr2* (Kruskal-Wallis *H*=6.52, *df*=2, $p<0.05$) among groups of animals with different goblet cell states (Fig. 6). *Clca1* showed significant downregulation in hypotrophic cells compared to hypertrophic cells (post-hoc Wilcoxon $p<0.05$) but not compared to normal cells, while neither hyper- nor hypotrophic cells showed significant difference in expression in post-hoc tests. Two other mucosal secretion related genes, *Fcgbp* and *Zg16*, showed a nonsignificant trend of downregulation in samples with hypotrophic goblet cells.

Characterization of bank vole populations by host phenotype and fecal metabolites

Principal component analysis of host phenotype revealed a cluster of animals from the contaminated locations that was separated from the cluster of samples from the two uncontaminated locations along the first two principal components (that explained a total of 41% of variance in the data) (Fig. 7). There was also a notable separation of samples among the two contaminated study areas. Bank vole phenotype such as gene expression, colon goblet cell size and formate, acetate and propionate concentrations in plasma showed an association with exposure to radionuclides, while fecal SCFAs, particularly acetate and

propionate were associated with the study area at Gluboke rather than radiation.

Bank vole gut microbiota

Exposure to radionuclides was associated with changes in the composition of the gut microbiota, and also with the concentration of some fecal SCFAs. Variation in gut microbiota composition could also be explained by the features of the bank vole colon that associated with exposure to radionuclides, such as the pattern of transcription and goblet cell morphology.

Compositional changes in bank vole gut microbiota in response to radiation and colon environment

We identified 3310 ASVs from 12 bacterial phyla in the bank vole gut microbiota inhabiting the CEZ and forests near Kyiv (Table S9). Specifically, three bacterial phyla accounted for 96% of the gut microbiota community, Firmicutes (mean = 46%), Bacteroidetes (44%), and Proteobacteria (6.1%). Bacteroidetes were dominated by members of the *S24–7* (*Muribaculaceae*) family (93% of Bacteroidetes, 42% of total community), while Firmicutes mainly comprised three families: *Ruminococcaceae* (40%), *Lachnospiraceae* (25%), an unidentified family of order Clostridiales (21%) and *Lactobacillaceae* (3.2%). This community composition is typical for the gut microbiota of bank voles and other wild rodents (Maurice *et al.* 2015, Lavrinienko *et al.* 2021).

Animals from Gluboke had significantly fewer ASVs than did samples from other areas (Kruskal-Wallis *H*=16.75, *p*<0.001, post-hoc Wilxocon *p*<0.01 compared to all other areas), while also showing reduction in species evenness (*H*=16.64, *p*<0.001, post-hoc Wilxocon *p*<0.01 compared to all other areas) (Fig. 8). ASV richness and evenness in Vesnyane did not significantly differ from the two uncontaminated groups of samples (Fig. 8), indicating no radiation effect on alpha diversity.

Bank vole gut microbiota community composition was affected by differences in the environment, with the individual study area (pseudo-F=2.601, R^2=0.16, *p*<0.001), inhabiting a contaminated/uncontaminated location (pseudo-F=3.250, R^2=0.07, *p*<0.001), and the total received dose rate (pseudo-F = 2.024, R2 = 0.045, p < 0.01) having a significant association with gut microbiota beta-diversity (Fig. 9, Table 1). Samples from the contaminated group had a 21.7% increase in proportion of Bacteroidetes and a 17.7% decrease in Firmicutes compared to uncontaminated group (Fig. 10A, S1, S2). In further detail, LEfSe analysis revealed fifteen bacterial families that exhibited a significant difference in proportion between samples from contaminated and uncontaminated groups (LDA-score >2 or <-2, *p*<0.05) (Fig. 10B). Most prominently, S24-7 (Bacteroidetes) were increased in proportion in animals from the CEZ, while decrease in Firmicutes were attributed to five families of order Clostridiales: *Ruminococcaceae*, *Lachnospiraceae*, *Syntrophomonadaceae*, *Clostridiaceae* and *Mogibacteriaceae*. At the ASV level, ALDEx2 analysis identified 17 ASVs whose abundance

significantly differed between contaminated and uncontaminated groups (*FDR*<0.05) (Fig. 11, Table 2, Table S10), including four members of the *S24-7* with a positive association with the CEZ and ten members of Clostridiales with both positive and negative associations. Notably, *Lactobacillus salivarius*, a probiont (Chaves *et al.* 2017), showed a strong decrease in the colon of bank voles in the CEZ with concomitant increase in a member of genus *Treponema*. Goblet cell hypotrophy was associated with only one ASV belonging to *S24-7* (Table S11). Notably, this one ASV also had the highest increase in abundance in the CEZ and was the most abundant in the dataset overall, accounting for 2.8% of all mapped reads.

Our data also revealed that physiological differences in the bank vole colon were associated with changes in the composition of bank vole gut bacteria. Thus, colon goblet cell classification (normal, hypotrophic and hypertrophic) (pseudo-F = 1.277, R2 = 0.057, p < 0.05) and pattern of gene expression in colon tissue on the second principal component of expression data (pseudo-F = 2.391, R2 = 0.054, p < 0.001)) had significant impacts on gut microbiota beta diversity.

Fecal short chain fatty acid (SCFA) concentration

Fecal SCFAs had significantly different concentrations among one or both contaminated areas and elsewhere (Figure 3). Bank voles from Gluboke had significantly higher median concentration of fecal propionate (Kruskal-Wallis *H*=17.00, *df*=3, *p*<0.001, post-hoc Wilxocon *p*<0.01 compared to all other areas), fecal isobutyrate (*H*=12.92, *df*=3, *p*<0.01, post-hoc Wilxocon *p*<0.05 compared to all other areas) and fecal isovalerate (*H*=13.84, *df*=3, *p*<0.01, post-hoc Wilcoxon *p*<0.05 compared to East Kyiv and Vesnyane) than did the animals sampled from all other areas. Animals from the other contaminated area, Vesnyane, had significantly reduced median concentrations of fecal valerate (*H*=19.42, *df*=3, *p*<0.001, post-hoc Wilxocon *p*<0.001 compared to all other areas). Fecal caproate showed reduction in both contaminated areas compared to uncontaminated areas (*H*=25.52, *df*=3, *p*<0.001, post-hoc Wilcoxon *p*<0.05). Fecal butyrate concentration showed some area-specific differences (*H*=7.85, *df*=3, *p*<0.05), although post-hoc analysis did not specify any particular area being different from the rest. Fecal propionate shows significant positive correlation with logarithm of total absorbed dose rate (R = 0.33, *p* < 0.05), while concentrations of valerate and caproate were significantly negatively correlated with logarithm of total dose rate (R = -0.35 and -0.61 respectively, *p* < 0.05) (Fig. 2).

Discussion

While changes in gut microbiota can associate with variation in habitat, including effects of pollution, it is rarely known whether different microbiota associate with an alteration to health of the host and/or possible services provided by the microbiota. We quantified the associations between host health (body condi-

tion, colon morphology and gene expression, plasma SCFA concentration), gut microbiota and variation in key services (faecal SCFAs) in wild bank voles exposed to environmental radionuclides. Exposure to radionuclides is associated with a distinct gut microbiota and alterations to colon function (goblet cell morphology, transcription associated with mucus layer formation, and transcription associated with immune function), with changes in the mucus-producing colon goblet cells. The total absorbed dose of radiation was associated more with levels of circulating SCFAs (formate, propionate, and butyrate) than faecal SCFAs, whose concentrations were more specific to study areas.

Impaired gut health in bank voles exposed to radionuclides is distinct from effects of radiotherapy

An acute dose of radiation (>8 Gy) in clinical settings elicits breakdown of the mucosal layer and activation of the immune system in the human colon (François *et al.* 2013, Malipatlolla *et al.* 2019). Through ingestion of soil particles and dietary items that accumulate radionuclides, such as mushrooms (Mousseau 2021), bank vole gastrointestinal tract (including the colon) may be exposed to chronic doses of radiation and thus poor health. Estimated total absorbed doses varied from 19 to 99 µGy/h, thus falling within the medium/high total dose rate band, based on the derived consideration reference level (DCRL) for rat reference (ICRP, 2008), where radiation-induced effects are expected. Colons of bank voles from contaminated areas did not show obvious signs of pathological damage, but an increase in frequency of colonic goblet cell hypotrophy that indicates reduced mucus production. The vertebrate gut mucus layer consists mainly of MUC2 glycoprotein, and other constituents such as antibacterial proteins, to form a chemo-mechanical barrier that separates the host's epithelial cells from the gut lumen (Paone and Cani 2020). In bank voles, goblet cell hypotrophy appears to associate with downregulation of *Clca1* and *Agr2* rather than a change in *Muc2* transcription. *Clca1* and *Agr2* are involved in secretion and expansion of the outer mucus layer, and indeed, *Agr2*-deficient mice lack MUC2 on protein level despite the transcription of *Muc2* on mRNA level in goblet cells (Park *et al.* 2009, Nyström *et al.* 2018). Moreover, local production of mucus in the colon is regulated by the immune system (Birchenough *et al.* 2015, Paone and Cani 2020).

The gut is a radiosensitive tissue, having a high cell turnover ratio and being connected to a major lymphatic system, the gut associated lymphoid tissue (GALT). Indeed, abdominal pain, incontinency and constipation, bleeding and mucus discharge are typical side effects of pelvic radiation therapy (François *et al.* 2013). IR has a complex dose-dependent association with inflammation and the immune system. Therapeutical doses typically cause inflammation, although conversely, lower doses (<1 Gy) may attenuate ongoing inflammation (Di Maggio *et al.* 2015, Frey *et al.* 2015), which may have stabilizing properties as chronic inflammation can cause inflammatory bowel disease. Conversely, chronic immunosuppression can lead to loss of immunocompetence (Acevedo-Whitehouse and Duffus 2009) and subsequent infection, which can be seen here

as enrichment of GO terms relating to phagocytosis and as activation of innate immunity in the spleen (Kesäniemi *et al.* 2019a). Hence, gut health of bank voles experiencing an elevated absorbed dose in the CEZ has few parallels to human and mouse models of radiotherapy.

Seasonal interactions between environmental radiation and gut microbiota

Our data add to the growing literature reporting an association between change in gut microbiota and exposure to radiation in laboratory (Liu *et al.* 2021), in space (da Silveira *et al.* 2020) and also in wild populations (via exposure to environmental radionuclides) (Lavrinienko *et al.* 2018a, 2021, Antwis *et al.* 2021) indicating that the response occurs at both acute and chronic exposures. Despite the association between radiation exposure and changes in gut bacteria, the drivers of altered gut microbiota of wild animals may include indirect consequences of radionuclide contamination. For example, the contaminated areas may have a change in vegetation that elicits a different type or quality of diet, that itself may alter the gut microbiota.

A key factor of the response of wild animal gut microbiota is the change in season (Maurice *et al.* 2015). There is apparent compositional stability in bank voles inhabiting contaminated areas of the CEZ, but a temporal compositional change in animals inhabiting uncontaminated areas from early to late summer characterized by reduction in *S24-7*, subsequently referred to as *Muribaculaceae* (Lagkouvardos *et al.* 2019), and increase in *Ruminococcaceae* and *Lachnospiraceae* families (Lavrinienko *et al.* 2020), with other studies also observing changes in proportions of *Muribaculaceae*, *Ruminococcaceae* and *Lachnospiraceae* in response to radiation in bank voles and other rodents (Antwis *et al.* 2021, Lavrinienko *et al.* 2021). Our data represents an autumn composition, where the bank vole gut microbiota is characterized by enrichment of *Muribaculaceae* in contaminated, and of *Ruminococcaceae* and *Lachnospiraceae* in uncontaminated areas. Apparently there is an interaction effect between environmental radiation and season, which manifests as proportional changes between various members of order Clostridiales and *Muribaculaceae*, with the latter being particularly sensitive to radiation. Nonetheless, the important question remains: how do changes in gut microbiota associated with radionuclide contamination relate with colon health of bank voles exposed to radionuclides within the CEZ?

Associations between microbial families and gut health

The overall reduction in *Ruminococcaceae* and *Lachnospiraceae* in contaminated areas provides one route to colon health, as these families contain several commensal species that regulate gut homeostasis and the host's immune system by forming close metabolic relationships with host colon cells and are significant butyrate producers in humans (Lopetuso *et al.* 2013, Vital *et al.* 2017, Pereira *et al.* 2020). As commensal Clostridia participate in maintenance of the mucus layer (Birchenough *et al.* 2015, Schroeder 2019), loss in abundance of radiosensitive commensal species may induce change in gene expression and thus causing ob-

served hypotrophy in goblet cells. Induction of gene expression is however mediated by butyrate (Chang *et al.* 2014, van der Hee and Wells 2021), which in this data was not associated with radiation. Alternatively, impaired mucus layer is the cause behind loss of Clostridia, as many Clostridia species feed on host glycans (Paone and Cani 2020, Guo *et al.* 2020), thus being deprived of substrate.

Muribaculaceae are a recently described family of Bacteroidetes primarily inhabiting the digestive tract in rodents with capacity to degrade both plant and host-derived glycans (Lagkouvardos *et al.* 2019). While radiation did not explain change in fecal butyrate despite loss in abundance of *Ruminococcaceae* and *Lachnospiraceae*, it is possible that *Muribaculaceae* filled this niche. Moreover, *Muribaculaceae* family in general appears to have functions relating to formate metabolism (Lagkouvardos *et al.* 2019), possibly contributing to high formate levels observed in contaminated bank voles. Nonetheless, as *Muribaculaceae* have only recently been described and are difficult to cultivate, further studies are needed to determine the exact radiation-responsive *Muribaculaceae* species and their interactions with the host and the mucosal layer.

Lactobacillus salivarius is an established probiotic, improving immunity and preventing colonization by pathogens human and animal hosts (Chaves *et al.* 2017). Here, abundance loss in commensals such as *Lactobacillus* and some Clostridiales may expose bank voles to colonization by pathogens, explaining activity of the innate immune system on gene expression level (Kesäniemi *et al.* 2019a).

Changes in circulating SCFAs but not fecal SCFAs associate with radiation exposure

Changes in circulating SCFAs represent possible outcome of radiation impacts that can affect host health. While colonocytes consume a large portion of SCFAs as energy, the remaining absorbed SCFAs are transported to the liver via the portal vein and then to peripheral tissues (Boets *et al.* 2017, Liu *et al.* 2018). In humans, circulating SCFAs but not fecal SCFAs associate with impacts on host metabolism (Müller *et al.* 2019), as fecal SCFA concentrations represent the net effect of factors such as microbial composition, absorption by host and time of day (Sakata 2019). Here, lower concentration of circulating propionate and butyrate, rather than fecal SCFAs in general, were associated with radiation. This suggests that environmental radiation directly impacts SCFA uptake from the gut, regulation of SCFA circulation by the liver or SCFA usage by host tissues instead of acting through changes in gut microbial composition. Propionate and acetate impact host metabolism in various tissues via histone deacetylase inhibition and ligation to G-protein coupled receptors, increasing fatty acid oxidation and reducing inflammation (van der Hee and Wells 2021). As such, reduction in circulating SCFAs may seem paradoxical, however, SCFAs, particularly butyrate, have been reported to have apparently conflicting effects in some conditions, e.g., in cancer tissue (Liu *et al.* 2018, van der Hee and Wells 2021). Future studies ascertaining the effect of radiation on SCFAs should include temporal

sampling as well as additional sampling from the portal vein to more accurately quantify the flux of SCFAs from the gut into host circulation.

Levels of formic acid in bank vole plasma (>300 µM) were about threefold greater than that reported for laboratory rodents and humans (10-100 µM) (Brosnan and Brosnan 2016, Pietzke *et al.* 2019). Moreover, the significant positive correlation between circulating formate and total absorbed dose rate implies an association between radiation exposure and one-carbon metabolism. Most formate (~50%) is produced in the mitochondria by catabolism of serine, with the remainder derived from various other metabolic pathways and dietary sources (Brosnan and Brosnan 2016). While it is possible that the increased formate levels are associated with *Muribaculaceae* (Lagkouvardos *et al.* 2019), in our previous studies we have observed upregulation of mitochondrial biogenesis regulator PCG1α and several genes relating to fatty acid oxidation and mitochondrial stress such as *Cpt1a*, *Atf5* and *Fgf21* in bank voles inhabiting the CEZ (Kesäniemi *et al.* 2019a, 2020). Similar effects were also observed in astronauts and mice as consequence of spaceflights (da Silveira *et al.* 2020), suggesting that mitochondrial function lies at a key position regarding metabolic responses to low-dose IR.

Formate overflow is associated with numerous diseases and conditions such as methanol poisoning, folate & vitamin B-12 deficiency, birth defects and oxidative cancer (Meiser *et al.* 2018, Pietzke *et al.* 2019). Benefits of formate overflow are an open question, and the potential benefits largely depend on the underlying causes of overflow. For instance, while catabolism of serine into formate also produces NADH and NADPH which could be used to maintain cellular redox balance (Fan *et al.* 2014) in the oxidative environment of the CEZ, aberrant formate levels may also implicate mitochondrial dysfunction. Whether formate overflow provides selective benefits in bank voles inhabiting the CEZ or is merely a side effect of metabolic remodeling or mitochondrial stress affecting one-carbon metabolism should be tested in future experiments.

Conclusions

There is some controversy among studies concerning effects of low dose ionizing radiation on wildlife of the CEZ (Beresford *et al.* 2020b). The CEZ is a wildlife reserve with an apparently vigorous ecosystem due to inadvertent rewilding, and some studies report little or no effects of radiation on abundance of wildlife in the zone (Murphy *et al.* 2011, Deryabina *et al.* 2015). On the other hand, while the ecosystem thrives due to absence of humans, organisms experience chronic oxidative stress (Einor *et al.* 2016) that, when combined with cumulative stressors of a natural environment, may lead to poor health in the wild.

We conducted a comprehensive survey of gut microbiome and intercorrelated environmental and host variables driving gut health in a wild animal population exposed to radionuclide contamination. Lack of visible inflammation together with earlier results of immunosuppression in the liver (Kesäniemi *et al.* 2019a) is consistent with immunosuppressive effects of prolonged stress reaction. Colon goblet cell hypotrophy and downregulation in related secreted

genes possibly indicate poor gut health resulting from stress, however further experiments are required to assess whether gut condition interacts with compositional changes between *Muribaculaceae, Ruminococcaceae* and *Lachnospiraceae*, bacterial families that include many members that inhabit the outer mucus layer. Although we cannot test microbiome-immunity associations in the wild, the lack of radiation impact on fecal SCFAs together with radiation-associated impacts on circulating SCFAs indicate that host metabolism is driven by the effect of radiation directly rather than through microbially produced SCFA affecting host physiology. Further evidence of this is provided by radiation dose - associated formate overflow that may be related to mitochondrial function and metabolic changes reported earlier (Kesäniemi *et al.* 2019a, 2020). These novel responses not observed in controlled clinical settings highlight the need of studying the effects of exposure to anthropogenic stressors on wildlife in natural settings.

Acknowledgements

Ethics statement

Authors declare no competing interests. All experiments complied with the legal requirements and adhered closely to international guidelines for the use of animals in research. All necessary permissions were obtained from the Animal Experimentation Committee for these experiments (permission no. ESAVI/7256/04.10.07/2014).

Author contributions

PW, TJ and AL conceived the project. TM provided sampling infrastructure and TJ, AL and ET performed sampling. TJ, AL, IV, RL, RF and OT performed laboratory work. TJ and AL performed bioinformatic analyses. TJ wrote the manuscript in collaboration with all authors.

References

Acevedo-Whitehouse K. & Duffus A.L.J. 2009. Effects of environmental change on wildlife health. *Philos. Trans. R. Soc. B Biol. Sci.* 364: 3429–3438.

Alberdi A., Aizpurua O., Bohmann K., Zepeda-Mendoza M.L. & Gilbert M.T.P. 2016. Do Vertebrate Gut Metagenomes Confer Rapid Ecological Adaptation? *Trends Ecol. Evol.* 31: 689–699.

Amato K.R., Yeoman C.J., Kent A., Righini N., Carbonero F., Estrada A., Rex

Gaskins H., Stumpf R.M., Yildirim S., Torralba M., Gillis M., Wilson B.A., Nelson K.E., White B.A. & Leigh S.R. 2013. Habitat degradation impacts black howler monkey (Alouatta pigra) gastrointestinal microbiomes. *ISME J.*

Anderson M.J. 2001. A new method for non-parametric multivariate analysis of variance. *Austral Ecol.* 26: 32–46.

Antwis R.E., Beresford N.A., Jackson J.A., Fawkes R., Barnett C.L., Potter E., Walker L., Gaschak S. & Wood M.D. 2021. Impacts of radiation exposure on the bacterial and fungal microbiome of small mammals in the Chernobyl Exclusion Zone. *J. Anim. Ecol.*: 1365-2656.13507.

Ashburner M., Ball C.A., Blake J.A., Botstein D., Butler H., Cherry J.M., Davis A.P., Dolinski K., Dwight S.S., Eppig J.T., Harris M.A., Hill D.P., Issel-Tarver L., Kasarskis A., Lewis S., Matese J.C., Richardson J.E., Ringwald M., Rubin G.M. & Sherlock G. 2000. Gene Ontology: tool for the unification of biology. *Nat. Genet.* 25: 25–29.

Baker R.J., Hamilton M.J., Bussche R.A. Van Den, Wiggins L.E., Sugg D.W., Smith M.H., Lomakin M.D., Gaschak S.P., Bundova E.G., Rudenskaya G.A. & Chesser R.K. 1996. Small Mammals from the Most Radioactive Sites Near the Chornobyl Nuclear Power Plant. *J. Mammal.* 77: 155–170.

Beresford N.A., Barnett C.L., Gashchak S., Maksimenko A., Guliaichenko E., Wood M.D. & Izquierdo M. 2020a. Radionuclide transfer to wildlife at a 'Reference site' in the Chernobyl Exclusion Zone and resultant radiation exposures. *J. Environ. Radioact.* 211: 105661.

Beresford N.A., Fesenko S., Konoplev A., Skuterud L., Smith J.T. & Voigt G. 2016. Thirty years after the Chernobyl accident: What lessons have we learnt? *J. Environ. Radioact.* 157: 77–89.

Beresford N.A., Gaschak S., Barnett C.L., Howard B.J., Chizhevsky I., Strømman G., Oughton D.H., Wright S.M., Maksimenko A. & Copplestone D. 2008. Estimating the exposure of small mammals at three sites within the Chernobyl exclusion zone – a test application of the ERICA Tool. *J. Environ. Radioact.* 99: 1496–1502.

Beresford N.A.A., Horemans N., Copplestone D., Raines K.E.E., Orizaola G., Wood M.D.D., Laanen P., Whitehead H.C.C., Burrows J.E.E., Tinsley M.C.C., Smith J.T.T., Bonzom J.-M.M., Gagnaire B., Adam-Guillermin C., Gashchak S., Jha A.N.N., Menezes A. de, Willey N. & Spurgeon D. 2020b. Towards solving a scientific controversy – The effects of ionising radiation on the environment. *J. Environ. Radioact.* 211: 106033.

Besten G. den, Eunen K. van, Groen A.K., Venema K., Reijngoud D.-J. & Bakker B.M. 2013. The role of short-chain fatty acids in the interplay between diet, gut microbiota, and host energy metabolism. *J. Lipid Res.* 54: 2325–2340.

Birchenough G.M.H., Johansson M.E.V., Gustafsson J.K., Bergström J.H. & Hansson G.C. 2015. New developments in goblet cell mucus secretion and function. *Mucosal Immunol.* 8: 712–719.

Boets E., Gomand S. V., Deroover L., Preston T., Vermeulen K., Preter V. De, Hamer H.M., Mooter G. Van den, Vuyst L. De, Courtin C.M., Annaert P., Delcour J.A. & Verbeke K.A. 2017. Systemic availability and metabolism of

colonic-derived short-chain fatty acids in healthy subjects: a stable isotope study. *J. Physiol.* 595: 541–555.

Bokulich N.A., Kaehler B.D., Rideout J.R., Dillon M., Bolyen E., Knight R., Huttley G.A. & Gregory Caporaso J. 2018. Optimizing taxonomic classification of marker-gene amplicon sequences with QIIME 2's q2-feature-classifier plugin. *Microbiome* 6: 90.

Bolyen E., Rideout J.R., Dillon M.R., Bokulich N.A., Abnet C.C., Al-Ghalith G.A., Alexander H., Alm E.J., Arumugam M., Asnicar F., Bai Y., Bisanz J.E., Bittinger K., Brejnrod A., Brislawn C.J., Brown C.T., Callahan B.J., Caraballo-Rodríguez A.M., Chase J., Cope E.K., Silva R. Da, Diener C., Dorrestein P.C., Douglas G.M., Durall D.M., Duvallet C., Edwardson C.F., Ernst M., Estaki M., Fouquier J., Gauglitz J.M., Gibbons S.M., Gibson D.L., Gonzalez A., Gorlick K., Guo J., Hillmann B., Holmes S., Holste H., Huttenhower C., Huttley G.A., Janssen S., Jarmusch A.K., Jiang L., Kaehler B.D., Kang K. Bin, Keefe C.R., Keim P., Kelley S.T., Knights D., Koester I., Kosciolek T., Kreps J., Langille M.G.I., Lee J., Ley R., Liu Y.-X., Loftfield E., Lozupone C., Maher M., Marotz C., Martin B.D., McDonald D., McIver L.J., Melnik A. V., Metcalf J.L., Morgan S.C., Morton J.T., Naimey A.T., Navas-Molina J.A., Nothias L.F., Orchanian S.B., Pearson T., Peoples S.L., Petras D., Preuss M.L., Pruesse E., Rasmussen L.B., Rivers A., Robeson M.S., Rosenthal P., Segata N., Shaffer M., Shiffer A., Sinha R., Song S.J., Spear J.R., Swafford A.D., Thompson L.R., Torres P.J., Trinh P., Tripathi A., Turnbaugh P.J., Ul-Hasan S., Hooft J.J.J. van der, Vargas F., Vázquez-Baeza Y., Vogtmann E., Hippel M. von, Walters W., Wan Y., Wang M., Warren J., Weber K.C., Williamson C.H.D., Willis A.D., Xu Z.Z., Zaneveld J.R., Zhang Y., Zhu Q., Knight R. & Caporaso J.G. 2019. Reproducible, interactive, scalable and extensible microbiome data science using QIIME 2. *Nat. Biotechnol.* 37: 852–857.

Bréchignac F., Oughton D., Mays C., Barnthouse L., Beasley J.C., Bonisoli-Alquati A., Bradshaw C., Brown J., Dray S., Geras'kin S., Glenn T., Higley K., Ishida K., Kapustka L., Kautsky U., Kuhne W., Lynch M., Mappes T., Mihok S., Møller A.P., Mothersill C., Mousseau T.A., Otaki J.M., Pryakhin E., Rhodes O.E., Salbu B., Strand P. & Tsukada H. 2016. Addressing ecological effects of radiation on populations and ecosystems to improve protection of the environment against radiation: Agreed statements from a Consensus Symposium. *J. Environ. Radioact.* 158–159: 21–29.

Brila I., Lavrinienko A., Tukalenko E., Ecke F., Rodushkin I., Kallio E.R., Mappes T. & Watts P.C. 2021. Low-level environmental metal pollution is associated with altered gut microbiota of a wild rodent, the bank vole (Myodes glareolus). *Sci. Total Environ.* 790: 148224.

Brosnan M.E. & Brosnan J.T. 2016. Formate: The Neglected Member of One-Carbon Metabolism. *Annu. Rev. Nutr.* 36: 369–388.

Bryant D.M., Johnson K., DiTommaso T., Tickle T., Couger M.B., Payzin-Dogru D., Lee T.J., Leigh N.D., Kuo T.H., Davis F.G., Bateman J., Bryant S., Guzikowski A.R., Tsai S.L., Coyne S., Ye W.W., Freeman R.M., Peshkin L., Tabin C.J., Regev A., Haas B.J. & Whited J.L. 2017. A Tissue-Mapped

Axolotl De Novo Transcriptome Enables Identification of Limb Regeneration Factors. *Cell Rep.* 18: 762–776.

Callahan B.J., McMurdie P.J., Rosen M.J., Han A.W., Johnson A.J.A. & Holmes S.P. 2016. DADA2: High-resolution sample inference from Illumina amplicon data. *Nat. Methods* 13: 581–583.

Cannon G. & Kiang J.G. 2020. A review of the impact on the ecosystem after ionizing irradiation: wildlife population. *Int. J. Radiat. Biol.* 0: 1–9.

Caporaso J.G., Lauber C.L., Walters W.A., Berg-Lyons D., Lozupone C.A., Turnbaugh P.J., Fierer N. & Knight R. 2011. Global patterns of 16S rRNA diversity at a depth of millions of sequences per sample. *Proc. Natl. Acad. Sci.* 108: 4516–4522.

Chang P. V., Hao L., Offermanns S. & Medzhitov R. 2014. The microbial metabolite butyrate regulates intestinal macrophage function via histone deacetylase inhibition. *Proc. Natl. Acad. Sci.* 111: 2247–2252.

Chassaing B., Raja S.M., Lewis J.D., Srinivasan S. & Gewirtz A.T. 2017. Colonic Microbiota Encroachment Correlates With Dysglycemia in Humans. *CMGH* 4: 205–221.

Chaves B.D., Brashears M.M. & Nightingale K.K. 2017. Applications and safety considerations of Lactobacillus salivarius as a probiotic in animal and human health. *J. Appl. Microbiol.* 123: 18–28.

Cheng K., Brunius C., Fristedt R. & Landberg R. 2020. An LC-QToF MS based method for untargeted metabolomics of human fecal samples. *Metabolomics* 16: 46.

Chesser R.K., Sugg D.W., Lomakin M.D., Bussche R.A. van den, DeWoody J.A., Jagoe C.H., Dallas C.E., Whicker F.W., Smith M.H., Gaschak S.P., Chizhevsky I. V, Lyabik V. V, Buntova E.G., Holloman K. & Baker R.J. 2000. Concentrations and dose rate estimates of 134137 cesium and 90 strontium in small mammals at chornobyl, Ukraine. *Environ. Toxicol. Chem.* 19: 305–312.

Cortés A., Clare S., Costain A., Almeida A., McCarthy C., Harcourt K., Brandt C., Tolley C., Rooney J., Berriman M., Lawley T., MacDonald A.S., Rinaldi G. & Cantacessi C. 2020. Baseline Gut Microbiota Composition Is Associated With Schistosoma mansoni Infection Burden in Rodent Models. *Front. Immunol.* 11: 1.

Deryabina T.G., Kuchmel S.V., Nagorskaya L.L., Hinton T.G., Beasley J.C., Lerebours A. & Smith J.T. 2015. Long-term census data reveal abundant wildlife populations at Chernobyl. *Curr. Biol.* 25: R824–R826.

Desouky O., Ding N. & Zhou G. 2015. Targeted and non-targeted effects of ionizing radiation. *J. Radiat. Res. Appl. Sci.* 8: 247–254.

Dill-McFarland K.A., Tang Z.Z., Kemis J.H., Kerby R.L., Chen G., Palloni A., Sorenson T., Rey F.E. & Herd P. 2019. Close social relationships correlate with human gut microbiota composition. *Sci. Rep.* 9: 1–10.

Einor D., Bonisoli-Alquati A., Costantini D., Mousseau T.A.A. & Møller A.P.P. 2016. Ionizing radiation, antioxidant response and oxidative damage: A meta-analysis. *Sci. Total Environ.* 548–549: 463–471.

Fan J., Ye J., Kamphorst J.J., Shlomi T., Thompson C.B. & Rabinowitz J.D. 2014.

Quantitative flux analysis reveals folate-dependent NADPH production. *Nature* 510: 298–302.

Fernandes A.D., Reid J.N., Macklaim J.M., McMurrough T.A., Edgell D.R. & Gloor G.B. 2014. Unifying the analysis of high-throughput sequencing datasets: characterizing RNA-seq, 16S rRNA gene sequencing and selective growth experiments by compositional data analysis. *Microbiome 2014 21* 2: 1–13.

François A., Milliat F., Guipaud O. & Benderitter M. 2013. Inflammation and immunity in radiation damage to the gut mucosa. *Biomed Res. Int.* 2013.

Frey B., Hehlgans S., Rödel F. & Gaipl U.S. 2015. Modulation of inflammation by low and high doses of ionizing radiation: Implications for benign and malign diseases. *Cancer Lett.* 368: 230–237.

Fu L., Niu B., Zhu Z., Wu S. & Li W. 2012. CD-HIT: accelerated for clustering the next-generation sequencing data. *Bioinformatics* 28: 3150–3152.

Gentile C.L. & Weir T.L. 2018. The gut microbiota at the intersection of diet and human health. *Science (80-.).* 362: 776–780.

Geras'kin S.A., Fesenko S.V. & Alexakhin R.M. 2008. Effects of non-human species irradiation after the Chernobyl NPP accident. *Environ. Int.* 34: 880–897.

Grabherr M.G., Haas B.J., Yassour M., Levin J.Z., Thompson D.A., Amit I., Adiconis X., Fan L., Raychowdhury R., Zeng Q., Chen Z., Mauceli E., Hacohen N., Gnirke A., Rhind N., Palma F. di, Birren B.W., Nusbaum C., Lindblad-Toh K., Friedman N. & Regev A. 2011. Full-length transcriptome assembly from RNA-Seq data without a reference genome. *Nat. Biotechnol.* 29: 644–652.

Guo P., Zhang K., Ma X. & He P. 2020. Clostridium species as probiotics: potentials and challenges. *J. Anim. Sci. Biotechnol.* 11: 24.

Haas B.J., Papanicolaou A., Yassour M., Grabherr M., Blood P.D., Bowden J., Couger M.B., Eccles D., Li B., Lieber M., MacManes M.D., Ott M., Orvis J., Pochet N., Strozzi F., Weeks N., Westerman R., William T., Dewey C.N., Henschel R., LeDuc R.D., Friedman N. & Regev A. 2013. De novo transcript sequence reconstruction from RNA-seq using the Trinity platform for reference generation and analysis. *Nat. Protoc.* 8: 1494–1512.

Han J., Lin K., Sequeira C. & Borchers C.H. 2015. An isotope-labeled chemical derivatization method for the quantitation of short-chain fatty acids in human feces by liquid chromatography–tandem mass spectrometry. *Anal. Chim. Acta* 854: 86–94.

Hee B. van der & Wells J.M. 2021. Microbial Regulation of Host Physiology by Short-chain Fatty Acids. *Trends Microbiol.* 29: 700–712.

Hooper L. V., Littman D.R. & Macpherson A.J. 2012. Interactions between the microbiota and the immune system. *Science (80-.).*

Hooper L. V., Xu J., Falk P.G., Midtvedt T. & Gordon J.I. 1999. A molecular sensor that allows a gut commensal to control its nutrient foundation in a competitive ecosystem. *Proc. Natl. Acad. Sci.* 96: 9833–9838.

Huang W., Guo H.-L., Deng X., Zhu T.-T., Xiong J.-F., Xu Y.-H. & Xu Y. 2017. Short-Chain Fatty Acids Inhibit Oxidative Stress and Inflammation in

Mesangial Cells Induced by High Glucose and Lipopolysaccharide. *Exp. Clin. Endocrinol. Diabetes* 125: 98–105.

Iacob S., Iacob D.G. & Luminos L.M. 2019. Intestinal Microbiota as a Host Defense Mechanism to Infectious Threats. *Front. Microbiol.* 9.

Jernfors T., Danforth J., Kesäniemi J., Lavrinienko A., Tukalenko E., Fajkus J., Dvořáčková M., Mappes T. & Watts P.C. 2021. Expansion of rDNA and pericentromere satellite repeats in the genomes of bank voles Myodes glareolus exposed to environmental radionuclides. *Ecol. Evol.*: ece3.7684.

Johansson M.E. V, Gustafsson J.K., Holmén-Larsson J., Jabbar K.S., Xia L., Xu H., Ghishan F.K., Carvalho F.A., Gewirtz A.T., Sjövall H. & Hansson G.C. 2014. Bacteria penetrate the normally impenetrable inner colon mucus layer in both murine colitis models and patients with ulcerative colitis. *Gut* 63: 281–291.

Kesäniemi J., Boratyński Z., Danforth J., Itam P., Jernfors T., Lavrinienko A., Mappes T., Møller A.P., Mousseau T.A. & Watts P.C. 2018. Analysis of heteroplasmy in bank voles inhabiting the Chernobyl exclusion zone: A commentary on Baker et al. (2017) "Elevated mitochondrial genome variation after 50 generations of radiation exposure in a wild rodent." *Evol. Appl.* 11: 820–826.

Kesäniemi J., Jernfors T., Lavrinienko A., Kivisaari K., Kiljunen M., Mappes T. & Watts P.C. 2019a. Exposure to environmental radionuclides is associated with altered metabolic and immunity pathways in a wild rodent. *Mol. Ecol.*: mec.15241.

Kesäniemi J., Lavrinienko A., Tukalenko E., Boratyński Z., Kivisaari K., Mappes T., Milinevsky G., Møller A.P., Mousseau T.A. & Watts P.C. 2019b. Exposure to environmental radionuclides associates with tissue-specific impacts on telomerase expression and telomere length. *Sci. Rep.* 9: 850.

Kesäniemi J., Lavrinienko A., Tukalenko E., Moutinho A.F., Mappes T., Møller A.P., Mousseau T.A. & Watts P.C. 2020. Exposure to environmental radionuclides alters mitochondrial DNA maintenance in a wild rodent. *Evol. Ecol.* 34: 163–174.

Kim C.H. 2021. Control of lymphocyte functions by gut microbiota-derived short-chain fatty acids. *Cell. Mol. Immunol.* 18: 1161–1171.

Labocha M.K., Schutz H. & Hayes J.P. 2014. Which body condition index is best? *Oikos* 123: 111–119.

Lagkouvardos I., Lesker T.R., Hitch T.C.A., Gálvez E.J.C., Smit N., Neuhaus K., Wang J., Baines J.F., Abt B., Stecher B., Overmann J., Strowig T. & Clavel T. 2019. Sequence and cultivation study of Muribaculaceae reveals novel species, host preference, and functional potential of this yet undescribed family. *Microbiome* 7: 1–15.

Langmead B., Trapnell C., Pop M. & Salzberg S.L. 2009. Ultrafast and memory-efficient alignment of short DNA sequences to the human genome. *Genome Biol.* 10: R25.

Lavrinienko A., Hämäläinen A., Hindström R., Tukalenko E., Boratyński Z., Kivisaari K., Mousseau T.A., Watts P.C. & Mappes T. 2021. Comparable response of wild rodent gut microbiome to anthropogenic habitat

contamination. *Mol. Ecol.*: mec.15945.

Lavrinienko A., Mappes T., Tukalenko E., Mousseau T.A., Møller A.P., Knight R., Morton J.T., Thompson L.R. & Watts P.C. 2018a. Environmental radiation alters the gut microbiome of the bank vole Myodes glareolus. *ISME J.* 12: 2801–2806.

Lavrinienko A., Tukalenko E., Kesäniemi J., Kivisaari K., Masiuk S., Boratyński Z., Mousseau T.A., Milinevsky G., Mappes T. & Watts P.C. 2020. Applying the Anna Karenina principle for wild animal gut microbiota: Temporal stability of the bank vole gut microbiota in a disturbed environment Hoye B. (ed.). *J. Anim. Ecol.*: 1365-2656.13342.

Lavrinienko A., Tukalenko E., Mappes T. & Watts P.C. 2018b. Skin and gut microbiomes of a wild mammal respond to different environmental cues. *Microbiome* 6: 209.

Lê S., Josse J. & Husson F. 2008. FactoMineR: An R package for multivariate analysis. *J. Stat. Softw.*

Lehmann P., Boratyński Z., Mappes T., Mousseau T.A. & Møller A.P. 2016. Fitness costs of increased cataract frequency and cumulative radiation dose in natural mammalian populations from Chernobyl. *Sci. Rep.* 6: 19974.

Li B. & Dewey C.N. 2011. RSEM: accurate transcript quantification from RNA-Seq data with or without a reference genome. *BMC Bioinformatics* 12: 323.

Liu J., Liu C. & Yue J. 2021. Radiotherapy and the gut microbiome: facts and fiction. *Radiat. Oncol. 2021 161* 16: 1–15.

Liu H., Wang J., He T., Becker S., Zhang G., Li D. & Ma X. 2018. Butyrate: A Double-Edged Sword for Health? *Adv. Nutr.* 9: 21–29.

Lopetuso L.R., Scaldaferri F., Petito V. & Gasbarrini A. 2013. Commensal Clostridia: Leading players in the maintenance of gut homeostasis. *Gut Pathog.* 5: 1–8.

Lourenço J., Mendo S. & Pereira R. 2016. Radioactively contaminated areas: Bioindicator species and biomarkers of effect in an early warning scheme for a preliminary risk assessment. *J. Hazard. Mater.* 317: 503–542.

Love M.I., Huber W. & Anders S. 2014. Moderated estimation of fold change and dispersion for RNA-seq data with DESeq2. *Genome Biol.* 15: 550.

Macdonald D.W. 2006. *The Encyclopedia of Mammals*. Oxford University Press.

Maggio F. Di, Minafra L., Forte G., Cammarata F., Lio D., Messa C., Gilardi M. & Bravatà V. 2015. Portrait of inflammatory response to ionizing radiation treatment. *J. Inflamm.* 12: 14.

Malipatlolla D.K., Patel P., Sjöberg F., Devarakonda S., Kalm M., Angenete E., Lindskog E.B., Grandér R., Persson L., Stringer A., Wilderäng U., Swanpalmer J., Kuhn H.G., Steineck G. & Bull C. 2019. Long-term mucosal injury and repair in a murine model of pelvic radiotherapy. *Sci. Rep.* 9: 4–13.

Mappes T., Boratyński Z., Kivisaari K., Lavrinienko A., Milinevsky G., Mousseau T.A., Møller A.P., Tukalenko E. & Watts P.C. 2019. Ecological mechanisms can modify radiation effects in a key forest mammal of Chernobyl. *Ecosphere* 10: e02667.

Maurice C.F., CL Knowles S., Ladau J., Pollard K.S., Fenton A., Pedersen A.B. &

Turnbaugh P.J. 2015. Marked seasonal variation in the wild mouse gut microbiota. *ISME J.* 9: 2423–2434.

Meiser J., Schuster A., Pietzke M., Voorde J. Vande, Athineos D., Oizel K., Burgos-Barragan G., Wit N., Dhayade S., Morton J.P., Dornier E., Sumpton D., Mackay G.M., Blyth K., Patel K.J., Niclou S.P., Vazquez A., Voorde J. Vande, Athineos D., Oizel K., Burgos-Barragan G., Wit N., Dhayade S., Morton J.P., Dornier E., Sumpton D., Mackay G.M., Blyth K., Patel K.J., Niclou S.P. & Vazquez A. 2018. Increased formate overflow is a hallmark of oxidative cancer. *Nat. Commun.* 9: 1368.

Møller A.P. & Mousseau T.A. 2006. Biological consequences of Chernobyl: 20 years on. *Trends Ecol. Evol.* 21: 200–207.

Morrison D.J. & Preston T. 2016. Formation of short chain fatty acids by the gut microbiota and their impact on human metabolism. *Gut Microbes* 7: 189–200.

Mousseau T.A. 2021. The Biology of Chernobyl. *Annu. Rev. Ecol. Evol. Syst.* 52: 87–109.

Müller M., Hernández M.A.G., Goossens G.H., Reijnders D., Holst J.J., Jocken J.W.E., Eijk H. van, Canfora E.E. & Blaak E.E. 2019. Circulating but not faecal short-chain fatty acids are related to insulin sensitivity, lipolysis and GLP-1 concentrations in humans. *Sci. Reports 2019 91* 9: 1–9.

Murphy J.F., Nagorskaya L.L. & Smith J.T. 2011. Abundance and diversity of aquatic macroinvertebrate communities in lakes exposed to Chernobyl-derived ionising radiation. *J. Environ. Radioact.* 102: 688–694.

Nakazawa M. 2019. fmsb: Functions for Medical Statistics Book with some Demographic Data. R package version 0.7.0.

Nyström E.E.L., Birchenough G.M.H., Post S. van der, Arike L., Gruber A.D., Hansson G.C. & Johansson M.E.V. 2018. Calcium-activated Chloride Channel Regulator 1 (CLCA1) Controls Mucus Expansion in Colon by Proteolytic Activity. *EBioMedicine* 33: 134–143.

Oksanen J., Blanchet F.G., Kindt R., Legen- P., Minchin P.R., Hara R.B.O., Simpson G.L., Soly- P., Stevens M.H.H. & Wagner H. 2018. Package ' vegan ' version 2.5-2. *Community Ecol. Packag.*

Paone P. & Cani P.D. 2020. Mucus barrier, mucins and gut microbiota: the expected slimy partners? *Gut* 69: 2232–2243.

Park S.W., Zhen G., Verhaeghe C., Nakagami Y., Nguyenvu L.T., Barczak A.J., Killeen N. & Erle D.J. 2009. The protein disulfide isomerase AGR2 is essential for production of intestinal mucus. *Proc. Natl. Acad. Sci. U. S. A.* 106: 6950–6955.

Pereira F.C., Wasmund K., Cobankovic I., Jehmlich N., Herbold C.W., Lee K.S., Sziranyi B., Vesely C., Decker T., Stocker R., Warth B., Bergen M. von, Wagner M. & Berry D. 2020. Rational design of a microbial consortium of mucosal sugar utilizers reduces Clostridiodes difficile colonization. *Nat. Commun.* 11.

Pickard J.M., Zeng M.Y., Caruso R. & Núñez G. 2017. Gut microbiota: Role in pathogen colonization, immune responses, and inflammatory disease. *Immunol. Rev.*

Pietzke M., Meiser J. & Vazquez A. 2019. Formate metabolism in health and disease. *Mol. Metab.*: 1–15.

Rodgers B.E., Wickliffe J.K., Phillips C.J., Chesser R.K. & Baker R.J. 2001. Experimental exposure of naive bank voles (Clethrionomys glareolus) to the Chornobyl, Ukraine, environment: A test of radioresistance. *Environ. Toxicol. Chem.* 20: 1936–1941.

Sakata T. 2019. Pitfalls in short-chain fatty acid research: A methodological review. *Anim. Sci. J.* 90: 3–13.

Schneider C.A., Rasband W.S. & Eliceiri K.W. 2012. NIH Image to ImageJ: 25 years of image analysis. *Nat. Methods* 9: 671–675.

Schroeder B.O. 2019. Fight them or feed them: how the intestinal mucus layer manages the gut microbiota. *Gastroenterol. Rep.* 7: 3–12.

Segata N., Izard J., Waldron L., Gevers D., Miropolsky L., Garrett W.S. & Huttenhower C. 2011. Metagenomic biomarker discovery and explanation. *Genome Biol.* 12.

Shreiner A.B., Kao J.Y. & Young V.B. 2015. The gut microbiome in health and in disease. *Curr. Opin. Gastroenterol.* 31: 69–75.

Silveira W.A. da, Fazelinia H., Rosenthal S.B., Laiakis E.C., Kim M.S., Meydan C., Kidane Y., Rathi K.S., Smith S.M., Stear B., Ying Y., Zhang Y., Foox J., Zanello S., Crucian B., Wang D., Nugent A., Costa H.A., Zwart S.R., Schrepfer S., Elworth R.A.L., Sapoval N., Treangen T., MacKay M., Gokhale N.S., Horner S.M., Singh L.N., Wallace D.C., Willey J.S., Schisler J.C., Meller R., McDonald J.T., Fisch K.M., Hardiman G., Taylor D., Mason C.E., Costes S. V. & Beheshti A. 2020. Comprehensive Multi-omics Analysis Reveals Mitochondrial Stress as a Central Biological Hub for Spaceflight Impact. *Cell* 183: 1185-1201.e20.

Simão F.A., Waterhouse R.M., Ioannidis P., Kriventseva E. V. & Zdobnov E.M. 2015. BUSCO: assessing genome assembly and annotation completeness with single-copy orthologs. *Bioinformatics* 31: 3210–3212.

Suvarna K.S., Layton C. & Bancroft J.D. 2013. *Bancroft's Theory and Practise of Histological Techniques (7th edition)*. Churchill Livingstone, London, UK.

The R Core Team. 2018. *R: A language and environment for statistical computing*.

Vital M., Karch A. & Pieper D.H. 2017. Colonic Butyrate-Producing Communities in Humans: an Overview Using Omics Data Shade A. (ed.). *mSystems* 2.

Ward J.F. 1988. DNA Damage Produced by Ionizing Radiation in Mammalian Cells: Identities, Mechanisms of Formation, and Reparability. In: pp. 95–125.

Wei T. & Simko V. 2017. R package 'corrplot': Visualization of a Correlation Matrix (Version 0.84).

Weiss S., Xu Z.Z., Peddada S., Amir A., Bittinger K., Gonzalez A., Lozupone C., Zaneveld J.R., Vázquez-Baeza Y., Birmingham A., Hyde E.R. & Knight R. 2017. Normalization and microbial differential abundance strategies depend upon data characteristics. *Microbiome* 5: 27.

Young M.D., Wakefield M.J., Smyth G.K. & Oshlack A. 2010. Gene ontology analysis for RNA-seq: accounting for selection bias. *Genome Biol.* 11: R14.

Zmora N., Suez J. & Elinav E. 2019. You are what you eat: diet, health and the gut microbiota. *Nat. Rev. Gastroenterol. Hepatol.* 16: 35–56.
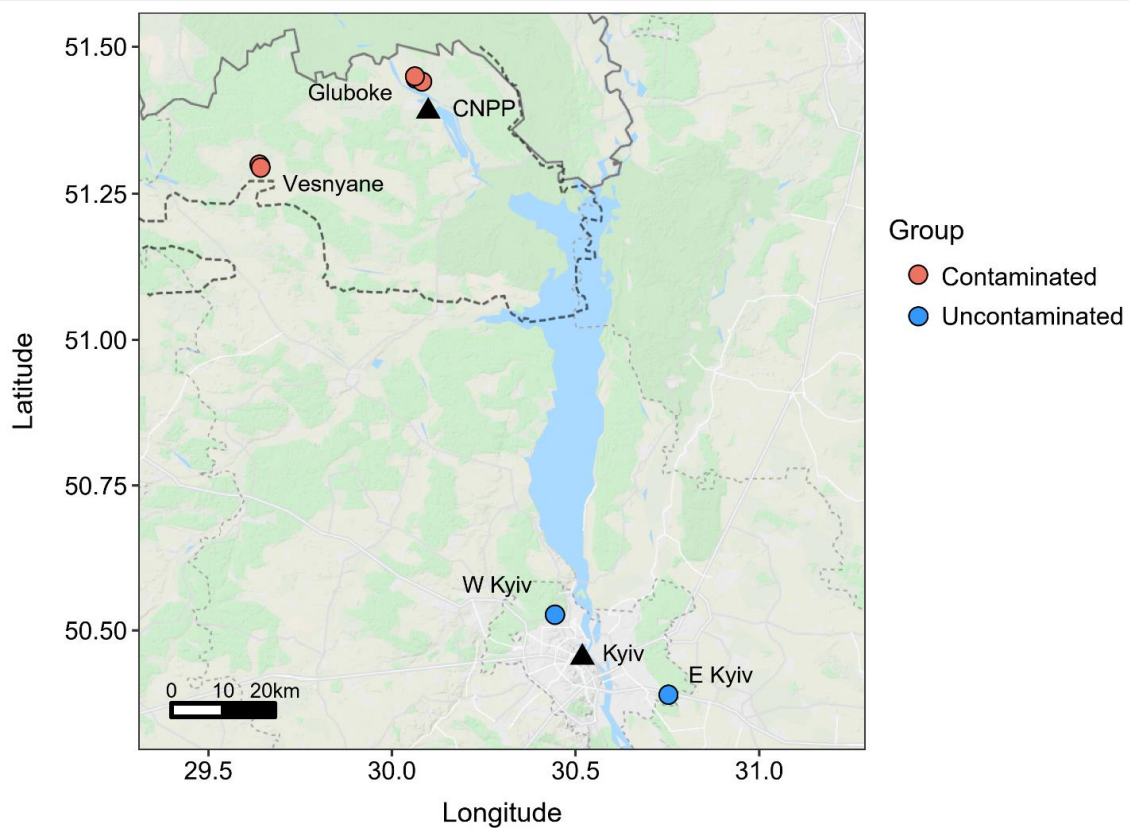
Chapter III: Figures and tables

Figure 1: Map of the Chernobyl exclusion zone (dashed border) and study areas used in this project in Ukraine. CNPP = Chernobyl Nuclear Power Plant. Map data © 2021 Google.
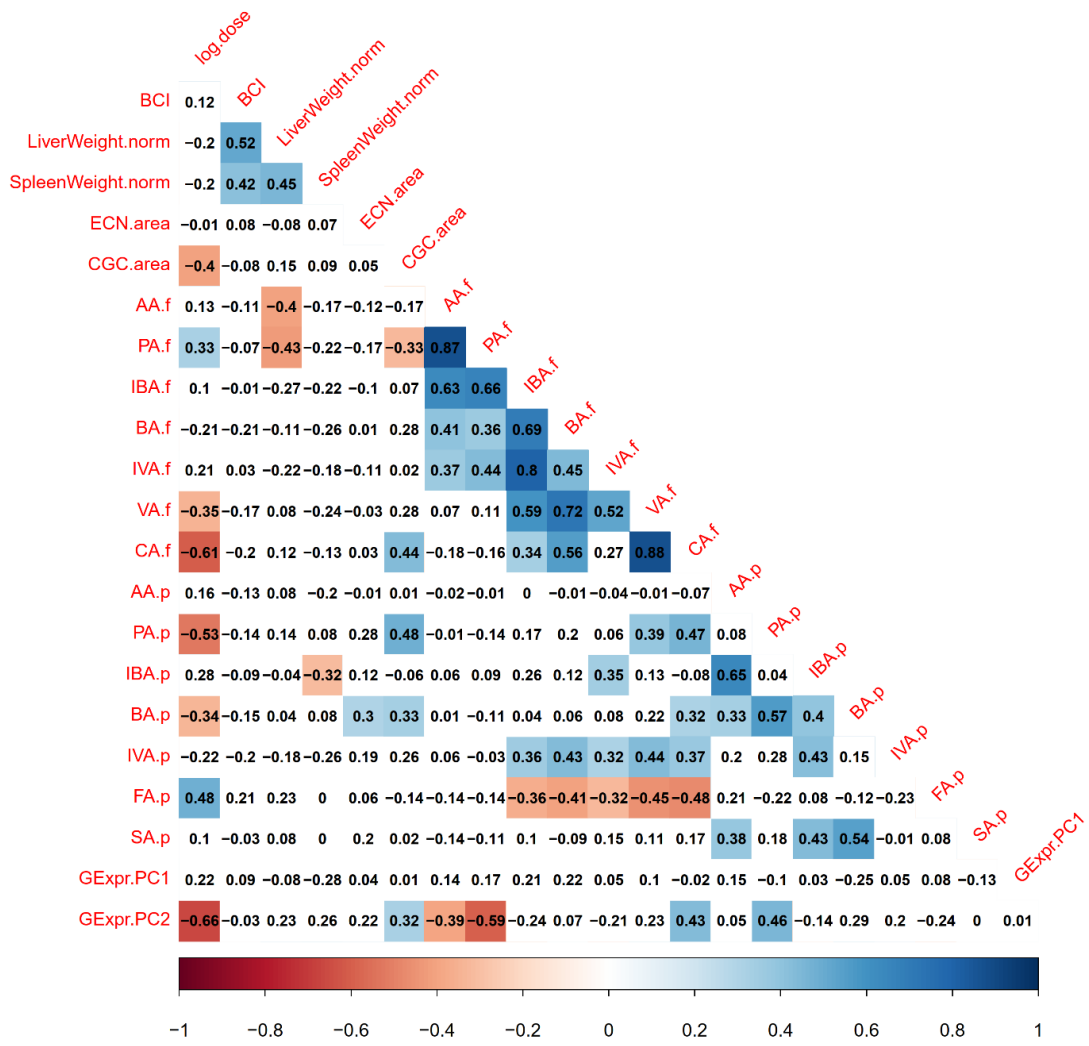
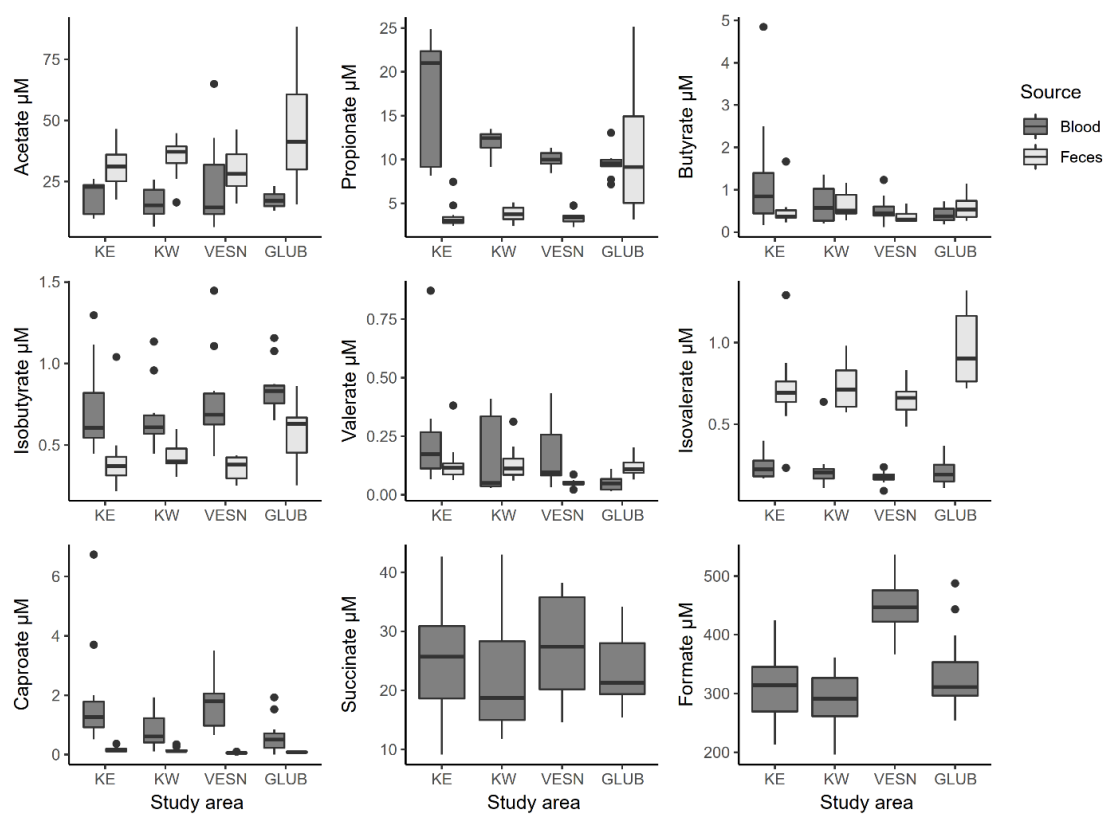**Figure 2:** Pairwise correlation coefficients of host phenotypic variables. Correlations significant at 0.05 significance level are indicated with coloured box.

Figure 3: Median concentrations of short-chain fatty acids in blood plasma (μM) and fecal matter (μM/g). KE = East Kyiv, KW = West Kyiv, VESN = Vesnyane, GLUB = Gluboke.
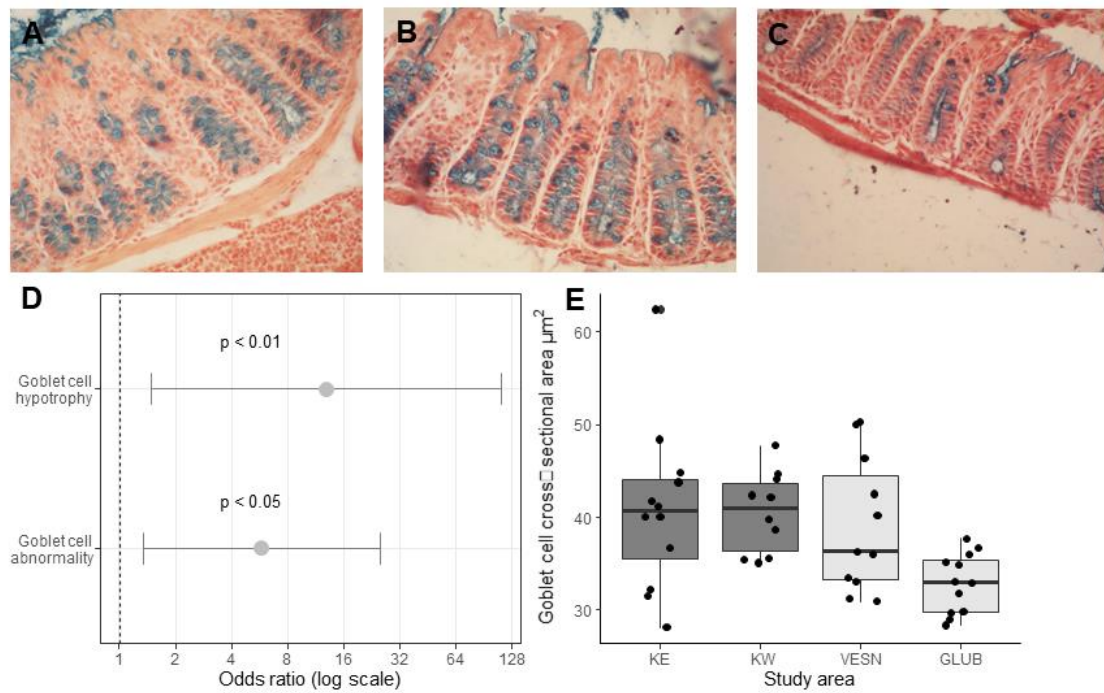
Figure 4: A) normal, B) hyper- and C) hypotrophic colonic mucous goblet cells (alcian blue with carmine supplementation; × 400). Mucin bodies (in blue) appear smaller and fewer in number in hypotrophic goblet cells than normal. D) Odds ratio of bank voles exposed to radionuclides exhibiting goblet cell hypotrophy and abnormality (hyper+hypotrophic cells). E) Goblet cell cross-sectional area across study areas.
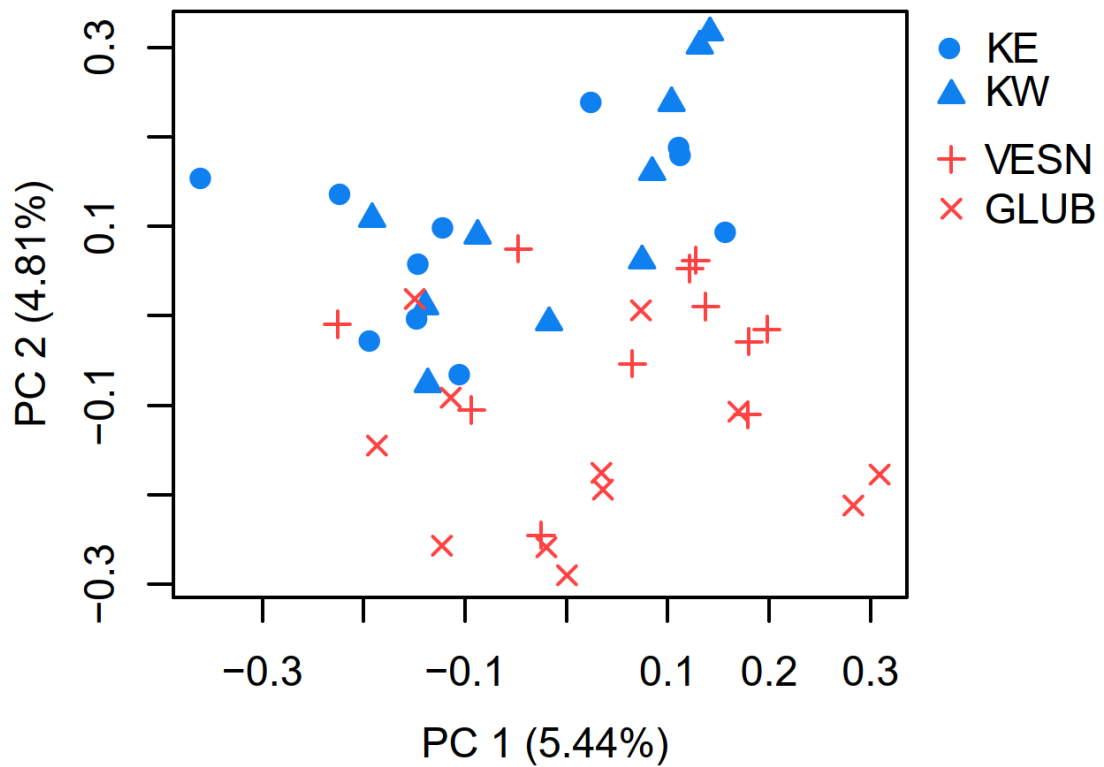
Figure 5: The first two principal component scores based on principal component analysis applied to transcript data. The scores exhibit clustering between treatment groups along component 2.
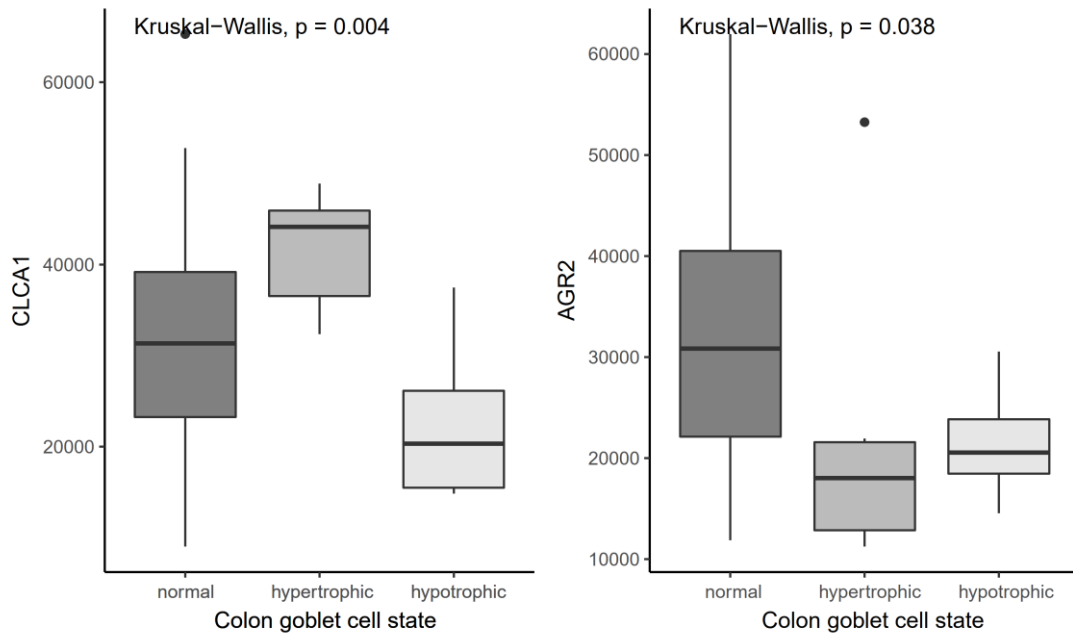
Figure 6: Boxplots of CLCA1 and AGR2 expression levels for different colon goblet cells.
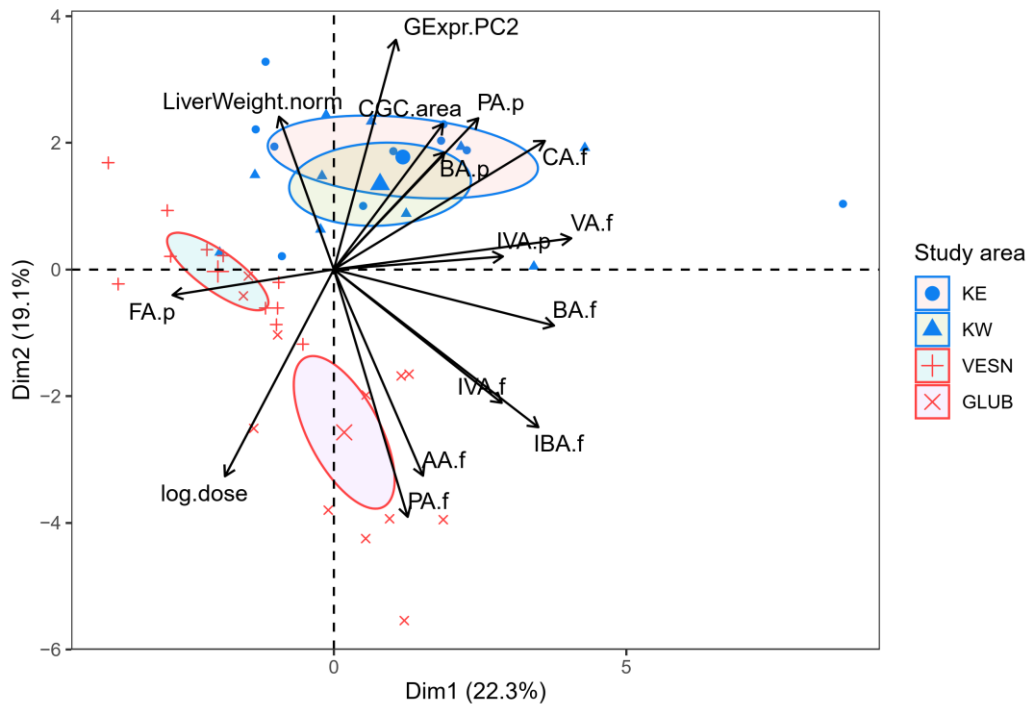
Figure 7: The first two principal component scores when PCA is applied to bank vole phenotypic data incorporating body, liver and spleen weights (corrected by head width), histological measurements (epitheliocyte height and cross-sectional area of the nucleus, colon crypt depth and cross-sectional area of goblet cells) and fecal and blood SCFA concentrations. The animals are labeled by study area and are superimposed with vectors showing top 15 variables based on quality of representation (cos2).
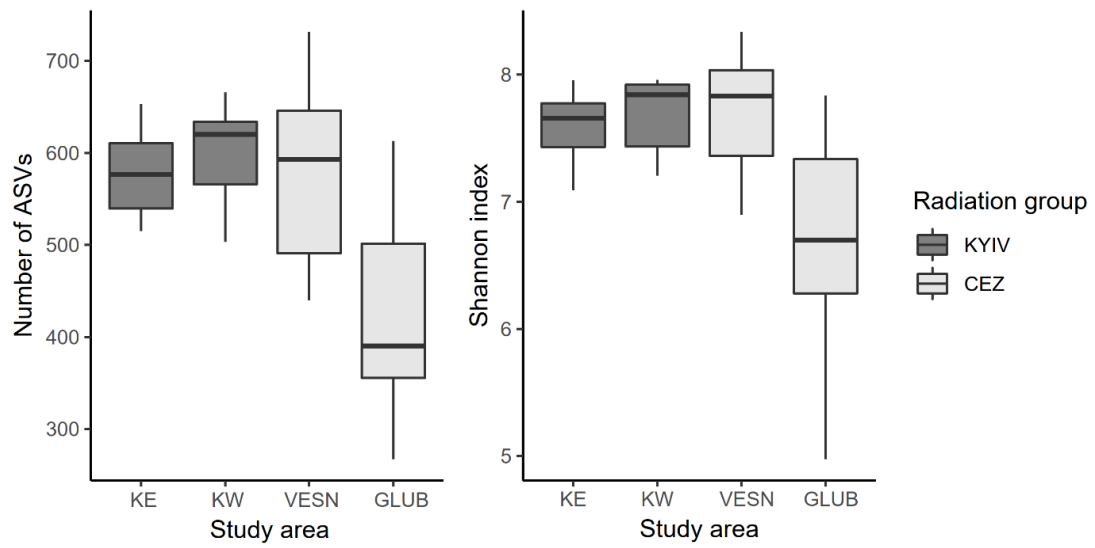
Figure 8: Species richness as number of unique ASVs and evenness measured in Shannon index in bank voles across study areas.
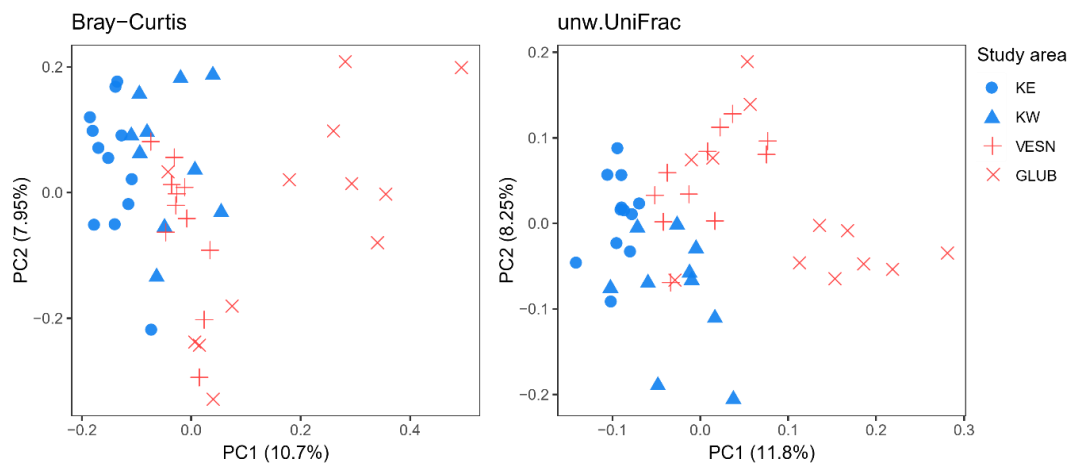
Figure 9: PCoA of radiation-associated differences in bank vole gut microbiota community composition using Bray-Curtis dissimilarities and unweighted UniFrac distances.

Table 1: PERMANOVA results (999 permutations) of various variables performed on gut microbiome composition using Bray-Curtis and unweighted UniFrac distance metrics. CGC state: three-factor classification of colonic goblet cells into normal, hypo- and hypertrophic cells. BCI: body condition index. Gene expression PC: principal components of gene expression data. ***: $p < 0.001$, **: $p < 0.01$, *: $p < 0.05$.

	Bray-Curtis			unw.UniFrac		
Variable	R2	pseudo-F		R2	pseudo-F	
Radiation group	0.07	3.250	***	0.053	2.447	***
Study area	0.16	2.601	***	0.126	1.965	***
Total absorbed dose rate (mGy/d)	0.045	2.024	**	0.057	2.606	***
CGC state	0.057	1.277	*	0.062	1.391	*
BCI	0.022	0.985		0.022	0.975	
Gene expression PC1	0.043	1.909	**	0.029	1.244	
Gene expression PC2	0.054	2.391	***	0.037	1.608	**
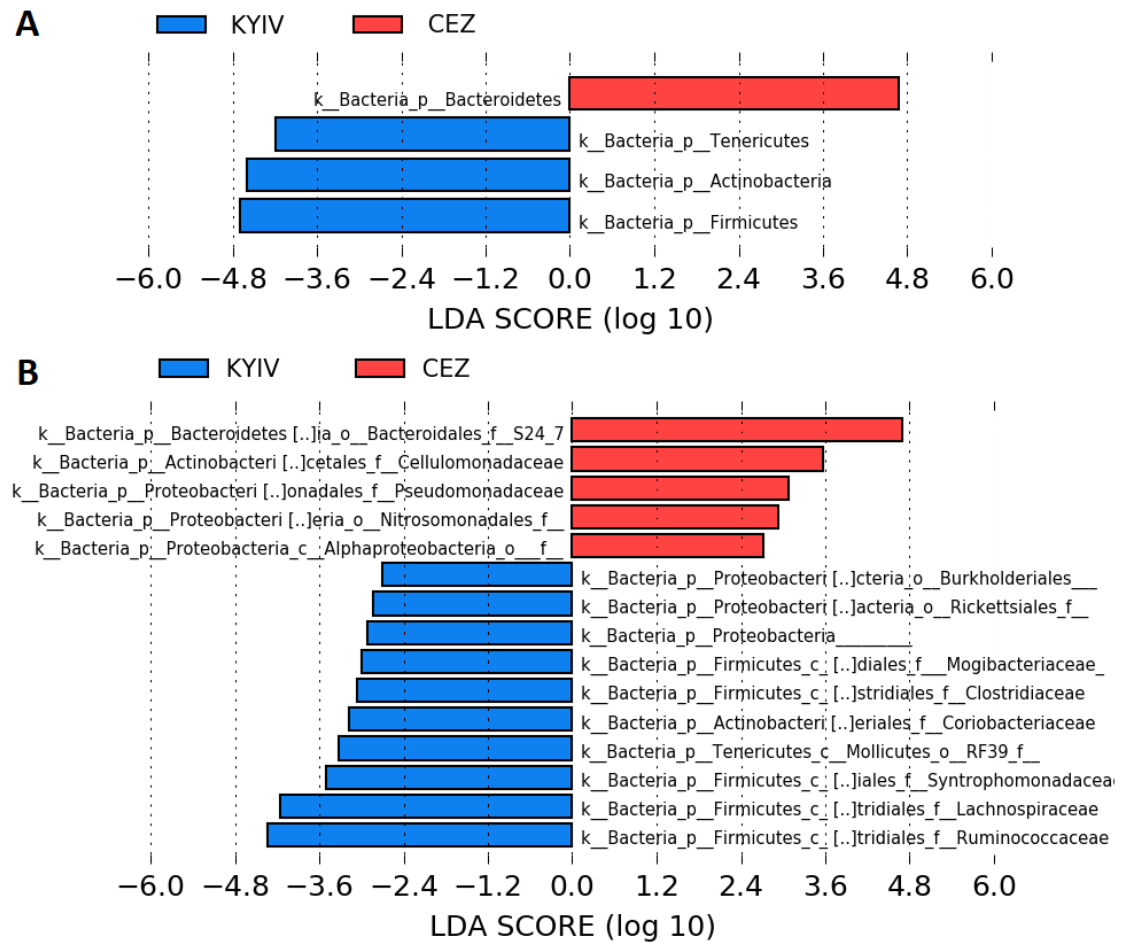
Figure 10: Log-transformed LDA-scores for different bacterial phyla (A) and families (B) between groups.
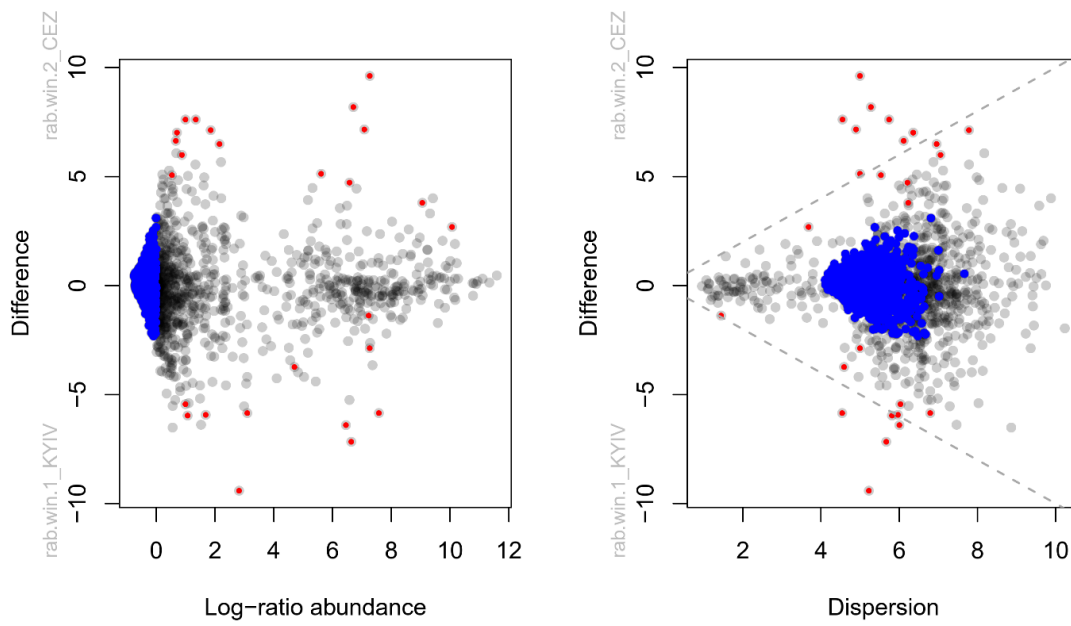
Figure 11: MA and effect plots of Aldex2 output. Red dots signify differentially abundant ASVs with statistical significance between contaminated and uncontaminated groups.

Table 2: Differentially abundant ASVs (*FDR*<0.05) between contaminated and uncontaminated groups. Positive effect size indicates increased relative abundance in animals from the CEZ. Overlap indicates proportion of effect size that overlaps 0 (no effect). In addition, S24-7 family member 1 was the only ASV associated with goblet cell hypotrophy (Table S11).

| Phylum /Order	ASV	Effect size	Overlap	p-value	FDR
Bacteroidales /Bacteroidales	S24-7 family member 1	1.629853	0.06108	1.04E-07	6.84E-05
	S24-7 family member 2	0.967744	0.193754	0.002319	0.038966
	S24-7 family member 3	0.779687	0.178267	0.000155	0.024177
	S24-7 family member 4	0.672805	0.135653	0.000357	0.037049
Firmicutes /Lactobacillales	Lactobacillus salivarius	-1.51825	0.083038	9.40E-07	0.000301
Firmicutes /Clostridiales	Clostridiales order member 1	-0.89611	0.198013	0.000185	0.02148
	Clostridiales order member 2	-0.91012	0.198723	0.000615	0.034021
	Clostridiales order member 3	-1.11462	0.088715	3.82E-05	0.003561
	Lachnospiraceae family member	1.123097	0.150568	5.51E-05	0.006997
	Ruminococcaceae family member 1	-1.15595	0.105749	4.56E-05	0.005403
	Ruminococcaceae family member 2	1.470684	0.093684	5.57E-06	0.001387
	Ruminococcaceae family member 3 - genus Oscillospira	1.360572	0.083097	7.97E-07	0.000378
	Ruminococcaceae family member 4 - genus Oscillospira	1.263068	0.086648	2.21E-06	0.000777
	Ruminococcaceae family member 5 - genus Oscillospira	-0.71191	0.154119	0.00061	0.046936
	Ruminococcaceae family member 6 - genus Ruminococcus	0.87122	0.124202	0.000186	0.019826
Spirochaetes /Spirochaetales	Treponema genus member	0.926208	0.192472	0.000555	0.031483
Tenericutes /Mycoplasmatales	Mycoplasmataceae family member	-0.91171	0.171043	0.000299	0.025607

Chapter III: Supplementary figures
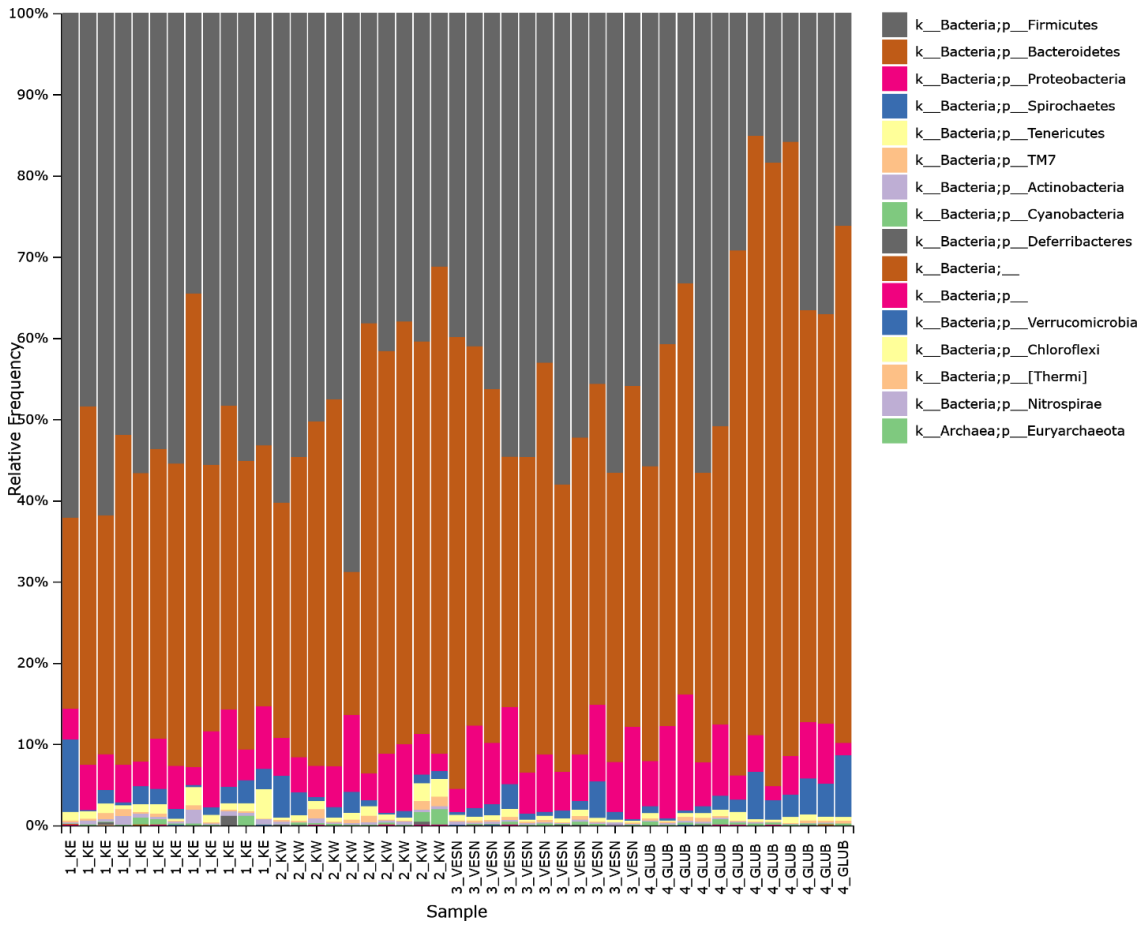
Figure S1: Phylum-level relative abundances of gut microbiota among bank voles from different study sites. KE = East Kyiv, KW = West Kyiv, VESN = Vesnyane, GLUB = Gluboke.
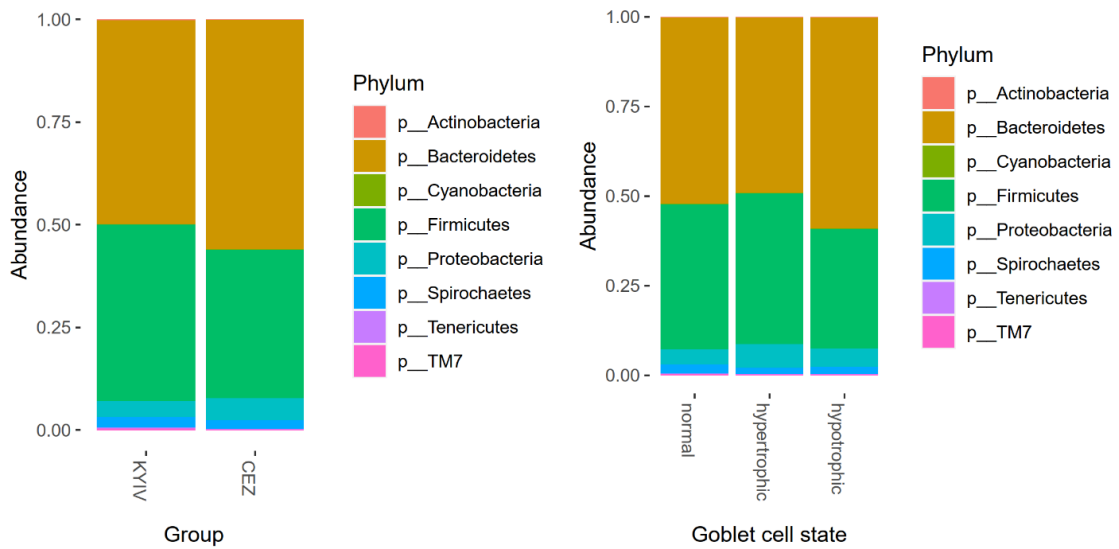

Figure S2: Relative abundances of bacterial phyla grouped by radiation group and colonic goblet cell conditions.

Chapter III: Supplementary methods

Internal dosimetry

To estimate internal dose rate ^{137}Cs activity was measured with the use of the SAM 940 radionuclide identifier system (Berkeley Nucleonics Corporation, San Rafael, CA, USA) equipped with a 3"x3" NaI detector. The detector was enclosed in 10 cm thick lead shielding to reduce the noise from background radioactivity. The system was calibrated with reference standard sources. With corrections for laboratory background, the ^{137}Cs activity of whole bodies was evaluated from the obtained spectra in the energies range 619-707 keV (with caesium photopeak at 662 keV) with the use of the phantom with known activity and geometry similar to the samples. The activities were above the critical level (decision threshold) were used for internal dose rate estimation. According to (Cristy and Eckerman 1987; Baltas *et al.* 2019), the individual internal absorbed dose from caesium-137 acquired during one day were calculated as:

$$D\text{int} = A \cdot T \cdot C_u \cdot \left(\sum_i \phi_i \cdot E_i \cdot f_i \right),$$

where: D_{int} is the absorbed dose rate due to internal exposure from [137]Cs (mGy/d); A is the activity of ^{137}Cs incorporated in the animal body (Bq/kg); C_u is the unit conversion coefficient; ϕ_i is the absorbed fractions for electron, positron or photon of the specific energy line; E_i is the self-absorption in tissue for the ^{137}Cs source which is uniformly distributed throughout homogeneous sphere of mass 20 grams of unit density and tissue-equivalent composition (Stabin and Konijnenberg 2000); f_i is the intensity (or emission frequency) of the specific energy line E_i (MeV) emitted per decay of ^{137}Cs and it daughter radionuclide [137m]Ba (ICRP 1983), the sum is taken over all electron, positron and photon energies E_i of ^{137}Cs spectrum. The similar way of bank voles internal dose calculations was reported earlier (Chesser *et al.* 2000). Despite of considerable contribution of ^{90}Sr to the total internal absorbed dose, that is considered as approximately the same as from cesium-137 (Beresford *et al.* 2020), in our study we neglected it because of characteristics of this beta-emitting radionuclide (tissue-specific strontium distribution in body: [90]Sr deposites mainly in bones and adds its adsorbed dose contribution there). As a total absorbed dose rate we considered a sum of internal and external absorbed dose rates per each animal per day.

SCFA quantification

SCFA in plasma samples. Short-chain fatty acids (SCFAs) (formic, acetic, propionic, isobutyric, butyric, succinic, isovaleric, valeric and caproic acid) were analyzed in plasma by LC-MS according to a method described before (J. Han et al. / Analytica Chimica Acta 854 (2015) 86–94 87) with the described modifications. Compounds of nine straight and branched-chain SCFAs were purchased from

Sigma–Aldrich. Analytical reagent-grade 3-nitrophenylhydrazine (3NPH)HCl (97%) and N-(3-dimethylaminopropyl)-N0-ethylcarbodiimide (EDC), HPLC grade pyridine, LC–MS grade acetonitrile, were also purchased from Sigma–Aldrich. To avoid SCFAs contamination hypergrade LC-MS water and MeOH (LiChrosolv®) was obtained from Sigma–Aldrich. All reagents and solvents were used for a maximum of 5 days. 13C6-3NPH was custom synthesized by IsoSciences Inc. (King of Prussia, PA, USA) and used as internal standard for all SCFAs. 10 µl plasma was incubated with 60 µl 75% methanol, 10 µl 200 mM 3-NPH and 10 µl 120 mM EDC-6% pyridine at ambient temperature for 45 min with gentle shaking. The reaction was quenched by addition of 10 µl of 200 mM quinic acid (15 min with gentle shaking at ambient temperature). The samples were centrifuged at 15 000 g for 5 min and the supernatant moved to a new tube. The samples were made up to 1 mL by 10% methanol in water and again centrifuged at 15 000 g for 5 min. 100 µl of the derivatized (12C) sample was mixed with 100 µl of labelled (13C) internal standard. The samples were analysed by a 6500+ QTRAP triple-quadrupole mass spectrometer (AB Sciex, 11432 Stockholm, Sweden) which was equipped with an APCI source and operated in the negative-ion mode. Chromatographic separations were performed on a Phenomenex Kinetix Core-Shell C18 (2.1, 100 mm, 1.7 um 100Å) UPLC column with SecurityGuard ULTRA Cartridges (C18 2.1mm ID) (changed at regular intervals). The column was backflushed for 60 min between each batch to ensure good chromatographic separation. LC-MS grade water (100% solvent A) and acetonitrile (100% solvent B) was the mobile phases for gradient elution. The column flow rate was 0.4 mL/min and the column temperature was 40°C, the autosampler was kept at 5°C. LC starting conditions at 0.5% B, held for 3 min, 3 min 2.5% B ramping linearly to 17% B at 6 min, then to 45% B at 10 min and 55% B at 13 min. Followed by a flush (100% B) and recondition (0.5% B), total runtime 15 min. The MRM transitions were optimized for the analytes one by one by direct infusion of the derivatives containing 50 mM of each fatty acid. The Q1/Q3 pairs were used in the MRM scan mode to optimize the collision energies for each analyte, and the two most sensitive pairs per analyte were used for the subsequent analyses. The retention time window for the scheduled MRM was 1 min for each analyte. The two MRM transitions per analyte, the Q1/Q3 pair that showed the higher sensitivity was selected as the MRM transition for quantitation. The other transition acted as a qualifier for the purpose of verification of the identity of the compound.

SCFA in fecal samples. 20 mg fresh frozen fecal samples were weighed into test tubes. Samples were then diluted in 4 mL MilliQ H2O and mixed thoroughly with metal beads (2 mm) for 5 min. A portion of 400 µL of the supernatants was mixed with 100 µL meta- phosphoric acid (16% w/v in MilliQ H2O) containing internal standard (15 nmol acrylic acid, L04280, Alfa Aesar, USA) for 5 min using a vortex. Propyl formate (300 µL) was added to the samples and mixed for 5 min. Samples were centrifuged at 16,000 g 4 °C for 15 min and 150 µL of the upper organic layer was collected in GC vials for analysis. Samples were analyzed by a Shimadzu GC–MS-TQ8030 (Tokyo, Japan), fast scanning triple quadrupole GC system with a PAL autosampler. The sample (2 µL) was

injected in split-less mode and helium (2 mL/min) was used as carrier gas. SCFA were separated on a ZB-FFAP column (30 m, 0.25 µm ID, no. 7HG-G009-11; Phenomenex, USA). The initial oven temperature was set at 40 °C for 1 min, then ramped to 250 °C at a rate of 40 °C/min. The final temperature was held for 2 min giving a total runtime of 8 min per sample. Electron impact ionization (250 °C) mode was used. Selected ion monitoring was performed with one quantification ion and one confirmation ion (m/z), respectively: Acetic acid m/z 60 and 45, propionic acid m/z 74 and 57, isobutyric acid m/z 73 and 57, butyric acid 73 and 60, isovaleric acid m/z 87 and 60, valeric acid m/z 73 and 60, caproic acid m/z 73 and 60 and for the internal standard acrylic acid m/z 72 and 45. Quantification was made based on an 8 point standard curve in ranges normally observed in fecal samples: 10–1280 µM for acetic acid (Honeywell), 4–512 µM for propionic acid (Alfa Aesar) and butyric acid (Sigma-Aldrich) and 0.5–64 µM for the other SCFA (isobutyric acid and valeric acid purchased from Alfa Aesar; isovaleric acid and caproic acid from Sigma-Aldrich). The SCFA concentrations were linearly regressed against the ratio of SCFA/acrylic acid. Samples, standards and blanks were analyzed randomly by the GC–MS system. Integrations were performed with GCMSsolution workstation software (Shimadzu GCMS-TQ series).

Supplementary references

Baltas D., Sakelliou L. & Zamboglou N. 2019. *The Physics of Modern Brachytherapy for Oncology*. CRC Press.

Beresford N.A., Barnett C.L., Gashchak S., Maksimenko A., Guliaichenko E., Wood M.D. & Izquierdo M. 2020. Radionuclide transfer to wildlife at a 'Reference site' in the Chernobyl Exclusion Zone and resultant radiation exposures. *J. Environ. Radioact.* 211: 105661.

Chesser R.K., Sugg D.W., Lomakin M.D., Bussche R. a Van den, DeWoody J. a, Jagoe C.H., Dallas C.E., Whicker F.W., Smith M.H., Gaschak S.P., Chizhevsky I. V, Lyabik V. V, Buntova E.G., Holloman K. & Baker R.J. 2000. Concentrations and dose rate estimates of (134,137)cesium and (90)strontium in small mammals at Chornobyl, Ukraine. *Environ. Toxicol. Chem.* 19: 305–312.

Cristy M. & Eckerman K.F. 1987. Specific absorbed fractions of energy at various ages from internal photon sources: 7, Adult male.

ICRP. 1983. Radionuclide transformations. Energy and intensity of emissions. *Ann. ICRP*.

Stabin M.G. & Konijnenberg M.W. 2000. Re-evaluation of absorbed fractions for photons and electrons in spheres of various sizes. *J. Nucl. Med.* 41: 149–160.

IV

EXPANSION OF rDNA AND PERICENTROMERE SATELLITE REPEATS IN THE GENOMES OF BANK VOLES MYODES GLAREOLUS EXPOSED TO ENVIRONMENTAL RADIONUCLIDES

by

Jernfors T, Danforth J, Kesäniemi J, Lavrinienko A, Tukalenko E, Fajkus J, Dvořáčková M, Mappes T & Watts PC. 2021

ORIGINAL RESEARCH

Expansion of rDNA and pericentromere satellite repeats in the genomes of bank voles *Myodes glareolus* exposed to environmental radionuclides

Toni Jernfors[1] | John Danforth[2] | Jenni Kesäniemi[1] | Anton Lavrinienko[1] |
Eugene Tukalenko[1,3] | Jiří Fajkus[4,5,6] | Martina Dvořáčková[4] | Tapio Mappes[1] |
Phillip C. Watts[1]

[1]Department of Biological and Environmental Science, University of Jyväskylä, Jyväskylä, Finland

[2]Department of Biochemistry & Molecular Biology, Robson DNA Science Centre, Arnie Charbonneau Cancer Institute, Cumming School of Medicine, University of Calgary, Calgary, Canada

[3]National Research Center for Radiation Medicine of the National Academy of Medical Science, Kyiv, Ukraine

[4]Mendel Centre for Plant Genomics and Proteomics, Central European Institute of Technology (CEITEC), Masaryk University, Brno, Czech Republic

[5]Laboratory of Functional Genomics and Proteomics, NCBR, Faculty of Science, Masaryk University, Brno, Czech Republic

[6]Department of Cell Biology and Radiobiology, Institute of Biophysics of the Czech Academy of Sciences, Brno, Czech Republic

Correspondence
Toni Jernfors, Department of Biological and Environmental Science, University of Jyväskylä, Jyväskylä 40014, Finland.
Email: toni.m.jernfors@jyu.fi

Funding information
Suomen Kulttuurirahasto; Academy of Finland, Grant/Award Number: 268670, 287153, 324602 and 324605

Abstract

Altered copy number of certain highly repetitive regions of the genome, such as satellite DNA within heterochromatin and ribosomal RNA loci (rDNA), is hypothesized to help safeguard the genome against damage derived from external stressors. We quantified copy number of the 18S rDNA and a pericentromeric satellite DNA (Msat-160) in bank voles (*Myodes glareolus*) inhabiting the Chernobyl Exclusion Zone (CEZ), an area that is contaminated by radionuclides and where organisms are exposed to elevated levels of ionizing radiation. We found a significant increase in 18S rDNA and Msat-160 content in the genomes of bank voles from contaminated locations within the CEZ compared with animals from uncontaminated locations. Moreover, 18S rDNA and Msat-160 copy number were positively correlated in the genomes of bank voles from uncontaminated, but not in the genomes of animals inhabiting contaminated, areas. These results show the capacity for local-scale geographic variation in genome architecture and are consistent with the genomic safeguard hypothesis. Disruption of cellular processes related to genomic stability appears to be a hallmark effect in bank voles inhabiting areas contaminated by radionuclides.

KEYWORDS
anthropogenic disturbance, chernobyl, copy number, ionizing radiation, *myodes glareolus*, rDNA

---

1 | INTRODUCTION

Release of pollutants into the environment has diverse impacts upon wildlife, such as the bank vole (*Myodes glareolus*) (Figure 1) and the ecosystems they inhabit (Acevedo-Whitehouse & Duffus, 2009; Isaksson, 2010). An example of environmental pollution whose potential impacts on wildlife have stimulated scientific debate is the fallout derived from the accident (April 26, 1986) at reactor 4 of the Chernobyl nuclear power plant, Ukraine, when approximately 9 million terabecquerels of radionuclides were released into the atmosphere and deposited across much of Eastern Europe, Russia, and Fenno-Scandinavia (Beresford et al., 2016; Lourenço et al., 2016; Mousseau et al., 2014). The Chernobyl Exclusion Zone (CEZ) was established at an approximately 30-km radius around the accident site (Figure 2) to limit human exposure to persistent radionuclides, notably strontium-90, cesium-137, and plutonium-239 that have half-lives of about 29, 30, and 24,100 years, respectively. In addition to controlled laboratory experiments, there is a need to study exposure to radionuclides in wildlife in natural habitats (Garnier-Laplace et al., 2013), for which the CEZ provides a natural laboratory. Accordingly, the wildlife inhabiting the CEZ provide the best-studied models of the biological impacts of exposure to environmental radionuclides (Beresford & Copplestone, 2011; Beresford et al., 2016; Bréchignac et al., 2016; Mappes et al., 2019; Mousseau et al., 2014).

Concern about the release of anthropogenic radionuclides into the environment stems from the potential damaging effects of exposure to ionizing radiation (IR) (Ward, 1988). For example, IR can damage DNA by direct impact that causes structural damage to DNA molecules, and/or by an indirect effect of radiolysis of cellular water that releases free radicals and causes an increase in oxidative stress (Desouky et al., 2015; Einor et al., 2016). Structural damage to DNA can induce, for example, genetic instability and abnormalities (such as cancers) or cell death. Elevated oxidative stress has diverse impacts on cell function, including an increase in DNA damage (Gonzalez-Hunt et al., 2018; Poetsch et al., 2018). Indeed, many organisms inhabiting areas within the CEZ that are contaminated by radionuclides

exhibit signs of elevated levels of genetic damage, such as increased frequency of chromosome aberrations (Dzyubenko & Gudkov, 2009) and/or an elevated mutation rate (Ellegren et al., 1997; Lourenço et al., 2016; Møller & Mousseau, 2015). Conversely, other studies have failed to find evidence for an increase in DNA damage (Rodgers & Baker, 2000), activation of DNA repair pathways (Kesäniemi, Jernfors, et al., 2019), or increase in mutation rate as measured by the level of heteroplasmy (Kesäniemi et al., 2018) in wildlife exposed to the persistent fallout from the Chernobyl accident. There are several possible reasons for the apparent support both for and against evidence of an increase in DNA damage in wildlife exposed to environmental radionuclides, such as interspecific variation in radiosensitivity (Beresford & Copplestone, 2011; Mousseau et al., 2014) and variation in received dose in the studied samples. Another key issue when quantifying DNA damage in wildlife exposed to environmental radionuclides is that certain regions of the genome preferentially accumulate damage when exposed to oxidative stress (Poetsch et al., 2018).

That regions of the genome differ in radiosensitivity is highlighted by evidence that an increase in frequency of four-stranded G-quadruplex (G4-DNA) motifs can shield DNA against the direct damaging effects of IR in the human genome (Kumari et al., 2019). Also, radiosensitivity has been associated with telomeric DNA content in laboratory experiments on cell lines (Ayouaz et al., 2008; Zhang et al., 2016) and with minisatellite DNA in laboratory experiments on mice (Dubrova, 1998), although studies on the mutation rate at minisatellite loci in Chernobyl workers and their families have

FIGURE 1 The bank vole *Myodes glareolus*

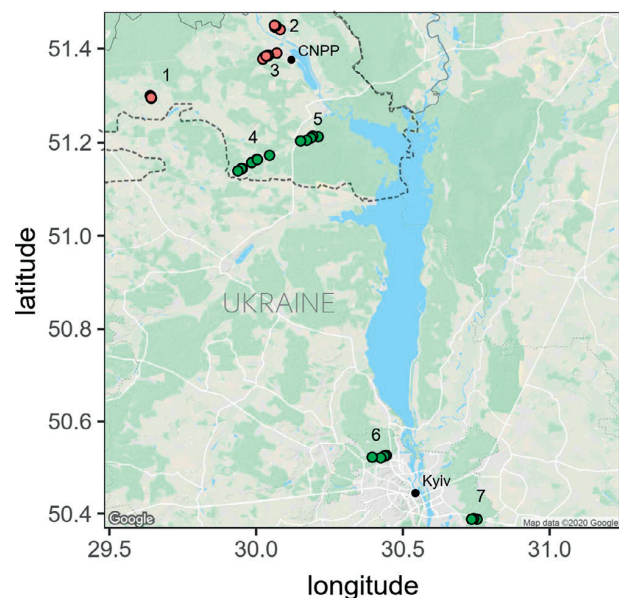**FIGURE 2** Location of *M. glareolus* sampling areas: contaminated CEZ (CEZ-CNTM) areas (1) Vesnyane, (2) Gluboke, and (3) Chistogalovka; uncontaminated CEZ (CEZ-CTRL) areas (4) Rosoha and (5) Yampil; and Kyiv (KYV-CTRL) areas (6) Kyiv West and (7) Kyiv East. Dashed line represents the border around the CEZ in Ukraine (area of ~2,050 km^2). Figure was created using ggmap v.3.0.0 package in R

proven inconclusive (Bouffler et al., 2006). Interestingly, short telomeres characterized some tissues of bank voles inhabiting areas contaminated by radionuclides within the CEZ (Kesäniemi, Lavrinienko, et al., 2019), while slightly longer telomeres were found in blood of humans potentially exposed to high levels of radiation during the Chernobyl accident (Reste et al., 2014). It has been suggested that heterochromatin content can play a role in safeguarding transcribed genomic regions against the damaging effects of exposure to IR (Qiu, 2015).

Heterochromatin represents the transcriptionally suppressed, densely packed chromatin, which is mostly formed from repetitive non-protein-coding sequence (Grewal & Jia, 2007). The hypothesized role of heterochromatin in helping to safeguard the genome against IR-induced damage (Qiu, 2015) is derived from the tendency for heterochromatin to localize at the nuclear periphery where it forms a three-dimensional structure that physically surrounds the actively transcribed euchromatic regions (Geyer et al., 2011), possibly protecting these territories from impacts of IR and oxygen radicals. This "safeguard hypothesis" is supported by studies that demonstrate relationship between sensitivity to radiation, other mutagens or aging and loss in repetitive content such as telomeres (Goytisolo et al., 2000; Zhang et al., 2016), ribosomal DNA (rDNA) (Ide et al., 2010; Kobayashi, 2011, 2014), and heterochromatin in general (Larson et al., 2012; Yan et al., 2011). One paradox of the genomic safeguard hypothesis is that it should result in increased ratio of DNA damage in peripheral heterochromatin compared with euchromatin, contrary to observations where DNA repair activity is concentrated in the nuclear center than periphery (Gazave et al., 2005). However, damaged heterochromatic DNA is rarely repaired in situ (Chiolo et al., 2011), but is instead relocated to nuclear center for repair or to the nuclear pore complex to be expelled from the nucleus in the form of extrachromosomal circular DNAs (Chiolo et al., 2011; Jakob et al., 2011; Khadaroo et al., 2009; Qiu, 2015; Torres-Rosell et al., 2007). Nonetheless, heterochromatin content of wild animals in the CEZ has not been explored. Two common constituents of heterochromatin, (a) rDNA and (b) centromeric DNA, are important for proper cellular function in eukaryotes and have been found to associate with genome stability (Kobayashi, 2011, 2014; Kobayashi & Sasaki, 2017). This possible association with genome stability implies that these genomic regions should be examined with regard to organisms inhabiting the CEZ.

The cluster of loci that are transcribed into ribosomal RNAs (hereafter called rDNA) represent a remarkable and evolutionarily conserved component of eukaryotic genomes. rDNA is organized as tandem arrays of 45S rRNA units that are transcribed and spliced into 18S, 5.8S, and 28S rRNAs, which, together with ribosomal proteins, form ribosomes. rDNA is abundant in many eukaryotic genomes, typically varying from tens to thousands of copies depending upon the species (Lavrinienko et al., 2020; Parks et al., 2018; Prokopowich et al., 2003; Symonová, 2019). Moreover, rDNA copy number can vary widely among individuals within a species (Lavrinienko, Jernfors, et al., 2020; Symonová, 2019; Weider et al., 2005), and geographic variation in rDNA content has been documented in

diverse taxa (reviewed by Weider et al., 2005), for example, among plant populations that differ in altitude and latitude (Strauss & Tsai, 1988), in _Daphnia_ (Harvey et al., 2020), and among human populations (Parks et al., 2018). As a tandemly repeating locus, rDNA is prone to copy-number mutations, a feature that is exacerbated by topological stress from opening of the helical DNA structure and collisions between replication and transcription machinery due to frequent transcription (Salim & Gerton, 2019). Laboratory studies on fruit flies (_Drosophila melanogaster_) and baker's yeast (_Saccharomyces cerevisiae_) have demonstrated that exposure to stressors can elicit a rapid change in rDNA copy number within few generations (Aldrich & Maggert, 2015; Jack et al., 2015; Kobayashi, 2011; Paredes et al., 2011; Salim et al., 2017), making rDNA an apparently environmentally sensitive locus (Salim & Gerton, 2019). rDNA content is associated with genome stability and sensitivity to stress (Kobayashi & Sasaki, 2017). For example, strains of baker's yeast with fewer copies of rDNA are more sensitive to mutagens than strains with many rDNA copies (Ide et al., 2010). This interaction between rDNA and genome stability can be exemplified in plants, where dysfunction of chromatin assembly factor-1 results in progressive loss of rDNA and higher sensitivity to genotoxic stress (Mozgová et al., 2010).

Another major fraction of heterochromatin is comprised of centromeric sequences and pericentromeric sequences, which flank the centromeres (Biscotti et al., 2015; Plohl et al., 2008). In contrast to rDNA, centromeric sequence motifs often are not evolutionarily conserved, but tend to differ among species (Biscotti et al., 2015). Centromeric DNA is defined by its ability to recruit the centromere-specific histone 3 variant, centromere protein A (Foltz et al., 2006). Centromere and pericentromere regions are typically comprised of tandem arrays of satellite DNA such as α-satellites in primates (Alexandrov et al., 2001), minor and major satellites in mice (Komissarov et al., 2011), and an approximately 160-base-pair-long satellite motif (Msat-160) in arvicoline rodents (Acosta et al., 2010). Using fluorescence in situ hybridisation (FISH), Msat-160 has often been characterized as an abundant component of arvicoline rodent genomes, located primarily at the pericentromeric regions of chromosomes and with apparently high interspecific variation in copy number and the number of chromosomes that contain the satellite sequence (Acosta et al., 2007, 2010; Modi, 1992, 1993). While interspecific differences in centromere architecture are quite well described for some taxa (_e.g._, primates, Melters et al., 2013), perhaps consistent with the general lack of information about centromere and pericentromere sequence in most species, we are not aware of any studies to have quantified whether variation in pericentromeric satellite content associates with features of the environment. However, as constituents of heterochromatin, the centromeric and pericentromeric regions may represent a key component of the genome that interacts with exposure to environmental stress.

Bank voles appear to be relatively radioresistant, being one of the first mammals to recolonize the Chernobyl accident site (Chesser et al., 2000) and with animals exposed to environmental radionuclides showing equivocal evidence for genomic DNA damage (Rodgers & Baker, 2000), little upregulation of DNA repair pathways

(Jernfors et al., 2018; Kesäniemi, Jernfors, et al., 2019), and no elevated mutation rate (heteroplasmy) in their mitochondrial genomes (Kesäniemi et al., 2018). At a cellular level, fibroblasts isolated from bank voles exposed to radionuclides in the CEZ show increased resistance to oxidative stress and genotoxins (Mustonen et al., 2018). Given the genomic safeguard hypothesis, we expect that change in rDNA and pericentromere content will be a feature of the genomes of organisms exposed to radionuclides. To test this hypothesis, we used quantitative PCR (qPCR) to quantify the relative amounts of (a) 18S rDNA and (b) Msat-160 (a pericentromeric satellite sequence) as proxies for heterochromatin content in genomes of bank voles that have inhabited areas contaminated with radionuclides for estimated 50 generations (Baker et al., 2017).

2 | MATERIALS AND METHODS

2.1 | Sampling and dosimetry

Two hundred and two bank voles were captured using Ugglan Special2 live traps with sunflower seeds and potatoes as bait during fieldwork seasons of 2016–2017. Briefly, at each location 9–16 traps were placed either in a 3 × 3 or 4 × 4 grid with an intertrap distance of 15–20 m. In all locations, traps were kept for at least three consecutive nights and were checked each following morning. Animals were brought to a field laboratory in town of Chernobyl within the CEZ where they were euthanized by cervical dislocation within 24 hr of entering the laboratory and stored in dry ice for transport before long-term storage in −80°C. rDNA copy number can change within a generation (Aldrich & Maggert, 2015); in bank voles, stress during early (but not adult) life can affect rDNA copy number (van Cann, 2019). Animals were caught from seven study areas in Ukraine (Figure 2), with near-equal sex ratios at each location (Rosoha: 14 females/14 males, Yampil: 15F/15M, Chistogalovka: 15F/15M, Gluboke: 15F/14M, Vesnyane: 15F/15M, East Kyiv: 15F/12M, and West Kyiv: 15F/13M). We measured ambient radiation levels at all trapping locations using a handheld Geiger counter (Gamma-Scout GmbH & Co.) placed 1 cm above the ground, and taking an average of at least nine measurements from each trapping location. Ambient dose rate measurements provide a reasonable approximation of external absorbed dose rate for bank voles (Beresford et al., 2008; Lavrinienko, Tukalenko, et al., 2020). Internal absorbed cesium-137 dose rates were measured using a SAM 940 radionuclide identifier system (Berkeley Nucleonics Corporation). Full details on internal dosimetry and total received dose rate estimations are provided in Appendix 1 and supporting data.

To control for possible confounding variables, we use a robust study design that utilized samples from replicated contaminated areas within the CEZ and noncontaminated areas within and outside the CEZ. We classified our seven study areas into three exposure groups that reflect a likely radiation "treatment." Three areas within the CEZ (Chistogalovka, Gluboke, and Vesnyane) were contaminated by radionuclides and delivered elevated external dose rates

(0.24–1.49 mGy/day, median 0.41 mGy/day, representing ~4 chest X-rays per day) to wildlife inhabiting these areas: These three sites are collectively referred to as CEZ-CNTM (CEZ-contaminated). Two areas within the CEZ (Rosoha and Yampil) had little to no apparent soil radionuclide contamination, with near-background external dose rates (median $6.4*10^{-3}$ mGy/day), and are referred to as CEZ-CTRL (CEZ-control). Finally, the two areas outside the CEZ (Kyiv East and Kyiv West) also are uncontaminated by environmental radionuclides (median $3.6*10^{-3}$ mGy/day) and are referred to as KYV-CTRL (KYIV-control). As the CEZ presents a mosaic of radionuclide contamination (Mousseau et al., 2014), we make the distinction between the locations defined as CEZ-CTRL and KYV-CTRL. At CEZ-CTRL, it is possible that some animals caught in these uncontaminated areas may have dispersed into these areas from contaminated areas (and indeed vice versa). By contrast, KYV-CTRL presents a sample of animals that have not directly encountered a large dose of IR from environmental radionuclides, because the distance between the KYV-CTRL site and the CEZ (~90 km) is much further than bank voles' dispersal ability (*ca.* ~1 km per breeding season, Kozakiewicz et al., 2007; and an estimated <5 km per year rate of range expansion, White et al., 2012; Smiddy et al., 2016).

2.2 | Characterization of bank vole 18S rDNA and Msat-160 satellite sequences and primer design

Sequences for ribosomal rDNA were identified by BLASTn search (Altschul et al., 1990; parameters: default) of mouse 18S rDNA (GenBank Accession NR_003278.3) against a draft bank vole genome (GenBank Accession GCA_001305785.1). The putative bank vole pericentromere satellite DNA sequence was identified by its similarity (70% identity, *e*-value = $3e^{-14}$) with the satellite DNA Msat-160, clone 960-47 isolated from the genome of the Eurasian water vole *Arvicola amphibius* (synonym *A. terrestris*) (GenBank Accession FN859393.1). Quantitative PCR (qPCR) primers for 18S rDNA and Msat-160 sequences were designed using Primer3web v.4.1.0 (Untergasser et al., 2012) and BLAST to ascertain primer specificity.

2.3 | Fluorescence in situ hybridization of Msat-160 satellite in the bank vole genome

Arvicoline rodents display high variability in centromere sequence composition owing to rapid species radiation (Acosta et al., 2010). To identify genomic locations of the Msat-160 satellite sequence in the bank vole genome, fluorescence in situ hybridization (FISH) was used using the same fibroblast source as Mustonen et al. (2018). Fibroblasts were isolated from male bank voles collected from Gluboke (Figure 2) and from near Kyiv, cultured according to Mustonen et al. (2018), and fixed in 3:1 methanol:glacial acetic acid according to the standard protocol (Franek et al., 2015). Full details of chromosomal preparations are given in Appendix 2. FISH images were taken using Zeiss Axio Imager Z2 microscope, using

a Plan-Apochromat 100×/1.4 OIL objective and an ORCA Flash 4 camera. Images were analyzed with CellProfiler 2.4.

2.4 | Quantitative PCR to detect relative copy number of 18S rDNA and Msat-160

Genomic DNA was extracted from ear tissue samples using DNeasy Blood & Tissue Kit (Qiagen) following the manufacturer's protocol. Quantitative PCRs were carried out on a LightCycler 480 Real-Time PCR System (Roche), using ribosomal phosphoprotein P0-coding gene _36b4_ as a single-copy reference gene (see Cawthon, 2002). Each 96-well plate of qPCRs contained triplicate reactions for the same reference bank vole DNA sample that acted as a golden standard (GS). Raw quantification cycle (Cq) data were corrected for PCR efficiency (E) and transformed into relative values compared with a single-copy reference using the Pfaffl method (Pfaffl, 2001), where

$$\text{ratio} = \frac{(E\text{target})^{\Delta Cq\text{target(control - sample)}}}{(E\text{ref})^{\Delta Cq\text{ref(control - sample)}}}.$$

All qPCRs were run in 15 μl final reaction volumes using LightCycler 580 SYBR Green I Master (Roche). Reactions for Msat-160 and _36b4_ included 15 ng template DNA, 500 nM of both forward and reverse primers for Msat-160, and 200 nM of both primers for _36b4_. Reactions for 18S rDNA included 3 ng genomic DNA and 333 nM of both forward and reverse primers. Amplification conditions for Msat-160 were as follows: denaturation at 95°C for 5 min, and 40 cycles of amplification (95°C for 10 s, 58°C for 5 s, and 72°C for 5 s). Amplification conditions for _36b4_ were as follows: 95°C 5 min and 40 × (95°C 10 s; 58°C 15 s; 72°C 10 s). Amplification conditions for 18S were as follows: 95°C and 45 × (95°C 10 s; 60°C 15 s; 72°C 10 s). A standard melt curve analysis included in the LightCycler software was included in each analysis run to ascertain product specificity. All samples whose duplicate C_t values had standard deviations above 0.2 cycles were rerun. Dilution series of GS DNA were run on each qPCR plate to generate PCR efficiencies: For Msat-160, we used a 1:5 dilution series from 40 to 0.064 ng/μl; for _36b4_, we used a 1:3 dilution series from 40 to 0.49 ng/μl; and for 18S, we used a 1:5 dilution series from 12.0 ng to 0.0192 ng/μl.

Variation in relative copy number for 18s rDNA and for Msat-160 (response variables) was evaluated using linear mixed models in lme4 (Bates et al., 2015) in R v.3.5.0 (The R Core Team, 2018), including radiation treatment group (CEZ-CNTM, CEZ-CTRL, and KYV-CTRL) and sex as fixed factors and trap point ($N = 56$) or trapping area ($N = 7$) as a random factor. Marginal R_m^2 (variance explained by fixed effects) and conditional R_c^2 (variance derived from fixed and random effects), as well as the significance of post hoc comparisons, were calculated using MuMIn (Burnham & Anderson, 2002) and multcomp (Hothorn et al., 2008), also in R. We also ran models that examined the total received dose rates as a continuous variable (instead of treatment).

3 | RESULTS

FISH confirmed that Msat-160 is located in the pericentromeric heterochromatin regions in the bank vole genome. Most bank vole chromosomes are acrocentric (one-armed), a feature that is common among rodents (Pardo-Manuel de Villena & Sapienza, 2001) (Figure 3).

We observed significant differences in the relative copy number of 18S rDNA in bank voles among the three radiation treatments ($R_m^2 = 0.128$, $R_c^2 = 0.137$, Table 2, Figure 4a). Consistent with the genomic safeguard hypothesis, average rDNA content was significantly higher in animals caught from CEZ-CNTM compared with animals from CEZ-CTRL areas ($\beta = 0.195$, $df = 7.12$, $t = 3.15$, $p < 0.05$), although then comparison between CEZ-CNTM and KYV-CTRL was not significantly different. Male bank voles had significantly more copies of 18S rDNA than females ($\beta = 0.182$, $df = 195.34$, $t = 4.01$, $p < 0.001$), except in the sample from East Kyiv.
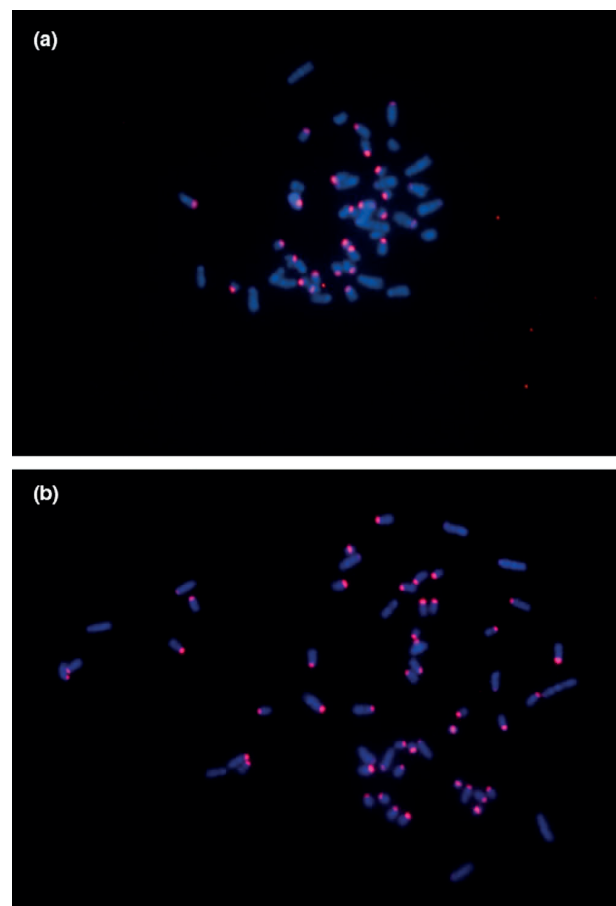

FIGURE 3 Fluorescence in situ hybridization (FISH) staining of Msat-160 regions in _M. glareolus_ fibroblast cells (red). (a) Cells from a male individual sampled from the Kyiv West site and (b) cells from a male individual from CEZ-CNTM Gluboke site. Chromosomes were counterstained with DAPI (blue)

Msat-160 satellite motif (pericentromere) also exhibited significant spatial variation in copy number among treatment groups ($R_m^2 = 0.135$, $R_c^2 = 0.192$, Table 2, Figure 4b). Again, consistent with the genome safeguard hypothesis, bank voles caught from contaminated areas within the CEZ had significantly more copies of Msat-160 than did animals caught from uncontaminated areas within the CEZ ($\beta = 0.251$, $df = 68.26$, $t = 4.949$, $p < 0.001$). Mean copy number in KYV-CTRL was significantly higher than in CEZ-CTRL ($\beta = 0.174$, $df = 32.55$, $t = 2.725$, $p < 0.05$). Male voles have higher Msat-160 content than females in all areas except at East Kyiv, where females have elevated Msat-160 content, thus increasing the average Msat-160 content in the KYV-CTRL sample.

Both 18S rDNA and Msat-160 copy number also significantly correlated with radiation levels when modeling total absorbed dose rate as a continuous variable ($\beta = 0.020$, $df = 7.26$, $t = 0.042$, $p < 0.05$ and $\beta = 0.028$, $df = 70.38$, $t = 3.985$, $p < 0.001$, respectively) (Table 3). When considering bank voles only within the CEZ-CNTM group (as other areas had near-zero radiation levels), neither 18S rDNA nor Msat-160 copy number correlated with the total received dose rate ($R = 0.02$ and 0.11, respectively, for log dose, $p > 0.05$).

Given the similar increase in 18S rDNA and Msat-160 content in the genomes of animals exposed to environmental radionuclides, we quantified (a) whether the copy number at these loci was correlated within individuals (i.e., is there an intragenomic correlation in rDNA and Msat-160 content) and (b) whether the strength of any such intragenomic correlations was impacted by exposure to environmental radionuclides. Significant positive correlations were found (Pearson's correlation, $R > 0.5$ and $p < 0.05$, with weaker correlation in the West Kyiv sample) between the copy number of 18S rDNA and Msat-160 in animals at all uncontaminated areas (Table 4, Figure 5). However, this intragenomic correlation in copy number among 18S rDNA and Msat-160 was not observed ($R < 0.3$, $p > 0.1$) at the contaminated areas (CEZ-CNTM).

4 | DISCUSSION

4.1 | Increased genomic repeat copy number may mitigate radiation stress

It is hypothesized that heterochromatin may uphold genomic stability by safeguarding the genome against environmental stresses such as ionizing radiation (Qiu, 2015). We found (a) that both 18S rDNA and Msat-160 satellite (both of which are major constituents of heterochromatin) copy numbers were higher in contaminated areas than uncontaminated areas within the CEZ, (b) extensive variation in copy number at KYV-CTRL, and also (c) intragenomic correlations in rDNA and Msat-160 content at CEZ-CTRL and at KYV-CTRL, but not in the samples from the contaminated areas (CEZ-CNTM).

An apparent increase in both Msat-160 and rDNA copy number in contaminated sites is consistent with the genomic safeguard hypothesis (Qiu, 2015). Loss of heterochromatin as an expectation of the hypothesis is mainly a result of relocation and expulsion of DNA double-strand breaks that we do not expect in the CEZ due to the

TABLE 1 Sequences of qPCR primers that amplify fragments of the 18S rDNA and Msat-160 (and 36b4 as a single-copy control gene) in the bank vole *Myodes glareolus*

locus		Sequence (5′→3′)	Amplicon length (bp)
18S rDNA	F	AAG ACG GAC CAG AGC GAA AG	238
	R	TGG TGC CCT TCC GTC AAT TC	
Msat-160	F	CAG CAT TTA GAA AGT GAA GCA ACA	101
	R	CCA AGA AAC TCA CAG GCA TTT C	
36b4	F	GTC CCG TGT GAA GTC ACT GT	87
	R	AGC GGT GTT GTC TAA AGC CT	

TABLE 2 Primary models explaining variation in mean relative copy number of ribosomal 18S DNA and centromeric repeat Msat-160 as dependent variables (DV) between treatment groups (Ex. grp) using CEZ-CTRL and female voles as reference level

DV (fixed effects)		β (SE)	df	t
18S copy number	Intercept	0.483 (0.053)	10.762	9.087***
(Ex. Grp+Sex)[a]	CEZ-CNTM	0.195 (0.062)	7.120	3.153*
	CTRL-KYV	0.073 (0.069)	7.540	1.057
	Sex (Male)	0.182 (0.045)	195.337	4.008***
Msat–160 copy number	Intercept	0.352 (0.044)	77.86	7.968***
(Ex. Grp+Sex)[b]	CEZ-CNTM	0.251 (0.051)	68.26	4.949***
	CTRL-KYV	0.174 (0.064)	32.55	2.725*
	Sex (Male)	0.007 (0.038)	197.7	0.180

[a]Random factor: trapping area, $N = 7$, Var = 0.001 (trapping point resulted in singular fit).
[b]Random factor: trapping point, $N = 56$, Var = 0.005.
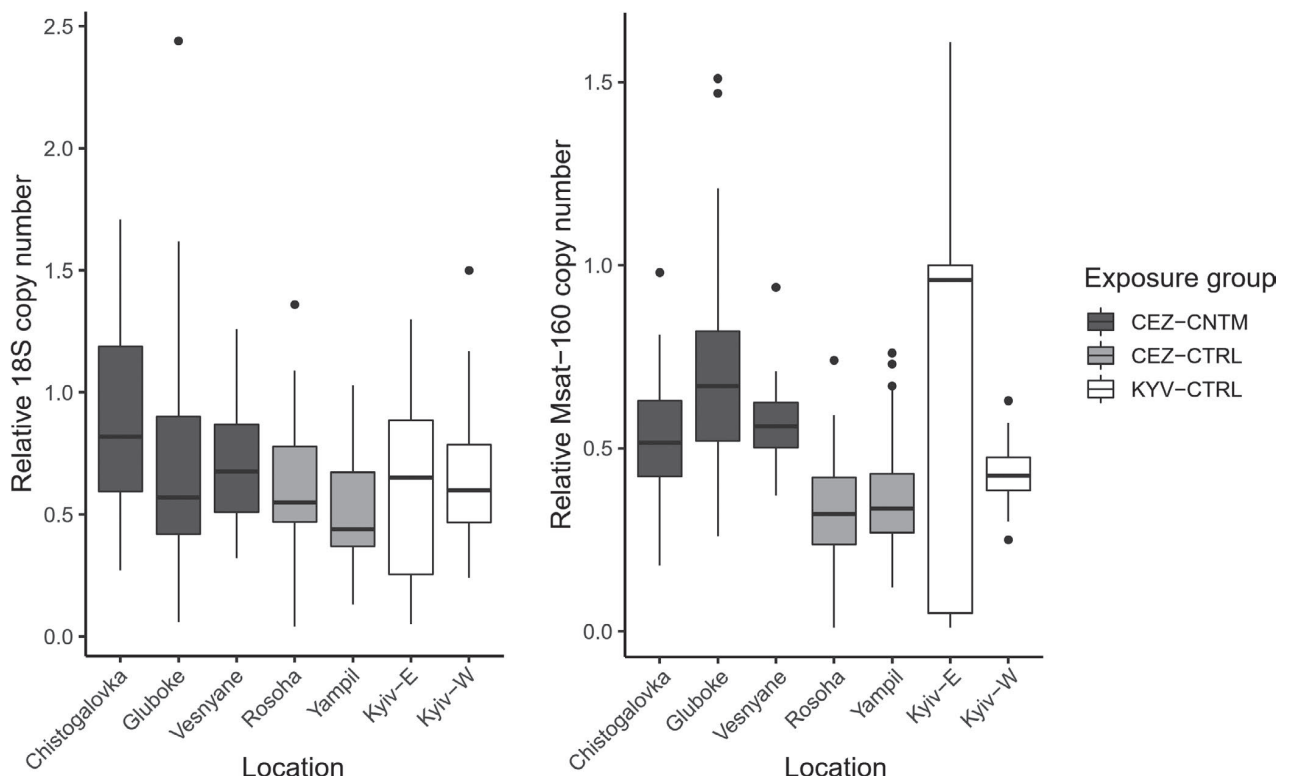*$p < 0.05$; ***$p < 0.001$.

FIGURE 4 Genomic changes in response to exposure to ionizing radiation as measured by (a) relative 18S rDNA and (b) Msat-160 copy number in bank voles inhabiting areas contaminated by radionuclides (CEZ-CNTM) and uncontaminated areas (CEZ-CTRL and KYV-CTRL). Relative copy numbers of both repeats are normalized to a reference golden standard DNA sample. Dots represent data points above 1.5 * interquartile range

low-dose rates generally thought to be too weak to induce them. Increased heterochromatin content could provide stability against oxidative stress, and thus, changes in rDNA and Msat-160 content, either by selection on existing copy-number variation or by affecting copy-number maintenance during development, may be an adaptive response to exposure to environmental radionuclides. Interestingly, our data show how this change in genome architecture can occur at a local geographic scale (i.e., within a few tens of km). Considering animals within contaminated areas (CEZ-CNTM) only, direct effect of IR on heterochromatin content is not expected, for example, because we do not expect DNA content to have linear response to IR, and dose measured may not reflect that experienced at the relevant time of life, that is, embryonic development.

rDNA copy-number variation has been associated with diverse cellular functions (Gibbons et al., 2014; Kobayashi & Sasaki, 2017), and loss of rDNA copies correlates with, for example, cellular senescence and susceptibility to mutagens in yeast (Ide et al., 2010; Kobayashi, 2011). Aside from possible safeguarding the genome as part of heterochromatin, changes in rDNA content can affect cell processes such as transcription (Gibbons et al., 2014; Jack et al., 2015; Paredes et al., 2011; Parks et al., 2018; Salim et al., 2017) and nucleolus organization (Potapova & Gerton, 2019). Loss of rDNA in mouse cancer lines is associated with vulnerability to DNA damage and activation of the mTOR pathway, which promotes cell growth

and division (Xu et al., 2017). Interestingly, mTOR activation is antagonistic to a fatty acid oxidating mode of metabolism. Bank voles inhabiting contaminated areas within the CEZ upregulate genes associated with fatty acid oxidation (Kesäniemi, Jernfors, et al., 2019), which is associated with genomic stability (Heydari et al., 2007; Yuan et al., 2013) in the form of antioxidative capabilities and longevity in captivity. While the explicit link between rDNA CN variation and metabolic changes in the bank vole remains unclear, fibroblasts isolated from bank voles exposed to radionuclides show increased tolerance of oxidative stress and genotoxic agents (Mustonen et al., 2018). Increase in rDNA copy number may thus provide certain advantages to bank voles exposed to environmental radionuclides, although this idea remains to be tested experimentally.

Like a change in rDNA copy number, change in pericentromeric content associated with environmental radionuclides is interesting as this change in genome architecture can have diverse impacts on cell function. For example, centromeric and pericentromeric regions contain noncoding RNA (ncRNA) sequences that are involved in centromere maintenance and gene silencing (Ideue & Tani, 2020). Altered centromere structure can change patterns of histone binding with a concomitant impact on gene expression (Vaissière et al., 2008). Also, given the shorter telomeres in bank voles exposed to radionuclides (Kesäniemi, Lavrinienko, et al., 2019), it is interesting that many bank vole chromosomes are acrocentric (Figure 3) as

TABLE 3 Alternative models for Msat-160 and 18S rDNA content using logarithm of the total received dose rate (D.rate, mGy/day) as a continuous variable in place of treatment group-based models. Female voles are used as reference level

DV (fixed effects)		β (SE)	df	t
18S copy number	Intercept	0.676 (0.050)	10.75	13.461[***]
(D.rate+Sex)[a]	D.rate	0.020 (0.008)	7.26	0.042[*]
	Sex (Male)	0.180 (0.046)	195.20	3.939[***]
Msat–160 copy number	Intercept	0.614 (0.041)	118.90	14.995[***]
(D.rate+Sex)[b]	D.rate	0.028 (0.007)	70.38	3.985[***]
	Sex (Male)	0.010 (0.039)	201.70	0.267

[a]Random factor: trapping area, $N = 7$, Var = 0.002 (trapping point resulted in singular fit).
[b]Random factor: trapping point, $N = 56$, Var = 0.009.
[*]$p < 0.05$; [***]$p < 0.001$.

this possibly makes Msat-160 simultaneously pericentromeric and subtelomeric. Subtelomeric heterochromatin can contribute to telomere protection, for example, by inducing compaction of telomere chromatin to a less accessible chromatin structure or even replacing canonical telomeres in telomerase-independent pathways of telomere maintenance (Jain et al., 2010). Subtelomeric repeats also show high copy-number variation under some stress conditions with detrimental consequences (Chow et al., 2012; van der Maarel & Frants, 2005; Vyskot et al., 1991).

It is perhaps important to note that, even with an attempt at genomic safeguard to mitigate some of the genomic consequences of stress, animals inhabiting contaminated areas can still experience diverse impacts of exposure to radionuclides. For example, bank voles inhabiting contaminated areas within the CEZ show reduced breeding success (Mappes et al., 2019) and elevated frequency of cataracts (Lehmann et al., 2016). Also, bank voles exposed to radionuclides show an increase in damage to their mitochondrial genomes (Kesäniemi et al., 2020), possibly because the mitochondria do not use certain DNA repair pathways (e.g., nucleotide excision repair) and/or the mitochondrial DNA lacks heterochromatin (Kazak et al., 2012; Yakes & Van Houten, 1997).

4.2 | Breakdown of intragenomic correlations as a hallmark of radioactively contaminated habitat

The correlation between rDNA and Msat-160 copy number in bank voles from uncontaminated areas within and outside the CEZ, but not in animals from contaminated areas, implies some disruption to typical genome architecture when animals are exposed to environmental radionuclides. Repetitive genome fraction generally correlates with genome size between species (Gregory, 2001; Prokopowich et al., 2003). Data on expected intraspecific correlations among different genomic regions are lacking, although there is some evidence that rDNA content negatively associates with mitochondrial DNA content in humans (Gibbons et al., 2014). We are not aware of any previous report that rDNA and pericentromere content would be correlated. Regardless, disruption to processes that maintain typical cell and genome integrity is a notable feature of bank voles inhabiting areas contaminated by radionuclides, such as (a) a lack of

TABLE 4 Pearson's correlation between 18S rDNA and Msat-160 copy numbers among treatment groups and trapping areas

Exposure group	Trapping area	R	df	t
CEZ-CNTM	Combined	0.130	87	1.213
	Gluboke	0.165	27	0.868
	Vesnyane	0.251	28	1.374
	Chistogalovka	0.279	28	1.540
CEZ-CTRL	Combined	0.755	56	8.618[***]
	Yampil	0.831	28	7.890[***]
	Rosoha	0.808	26	7.005[***]
KYV-CTRL	Combined	0.515	53	4.370[***]
	East	0.724	25	5.540[***]
	West	0.387	26	2.141[*]

[*]$p < 0.05$; [***]$p < 0.001$.

correlation in telomere length among different tissues (Kesäniemi, Lavrinienko, et al., 2019), (b) no relationship between mitochondrial DNA copy number and expression of PGC1α (the gene that regulates mitochondrial synthesis) in brain tissue (Kesäniemi et al., 2020), and (c) a weakening of gene coexpression networks in liver and spleen (Kesäniemi, Jernfors, et al., 2019).

4.3 | Safeguard by genomic repeats may respond to diverse stressors

The comparison between samples from the CEZ and West Kyiv is consistent with the genomic safeguard hypothesis, but the general increase in rDNA and Msat-160 copy number in the genomes of animals from East Kyiv cannot be explained. On the one hand, these data could be used to argue against an increase in rDNA and centromeric DNA to exposure to IR. However, as diverse stressors can elicit intraspecific heterogeneity in rDNA content (Govindaraju & Cullis, 1992; Harvey et al., 2020; Salim et al., 2017), and potentially centromeric architecture, it is possible that voles at East Kyiv experienced some other feature of the environment that selected for an increase in rDNA/centromere content. As such, the data from East Kyiv do not necessarily refute the idea of genome safeguard
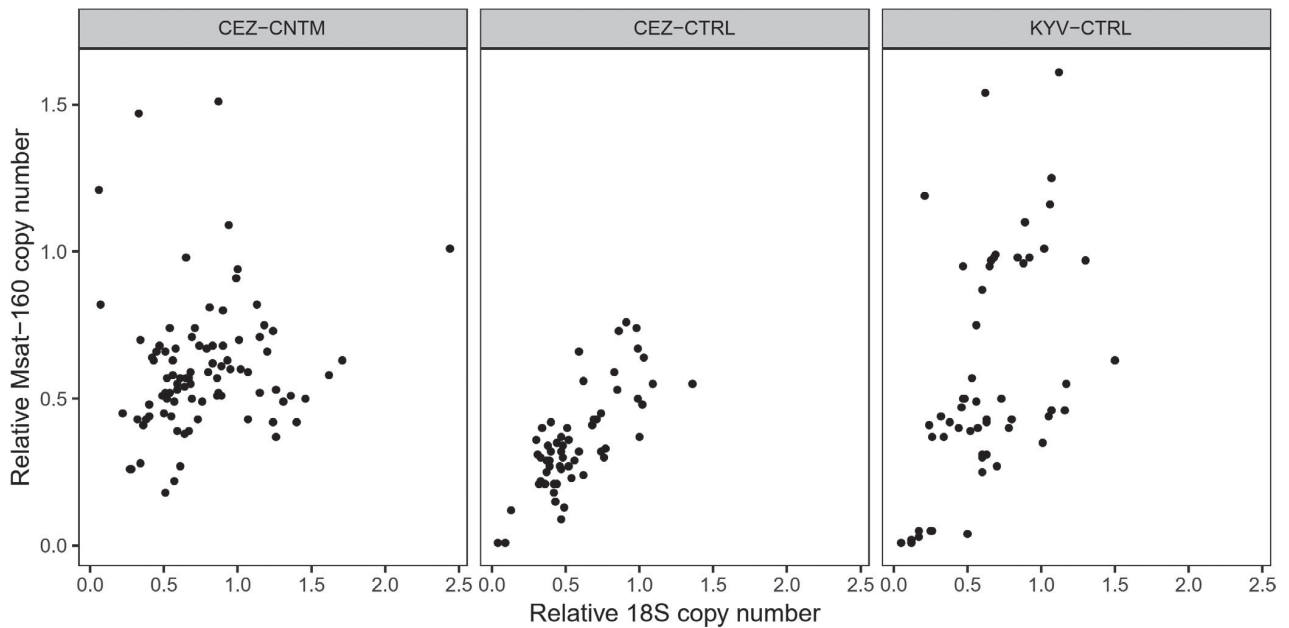
FIGURE 5 Association between 18S rDNA and Msat-160 content. 18S rDNA and Msat-160 content are correlated in all uncontaminated areas (CEZ-CTRL and KYV-CTRL), but not in contaminated areas (CEZ-CNTM)

by heterochromatin. Also, we are not aware of other reports of sex differences in rDNA content in mammals. In _Drosophila melanogaster,_ the rDNA cluster is located on sex chromosomes. However, the rDNA clusters in mammals, such as humans and mice, are located on several autosomes (Coen & Dover, 1983) and not sex chromosomes. In any case, an animal's sex and its rDNA content do not interact with radionuclide exposure. Hence, our data highlight the capacity for wild animals to show macro- and microgeographic variation in DNA and Msat-160 (_i.e._, centromeric) content, and this emphasizes the need for further research to understand the biological driver(s) of this genetic variation. Particularly important will be the use of experiments to quantify how specific stressors, such as environmental radionuclide exposure, impact these apparently labile regions of the genome. Moreover, heterochromatin architecture as a potential mitigator of genome damage should be explored in more detail, not only in bank voles, but also in other species that differ in apparent radiosensitivity (Lourenço et al., 2016) and amount of noncoding DNA (Gregory, 2001; Prokopowich et al., 2003).

5 | CONCLUSION

In conclusion, we uncovered geographic variation in Msat-160 and 18S rDNA content in bank vole genomes that is consistent with the hypothesized role of heterochromatin and rDNA in responding to, and safeguarding the genome against, environmental stress. Furthermore, we show loss of an apparent intragenomic correlation in rDNA-(peri-)centromere content in bank voles exposed to radionuclides. While the role of non-protein-coding DNA, and particularly rDNA, is well researched in a medical context (Kobayashi, 2014;

Wang & Lemos, 2017; Xu et al., 2017), our data indicate clear potential for environmental pollution to have a broad effect in genome architecture. Additional studies are required to partition the plastic and heritable components of these copy-number changes, and also whether this change in genome architecture is part of an adaptive response to exposure to elevated radiation dose or, indeed, other pollutants.

CONFLICT OF INTEREST

The authors declare no competing interests.

AUTHOR CONTRIBUTION

Toni Jernfors: Conceptualization (equal); Formal analysis (lead); Investigation (equal); Writing-original draft (lead). **John Danforth:** Conceptualization (equal); Investigation (equal); Writing-review & editing (equal). **Jenni Kesäniemi:** Investigation (equal); Writing-review & editing (equal). **Anton Lavrinienko:** Investigation (equal); Resources (equal); Writing-review & editing (equal). **Eugene Tukalenko:** Investigation (equal); Resources (equal); Writing-review & editing (equal). **Jiří Fajkus:** Resources (equal); Writing-review &

editing (equal). **Martina Dvořáčková:** Investigation (equal); Writing-review & editing (equal). **Tapio Mappes:** Resources (equal); Writing-review & editing (equal). **Phillip Watts:** Conceptualization (lead); Project administration (lead); Supervision (lead); Writing-review & editing (lead).

ETHICAL APPROVAL

All experiments complied with the legal requirements and adhered closely to international guidelines for the use of animals in research. All necessary permissions were obtained from the Animal Experimentation Committee for these experiments (permission no. ESAVI/7256/04.10.07/2014).

DATA AVAILABILITY STATEMENT

Sampling metadata, morphological measurements, and radiation dosimetry data are available in Dryad (https://doi.org/10.5061/dryad.1zcrjdfrt).

ORCID

Toni Jernfors (ID) https://orcid.org/0000-0002-8657-574X
Jenni Kesäniemi http://orcid.org/0000-0001-8328-558X
Anton Lavrinienko (ID) https://orcid.org/0000-0002-9524-8054
Jiří Fajkus (ID) https://orcid.org/0000-0002-3112-1716
Martina Dvořáčková (ID) https://orcid.org/0000-0001-5998-6159
Tapio Mappes (ID) https://orcid.org/0000-0002-5936-7355
Phillip C. Watts (ID) https://orcid.org/0000-0001-7755-187X

REFERENCES

Acevedo-Whitehouse, K., & Duffus, A. L. J. (2009). Effects of environmental change on wildlife health. _Philosophical Transactions of the Royal Society B: Biological Sciences_, _364_, 3429–3438. https://doi.org/10.1098/rstb.2009.0128

Acosta, M. J., Marchal, J. A., Fernández-Espartero, C., Romero-Fernández, I., Rovatsos, M. T., Giagia-Athanasopoulou, E. B., Gornung, E., Castiglia, R., & Sánchez, A. (2010). Characterization of the satellite DNA Msat-160 from species of Terricola (Microtus) and Arvicola (Rodentia, Arvicolinae). _Genetica_, _138_, 1085–1098. https://doi.org/10.1007/s10709-010-9496-2

Acosta, M. J., Marchal, J. A., Martínez, S., Puerma, E., Bullejos, M., de Guardia, R. D. L., & Sánchez, A. (2007). Characterization of the satellite DNA Msat-160 from the species _Chionomys nivalis_ (Rodentia, Arvicolinae). _Genetica_, _130_, 43–51. https://doi.org/10.1007/s10709-006-0018-1

Aldrich, J. C., & Maggert, K. A. (2015). Transgenerational inheritance of diet-induced genome rearrangements in _Drosophila_. _PLoS Genetics_, _11_, 1–21. https://doi.org/10.1371/journal.pgen.1005148

Alexandrov, I., Kazakov, A., Tumeneva, I., Shepelev, V., & Yurov, Y. (2001). Alpha-satellite DNA of primates: Old and new families. _Chromosoma_, _110_, 253–266. https://doi.org/10.1007/s004120100146

Altschul, S. F., Gish, W., Miller, W., Myers, E. W., & Lipman, D. J. (1990). Basic local alignment search tool. _Journal of Molecular Biology_, _215_, 403–410. https://doi.org/10.1016/S0022-2836(05)80360-2

Ayouaz, A., Raynaud, C., Heride, C., Revaud, D., & Sabatier, L. (2008). Telomeres: Hallmarks of radiosensitivity. _Biochimie_, _90_, 60–72. https://doi.org/10.1016/j.biochi.2007.09.011

Baker, R. J., Dickins, B., Wickliffe, J. K., Khan, F. A. A., Gaschak, S., Makova, K. D., & Phillips, C. D. (2017). Elevated mitochondrial genome variation after 50 generations of radiation exposure in a

wild rodent. _Evolutionary Applications_, _10_, 784–791. https://doi.org/10.1111/eva.12475

Baltas, D., Sakelliou, L., & Zamboglou, N. (2019). _The physics of modern brachytherapy for oncology_. CRC Press.

Bates, D., Mächler, M., Bolker, B., & Walker, S. (2015). Fitting Linear Mixed-Effects Models Using lme4. _Journal of Statistical Software_, _67_(1). https://doi.org/10.18637/jss.v067.i01

Beresford, N. A., Barnett, C. L., Gashchak, S., Maksimenko, A., Guliaichenko, E., Wood, M. D., & Izquierdo, M. (2020). Radionuclide transfer to wildlife at a 'Reference site' in the Chernobyl Exclusion Zone and resultant radiation exposures. _Journal of Environmental Radioactivity_, _211_, 105661. https://doi.org/10.1016/j.jenvrad.2018.02.007

Beresford, N. A., & Copplestone, D. (2011). Effects of ionizing radiation on wildlife: What knowledge have we gained between the chernobyl and fukushima accidents? _Integrated Environmental Assessment and Management_, _7_, 371–373. https://doi.org/10.1002/ieam.238

Beresford, N. A., Fesenko, S., Konoplev, A., Skuterud, L., Smith, J. T., & Voigt, G. (2016). Thirty years after the Chernobyl accident: What lessons have we learnt? _Journal of Environmental Radioactivity_, _157_, 77–89. https://doi.org/10.1016/j.jenvrad.2016.02.003

Beresford, N. A., Gaschak, S., Barnett, C. L., Howard, B. J., Chizhevsky, I., Strømman, G., Oughton, D. H., Wright, S. M., Maksimenko, A., & Copplestone, D. (2008). Estimating the exposure of small mammals at three sites within the Chernobyl exclusion zone – A test application of the ERICA Tool. _Journal of Environmental Radioactivity_, _99_, 1496–1502. https://doi.org/10.1016/j.jenvrad.2008.03.002

Biscotti, M. A., Canapa, A., Forconi, M., Olmo, E., & Barucca, M. (2015). Transcription of tandemly repetitive DNA: Functional roles. _Chromosome Research_, _23_, 463–477. https://doi.org/10.1007/s10577-015-9494-4

Biscotti, M. A., Olmo, E., & Heslop-Harrison, J. S. (2015). Repetitive DNA in eukaryotic genomes. _Chromosome Research_, _23_, 415–420. https://doi.org/10.1007/s10577-015-9499-z

Bouffler, S. D., Bridges, B. A., Cooper, D. N., Dubrova, Y., McMillan, T. J., Thacker, J., Wright, E. G., & Waters, R. (2006). Assessing radiation-associated mutational risk to the germline: Repetitive DNA sequences as mutational targets and biomarkers. _Radiation Research_, _165_, 249–268. https://doi.org/10.1667/rr3506.1

Bréchignac, F., Oughton, D., Mays, C., Barnthouse, L., Beasley, J. C., Bonisoli-Alquati, A., Bradshaw, C., Brown, J., Dray, S., Geras'kin, S., Glenn, T., Higley, K., Ishida, K., Kapustka, L., Kautsky, U., Kuhne, W., Lynch, M., Mappes, T., Mihok, S., … Tsukada, H. (2016). Addressing ecological effects of radiation on populations and ecosystems to improve protection of the environment against radiation: Agreed statements from a Consensus Symposium. _Journal of Environmental Radioactivity_, _158–159_, 21–29. https://doi.org/10.1016/j.jenvrad.2016.03.021

Burnham, K. P., & Anderson, D. R. (2002). _Model selection and multimodel inference: A practical information-theoretic approach_ (2nd ed.). Springer-Verlag.

Cawthon, R. M. (2002). Telomere measurement by quantitative PCR. _Nucleic Acids Research_, _30_, 47e–47. https://doi.org/10.1093/nar/30.10.e47

Chesser, R. K., Sugg, D. W., Lomakin, M. D., van den Bussche, R. A., DeWoody, J. A., Jagoe, C. H., Dallas, C. E., Whicker, F. W., Smith, M. H., Gaschak, S. P., Chizhevsky, I. V., Lyabik, V. V., Buntova, E. G., Holloman, K., & Baker, R. J. (2000). Concentrations and dose rate estimates of 134137 cesium and 90 strontium in small mammals at chornobyl, Ukraine. _Environmental Toxicology and Chemistry_, _19_, 305–312. https://doi.org/10.1002/etc.5620190209

Chiolo, I., Minoda, A., Colmenares, S. U., Polyzos, A., Costes, S. V., & Karpen, G. H. (2011). Double-strand breaks in heterochromatin move outside of a dynamic HP1a domain to complete recombinational repair. _Cell_, _144_, 732–744. https://doi.org/10.1016/j.cell.2011.02.012

Chow, E. W. L., Morrow, C. A., Djordjevic, J. T., Wood, I. A., & Fraser, J. A. (2012). Microevolution of *Cryptococcus neoformans* driven by massive tandem gene amplification. *Molecular Biology and Evolution*, *29*, 1987–2000. https://doi.org/10.1093/molbev/mss066

Coen, E. S., & Dover, G. A. (1983). Unequal exchanges and the coevolution of X and Y rDNA arrays in drosophila melanogaster. *Cell*, *33*, 849–855. https://doi.org/10.1016/0092-8674(83)90027-2

Cristy, M., & Eckerman, K. F. (1987). Specific absorbed fractions of energy at various ages from internal photon sources: 7, Adult male. Oak Ridge National Laboratory, Tennessee, USA. https://www.osti.gov/servlets/purl/6233638

Desouky, O., Ding, N., & Zhou, G. (2015). Targeted and non-targeted effects of ionizing radiation. *Journal of Radiation Research and Applied Sciences*, *8*, 247–254. https://doi.org/10.1016/j.jrras.2015.03.003

Dubrova, Y. E. (1998). Radiation-induced germline instability at minisatellite loci. *International Journal of Radiation Biology*, *74*, 689–696. https://doi.org/10.1080/095530098140952

Dzyubenko, E. V., & Gudkov, D. I. (2009). Cytogenetical and haematological effects of long-term irradiation on freshwater gastropod snails in the Chernobyl accident Exclusion Zone. *Radioprotection*, *44*, 933–936. https://doi.org/10.1051/radiopro/20095166

Einor, D., Bonisoli-Alquati, A., Costantini, D., Mousseau, T. A., & Møller, A. P. (2016). Ionizing radiation, antioxidant response and oxidative damage: A meta-analysis. *Science of the Total Environment*, *548–549*, 463–471. https://doi.org/10.1016/j.scitotenv.2016.01.027

Ellegren, H., Møller, A. P., Lindgren, G., & Primmer, C. R. (1997). Fitness loss and germline mutations in barn swallows breeding in Chernobyl. *Nature*, *389*, 593–596. https://doi.org/10.1038/39303

Foltz, D. R., Jansen, L. E. T., Black, B. E., Bailey, A. O., Yates, J. R., & Cleveland, D. W. (2006). The human CENP-A centromeric nucleosome-associated complex. *Nature Cell Biology*, *8*, 458–469. https://doi.org/10.1038/ncb1397

Franek, M., Legartová, S., Suchánková, J., Milite, C., Castellano, S., Sbardella, G., Kozubek, S., & Bártová, E. (2015). CARM1 modulators affect epigenome of stem cells and change morphology of nucleoli. *Physiological Research*, *64*, 769–782. https://doi.org/10.33549/physiolres.932952

Garnier-Laplace, J., Geras'kin, S., Della-Vedova, C., Beaugelin-Seiller, K., Hinton, T. G., Real, A., & Oudalova, A. (2013). Are radiosensitivity data derived from natural field conditions consistent with data from controlled exposures? A case study of Chernobyl wildlife chronically exposed to low dose rates. *Journal of Environmental Radioactivity*, *121*, 12–21. https://doi.org/10.1016/j.jenvrad.2012.01.013

Gaschak, S. P., Maklyuk, Y. A., Maksimenko, A. M., Bondarkov, M. D., Jannik, G. T., & Farfán, E. B. (2011). Radiation ecology issues associated with murine rodents and shrews in the chernobyl exclusion zone. *Health Physics*, *101*, 416–430. https://doi.org/10.1097/HP.0b013e31821e123f

Gazave, E., Gautier, P., Gilchrist, S., & Bickmore, W. A. (2005). Does radial nuclear organisation influence DNA damage? *Chromosome Research*, *13*, 377–388. https://doi.org/10.1007/s10577-005-3254-9

Geyer, P. K., Vitalini, M. W., & Wallrath, L. L. (2011). Nuclear organization: Taking a position on gene expression. *Current Opinion in Cell Biology*, *23*, 354–359.

Gibbons, J. G., Branco, A. T., Yu, S., & Lemos, B. (2014). Ribosomal DNA copy number is coupled with gene expression variation and mitochondrial abundance in humans. *Nature Communications*, *5*, 4850. https://doi.org/10.1038/ncomms5850

Gonzalez-Hunt, C. P., Wadhwa, M., & Sanders, L. H. (2018). DNA damage by oxidative stress: Measurement strategies for two genomes. *Current Opinion in Toxicology*, *7*, 87–94. https://doi.org/10.1016/j.cotox.2017.11.001

Govindaraju, D. R., & Cullis, C. A. (1992). Ribosomal DNA variation among populations of a *Pinus rigida* Mill. (pitch pine) ecosystem: I. Distribution of copy numbers. *Heredity*, *69*, 133–140. https://doi.org/10.1038/hdy.1992.106

Goytisolo, F. A., Samper, E., Martín-Caballero, J., Finnon, P., Herrera, E., Flores, J. M., Bouffler, S. D., & Blasco, M. A. (2000). Short telomeres result in organismal hypersensitivity to ionizing radiation in mammals. *Journal of Experimental Medicine*, *192*, 1625–1636. https://doi.org/10.1084/jem.192.11.1625

Gregory, T. R. (2001). Coincidence, coevolution, or causation? DNA content, cellsize, and the C-value enigma. *Biological Reviews*, *76*, 65–101. https://doi.org/10.1111/j.1469-185X.2000.tb00059.x

Grewal, S. I. S., & Jia, S. (2007). Heterochromatin revisited. *Nature Reviews Genetics*, *8*, 35–46. https://doi.org/10.1038/nrg2008

Harvey, E. F., Cristescu, M. E., Dale, J., Hunter, H., Randall, C., & Crease, T. J. (2020). Metal exposure causes rDNA copy number to fluctuate in mutation accumulation lines of Daphnia pulex. *Aquatic Toxicology*, *226*, 105556. https://doi.org/10.1016/j.aquatox.2020.105556

Heydari, A. R., Unnikrishnan, A., Lucente, L. V., & Richardson, A. (2007). Caloric restriction and genomic stability. *Nucleic Acids Research*, *35*, 7485–7496. https://doi.org/10.1093/nar/gkm860

Hothorn, T., Bretz, F., & Westfall, P. (2008). Simultaneous Inference in General Parametric Models. *Biometrical Journal*, *50*, 346–363. https://doi.org/10.1002/bimj.200810425

ICRP (1983). *Radionuclide transformations. Energy and intensity of emissions*. Ann ICRP.

Ide, S., Miyazaki, T., Maki, H., & Kobayashi, T. (2010). Abundance of ribosomal RNA gene copies maintains genome integrity. *Science*, *327*, 693–696. https://doi.org/10.1126/science.1179044

Ideue, T., & Tani, T. (2020). Centromeric non-coding RNAs: Conservation and diversity in function. *Non-Coding RNA*, *6*, 4. https://doi.org/10.3390/ncrna6010004

Isaev, A. G., Babenko, V. V., Kazimirov, A. S., Grishin, S. N., & Ievlev, S. M. (2010). Minimum detectable activity. Basic concepts and definitions. *Problemi Bezpeki Atomnikh Elektrostantsyij Yi Chornobilya*, *13*, 103–110.

Isaksson, C. (2010). Pollution and its impact on wild animals: A meta-analysis on oxidative stress. *EcoHealth*, *7*, 342–350. https://doi.org/10.1007/s10393-010-0345-7

Jack, C. V., Cruz, C., Hull, R. M., Keller, M. A., Ralser, M., & Houseley, J. (2015). Regulation of ribosomal DNA amplification by the TOR pathway. *Proceedings of the National Academy of Sciences of the United States of America*, *112*, 9674–9679. https://doi.org/10.1073/pnas.1505015112

Jain, D., Hebden, A. K., Nakamura, T. M., Miller, K. M., & Cooper, J. P. (2010). HAATI survivors replace canonical telomeres with blocks of generic heterochromatin. *Nature*, *467*, 223–227. https://doi.org/10.1038/nature09374

Jakob, B., Splinter, J., Conrad, S., Voss, K.-O., Zink, D., Durante, M., Löbrich, M., & Taucher-Scholz, G. (2011). DNA double-strand breaks in heterochromatin elicit fast repair protein recruitment, histone H2AX phosphorylation and relocation to euchromatin. *Nucleic Acids Research*, *39*(15), 6489–6499. https://doi.org/10.1093/nar/gkr230

Jernfors, T., Kesäniemi, J., Lavrinienko, A., Mappes, T., Milinevsky, G., Møller, A. P., Mousseau, T. A., Tukalenko, E., & Watts, P. C. (2018). Transcriptional upregulation of DNA damage response genes in bank voles (*Myodes glareolus*) inhabiting the chernobyl exclusion zone. *Frontiers in Environmental Science*, *5*, 95. https://doi.org/10.3389/fenvs.2017.00095

Kazak, L., Reyes, A., & Holt, I. J. (2012). Minimizing the damage: Repair pathways keep mitochondrial DNA intact. *Nature Reviews Molecular Cell Biology*, *13*, 659–671. https://doi.org/10.1038/nrm3439

Kesäniemi, J., Boratyński, Z., Danforth, J., Itam, P., Jernfors, T., Lavrinienko, A., Mappes, T., Møller, A. P., Mousseau, T. A., & Watts, P. C. (2018). Analysis of heteroplasmy in bank voles inhabiting the Chernobyl exclusion zone: A commentary on Baker et al. (2017) "Elevated mitochondrial genome variation after 50 generations of

radiation exposure in a wild rodent. _Evolutionary Applications_, 11, 820–826. https://doi.org/10.1111/eva.12578

Kesäniemi, J., Jernfors, T., Lavrinienko, A., Kivisaari, K., Kiljunen, M., Mappes, T., & Watts, P. C. (2019). Exposure to environmental radionuclides is associated with altered metabolic and immunity pathways in a wild rodent. _Molecular Ecology_, 28(20), 4620–4635. https://doi.org/10.1111/mec.15241

Kesäniemi, J., Lavrinienko, A., Tukalenko, E., Boratyński, Z., Kivisaari, K., Mappes, T., Milinevsky, G., Møller, A. P., Mousseau, T. A., & Watts, P. C. (2019). Exposure to environmental radionuclides associates with tissue-specific impacts on telomerase expression and telomere length. _Scientific Reports_, 9, 850. https://doi.org/10.1038/s41598-018-37164-8

Kesäniemi, J., Lavrinienko, A., Tukalenko, E., Moutinho, A. F., Mappes, T., Møller, A. P., Mousseau, T. A., & Watts, P. C. (2020). Exposure to environmental radionuclides alters mitochondrial DNA maintenance in a wild rodent. _Evolutionary Ecology_, 34, 163–174. https://doi.org/10.1007/s10682-019-10028-x

Khadaroo, B., Teixeira, M. T., Luciano, P., Eckert-Boulet, N., Germann, S. M., Simon, M. N., Gallina, I., Abdallah, P., Gilson, E., Géli, V., & Lisby, M. (2009). The DNA damage response at eroded telomeres and tethering to the nuclear pore complex. _Nature Cell Biology_, 11, 980–987. https://doi.org/10.1038/ncb1910

Kobayashi, T. (2011). Regulation of ribosomal RNA gene copy number and its role in modulating genome integrity and evolutionary adaptability in yeast. _Cellular and Molecular Life Sciences_, 68, 1395–1403. https://doi.org/10.1007/s00018-010-0613-2

Kobayashi, T. (2014). Ribosomal RNA gene repeats, their stability and cellular senescence. _Proceedings of the Japan Academy, Series B_, 90, 119–129. https://doi.org/10.2183/pjab.90.119

Kobayashi, T., & Sasaki, M. (2017). Ribosomal DNA stability is supported by many 'buffer genes'—introduction to the Yeast rDNA Stability Database. _FEMS Yeast Research_, 17, 1–8. https://doi.org/10.1093/femsyr/fox001

Komissarov, A. S., Gavrilova, E. V., Demin, S. J., Ishov, A. M., & Podgornaya, O. I. (2011). Tandemly repeated DNA families in the mouse genome. _BMC Genomics_, 12, 531. https://doi.org/10.1186/1471-2164-12-531

Kozakiewicz, M., Chołuj, A., & Kozakiewicz, A. (2007). Long-distance movements of individuals in a free-living bank vole population: An important element of male breeding strategy. _Acta Theriologica_, 52, 339–348. https://doi.org/10.1007/BF03194231

Kumari, N., Vartak, S. V., Dahal, S., Kumari, S., Desai, S. S., Gopalakrishnan, V., Choudhary, B., & Raghavan, S. C. (2019). G-quadruplex structures contribute to differential radiosensitivity of the human genome. _iScience_, 21, 288–307. https://doi.org/10.1016/j.isci.2019.10.033

Larson, K., Yan, S.-J., Tsurumi, A., Liu, J., Zhou, J., Gaur, K., Guo, D., Eickbush, T. H., & Li, W. X. (2012). Heterochromatin formation promotes longevity and represses ribosomal RNA synthesis. _PLoS Genetics_, 8, e1002473. https://doi.org/10.1371/journal.pgen.1002473

Lavrinienko, A., Jernfors, T., Koskimäki, J. J., Pirttilä, A. M., & Watts, P. C. (2020). Does intraspecific variation in rDNA copy number affect analysis of microbial communities? _Trends in Microbiology_, 29, 19–27. https://doi.org/10.1016/j.tim.2020.05.019

Lavrinienko, A., Tukalenko, E., Kesäniemi, J., Kivisaari, K., Masiuk, S., Boratyński, Z., Mousseau, T. A., Milinevsky, G., Mappes, T., & Watts, P. C. (2020). Applying the Anna Karenina principle for wild animal gut microbiota: Temporal stability of the bank vole gut microbiota in a disturbed environment. _Journal of Animal Ecology_, 1365–2656, 13342. https://doi.org/10.1111/1365-2656.13342

Lehmann, P., Boratyński, Z., Mappes, T., Mousseau, T. A., & Møller, A. P. (2016). Fitness costs of increased cataract frequency and cumulative radiation dose in natural mammalian populations from Chernobyl. _Scientific Reports_, 6, 19974. https://doi.org/10.1038/srep19974

Lourenço, J., Mendo, S., & Pereira, R. (2016). Radioactively contaminated areas: Bioindicator species and biomarkers of effect in an early warning scheme for a preliminary risk assessment. _Journal of Hazardous Materials_, 317, 503–542. https://doi.org/10.1016/j.jhazmat.2016.06.020

Mappes, T., Boratyński, Z., Kivisaari, K., Lavrinienko, A., Milinevsky, G., Mousseau, T. A., Møller, A. P., Tukalenko, E., & Watts, P. C. (2019). Ecological mechanisms can modify radiation effects in a key forest mammal of Chernobyl. _Ecosphere_, 10, e02667. https://doi.org/10.1002/ecs2.2667

Melters, D. P., Bradnam, K. R., Young, H. A., Telis, N., May, M. R., Ruby, J., Sebra, R., Peluso, P., Eid, J., Rank, D., Garcia, J., DeRisi, J. L., Smith, T., Tobias, C., Ross-Ibarra, J., Korf, I., & Chan, S. W. L. (2013). Comparative analysis of tandem repeats from hundreds of species reveals unique insights into centromere evolution. _Genome Biology_, 14, 1–20. https://doi.org/10.1186/gb-2013-14-1-r10

Modi, W. S. (1992). Nucleotide sequence and genomic organization of a tandem satellite array from the rock vole _Microtus chrotorrhinus_ (Rodentia). _Mammalian Genome_, 3, 226–232. https://doi.org/10.1007/BF00355723

Modi, W. S. (1993). Heterogeneity in the concerted evolution process of a tandem satellite array in meadow mice (Microtus). _Journal of Molecular Evolution_, 37, 48–56. https://doi.org/10.1007/BF00170461

Møller, A. P., & Mousseau, T. A. (2015). Strong effects of ionizing radiation from Chernobyl on mutation rates. _Scientific Reports_, 5, 8363. https://doi.org/10.1038/srep08363

Mousseau, T. A., Moller, A. P., Møller, A. P., & Moller, A. P. (2014). Genetic and ecological studies of animals in Chernobyl and Fukushima. _Journal of Heredity_, 105, 704–709. https://doi.org/10.1093/jhered/esu040

Mozgová, I., Mokroš, P., & Fajkus, J. (2010). Dysfunction of chromatin assembly factor 1 induces shortening of telomeres and loss of 45s rDNA in Arabidopsis Thaliana. _The Plant Cell_, 22, 2768–2780. https://doi.org/10.1105/tpc.110.076182

Mustonen, V., Kesäniemi, J., Lavrinienko, A., Tukalenko, E., Mappes, T., Watts, P. C., & Jurvansuu, J. (2018). Fibroblasts from bank voles inhabiting Chernobyl have increased resistance against oxidative and DNA stresses. _BMC Cell Biology_, 19, 17. https://doi.org/10.1186/s12860-018-0169-9

Pardo-Manuel de Villena, F., & Sapienza, C. (2001). Female meiosis drives karyotypic evolution in mammals. _Genetics_, 159, 1179–1189. https://doi.org/10.1093/genetics/159.3.1179

Paredes, S., Branco, A. T., Hartl, D. L., Maggert, K. A., & Lemos, B. (2011). Ribosomal dna deletions modulate genome-wide gene expression: "rDNA-sensitive" genes and natural variation. _PLoS Genetics_, 7, 1–10. https://doi.org/10.1371/journal.pgen.1001376

Parks, M. M., Kurylo, C. M., Dass, R. A., Bojmar, L., Lyden, D., Vincent, C. T., & Blanchard, S. C. (2018). Variant ribosomal RNA alleles are conserved and exhibit tissue-specific expression. _Science Advances_, 4(2), eaao0665. https://doi.org/10.1126/sciadv.aao0665

Pfaffl, M. W. (2001). A new mathematical model for relative quantification in RT-PCR. _Nucleic Acids Research_, 29, 16–21. https://doi.org/10.1093/nar/29.9.e45

Plohl, M., Luchetti, A., Meštrović, N., & Mantovani, B. (2008). Satellite DNAs between selfishness and functionality: Structure, genomics and evolution of tandem repeats in centromeric (hetero)chromatin. _Gene_, 409, 72–82. https://doi.org/10.1016/j.gene.2007.11.013

Poetsch, A. R., Boulton, S. J., & Luscombe, N. M. (2018). Genomic landscape of oxidative DNA damage and repair reveals regioselective protection from mutagenesis 06 Biological Sciences 0604 Genetics. _Genome Biology_, 19, 1–23. https://doi.org/10.1186/s13059-018-1582-2

Potapova, T. A., & Gerton, J. L. (2019). Ribosomal DNA and the nucleolus in the context of genome organization. _Chromosome Research_, 27, 109–127. https://doi.org/10.1007/s10577-018-9600-5

Prokopowich, C. D., Gregory, T. R., & Crease, T. J. (2003). The correlation between rDNA copy number and genome size in eukaryotes. _Genome_, _46_, 48–50. https://doi.org/10.1139/g02-103

Qiu, G. H. (2015). Protection of the genome and central protein-coding sequences by non-coding DNA against DNA damage from radiation. _Mutation Research/Reviews in Mutation Research_, _764_, 108–117. https://doi.org/10.1016/j.mrrev.2015.04.001

Reste, J., Zvigule, G., Zvagule, T., Kurjane, N., Eglite, M., Gabruseva, N., Berzina, D., Plonis, J., & Miklasevics, E. (2014). Telomere length in Chernobyl accident recovery workers in the late period after the disaster. _Journal of Radiation Research_, _55_, 1089–1100. https://doi.org/10.1093/jrr/rru060

Rodgers, B. E., & Baker, R. J. (2000). Frequencies of micronuclei in bank voles from zones of high radiation at Chornobyl, Ukraine. _Environmental Toxicology and Chemistry_, _19_, 1644–1648. https://doi.org/10.1002/etc.5620190623

Salim, D., Bradford, W. D., Freeland, A., Cady, G., Wang, J., Pruitt, S. C., & Gerton, J. L. (2017). DNA replication stress restricts ribosomal DNA copy number. _PLoS Genetics_, _13_, 1–20. https://doi.org/10.1371/journal.pgen.1007006

Salim, D., & Gerton, J. L. (2019). Ribosomal DNA instability and genome adaptability. _Chromosome Research_, _27_, 73–87. https://doi.org/10.1007/s10577-018-9599-7

Smiddy, P., Sleeman, D. P., & Lysaght, L. (2016). Expansion of range in the Bank Vole (_Myodes glareolus_) in Co., Waterford: 1994–2009. _Irish Naturalists Journal_, _35_, 17–21.

Stabin, M. G., & Konijnenberg, M. W. (2000). Re-evaluation of absorbed fractions for photons and electrons in spheres of various sizes. _Journal of Nuclear Medicine_, _41_, 149–160.

Strauss, S. H., & Tsai, C.-H. (1988). Ribosomal gene number variability in Douglas-Fir. _Journal of Heredity_, _79_, 453–458. https://doi.org/10.1093/oxfordjournals.jhered.a110550

Symonová, R. (2019). Integrative rDNAomics—Importance of the oldest repetitive fraction of the eukaryote genome. _Genes (Basel)_, _10_, 345. https://doi.org/10.3390/genes10050345

The R Core Team (2018). _R: A language and environment for statistical computing_. Vienna, Austria: R Foundation for Statistical Computing. https://www.r-project.org/

Torres-Rosell, J., Sunjevaric, I., De Piccoli, G., Sacher, M., Eckert-Boulet, N., Reid, R., Jentsch, S., Rothstein, R., Aragón, L., & Lisby, M. (2007). The Smc5–Smc6 complex and SUMO modification of Rad52 regulates recombinational repair at the ribosomal gene locus. _Nature Cell Biology_, _9_(8), 923–931. https://doi.org/10.1038/ncb1619

Untergasser, A., Cutcutache, I., Koressaar, T., Ye, J., Faircloth, B. C., Remm, M., & Rozen, S. G. (2012). Primer3–new capabilities and interfaces. _Nucleic Acids Research_, _40_, e115. https://doi.org/10.1093/nar/gks596

Vaissière, T., Sawan, C., & Herceg, Z. (2008). Epigenetic interplay between histone modifications and DNA methylation in gene silencing. _Mutation Research/Reviews in Mutation Research_, _659_, 40–48. https://doi.org/10.1016/j.mrrev.2008.02.004

van Cann, J. (2019). _Intergenerational responses to a changing environment: Maternal and paternal early life shape fitness components in the bank vole_. University of Jyväskylä.

van der Maarel, S. M., & Frants, R. R. (2005). The D4Z4 repeat-mediated pathogenesis of facioscapulohumeral muscular dystrophy. _American Journal of Human Genetics_, _76_, 375–386. https://doi.org/10.1086/428361

Vyskot, B., Reich, J., Fajkus, J., Bezdek, M., & Soska, J. (1991). Genome modifications in protoplast-derived tobacco plants: Contents of repetitive DNA sequences. _Biologia Plantarum_, _33_, 448–454. https://doi.org/10.1007/BF02897717

Wang, M., & Lemos, B. (2017). Ribosomal DNA copy number amplification and loss in human cancers is linked to tumor genetic context, nucleolus activity, and proliferation. _PLoS Genetics_, _13_, e1006994. https://doi.org/10.1371/journal.pgen.1006994

Ward, J. F. (1988). DNA damage produced by ionizing radiation in mammalian cells: Identities, mechanisms of formation, and reparability. _Progress in Nucleic Acid Research and Molecular Biology_, _35_, 95–125.

Weider, L. J., Elser, J. J., Crease, T. J., Mateos, M., Cotner, J. B., & Markow, T. A. (2005). The functional significance of ribosomal (r)DNA variation: Impacts on the evolutionary ecology of organisms. _Annual Review of Ecology Evolution and Systematics_, _36_, 219–242. https://doi.org/10.1146/annurev.ecolsys.36.102003.152620

White, T. A., Lundy, M. G., Montgomery, W. I., Montgomery, S., Perkins, S. E., Lawton, C., Meehan, J. M., Hayden, T. J., Heckel, G., Reid, N., & Searle, J. B. (2012). Range expansion in an invasive small mammal: Influence of life-history and habitat quality. _Biological Invasions_, _14_, 2203–2215. https://doi.org/10.1007/s10530-012-0225-x

Xu, B., Li, H., Perry, J. M., Singh, V. P., Unruh, J., Yu, Z., Zakari, M., McDowell, W., Li, L., & Gerton, J. L. (2017). Ribosomal DNA copy number loss and sequence variation in cancer. _PLoS Genetics_, _13_, 1–25. https://doi.org/10.1371/journal.pgen.1006771

Yakes, F. M., & Van Houten, B. (1997). Mitochondrial DNA damage is more extensive and persists longer than nuclear DNA damage in human cells following oxidative stress. _Proceedings of the National Academy of Sciences of the United States of America_, _94_, 514–519. https://doi.org/10.1073/pnas.94.2.514

Yan, S.-J., Lim, S. J., Shi, S., Dutta, P., & Li, W. X. (2011). Unphosphorylated STAT and heterochromatin protect genome stability. _The FASEB Journal_, _25_, 232–241. https://doi.org/10.1096/fj.10-169367

Yuan, H.-X.-X., Xiong, Y., & Guan, K.-L.-L. (2013). Nutrient sensing, metabolism, and cell growth control. _Molecular Cell_, _49_, 379–387. https://doi.org/10.1016/j.molcel.2013.01.019

Zhang, X., Ye, C., Sun, F., Wei, W., Hu, B., & Wang, J. (2016). Both complexity and location of DNA damage contribute to cellular senescence induced by ionizing radiation. _PLoS One_, _11_, e0155725. https://doi.org/10.1371/journal.pone.0155725

APPENDIX 1

INTERNAL DOSIMETRY

To estimate internal dose rate caused by exposure to radio-cesium contamination, ^{137}Cs activity was measured by SAM 940 radionuclide identifier system (Berkeley Nucleonics Corporation) equipped with a 3" × 3" NaI detector. The detector was enclosed in 10-cm-thick lead shielding to reduce the noise from background radioactivity. The system was calibrated with reference standard sources. With corrections for laboratory background, the ^{137}Cs activity of whole bodies was evaluated from the obtained spectra in the energies range from 619 to 707 keV (with cesium photopeak at 662 keV) with the use of the phantom with known activity and geometry similar to measured samples. Given the different time from capturing animals till their sacrificing, the initial ^{137}Cs activity (at the trapping timepoint) was calculated with the model $A = be^{\lambda x}$, where A is calculated initial cesium activity; b is activity

that was measured in animal bodies; x is time in hours (after trapping and before sacrificing); e is 2.72; and λ is elimination constant. The parameters of ^{137}Cs elimination were found in our other study (Tukalenko et al., unpublished), and they were close to ones reported earlier (Gaschak et al., 2011).

For each measurement, the critical detectable level (decision threshold) was found as $Lc = k[Rb/Tb(1+Tb/Ts]^{1/2}$, where Lc is critical level; k is 1.65 (coefficient, which determines 0.05 probability of type I error or false positive); Rb is counting rate of background; Tb is time of background measurement; and Ts is time of sample measurement (Isaev et al., 2010). The cesium activities above the critical level (decision threshold) were used for internal dose rate estimation; otherwise, the ^{137}Cs activity was considered as zero.

With the use of conventional approach (Baltas et al., 2019; Cristy & Eckerman, 1987), an individual bank vole's internal absorbed dose from incorporated ^{137}Cs acquired during one day was calculated (mGy/day) as a product of the activity of ^{137}Cs incorporated in the animal's body (Bq/kg) and the unit conversion coefficient and the sum of all electron, positron, and photon energies emitted per decay of ^{137}Cs and its daughter radionuclide ^{137m}Ba. The energies were calculated taking into account the absorbed fractions for electron or positron or photon of the specific energy line, the intensity (or emission frequency) of the specific energy line (MeV) emitted per decay of ^{137}Cs and its daughter radionuclide ^{137m}Ba (ICRP, 1983), and the assumption that ^{137}Cs source is uniformly distributed throughout homogeneous sphere of 20 g mass of unit density and tissue-equivalent composition (Stabin & Konijnenberg, 2000). Despite the considerable contribution of ^{90}Sr to the total internal absorbed dose, that is considered to be approximately the same as from cesium-137 in Chernobyl (Beresford et al., 2020), in our study we neglected it because of characteristics of this beta-emitting radionuclide (tissue-specific strontium distribution in a body: ^{90}Sr deposits mainly in bones and adds its adsorbed dose contribution there). The energies from alpha-emitters (plutonium and americium: radioisotopes of transuranium elements) were neglected because of their low contribution to the total internal absorbed dose, less than 5% (Beresford et al., 2020).

Thus, the internal absorbed dose rates were as follows (median[interquartile range]): $0.0[0.0;0.0]*10^{-3}$ mGy/day at KYV-CTRL in range of $0.0–1.5*10^{-3}$ mGy/day, $3.7[1.6;3.7]*10^{-3}$ mGy/day at CEZ-CTRL in range of $1.6–3.7*10^{-3}$ mGy/day, and $1.4[0.4;3.7]*10^{-1}$ mGy/day at CEZ-CNTM in range of $0.04–20.0*10^{-1}$ mGy/day.

As individual total absorbed dose rate, we considered the sum of estimations of internal and external absorbed dose rates per each animal. The total absorbed dose rates were as follows (median[interquartile range]): $5.1[3.6;7.2]*10^{-3}$ mGy/day at KYV-CTRL in the range of $3.6–7.9*10^{-3}$ mGy/day, $9.5[6.0;10.3]*10^{-3}$ mGy/day at CEZ-CTRL in the range of $3.6–11.1*10^{-3}$ mGy/day, and $5.3[4.2;9.3]*10^{-1}$ mGy/day at CEZ-CNTM in the range of $2.7–34.1*10^{-1}$ mGy/day.

APPENDIX 2

FLUORESCENCE IN SITU HYBRIDIZATION (FISH) TO IDENTIFY PRINCIPAL LOCATIONS OF MSAT-160 SATELLITE IN THE BANK VOLE GENOME.

Fibroblasts were isolated from male bank voles collected from contaminated area within the CEZ (Gluboke, mean external dose rate 21 μGy/hr) and from a control areas near Kyiv (see Mustonen et al. (2018) for cell culture conditions). Fibroblasts were treated with 0.01 μg/ml colcemid for 2 hr, after which the cells were trypsinized and resuspended to hypotonic 0.075 M prewarmed KCl. Cells were incubated for 20 min at 37°C, after which the cells were fixed in 3:1 methanol:glacial acetic acid according to the standard protocol (Franek et al., 2015).

For the chromosome preparations, 10 μl of the fixed sample was dropped on Superfrost slide and the slides were air-dried. Slides were then quickly washed in 2× SCC and incubated for 1.5 hr in RNAse A (200 μg/ml, AppliChem) in 2× SSC. Slides were washed 3 times for 5 min in 2× SSC and incubated for 2 min in 0.01 M HCl, then for 5 min in pepsin (16 μg/ml in 100 mM HCl, 37°C), followed by 3 × 5 min wash in 2× SSC. Slides were incubated for 10 min in 4% formaldehyde in 2× SSC, washed for 3 × 5 min in 2× SSC, and dried in EtOH series (70%, 80%, and 96%). Biotin-labeled PCR probes were hybridized on the slides overnight at 37°C. After the hybridization, slides were washed for 5 min in 2× SCC, then 3 × 5 min in 40% formamide/2× SCC (at 42°C), 1 × 5 min in 2× SCC at 42°C, 1 × 5 min in 2× SSC at RT, and 5 min in 4T buffer (4× SSC and 0.05% Tween-20). 80 μl of blocking solution (4× SSC, 5% BSA, and 0.2% Tween-20) was applied on the slides, incubated for 30 min at RT, and washed for 5 min in 4T buffer. For visualization of the Msat-160 region, 80 μl of streptavidin-AF594 (1:1,000 in blocking solution) was added to the slides and incubated for 30 min at 37°C, followed by 3 × 5 min washes in 4T, 1 × 5 min wash in 2× SSC, and dehydration in ethanol (70%, 80%, and 90%). Chromosomes were stained with DAPI (1 μg/ml in Vectashield, Vector Laboratories). Images were taken using Zeiss Axio Imager Z2 microscope, using a Plan-Apochromat 100×/1.4 OIL objective and an ORCA Flash 4 camera. Images were analyzed with CellProfiler 2.4. (GFP for DAPI, Texas Red channel for Msat-160).

The biotin-dUTP-labeled DNA probe for Msat-160 was prepared in a 50 μl PCR with 0.25 mM of each dA/G/CTP, 0.05 mM of dTTP, 0.20 mM of biotin-dUTP, 0.4 μM of both forward and reverse Msat-160 primers (Table 1), 1.5 mM of $MgCl_2$, 1X Taq Buffer with KCl, 2.5 U of Taq DNA polymerase (Thermo Scientific), and 10 μl of PCR product as a template. PCR program was as follows: 95°C for 3 min, and 30 cycles of 95°C for 10 s, 58°C for 5 s, and 72°C for 5 s, followed by elongation of 1 min at 72°C. MJ Thermal Cycler from Bio-Rad was used. Template PCR product was produced with same conditions as above, except with 0.05 mM of dNTPs and 2.5 μl of DNA extracted from a bank vole liver sample (approximately 70 ng) as a template.